Construction of the Hasubanan Alkaloid Core Through an Oxidative Dearomatization/Lewis Acid Catalyzed Cyclization

A Dissertation

SUBMITTED TO THE FACULTY OF

UNIVERSITY OF MINNESOTA

BY

Karen L. Beckman

IN PARTIAL FULFILLMENT OF THE REQUIREMENTS

FOR THE DEGREE OF

DOCTOR OF PHILOSOPHY

Andrew M. Harned, Advisor

July 2014

Acknowledgements

First, I want to thank my advisor, Prof. Andrew Harned. Your passion and enthusiasm for chemistry, as well as your unwavering support for your students has created a superb environment for fostering young scientists. I truly appreciate your dedication and all time you invested into my graduate education.

Next, I would like to thank my family, my mom, Peggy, sister, Joan, and brother-in-law Matthew, your love and support has meant so much to me throughout this process.

I would also like to thank my group members who created a supportive and exciting atmosphere for conducting research. Dr. Kyle Kalstabakken, thank you for answering my questions, no matter how silly they were, your patience is second to none. To Dr. Rodolfo Tello-Aburto, your optimism and generosity are truly inspirational; I wish I were half the person and chemist you are. Dr. Kelly Volp: your friendship has meant so much to me over these years. I could not image getting through without having you standing beside me (literally and figuratively). Nick Moon, Erik Goebel, and all of the other past members of the Harned Group, it has been an honor to have you as my friends and co-workers.

Dr. Letitia Yao, thank you for being such a positive force in my life. I truly loved getting to know you and being your NMR TA.

And finally, I want to thank David MacKenzie for being my partner and constant cheerleader, your support means so much to me.

Dedication

For my mother, Peggy Beckman

Abstract

Access to novel opioid receptor binding ligands is important as chronic pain continues to be a pervasive problem in healthcare. The hasubanan (HB) alkaloids have been identified as potential candidates for selective opioid receptor binding. These alkaloids are a family of compounds, primarily isolated from the flowering plants of the sp *Stephania*, which have been used for centuries in traditional medicinal remedies. While morphine and HB alkaloids share several structural features, the natural occurring HB alkaloids have a configuration opposite to that of morphine. The unnatural antipodes of the HB alkaloids have a similar spatial orientation to morphine, making then increasingly attractive as potential analgesic therapeutics. Based on these observations we were inspired to develop a synthetic strategy that allows access to both the natural and unnatural enantiomers for several of the HB alkaloid family members.

Chapter One provides a detailed background on pain and the involvement of the opioid receptors. Chapter Two covered the isolation and biosynthetic proposals of the HB alkaloids as well as a discussion of synthetic efforts that have been carried out and a structural analysis of the HB alkaloids. Chapter Three will cover our own synthetic efforts toward the synthesis of the HB alkaloid core.

Table of Contents

List of Tables

Table of Figures

List of Schemes

List of Abbreviations

Ac	acetyl
AcOH	acetic acid
AIBN	azobisisobutyronitrile
aq.	aqueous
Ar	generic aryl group
Bn	benzyl
BOC	*tert*-butyloxycarbonyl
BP or bp	boiling point, °C
br	broad
t-Bu	*tertiary*-Butyl
bu	butyl
calcd	calculated
cat.	catalytic amount
conc.	concentrated
COX-2	cycloxygenase-2
D	deuterium
d	doublet
DCE	1,2-dichloroethane
DDQ	2,3-dichloro-5,6-dicyano-1,4-benzoquinone
DEPT	Distortionless enhancement by polarization transfer
DBDMH	1,3-dibromo-*N,N*-dimethylhydantoin
DIBAL-H	diisobutylaluminum hydride
DIPEA	*N,N*-di-*iso*-propylethylamine
DMAP	4-dimethylaminopyridine
DMF	*N,N*-dimethylformamide
DMA	*N,N*-dimethylacetamide

DMSO	dimethylsulfoxide
DOR	delta (δ) opioid receptor
dr	diastereomeric ratio
ee	enantiomeric excess
EI	electron impact ionization
equiv	equivalent(s)
ESI	electrospray ionization
ex	excess
FCC	flash column chromatography
GC	gas chromatography
GPCR	G-protein coupled receptor
GRK	G-protein coupled receptor kinase
h	hour
HB	hasubanan
HRMS	high-resolution mass spectrometry
Hz	hertz
IBX	1-hydroxy-1,2-benziodoxol-3(1*H*)-one 1-oxide
IC	inhibitory concentration
IR	infrared spectroscopy
KOR	kappa (κ) opioid receptor
LA	Lewis acid
LAH	lithium aluminum hydride
M	molar (concentration, moles/L)
M	generic metal, usually group 1 or 2, possibly with ligands
m-CPBA	3-chloroperoxybenzoic acid
Me	Methyl
min	minutes
mol	mole
mol %	molecular percentage

MOM	methoxymethyl
MP or mp	melting point, °C
MS	mass spectrometry
MOR	mu (μ) opioid receptor
NBS	*N*-bromosuccinimide
nM	nanomolar
NMR	nuclear magnetic resonance spectroscopy
NOE	nuclear Overhauser enhancement/effect
NSAID	non-steroidal anti-inflammatory drug
Nu	nucleophile
[O]	oxidation
Pd	palladium
Ph	phenyl
PhH	benzene
PIDA	phenyliodine diacetate
PIFA	[bis(trifluoroacetoxy)iodo]benzene
Piv	pivaloyl
ppm	parts per million (NMR spectroscopy)
PPTS	pyridinium *p*-toluenesulfonate
i-Pr	*iso*-propyl
pyr	pyridine
Quant.	Quantitative
R	generic substituent
rt	room temperature
s	singlet
sat'd	saturated
SSRI	selective serotonin reuptake inhibitor
t	triplet
taut.	tautomerization
TBAF	tetra-*n*-butylammonium fluoride

TBS	*tertiary*-butyldimethylsilyl
TCA	tricyclic antidepressant
TFA	trifluoroacetic acid
TFE	2,2,2-trifluoroethanol
TfOH	trifloromethanesulfonic acid
THF	tetrahydrofuran
TIPS	triisopropylsilyl
TLC	thin layer chromatography
TMS	trimethylsilyl
TROC	2,2,2-trichloroethoxycarbonyl
Ts	4-tosyl (4-toluenesulfonyl)
X	generic atom, possibly substituted

CHAPTER 1

INRODUCTION AND BACKGROUND

Pain is defined as an unpleasant sensory and emotional experience associated with actual or potential tissue damage.[1] The prevalence of chronic pain in the United States is estimated to be 35.5 % or 105 million people; costs an estimated $100 billion USD per year in health-care expenditures and is the most common ailment for which patients seek medical attention.[2,3] The experience of pain is highly subjective, with individuals developing pain thresholds through experiences of injury or pathology in early life. This inherit patient variability complicates clinical strategies for pain management with 50 % of individuals seeking treatment dissatisfied with their present treatment options.[4]

Despite recent advancements in the use of analgesic adjuvants and the controversial selective cyclooxygenase 2 (COX-2) inhibitors, the mainstays of pain management continue to be non-steroidal anti-inflammatory drugs (NSAIDs), and opioid analgesics.[5,6] Unfortunately, many of these can be ineffectual at managing pain and are further marred by adverse effects including the potential for abuse or dependence. Therefore, there is a major unmet challenge in the identification of compounds that can more effectively manage chronic pain, with fewer adverse side effects. We feel this challenge is best met through the synthesis of novel compounds derived from the hasubanan (HB) family of alkaloids.

The HB alkaloids, primarily isolated from the vine *Stephania japonica*, have been used in traditional medicinal remedies for centuries.[7,8] There has been significant interest in the HB alkaloids due to the close resemblance of the HB skeleton to that of morphinan alkaloids.[9] Additionally, recent studies by Quinn and co-workers revealed an affinity of HB alkaloids for binding opioid receptors, which are common targets of several analgesic drug classes.[10]

There have been numerous synthetic studies of the HB alkaloids, but none have established the analgesic potential of the HB alkaloids, and only a few of these synthetic routes are amenable to the necessary structural activity studies.[11–14] The goal of this dissertation research is to develop a synthetic strategy that allows for the rapid synthesis of several HB alkaloids derivatives, which is required to complete a full biological evaluation of the HB alkaloids.

This introduction (Chapter One) will provide background on the current approaches to pain management including by a description of analgesic drug classes and their respective mechanisms of action. Chapter Two, will provide an overview of the HB alkaloids and a discussion of the structural similarities between morphine and the HB alkaloids and the biological implications. Finally, Chapter Three will provide an in depth analysis and discussion on the synthetic work that was involved in making these HB derivatives.

1.1 Pain Management

1.1.1 Classification and etiology

While several taxonomies for pain exist, the most commonly utilized is depicted below (Figure 1.1); where pain is categorized by both duration, acute versus chronic and by etiology, nociceptive vs. neuropathic.[15]

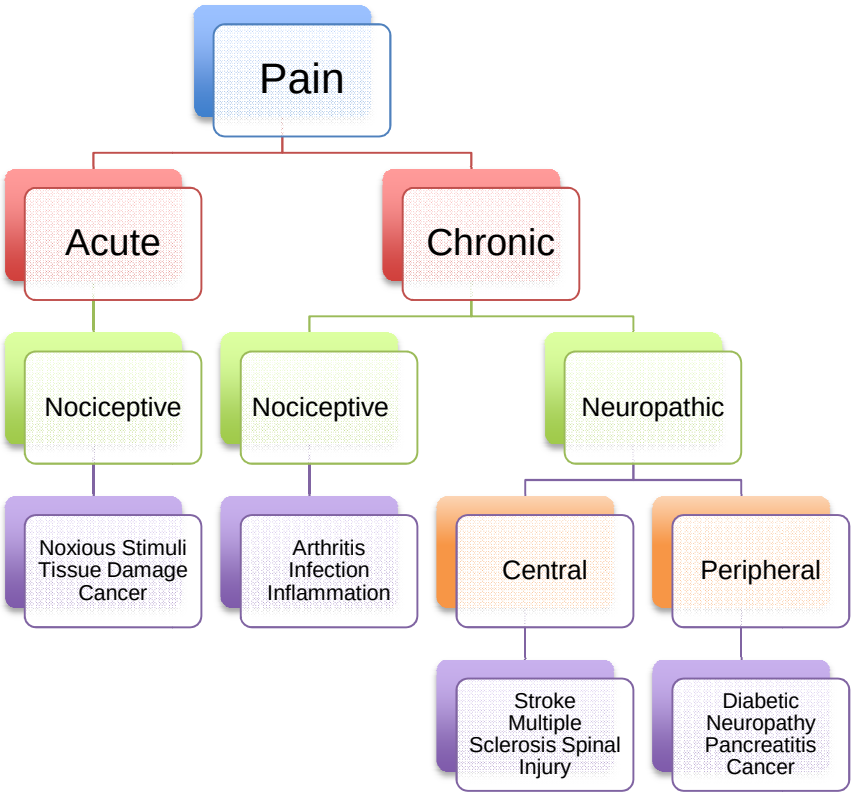

Figure 1.1. Pain classification by duration and etiology.

1.1.1.a Acute vs. Chronic

Acute and chronic are terms commonly used to describe the duration of painful sensations. In general, acute pain resolves within weeks of the initial onset, whereas chronic pain is continuous, long-term pain, which can last months or even years. The

demarcation between acute and chronic pain is somewhat arbitrary, and typically ranges from three months to six months.[16] Acute pain is highly receptive to treatment, as several classes of analgesics, including NSAIDs and weak opioids, are known to be clinically effective.

The complexity of chronic pain has represented a major dilemma for clinicians, with one in three adult Americans seeking treatment for chronic pain annually.[17] Chronic pain often has both adaptive (necessary for survival) and non-adaptive components. This multifactorial nature requires physicians to consider the origin of pain when developing treatment plans.[18] Below is a brief description of the most common pain etiologies, nociceptive and neuropathic pain.

1.1.1.b Nociceptive pain

Nociceptive pain is frequently described as stabbing, pricking, burning, throbbing or cramping. It is instigated through the stimulation of specialized sensory neurons, called nociceptors, by noxious stimuli such as, extremes of temperature, or mechanical or chemical excitation. This type of pain serves as a warning to protect individuals from potential injury as illustrated by the automatic response of pulling away caused by briefly touching a hot surface. Nociceptive pain is often subcategorized as somatic, derived from skin and deep tissue, or as visceral, originating from internal organs. Due to high concentrations of nociceptors in somatic tissues, chronic nociceptive pain is typically localized, as in arthritis, which results from degenerative or inflammatory processes

within the joints.[19] Nociceptive pain is often effectively managed with NSAIDs, or as in the case of post-operative pain, with a combination of NSAIDs and weak opioids.

1.1.1.c Neuropathic pain

Neuropathic pain results from actual damage to nerve fibers themselves in the central or peripheral nervous system.[20] This damage can lead to nerve dysfunction, causing numbness, weakness and/or loss of reflexes. Common descriptions accompanying neuropathic pain include “burning”, “shooting” or “shock-like” sensations. Central nervous system disorders of the brain or spinal cord, such as multiple sclerosis, and stroke frequently lead to neuropathic pain. Damage to peripheral nerves associated with amputation, radiculopathy, carpal tunnel syndrome also precipitate neuropathic pain.[21] The most common cases of chronic neuropathic pain include diabetic neuropathy, post-herpetic neuralgia, fibromyalgia, and lower back pain due to disc herniation.[22] There is a complex interplay between etiology, pathophysiology, and symptoms of neuropathic pain. Therefore, if one agent is not effective, physicians often use combination therapies that may mediate analgesia through different components of the involved pain pathways.

1.1.2 Traditional chronic pain management approaches

The treatment of chronic pain can be challenging because it is a complex condition influenced by genetic makeup as well as physiological and psychological factors. These factors are further complicated by the coexistence of both nociceptive and neuropathic pain. For instance, a cancer patient can experience pain from tumor encroachment, inflammatory pain due to tissue damage, and neuropathic pain resulting

from radiation or chemotherapy-induced neuropathies. Pain treatments are tailored to the individual, with a multidisciplinary approach, combining several of the methods (Figure 1.2).

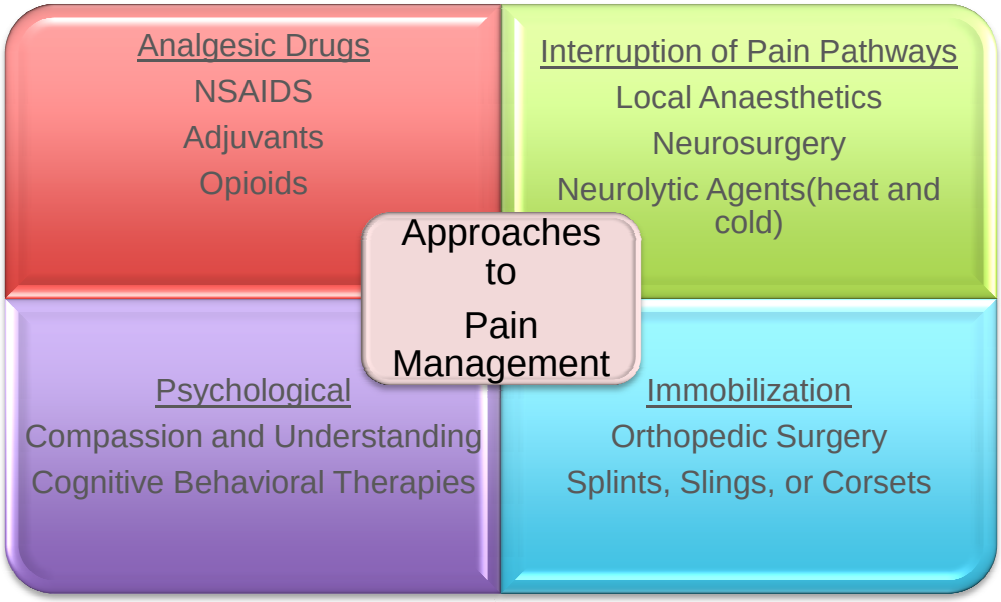

Figure 1.2. Approaches to pain management.

Physicians treat psychological factors of pain with cognitive behavioral therapies and analgesic adjuvants such as tricyclic antidepressants.[23] Nociceptive pain may be treated solely or in combination with surgery, immobilization, NSAIDs and weak opioids. Additionally, local anesthetics and some anticonvulsants (sodium channel- blocking drugs) are used as analgesic adjuvants for the treatment of pain. These pharmacotherapies presumably produce frequency and voltage-dependent blockade of sodium channels on damaged neurons, relieving some pain associated with some neuropathic pain.[24] However, no current pharmaceuticals optimally address chronic neuropathic pain.[25] Therefore,

management of neuropathic pain often requires a combination of drugs from different substance classes to produce adequate pain relief.

Several clinicians adhere to the guidelines laid out in the World Heath Organization's (WHO) Analgesic Ladder (Figure 1.3) for developing pain management plans.[26] The WHO analgesic ladder provides a three-step sequential approach for analgesic administration based on pain severity.

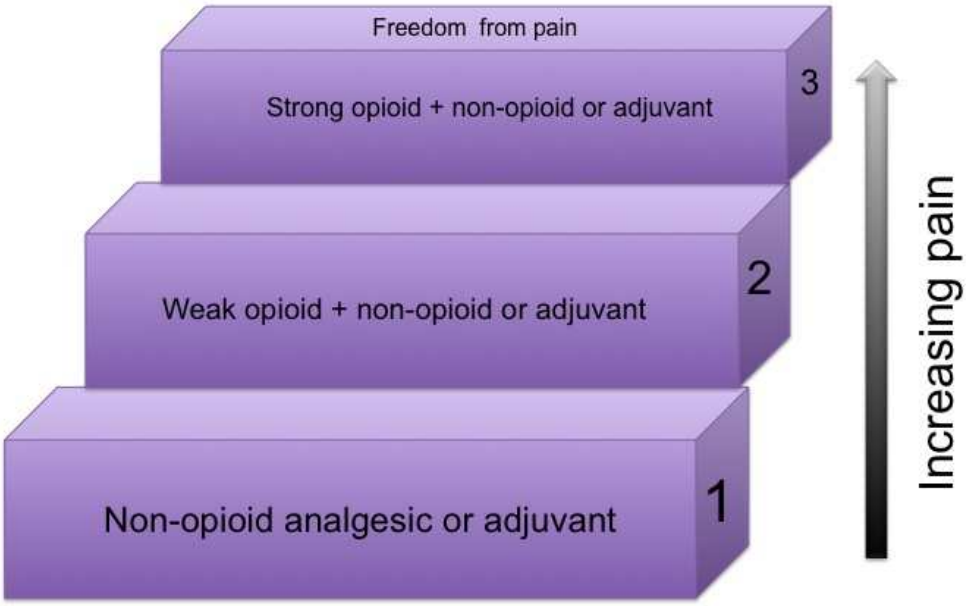

Figure 1.3. The WHO analgesic ladder.

The ladder recommends initial treatment of pain with non-opioids, such as NSAIDs and acetaminophen. If pain persists, treatment with a weak opioid, in combination with a non-opioid analgesic is recommended followed by a strong opioid, until the patient is free of pain.[27] At each stage of the treatment ladder, adjuvant

medications, such as antidepressants or anticonvulsants, may also be given to aid in alleviating patient pain and anxiety. Although recent advancements in the development of non-opioid analgesics have occurred, it is evident that opioids remain the mainstay of chronic pain management.

1.1.3 Analgesics utilized in pain management

1.1.3.a NSAIDs

Compounds such as aspirin and ibuprofen, act by disrupting the synthesis of prostaglandins by inhibiting the cyclooxygenase enzymes COX-1 and COX-2. This inhibition of prostaglandin synthesis results in the analgesic, anti-pyretic and anti-inflammatory properties of these drugs. Most NSAIDs are nonselective inhibitors of COX-1 and COX-2, but newly developed agents have much greater affinity for the COX-2 isoform.[28] Acetaminophen, which does not show anti-inflammatory affects, is also sometimes classified as an NSAID, but its mode of action for inhibiting prostaglandin synthesis has not been fully elucidated.[29] The structures and mechanism of action of the most commonly utilized NSAIDs are shown in Table 1.1. The most commonly reported side effects of NSAIDs are those involving the GI tract. Additionally, chronic or acutely toxic acetaminophen exposure can lead to liver toxicity through hepatocellular necrosis.[30,31]

Table 1.1. Examples of NSAIDs and mechanism of action.

Compound	Mechanism of Action
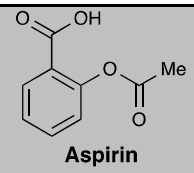 Aspirin	Non-selective inhibitor of COX-1 and COX-2 enzymes
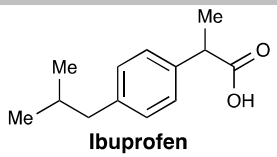 Ibuprofen	Non-selective inhibitor of COX-1 and COX-2 enzymes
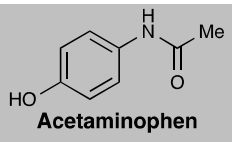 Acetaminophen	Inhibitor of prostaglandin synthesis; unknown mechanism
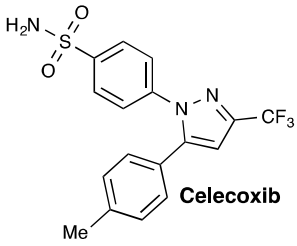 Celecoxib	Selective Inhibitor of COX-2 enzyme

The adverse GI side effects of NSAIDs are attributed to the reduced prostaglandin levels in the gastrointestinal mucosa, which decreases mucus and bicarbonate secretions, thereby reducing their protective effects against the acidic gastric environment. In addition, NSAIDs can be directly toxic to the gastric mucosa, leading to ulceration, and potentially fatal bleeding in the most extreme cases.[27] Selective COX-2 inhibitors cause less GI toxicity than non-selective COX-1 and COX-2 inhibitors, but several large studies have shown an increase in cardiovascular toxicity, including myocardial infarction and

stroke, associated with some selective COX-2 inhibitors.[32] These selective inhibitors were withdrawn from the market between 2004 and 2005 because of this toxicity. Celecoxib is one of the main drugs in this class still employed.[33]

1.1.3.b Analgesic adjuvants

The term adjuvant analgesic describes any drug with a primary indication other than pain, but with analgesic properties in some conditions.[34] Adjuvants are usually co-administered with other analgesics such as NSAIDs and opioids, although some have been shown to have analgesic properties when administered alone.[35] Tricyclic antidepressants (TCAs) and selective serotonin reuptake inhibitors (SSRIs) are commonly used as adjuvant therapy. The explicit way in which antidepressants are effective in pain management remains unknown, but multiple mechanisms are likely to be involved. It is speculated that analgesia is mediated through inhibition of neurotransmitter reuptake in the synaptic cleft. These mechanisms are related to pain signaling in descending spinal pain pathways.[36,37] Common side effects of TCAs are sedation, and anticholinergic consequences such as: dry mouth, constipation, postural hypotension and weight gain.[38] While SSRI side effects are generally more mild than TCAs, there is the risk of weight gain with the long-term use of SSRIs, as well as sexual dysfunction.[39]

Local anesthetics and some anticonvulsants are also used as analgesic adjuvants. These pharmacotherapies presumably produce a voltage-dependent blockade of calcium and/or sodium channels on damaged neurons, alleviating some pathologies associated

with neuropathic pain.[24] Local anesthetics are often highly sedating and have a small therapeutic window before reaching toxicity, so their use as analgesic therapies is primarily restricted to hospital or clinical settings, or administered with controlled release transdermal patches. Side effects of anticonvulsants include drowsiness, dizziness and less commonly gastrointestinal symptoms and mild peripheral edema. All these effects require close monitoring and regularly require dosage adjustment. The structures and drug classes of commonly prescribed analgesic adjuvants are listed in Table 1.2.

Table 1.2. Examples of analgesic adjuvants and drug classes.

Compound	Drug Class
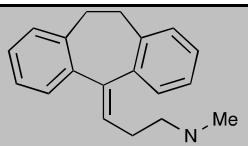 Amitriptyline	**Tricyclic antidepressant**: inhibit the reuptake of serotonin and norepinephrine at the synapse
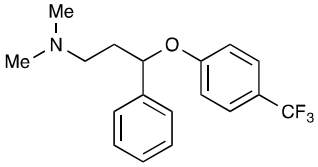 Fluoxetine	**Selective serotonin reuptake inhibitor**: inhibit the reuptake of serotonin at the synapse
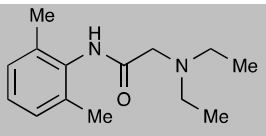 Lidocaine	**Local anesthetic**: inhibitor of voltage-gated sodium channels
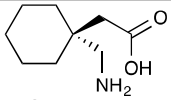 Gabapentin	**Anticonvulsant**: inhibitor of voltage-gated calcium channels

1.1.3.c Opioids[1]

Opioids play a unique role in society, with a history tracing back to 3400 BC, Mesopotamia; where the Sumerians used the juice from unripe seed pods of the poppy, *Papaver Sommniferum*, to treat pain and other ailments. In 1805, Friedrich Sertürner isolated morphine (named from the Greek god of dreams) from opium, helping transform the landscape of modern medicine.[40] Centuries later, opioids continue to be the cornerstone of treatment for moderate to severe pain.

Opioids exert their analgesic properties through the binding of opioid receptors within the central nervous system. The binding of these receptors produces signals causing a hyperpolarization of neuronal cell membranes and the suppression of neurotransmitter release, resulting in analgesia. Numerous natural, semisynthetic, and synthetic opioids have been commercialized for oral, transdermal and intravenous administration (Table 1.3). The single entity formulations on the market include morphine (Avinza™, Kadian™, MS Contin™), oxycodone (OxyContin™), hydromorphone (Dilaudid™), oxymorphone (Opana™), fentanyl (Duragesic™, Actiq™, Fentora™), and methadone. Additionally several combination opioid/NSAID products, such as those containing hydrocodone and acetaminophen (Vicodin™, Lorset™) or ibuprofen (Vicoprofen™), tramadol and acetaminophen (Ultracet™), oxycodone and

[1] The term *opioid* refers to *all compounds* that bind to the opioid receptors. Conventionally, the term *opiate* can be used to describe those opioids that are alkaloids, derived from the opium poppy. Opioids include semisynthetic opiates, endogenous peptides, as well as synthetic opioids.

acetaminophen or aspirin (Percocet™ or Percodan™), and those containing codeine and acetaminophen are frequently used for the treatment of chronic pain.[41]

Table 1.3. Examples opioids used in pain management.

Natural	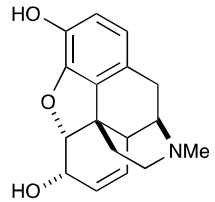 (−)-Morphine 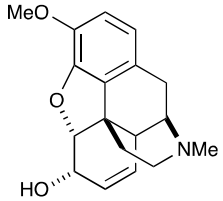 (−)-Codeine
Semi-synthetic	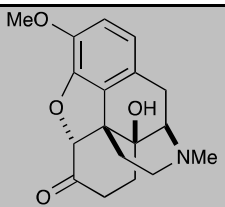 (−)-Oxycodone 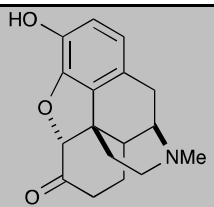 (−)-Hydromorphone 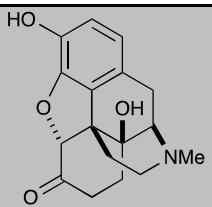 (−)-Oxymorphone
Synthetic	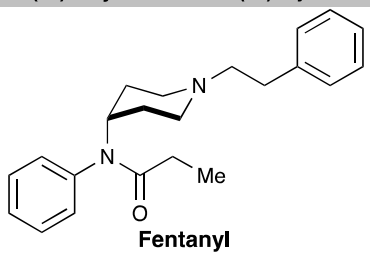 Fentanyl 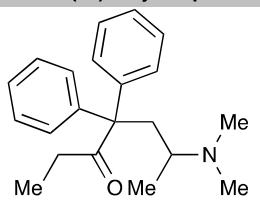 Methadone

Opioids are far from benign medications, their long-term use is associated with significant side effects, including sleep apnea,[42] constipation,[43] hyperalgesia,[44] tolerance, and addiction.[45] Tolerance and addiction are particularly troublesome given the rate of overdose deaths in the United States has more than tripled since 1990,[46] and the aberrant behaviors associated with addiction lead to significant criminal activity.

Since the time of morphine's isolation, scientists have attempted to develop opioids with a reduced propensity to cause the side effects associated with long-term use. Many

of these attempts have been based on flawed or incomplete hypotheses of tolerance development. As was the case of both diacetylmorphine (trade name Heroin) and sustained release oxycodone (trade name OxyContin), each initially was marketed as more effective and less habit forming than morphine.[47] Now, both are come of the most highly sought after opioid drugs of abuse.

Our understanding of the molecular mechanisms underlying opioid analgesia as well as tolerance and dependence has improved greatly with the study of the opioid receptors. The remainder of this chapter will focus on the insights into drug development gained through research of opioid receptor chemistry.

1.2 Opioid Receptors

1.2.1 Background and development of receptor pharmacophores

In 1973, three independent teams identified opiate binding membrane receptors within the brain.[48–50] Two years later scientists discovered endogenous peptides that bind to these receptors: enkephalins, β-endorphin, endomorphins, and dynorphins.[51,52] By 1976, scientists proposed the existence of three separate opioid receptor subtypes, μ (MOR), δ (DOR) and κ (KOR),[53,54] which differ in their function and ligand specificity.

The speed at which these discoveries were made was unprecedented compared to the discovery of other class of drugs. Early on, researchers observed the importance of subtle structural differences between agonists and antagonists (Figure 1.4 (A)).

Merely converting an *N*-methyl to an *N*-allyl substituent transformed the agonist (–)-morphine (**1.1**) to (–)-nalorphine (**1.2**), an opioid with partial antagonistic properties. The same modification of the agonist (–)- oxymorphone (**1.3**) leads to the full opioid receptor antagonist (–)-naloxone (**1.4**). By contrast, antagonists for most neurotransmitters and other drugs vary greatly in structure.

A three-point pharmacophore of MOR binding was developed (Figure 1.4 (B)) based on specific spatial orientation of critical functional groups.[55,56] These functional group requirements included a phenol, a hydrophobic region, and an amine. The size of the *N*-substituent dictated the compound's potency and its agonist vs. antagonist properties.

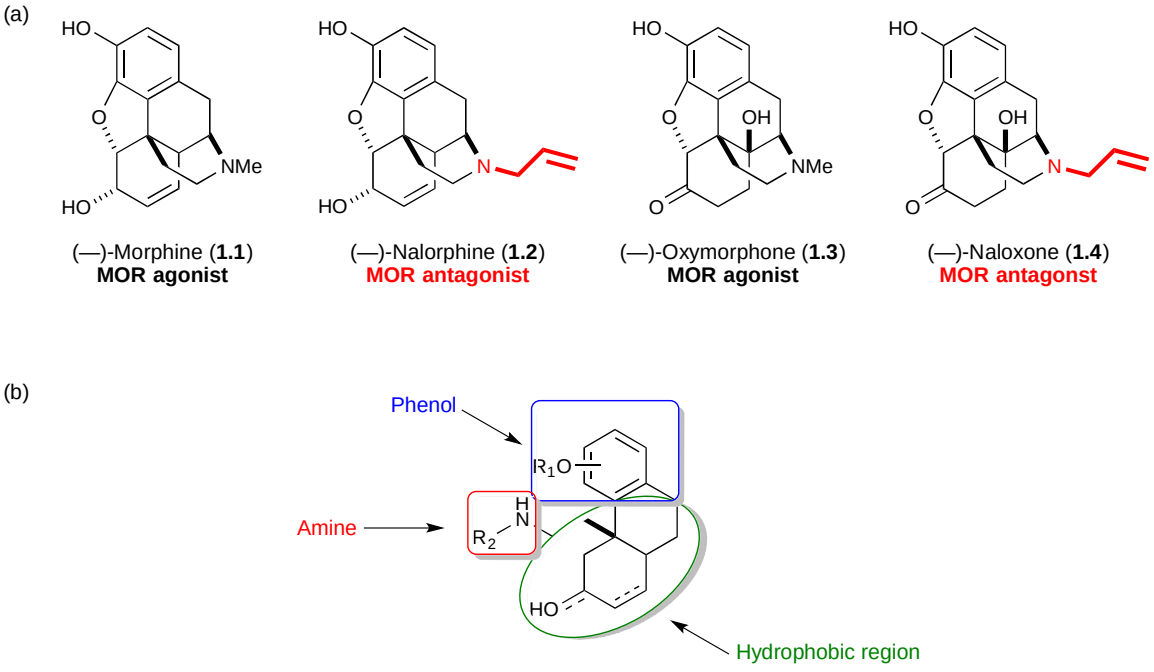

Figure 1.4. (a) Structural differences between MOR agonists and antagonists. (b) Generic 3-point pharmacophore for OR receptors.

Scientists used this knowledge to prepare large numbers of radiolabelled opiates with widely varying potencies and efficacies, allowing them to rapidly probe receptor pharmacology and other fundamental aspects drug activity.[57]

The advent of gene cloning and characterization further evolved our understanding of opioid receptors allowing the entire endogenous opioid system, including peptides and receptors to be characterized at the molecular level by the mid 90s.[58] Generation of chimeric receptors aided in identifying receptor regions important for binding, while site-directed mutagenesis studies were used to implicate individual residues involved in ligand binding.[59] This knowledge produced a significantly more detailed pharmacophore in which specific binding interactions were proposed. One such proposal suggests that the phenol (Figure 1.4, (B)) interacts with a trans-membrane helix histidine residue, the amine interacts with an aspartate residue and the hydrophobic region fits into a pocket of hydrophobic residues (See Section 1.2.2 for a description of receptor structure).[59]

Recently, after decades of studies, the crystal structures of MOR,[60] DOR,[61] and KOR[62] with antagonist bound were disclosed, confirming several of the binding hypotheses and revealing new insights into receptor conformation, For example, the presence of extraneous molecules, such as water, within the opioid binding pocket. These structures will allow for the development of sophisticated computer-based binding models, which will hopefully lead to drug discovery.

1.2.2 Receptor structure and function

The opioid receptors, MOR, DOR, and KOR resemble rhodopsin and belong to the γ subfamily of class A G-protein-coupled receptors (GPCR).[63] Each contains an extracellular *N*-terminus, seven counter-clockwise bundled trans-membrane helices, and an intracellular C-terminus.[59,64] Overall MOR, DOR, and KOR show 70 % amino acid sequence identity. The most homology occurs within the seven trans-membrane helical core, which contains the opioid binding pocket.[64] Three extracellular loops, including the *N*-terminal domain, differ strongly between receptors, and likely form a protein gate that selects agonists or antagonists entering the binding pocket, thereby contributing to μ, δ, and κ selectivity.[65]

As with all GPCRs, opioid receptors convey extracellular signals within the cell through conformational modulation of the cytoplasmic domains that interact with the G protein.[66] All three ORs interact with inhibitory G proteins of the G_o/G_i type. Opioid induced analgesia occurs when ligand binding modifies the helical packing of the receptor, rearranging the positioning of trans-membrane domains. This helical movement modifies the receptor's intracellular structure, disrupting the receptor-G protein interaction, catalyzing a nucleotide exchange on G_i and G_o, which leads to inhibition of adenylyl cyclase, neuronal hyperpolarization via activation of K^+ channels, and inhibition of neurotransmitter release via inhibition of Ca^{2+} channels.

Following activation, receptors are decoupled from the G protein through rapid phosphorylation by GPCR kinases (GRKs) and subsequent binding by arrestin, resulting

in receptor desensitization.[66] Arrestin additionally recruits clathrin and other components of the endocytic machinery, leading to endocytosis of the receptor, thus attenuating receptor signaling by removing ligand-receptor complexes from the cell surface. The receptors are re-sensitized by rapid recycling to the plasma membrane. There have been studies suggesting that ligands with the greatest addictive potential, promote interactions with G_i more strongly than they promote interactions with arrestins, leading researchers to believe that receptor trafficking plays a crucial role in the development of tolerance and dependence associated with the use of opioid drugs.[67,68]

1.2.3 Receptor pharmacology

The discrepancies in biological responses to the binding of opioids are due to differences in activity between the opioid receptors. The cloning of MOR, DOR and KOR receptors was an important step in probing these phenomena. Mice with genetic deletions of each of these receptors, as well as mice lacking two or three of the receptors have been generated, which has allowed researchers to identify unique pharmacological implications for each receptor.

The most extensive investigations have involved MOR knockout mice. These studies have established that MOR is primarily responsible for analgesia elicited by morphine and a variety of other opioids. Further work showed that deletion of MOR abolishes tolerance and physical dependence to morphine.[69]

Studies with KOR and DOR knockout mice have been also been fruitful. KOR was shown to mediate dysphoric activities and therefore was found to be useful in the

treatment of addiction by opposing the pleasure/reward response associated with MOR agonists.[70] DOR was shown to be very distinct from MOR and KOR, with implications in the regulation of emotional responses and as well as anxiolytic and antidepressant activity, leading to potential interest in the field of psychiatric disorders.[71] Selective DOR antagonists have also been shown to block the development of morphine tolerance and dependence[72] giving rise to promising combination therapies for neuropathic pain without the adverse side effects associated with MOR.[73]

1.2.4 Closing remarks

The tools of molecular biology and computational modeling have greatly augmented insights into receptors and their ligands. Unfortunately, the pharmacologic alterations observed with the three different receptor subtypes have failed to address the two key problems to be resolved: 1) what is the nature of the addictive process and 2) is there a rational approach to the design of a less addicting opioid based on differential influences within the opioid receptors? Thus the current challenges in developing new opioid analgesics are remarkably similar to those almost 40 years ago, when opioid receptors were first identified. This conclusion is only bolstered by the pharmaceutical industry's inability to develop treatments for chronic pain without the negative side effects associated with traditional MOR agonists. Drug development strategies, which have shown negligible success, continue to focus on solely on reformulation or drug combinations to attenuate the adverse side effects. If chronic pain is to be successfully treated, drug developers must look beyond improving efficacy and potency of MOR

agonists and consider additional properties that affect net receptor signaling, including receptor trafficking and signaling through non-canonical pathways such as arrestin.

The identification of novel opioid receptor ligands with unique selectivity is needed in order to probe developing strategies in downstream signaling pathways. We feel strongly that this need is be met by investigating the binding interactions between the HB alkaloids and the opioid receptors and further studying their downstream effects.

CHAPTER 2

THE HASUBANAN ALKALOIDS

2.1 Introduction

2.1.1 Isolation and structural elucidation

The HB alkaloids constitute, a large family of natural products, primarily isolated from the vine *Stephania japonica*. The greater than seventy HB family members which share a common aza[4.4.3]propellane core. The family is divided among four subclasses defined by the oxidation pattern of the C–ring (Figure 2.1). Runanine (**2.2**) and delavayine (**2.3**) are the most closely related to the parent compound hasubanonine (**2.1**), with minor variations in A–ring substitutions, whereas cepharamine (**2.4**) and longanine (**2.5**) vary in oxidation at the C8 position.

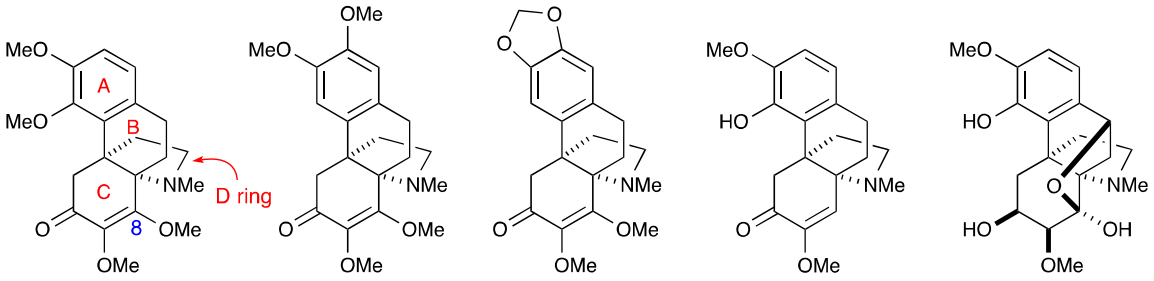

Figure 2.1. Representative members of the hasubanan family of alkaloids.

The premier family member hasubanonine (**2.1**), was isolated by Kondo and co-workers in 1951.[74] The structure of **2.1**, however, was not elucidated until over a decade

after initial discosure.[9] Due to the close structural resemblance to the morphinan alkaloids, the structure of hasubanonine was initially assigned as a morphinan analog, **2.6** (Figure 2.2). In 1956, the structure was errantly amended, based on biogenetic considerations to **2.7**.[75]

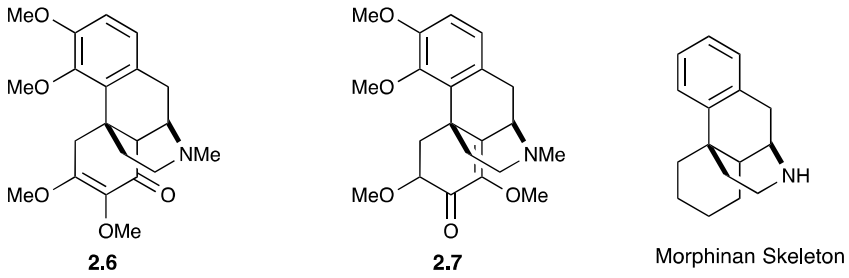

Figure 2.2. Proposed structures of hasubanonine (**2.1**).

The structure was not corrected until the mid-1960s, when Tomita and co-workers noted that the ^{1}H NMR spectrum of hasubanonine lacked the characteristic C_9–H resonance associated with the ethanamine bridge of the morphinan skeleton (**2.8**). This prompted the proposal of the hasubanan skeletal structure (**2.9**), which possesses a five-membered pyrrolidine ring as opposed to the six membered piperidine found in the morphinan alkaolids.[76]

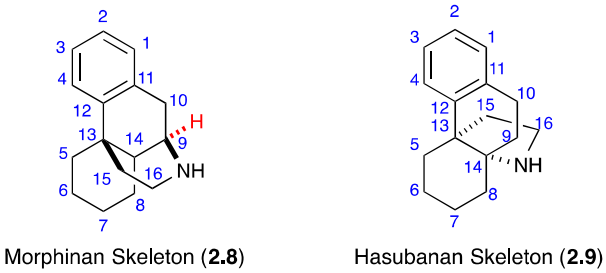

Figure 2.3. Numbered morphinan and hasubanan skeletons.

The authors confirmed their proposed structure by comparison of the physical and spectral properties of hasubanonine derivative **2.13** with known morphine derivative **2.14** (Scheme 2.1). Preparation of compound **2.13** commenced with sodium borohydride reduction of hasubanonine, followed by acid catalyzed loss of methanol, to yield enone **2.12**. Further reduction of **2.12** with zinc amalgam in concentrated hydrochloric acid afforded the fully saturated amine **2.13**.

Scheme 2.1. Structure elucidation of hasubanonine (**2.1**).

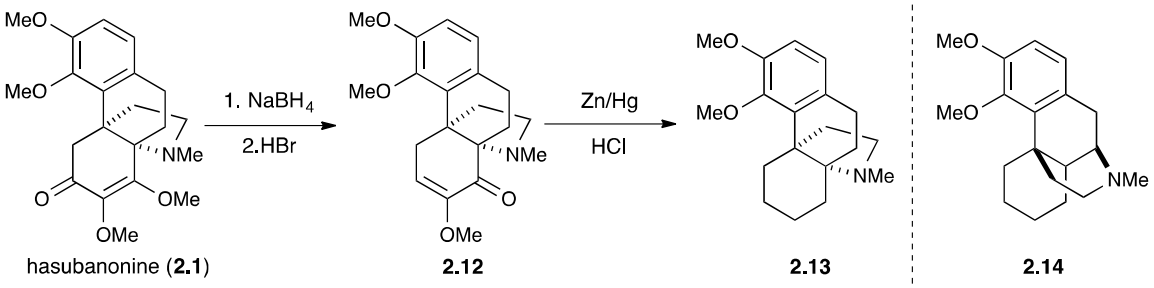

hasubanonine (**2.1**) **2.12** **2.13** **2.14**

The NMR spectra of **2.13** confirmed the presence of the proposed five-membered pyrrolidine D–ring, with no signals attributable to an ethanamine bridge. The authors also noted that the physical properties of compounds **2.13** and **2.14** are identical with the exception of specific rotation, **2.13** is antipodal to **2.14**, indicating an absolute configuration opposite to that of morphine. Thus the structure and absolute stereochemistry of (–)-hasubanonine (**2.1**) was unambiguously assigned.

2.1.2 Biosynthesis

Due to the similarities in structure, early studies into the biosynthesis of the HB alkaloids were first directed by the knowledge established through the investigations into the biosynthesis of (–)-morphine (**1.1**).

*2.1.2.a Biosynthesis of morphine (**1.1**)*

The concept of phenolic oxidative radical coupling is a central theme in the biosynthesis of morphine (Scheme 2.2).[75] The tyrosine derived 1-benzylisoquinoline intermediate, (*R*)-reticuline (**2.15**), undergoes oxidation to give **2.16**, with resonance-stabilized radicals at the ortho- position of the A–ring and para- position of the C–ring. Coupling of the intermediate radicals, followed by rearomatization leads to the dienone salutaridine (**2.17**). With the major framework established, subsequent cyclization, demethylation and reduction completes the biosynthesis of morphine (**1.1**).

Scheme 2.2. Biosynthesis of morphine (**1.1**).

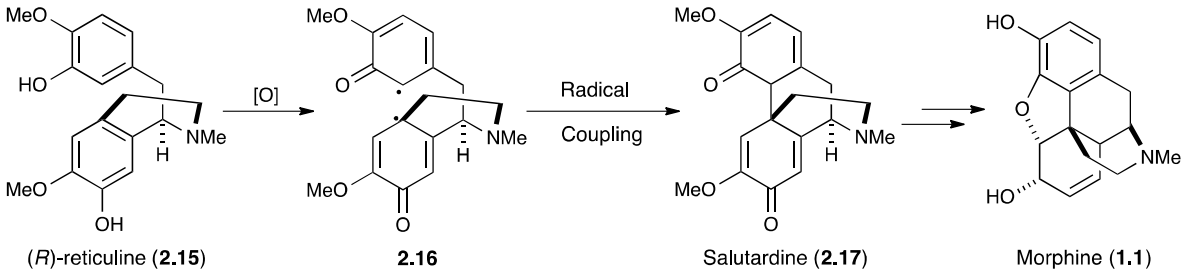

(*R*)-reticuline (**2.15**) **2.16** Salutardine (**2.17**) Morphine (**1.1**)

*2.1.2.b Biosynthetic studies of hasubanonine (**2.1**)*

To identify the radical cyclization precursor in the HB biosynthetic pathway, Battersby and co-workers, performed feeding experiments with several ^{13}C-labelled

synthetic derivatives of **2.15**.[77,78] Based on these studies, dihydoxyisoquinoline, **2.18**, was identified as an essential precursor for radical cyclization. The authors also concluded that the timing of the *N*-methylation was not pivotal, as secondary amino or *N*-methylated isoquinolines were both successfully incorporated into the alkaloid.

Little is known about the origins of the "enantiomeric" precursors **2.15** and **2.18**. Both the morphinan and HB alkaloids are derived from tyrosine dimerization products. It has been suggested the same mechanistic pathway is shared by both alkaloid families for the generation of **2.15** and **2.18**, but that the presence of different enzymes result in the formation of antipodal substrates.

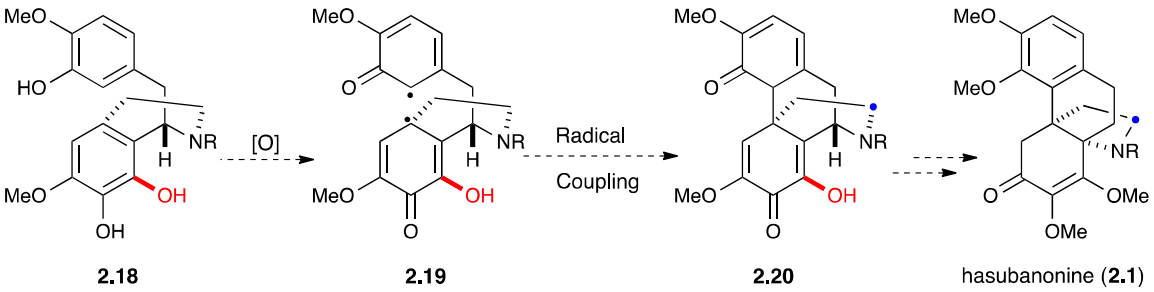

Scheme 2.3. Proposed biosynthesis of hasubanonine (**2.1**).

There is also limited information about the ring contraction of morphinan dienone **2.20**, or its antipode, to form the hasubanan skeleton. Synthetic investigations by Kirby have shown that the alkaloid **2.21**, bearing the morphinan framework, can be converted to the hasubanan framework through an aziridinium intermediate, by treatment with silver acetate (Scheme 2.4).[79]

Scheme 2.4. Conversion of the morphinan skeleton to the hasubanan skeleton.

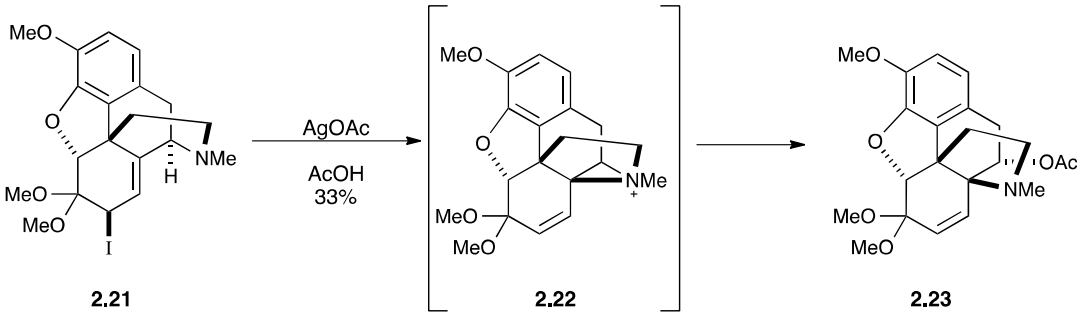

2.21 **2.22** **2.23**

Presumably, the coordination of the allylic iodide to the silver metal generates a transient allylic carbocation. The tertiary amine undergoes an intramolecular S_N2'-type substitution to give aziridinium ion **2.22**, which is opened by an acetate anion at the less substituted position to provide **2.23** in 33 % yield. Kirby speculates that the formation of a similar aziridinium intermediate followed by enzymatic reduction is involved in HB alkaloid biosynthetic pathway.

2.2 Synthetic Studies

The challenging structures of the hasubanan alkaloids have garnered significant attention from the scientific community, with synthetic studies dating back to the 1960s. Racemic syntheses of hasubanonine (**2.1**),[80] metaphanine,[81,82] and cepharamine (**2.4**),[83–85] as well as numerous partial and formal syntheses of other hasubanan alkaloids[86–97] have been reported. More recently, there has been a resurgence of interest in the HB alkaloids, with several disclosures of enantioselective syntheses within the last four years. The

discussion of this section will be focused on these enantioselective syntheses of the HB alkaloids.

2.2.1 Schultz's synthesis of (+)-cepharamine (2.33)

In 1998, Schultz reported the first asymmetric synthesis of a HB alkaloid. Inspired by the structural resemblance to the morphinan alkaloids, Schultz prepared the unnatural enantiomer, (+)-cepharamine,[11] featuring a highly convergent strategy dependent upon an asymmetric Birch reduction-alkylation protocol. To date this is the only reported synthesis of an unnatural HB alkaloid.

Scheme 2.5 highlights the asymmetric Birch reduction. Benzamine **2.24**, was prepared according to literature procedures in five steps from commercially available 2-bromo-5-methoxybenzoic acid; Birch reduction of **2.24**, with potassium in NH_3 (l), THF/*t*-BuOH (1 equiv) at –78 °C, followed by addition of LiBr and the alkylation reagent **2.25** provided 1,4-cyclohexadiene **2.26,** as a single diastereomer, in 95 % yield.

Scheme 2.5. Asymmetric Birch reduction and alkylation of benzamide **2.24**.

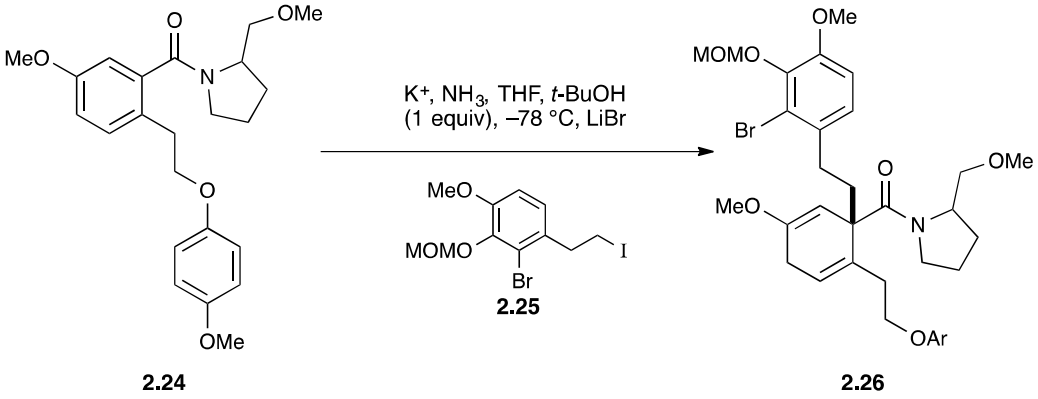

2.24 **2.25** **2.26**

With the success of the asymmetric Birch reduction the authors set out to close the A–B–C ring system utilizing a radical mediated cyclization to form both the C9–C14 and C12–C13 bonds of (+)-cepharamine (**2.33**) (Scheme 2.6).

Scheme 2.6. Radical cyclization of A–B–C ring system.

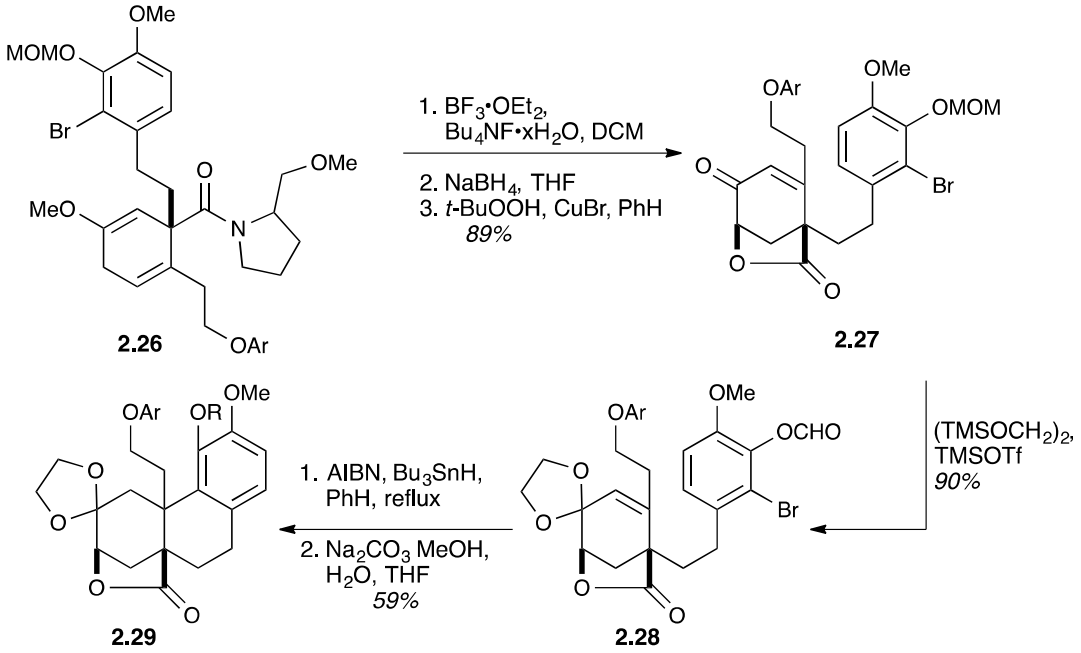

Enol ether hydrolysis and reduction of **2.26** with $NaBH_4$ gave a mixture (•1:1) of diastereomerically related alcohols. Protection of the phenolic hydroxyl group as the formate ester and allylic oxidation with *tert*-butyl hydrogen peroxide and CuBr gave enone **2.27**. Ketalization of **2.27** under aprotic conditions provided the radical cyclization precursor **2.28.** The formation of the A-B-C ring system occurred upon treatment of **2.28** with AIBN and tributyltin hydride, in refluxing toluene. Basic hydrolysis of the formate ester gave **2.29**.

Completion of the synthesis commenced with the very efficient Hofmann-type rearrangement of **2.29** to give the cyclic carbamate **2.30** (Scheme 2.7). Formation of the cis-fused *N*-methylpyrrolidine ring was then effected in one experimental operation by treatment of **2.30** with lithium aluminum hydride in refluxing THF. Swern oxidation of **2.31** provided a ketone, which was immediately converted into the enolate under O-alkylation conditions and reacted with MeI to afford enol ether **2.32**. Finally, acid-catalyzed ketal and MOM ether hydrolysis proceeded, without disruption of the enol ether, to give (+)-cepharamine (**2.33**) in 97 % yield.

Scheme 2.7. Completion of (+)–cepharamine

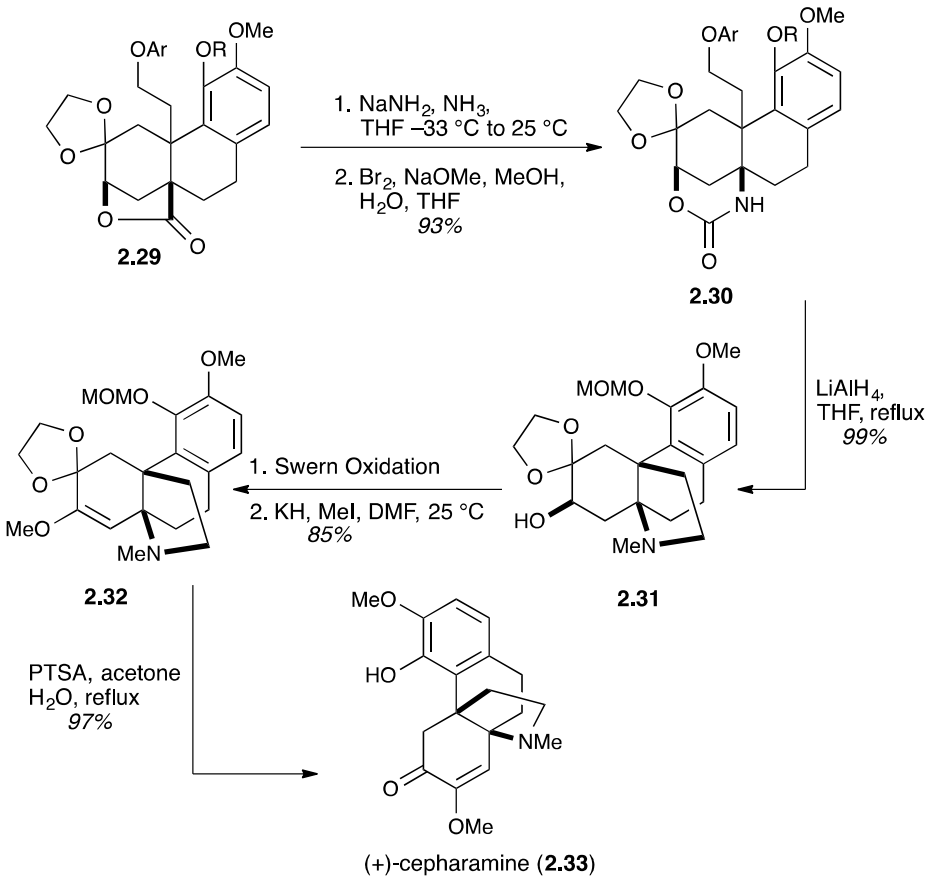

Although the authors mentioned the structural similarities between (–)-morphine (**1.1**) and (+)-cepharamine (**2.33**) and expressed interest in probing the biological activity of this unnatural HB alkaloid, there have been no reports of these biological studies.

2.2.2 Reisman synthesis of (–)-8-demethoxyrunanine

More recently, the Reisman[12] group reported a unified strategy for the enantioselective syntheses of the HB alkaloid (–)-8-demethoxyrunanine (**2.44**), and the structurally related alkaloids, (–)-cepharatine A, C, and D. This strategy called for the construction of an appropriate azapropellane skeleton, followed by systematic introduction of the peripheral oxidations, as dictated by the target compound.

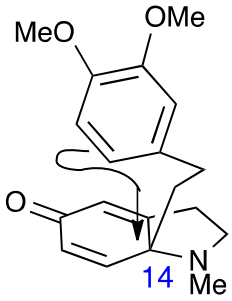

The authors envisioned formation of the azapropellane skeleton from the intramolecular Friedel-Crafts reaction of a dihydroindolone substrate, such as the one depicted in Figure 2.3.

Figure 2.4. Predicted electrophilic aromatic substitution in the Friedal-Crafts reaction.

The regioselectivity of the Friedal-Crafts reaction would be controlled by the steric factors driving the electrophilic aromatic substitution, directing substitution to the less sterically encumbered para-position. The stereocenter at C14 was to be installed using the previously developed[97] stereoselective alkylation of a mono-ketal-derived *N*-

tert-butanesulfide (**2.36**, Scheme 2.8) with an organometallic reagent, such as Grignard **2.37**.

The desired *N*-*tert*-butanesulfinimine, **2.36**, was prepared from commercially available phenol **2.34** (Scheme 2.8). Phenol **2.34** was dearomatized with the hypervalent iodide reagent, PIDA to give an intermediate cyclohexadienone, which was trapped as the *N*-*tert*-butanesulfinimine, **2.36**. Addition of Grignard reagent **2.37** at low temperatures followed by an *in situ N*-methylation provided sulfinamide **2.38**, which was isolated as a single diastereomer, 96:4 dr, in 77 % yield. The authors noted that the hydrolysis of the dimethyl acetal occurs during the mildly acidic workup without detectable quantities of undesired dienone-phenol rearrangement products.

Scheme 2.8. Synthesis of cyclohexadienone **2.38**.

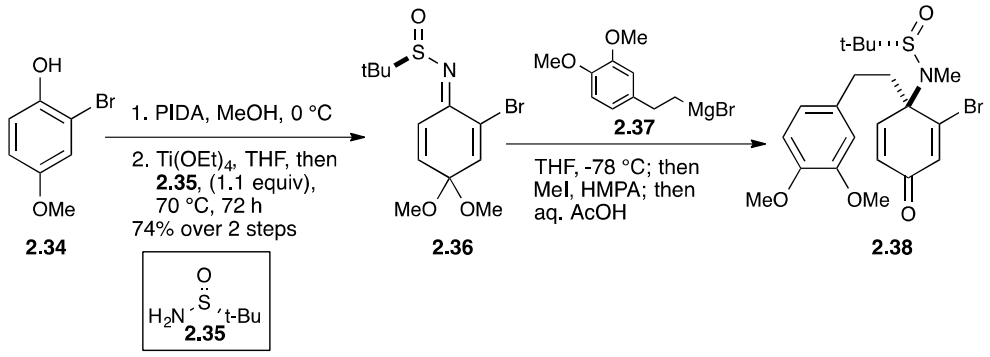

The requisite pyrrolidine ring was constructed in a three-step sequence, beginning with a Pd-catalyzed cross coupling between vinyl bromide **2.38** and ethoxyvinylstannane **2.49** to give enol ether **2.40** in 90 % yield (Scheme 2.9). Brief exposure of **2.40** to 1M HCl in THF at 0 °C resulted in cleavage of the sulfinamide and promoted intramolecular condensation to form an indolone. Chemoselective reduction of the indolone with sodium

borohydride and acetic acid furnished the desired dihydroindolone **2.41**, in 96 % yield over two steps.

Scheme 2.9. Construction of the requisite pyrrolidine ring.

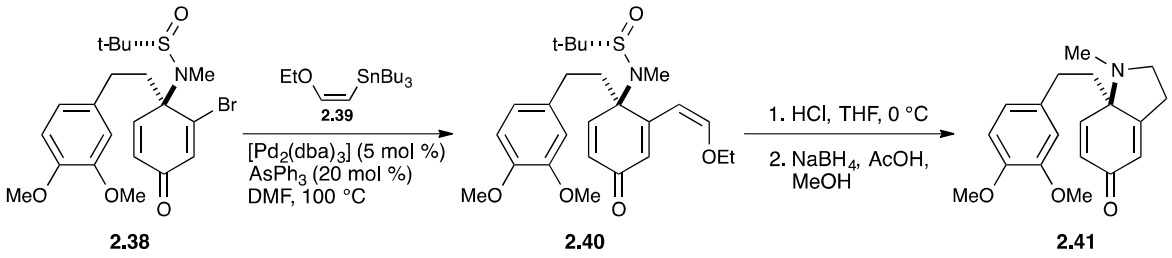

The authors had hoped to perform the pivotal azapropellane-forming Friedel-Crafts reaction by treating **2.41** with a Lewis acid. Unfortunately treatment of **2.41** with the Lewis acid BF_3•OEt_2 led low to moderate yields of the desired azapropellane. Happily, turning to the use of a strong Brønsted acid, such as TfOH, markedly increased the yields to 97 % (Scheme 2.10).

Scheme 2.10. Completion of the synthesis of (–)-(8)-demethoxyrunanine (**2.44**)

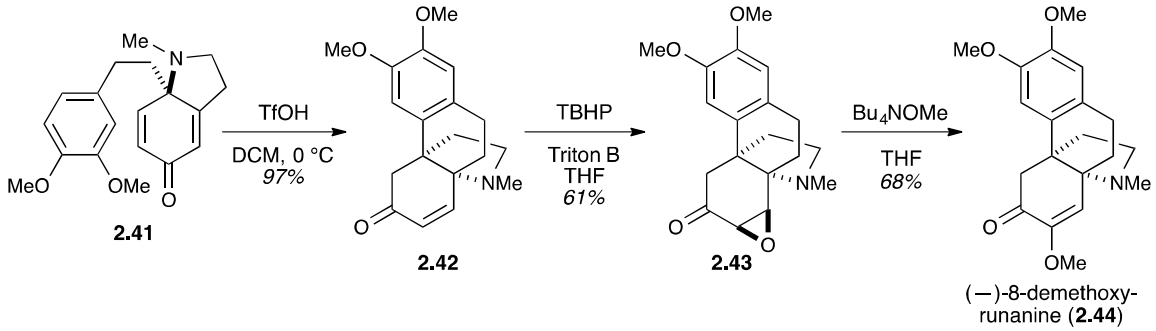

With the azapropellane core formed, the authors installed the C7 methoxy group by treating **2.42** with *tert*-butylhydroperoxide (TBHP) and Triton B in THF to form the

epoxide **2.43**. It was noted that epoxide **2.43,** was unstable in the presence of silica gel, leading to rearrangement products, therefore Florisil was utilized for the purification of epoxide. Additionally epoxide **2.43** was found to have a strong affinity for rearranging to the cepharatine skeleton **2.51** (Scheme 2.11). Presumably through a nitrogen-assisted epoxide opening, **2.45**, followed by β-elimination to give enol **2.50**, which is subsequently trapped to form the hemiaminal **2.51** bearing the cepharatine skeleton.

Scheme 2.11. Rearrangement of epoxide **2.43** to cepharatine skeleton **2.51**

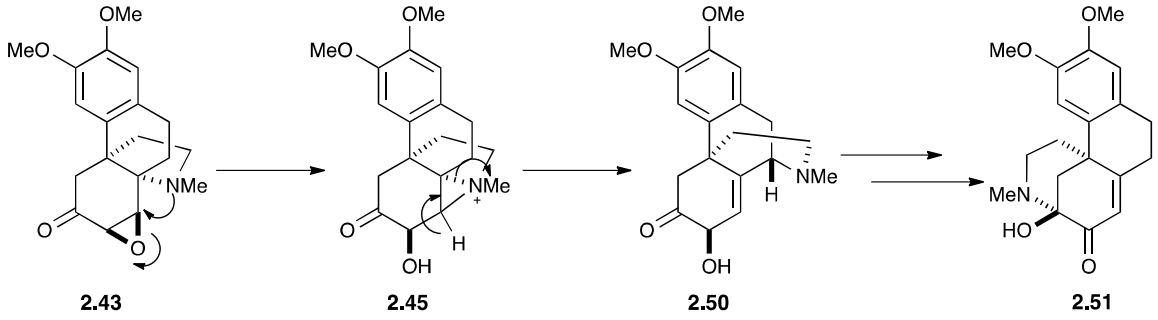

Despite issues with stability, (–)-8-demethoxyrunanine (**2.44**) was afforded from epoxide **2.43** by treatment with tetrabutylammonium methoxide. This concise synthesis provided access to the natural product in 9 steps from the commercially available phenol **2.34**, in a 19 % overall yield. To date this is the shortest reported synthesis of a HB alkaloid however, it is not without limitations.

The formation of indolone **2.41** (Scheme 2.9) required extensive experimentation and all attempts at isolation of the desired *des*-*N*-methyl- indolone resulted in failure, increasing the difficulty for pursuing analogs bearing non-methyl *N*-alkyl groups.

Additionally, there were significant stability issues with epoxide **2.43** during the installation of the C7 methoxy group (Scheme 2.11).

2.2.3 Herzon enantioselective synthesis of (–)-hasubanonine, (–)-runanine, and (–)-delavayine

2.2.3.a Retrosynthetic analysis

Coinciding with the Reisman synthesis of (–)-8-demethoxyrunanine, Herzon and co-workers[13] disclosed a unified route to several HB alkaloids, including the parent compound (–)-hasubanonine (**2.1**), as well as, (–)-runanine (**2.2**), (–)-delavayine (**2.3**), and (+)-periglaucine B.

While slightly longer, the Herzon strategy is more amenable to analog synthesis. This was accomplished through the development of a strategy in which the A and B rings of the hasubanan skeleton are formed through the reaction of a pro-nucleophile, such as **2.53** and the azaquinone **2.52** (Scheme 2.12). The pro-nucleophile **2.53** serves as a branching point for incorporation of the varying arene substitution patterns found in the A ring of the HB alkaloids. The azaquinone **2.52** contains the trioxygenated cyclohexanone fragment common to the C ring of the HB alkaloids as well as the electrophilic sites (labeled a and b) for attachment of **2.53**.

Scheme 2.12. Herzon retrosynthetic plan for analog synthesis.

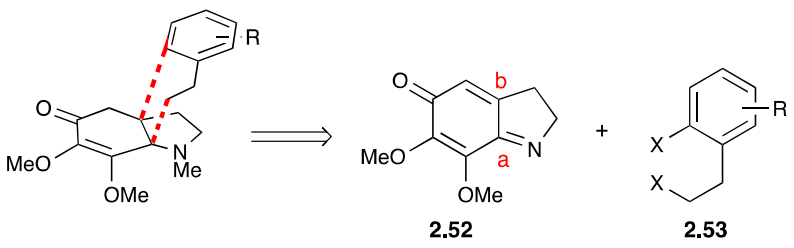

The authors noted that bicyclic azaquinones such as **2.52** are unstable, isomerizing to 5-hydroxyindole (**2.54**) by a proposed tautomerization and a 1,5-hydrogen atom shift, as shown (Scheme 2.13). The authors planned to mitigate this pathway through the transient introduction of a quaternary center on the azaquinone (at position b). The introduction of this quaternary center was to be accomplished by a Diels-Alder reaction of azaquinone **2.55** and 5-trimethylsilylcyclopentadiene **2.56**; a Staudinger reaction would then afford the tetracyclic imine **2.57**. Following bond formation to the imine (position a), the unsaturation required for addition to position b was to be regenerated by a retro-cycloaddition reaction, rendering **2.57** functionally equivalent to **2.52**. Additionally, it was envisioned that the cyclopentene fragment of **2.57** would provide a handle for stereocontrol through an enantioselective Diels-Alder reaction.

Scheme 2.13. Proposal for mitigating rearrangement of **2.52**

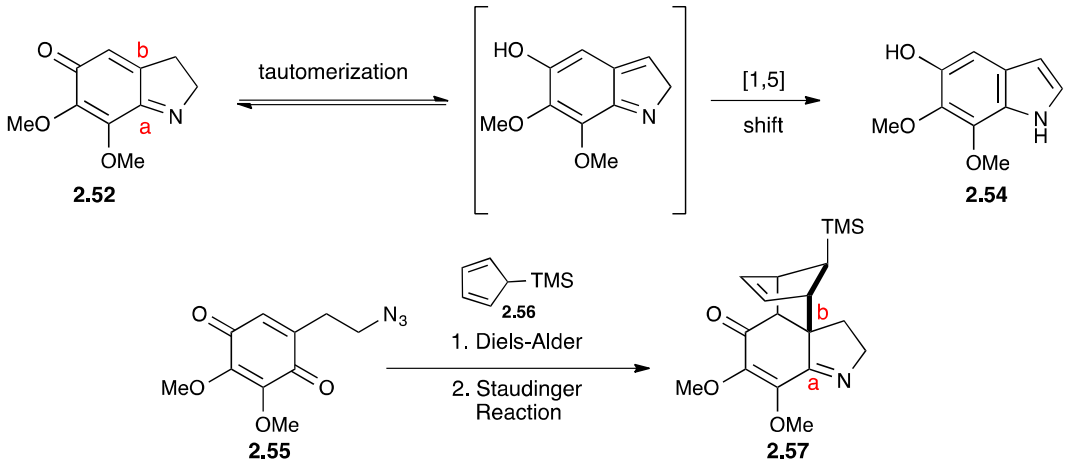

*2.2.3.b Synthesis of Diels-Alder adduct **2.57***

The synthesis of the key Diels-Alder adduct **2.57** began with the preparation of 5-(2-azidoethyl)-1,2,3-trimethoxybenzene (**2.58**) which was available in three steps from commercial reagents. Subsequent oxidation of **2.58** with hydrogen peroxide in formic acid afforded quinone **2.55** in a 48 % yield (Scheme 2.14). The regio- and stereoselective Diels–Alder reaction of **2.55** with 5-trimethylsilylcyclopentadiene (**2.56**) was mediated by the protonated form of the Corey–Bakshi–Shibata oxazaborolidine **2.59**, producing the *endo* adduct in 93 % ee. Staudinger reduction of the Diels-Alder adduct provided the imine **2.57**.

Scheme 2.14. Synthesis of key Diels-Alder adduct **2.57**.

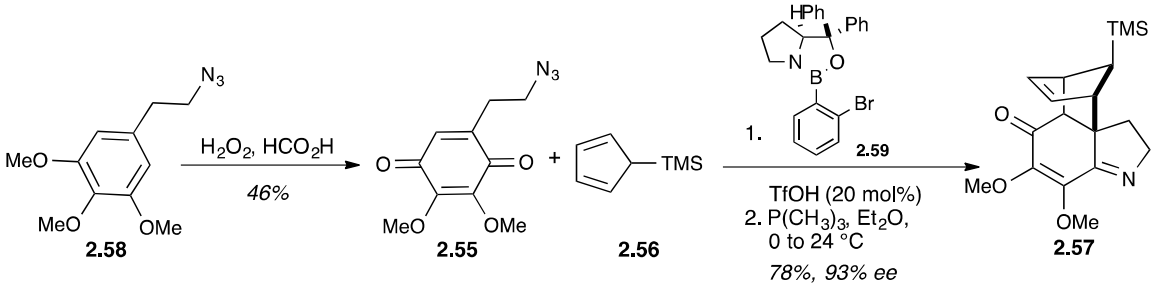

At this point, alkylation of imine **2.57** with the appropriately substituted A-ring appendage would provide access to several HB alkaloids as well as set the crucial C14 stereocenter. However, **2.57** needed to first be activated toward addition to the carbon–nitrogen π–bond (Figure 2.4). This was done by treatment with methyl triflate at – 60 °C.

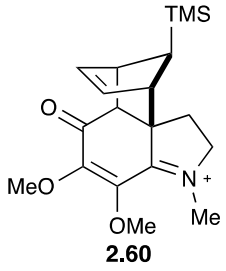

Figure 2.5. Activated iminium **2.60**

The temperature profile of this step was found to be critical; lower temperatures resulted in incomplete methylation, whereas further warming promoted rapid retro-cycloaddition of the iminium salt **2.60**. With the optimal activation conditions determined the syntheses of (–)-hasubanonine (**2.1**), (–)-runanine (**2.2**), (–)-delavayine (**2.3**), and (+)-periglaucine B could be completed.

*2.2.3.c Completion of (–)-hasubanonine (**2.1**), (–)-runanine (**2.2**), and (–)-delavayine*

Scheme 2.15. Completion of the synthesis of (–)-hasubanonine (**2.1**)

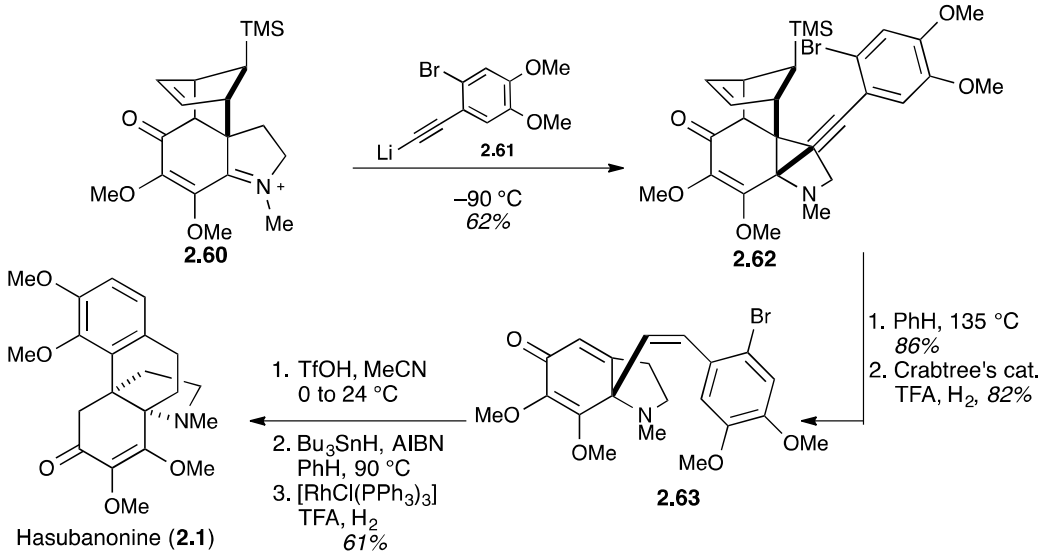

The completion of the synthesis of (–)-hasubanonine (**2.1**) (Scheme 2.15) commenced with the treatment of the iminium salt **2.60** with the acetylide **2.61** at – 90 °C, resulting in the formation of the 1,2-addition product **2.62** in 62 % yield as a single detectable diastereomer (verified by ^{1}H NMR analysis). The relative stereochemistry of the addition product **2.62** was assigned by elaboration to (–)-hasubanonine (**2.1**) and X-ray crystallography of later intermediates. Retro-cycloaddition of **2.62** was achieved, in

an 86 % yield by heating in toluene at 135 °C. Chemoselective hydrogenation using Crabtree's catalyst furnished the cis alkene **2.63**. A three-step sequence comprising acid-mediated cyclization, de-bromination, and hydrogenation provided synthetic (–)-hasubanonine (**2.1**). This synthetic pathway was used to prepare both (–)-runanine (**2.3**) and (–)-delavayine with minimal modifications (Scheme 2.16)

Scheme 2.16. Completion of (–)-runanine (**2.3**) and (–)-delavayine (**2.4**).

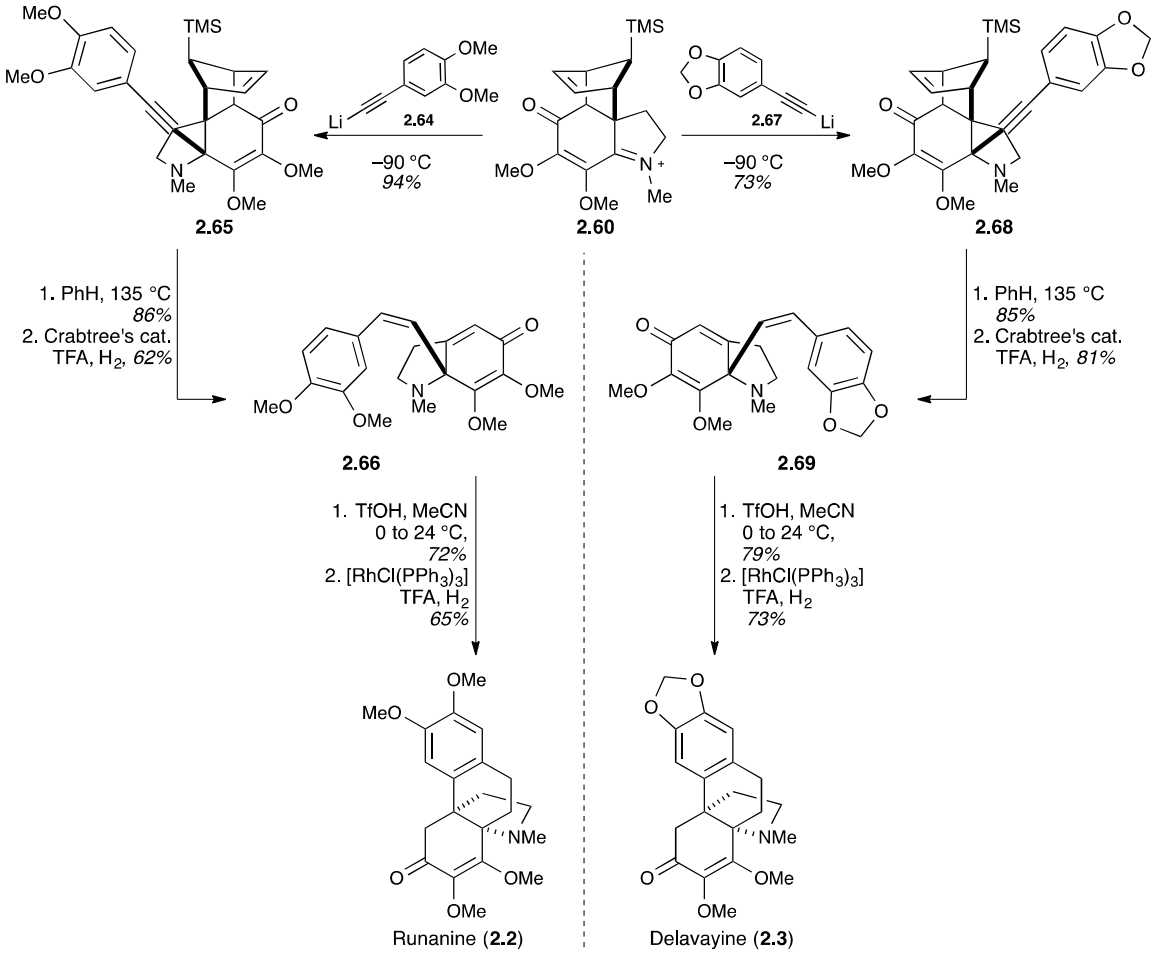

Again, the key iminium salt **2.60** was reacted with the acetylide bearing the appropriate A-ring substitutions (for (–)-runanine, **2.64** and for (–)-delavayine, **2.67**).

Retro Diels-Alder followed by reduction with Crabtree's catalyst gave intermediates **2.56** and **2.69**. These *cis* alkenes were each treated with triflouroacetic acid in MeCN, followed by reduction to yield the natural products in 5 steps from the common intermediate iminium salt **2.60**.

2.2.3.d Completion of (+)- periglaucine B

(+)-Periglaucine B bears the same A ring substitution as (–)-delavayine and therefore was directly accessed from the *cis* alkene intermediate **2.69** (Scheme 2.17) through a formal olefin hydration/conjugate addition sequence.

Scheme 2.17. Completion of (+)-periglaucine B

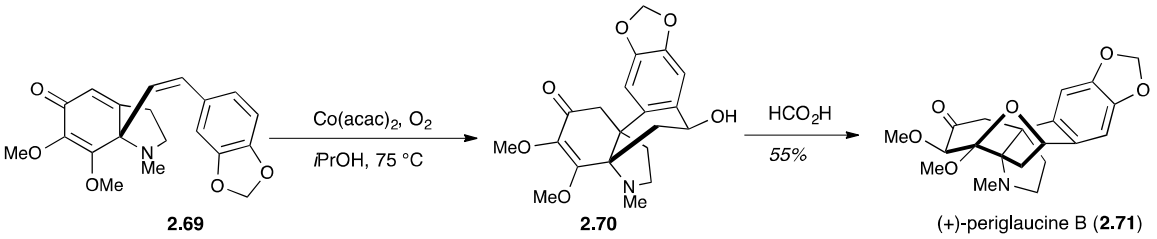

After surveying a number of conditions to effect this transformation, the authors found that the desired hydration product **2.70** could be formed by heating a mixture of **2.69** and cobalt bis(acetylacetonate) in isopropanol under an atmosphere of oxygen. The diastereoselectivity in the hydration step was 2.2:1 in favor of **2.70**. Addition of excess formic acid directly to the reaction mixture promoted cyclization of **2.70**, providing (+)-periglaucine B (**2.71**) in 55 % yield.

These represent the first enantioselective syntheses of (–)-hasubanonine (**2.1**), (–)-runanine (**2.2**), (–)-delavayine (**2.3**), and (+)-periglaucine B (**2.71**). The route to each

target proceeds in ten to twelve steps from commercially available reagents. Like the Reisman synthesis this route relies on substrate control for the formation of the stereogenic C14 center. Additionally the *N*-methyl is required for activation of iminium **2.60**, limiting the type of *N*-substituted analogs that can be prepared.

The authors expressed interest in studying the biological activities of these compounds and recently the results of cytotoxicity studies in human gastric cancer cells were published revealing that (–)-hasubanonine (**2.1**) and (–)-runanine (**2.2**) were sub-micromolar inhibitors of cancer cell growth.[98] However, to date no studies on the analgesic properties of the prepared HB alkaloids have been disclosed.

2.3 Biological Implications of Structural Similarities[**]

The resurgence in interest in the HB alkaloid is not only based the synthetic challenges associated with the construction of the HB skeleton, but is also due to the structural resemblance to the morphinan alkaloids.[9] As discussed in the previous section, Schulz and co-workers noted that the natural configuration of the HB alkaloids is "enantiomeric" to morphine, and suggested that the unnatural enantiomers of the HB alkaloids might demonstrate analgesic activity. However, no biological activity studies of (+)-cepharamine have been reported, nor have any analgesic studies been conducted on the other more recently, prepared HB alkaloids. Furthermore only limited studies on isolated alkaloids have been conducted.

[**] This section is part of a NIH R21-R33A1 grant proposal, submitted November 2012

2.3.1 Opioid receptor binding studies

In 2010, Quinn and co-workers reported the first study examining the affinity of natural HB alkaloids toward the δ opioid receptor.[10] Out of the limited number of compounds they investigated, longanine (**2.5**) was found to be the most potent binder to DOR (IC_{50} = 700 nM). In comparison, sinococuline **2.72**, a known "enantiomeric" morphinan alkaloid, has an IC_{50} of 37 μM for the same receptor, Figure 2.5. This IC_{50} value is in agreement with the previous observation that the binding affinity of (+)-morphine is much weaker than the natural enantiomer;[99–101] highlighting the specificity of the opioid receptors, with respect to the spatial placement of the required functional groups.

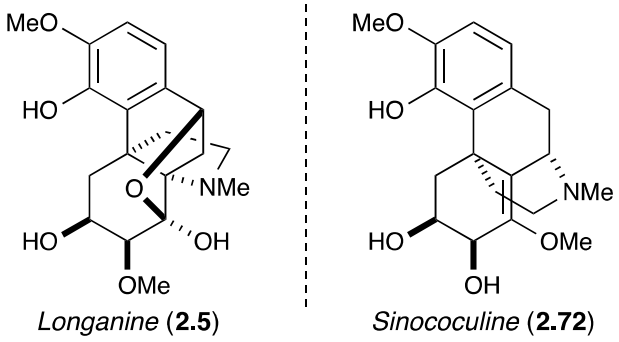

Longanine (**2.5**) *Sinococuline* (**2.72**)

Figure 2.6. Structural similarities of longanine (**2.5**) and known morphinan enantiomer sinococuline (**2.72**).

2.3.2 Receptor binding analysis

Since all of the tested compounds in Quinn's study were isolated from natural sources, they are of the opposite absolute configuration and therefore conclusions cannot be drawn about the analgesic properties of the *ent*-HB alkaloids from these studies. Figure 2.6, illustrates support for the hypothesis that *ent*-HB alkaloids will bind to the

opioid receptors. Here we show the energy-minimized structures of (–)-morphine (**1.1**) (Figure 2.6 (a)), and *ent*-hasubanonine (Figure 2.6 (b)). The aromatic A ring of each compound is oriented down and the *N*-methyl group of each (pink bond) to the left. As can be seen the pharmacophore region of morphine (blue bonds) aligns remarkably well with the A, B, and D rings of *ent*-**2.73** (blue bonds). It should also be noted that the *N*-methyl groups of each compound are also in a similar spatial arrangement.

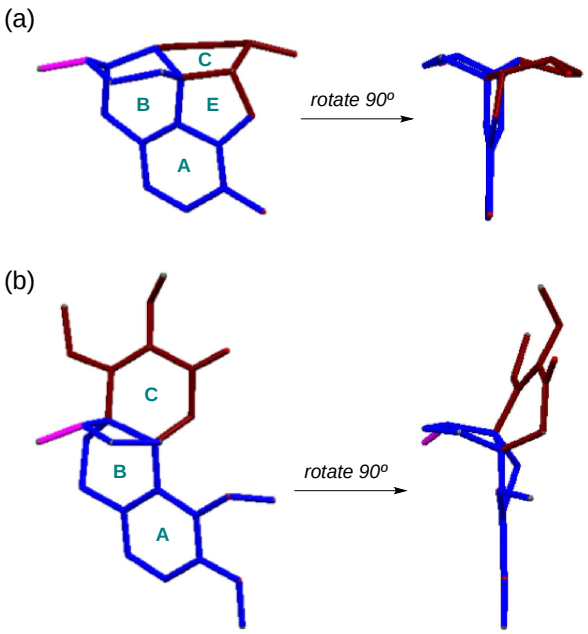

Figure 2.7. (a) Energy-minimized structure of (–)-morphine (**1.1**). (b) Energy-minimized structure of *ent*-hasubanonine .

The largest difference between the two structures in Figure 2.6 is found in the position of the C rings (red bonds). Upon rotating the two structures 90º so they are viewed down the edge of the A ring, it becomes clear that the C ring of *ent*-hasubanonine is oriented at about a 60º angle relative to the C ring of morphine. Previous studies on morphine derives showed that modifications to the C ring are generally well tolerated and

that these modifications can give rise to the receptor selectivity often observed with synthetic derivatives.[102–105] This large change in C ring orientation observed with *ent*-hasubanonine could give rise to receptor selectivity due to new interactions that are not possible with morphine-derived ligands.

We are particularly interested in developing selective ligands for DOR, as antagonists of DOR have been indicated as promising therapies for neuropathic pain without the adverse side effects associated with MOR.[73] With the recent disclosures of opioid receptor crystal structures we are now able to perform docking studies to better predict binding interactions that will lead to selectivity.

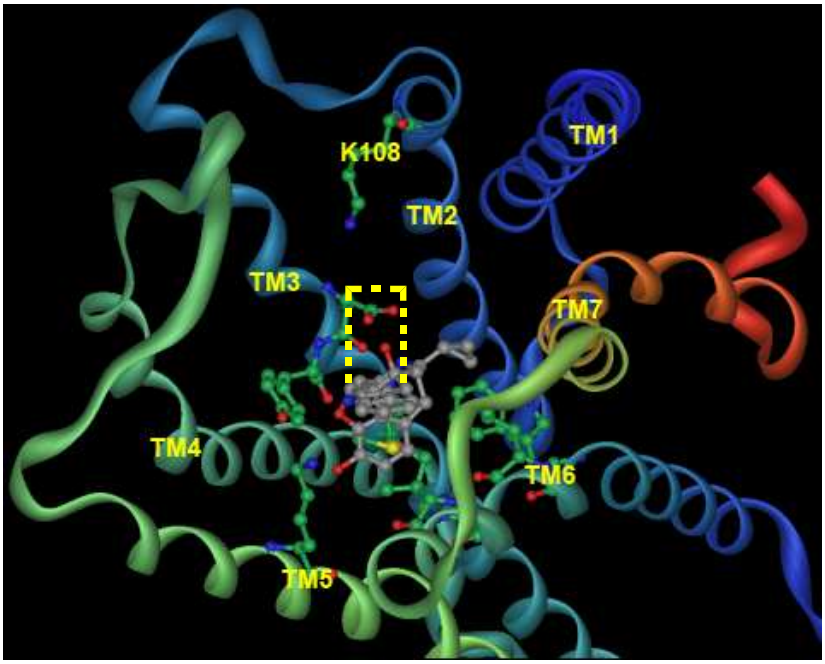

Figure 2.8. Crystal structure of DOR with naltrinole bound, *Adapted from PDB file 4EJ4*.

Figure 2.7 shows the interactions of the antagonist naltrinole (grey bounds), with DOR.[61] The dashed yellow lines represent the approximate orientation of the HB alkaloid C ring, if *ent*-hasubanonine was bound in the DOR. The HB alkaloid C ring is positioned closer to TM2 and TM3, whereas, the indole ring of the bound ligand is positioned closer to TM6 and TM7. Sequence analysis[106] of the DOR reveals K108 to be an interesting target for designing ligands that are selective for this receptor. This residue is an asparagine in MOR and a valine in KOR. Thus, it is reasonable to propose that an OR ligand capable of projecting an acidic functional group toward K108 would be more selective for binding the DOR.

2.3.3 Closing Remarks

Decades after their discovery, the HB alkaloids are still of interest to the synthetic community. While synthetically challenging, the primary reason for this interest has been due to the structural similarities to the morphinan alkaloids. There have been numerous synthetic studies on the HB alkaloids as well as recent disclosures of enantioselective syntheses but there have been no biological studies performed; nor have any unnatural analogs of the HB alkaloids been prepared and tested.

As discussed in Chapter One, there remains a significant need for the identification of novel and selective opioid receptor ligands. With the crystal structures of each of the opioid receptors finally available, we are now poised to develop such novel ligands and propose that the *ent*-hasubanan alkaloids and their derivatives would be ideal candidates. The remainder of this dissertation will discuss our strategy for the synthesis

of HB alkaloid analogs, particularly focusing on our efforts toward the aza[4.4.3]propellane HB core.

CHAPTER 3

PROGRESS TOWARD THE HB ALKALOID CORE

3.1 Synthetic Strategy

3.1.1 Retrosynthetic analysis

Our planned route (Scheme 3.1) differs from previous syntheses in that the formation of the C12–C13 and C14–N bonds are integrated with the formation of the B and D rings. This strategy is accomplished through the iodine(III) mediated oxidative dearomatization of an intermediate such as **3.2**, which in turn, arises from a Pd catalyzed cross coupling of aryl-halide **3.3** and appropriate coupling partner, **3.4**. Intermediate **3.2** bears both the C ring (**3.3**) and A ring (**3.4**) moieties of the final product allowing us to access a majority of the HB alkaloids through this common intermediate

Scheme 3.1. Oxidative dearomatization for the formation of the HB core.

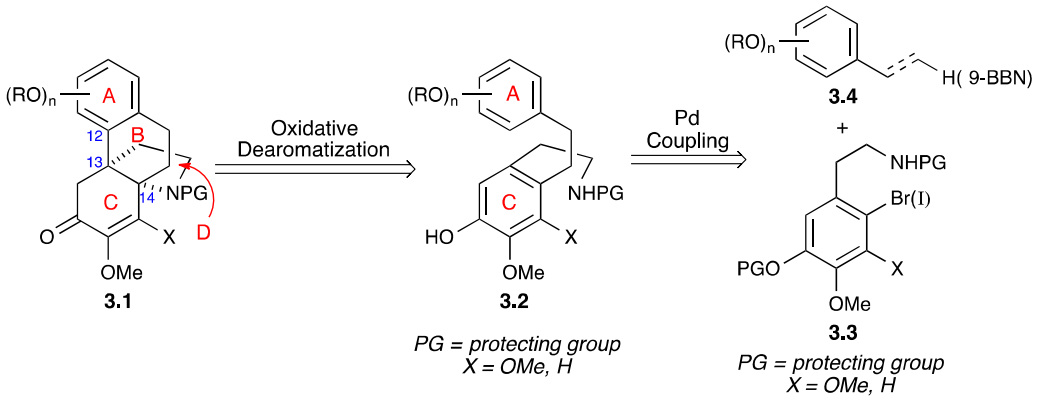

As discussed in Chapter Two, structural differences between the HB alkaloid family members are primarily found in the oxygen substitutions of the aromatic A ring (for examples see Figure 2.1), while little variation occurs in the C ring. Based on this, we hypothesized that the same starting material, gallic acid or isovanillin, could be used for all of the HB analogs, whereas the A ring would come from a benzaldehyde (**3.5**, Scheme 3.2) with varying substitutions.

Scheme 3.2. Construction of the common intermediate **3.2**.

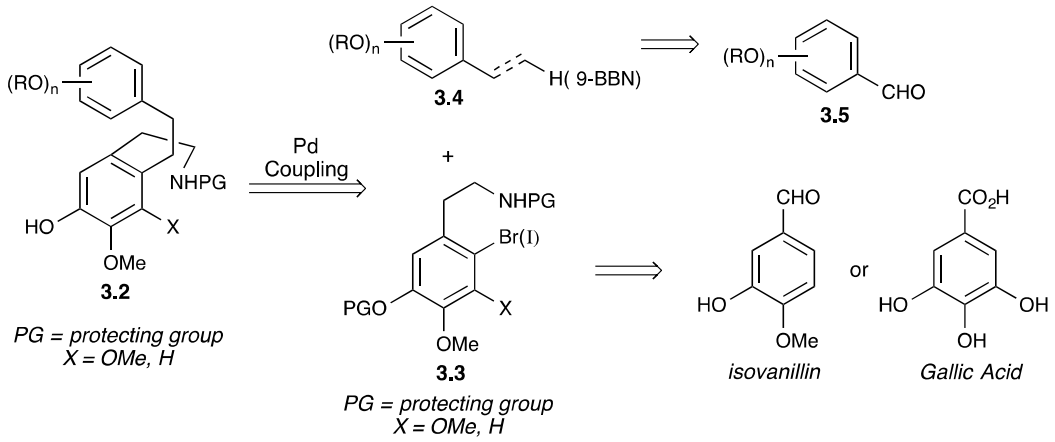

3.1.2 Possible dearomatization scenarios

The proposed dearomatization of **3.2** could lead to one of two possible scenarios (Scheme 3.3). The first involves initial attack by the nitrogen to give fused bicycle **3.6**. The use of hypervalent iodide for the formation of C–N bonds has been investigated,[107–111] however, generally these reactions lead the formation of amine spirocycles, with limited precedence for the formation of fused bicycles,[112] in our case we believe the five membered fused bicycle **3.6**, will be preferential to a less stable four membered amine

spriocycle.[112] Assuming the desired bicycle is formed, addition of a Lewis acid[113–115] to **3.6** would then result in conjugate addition of the electron-rich aryl ring to provide **3.1**; similar to the method used by Reisman, except, we anticipated being able to perform this sequence in a single pot without purification of the bicyclic intermediate.

Scheme 3.3. Possible scenarios for the dearomatization of **3.2**.

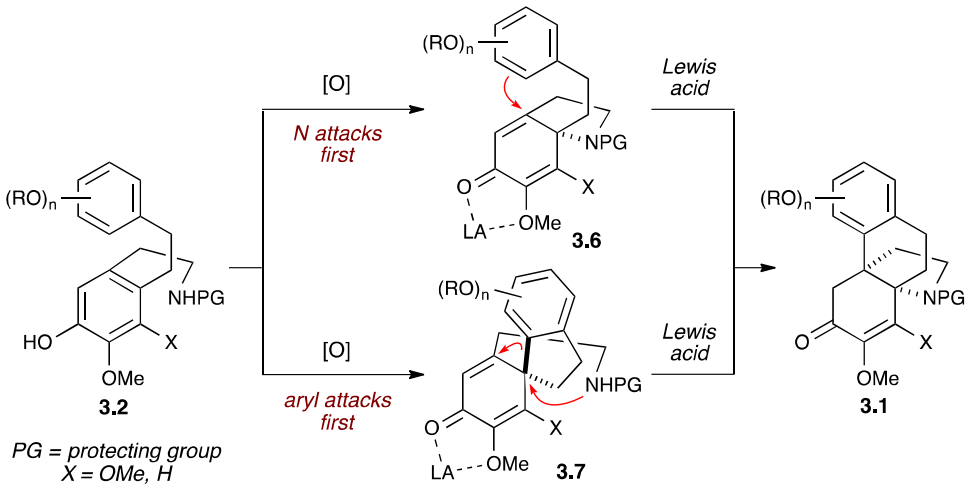

In the other dearomatization scenario, the aryl ring serves as the initial nucleophile leading to the formation of spirocycle **3.7**. Treating **3.7** with a Lewis acid would then promote migration of the arene together with addition of the proximal nitrogen. This sequence would also result in the formation of tetracycle **3.1**. While similar migrations of arene moieties have been reported to occur in the presence of Brønsted acids,[116–118] all have resulted in the formation of biaryl products. To the best of our knowledge, a nucleophile has not been used to trap the cationic intermediate generated during the migration. To test the feasibility of the proposed regioselective Lewis acid

promoted aryl migration, we investigated a simple model system (Scheme 3.4).[††] Treating phenol **3.8** with 1 equiv. of PIDA, followed by BF_3•OEt_2 smoothly promoted the desired rearrangement. Importantly the only product observed by NMR was the one in which aryl ring, A, had migrated to the olefin without the methoxy group, **3.10**. In this particular case, aromatization by proton loss was too facile to allow the intermediate carbocation to be trapped by a nucleophile. Fortunately, aromatization is not possible when the aryl group in **3.7** rearranges.

Scheme 3.4. Regioselectivity of LA promoted aryl migration.

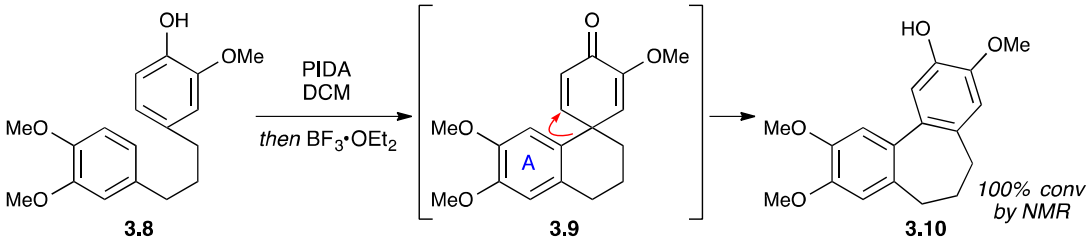

3.2 Synthesis of dearomatization substrate

Confident in our synthetic strategy we set out to construct the intermediate **3.2** for our dearomatization studies. The biaryl **3.2** (Scheme 3.1) is composed of the A ring, **3.4**, and C ring, **3.3** connected through an ethane bridge. Initially we proposed the use of a Pd catalyzed Sonogashira cross coupling reaction to connect **3.3** and **3.4**. Our hope was to utilize the newly formed alkyne as an additional point of derivatization. The A ring moiety was to be accessed from a Corey-Fuchs olefination of a benzaldehyde bearing

[††] Dr. Rodolfo Tello-Aburto conducted this experiment.

appropriate substitutions, whereas the C ring was to be derived from either isovanillin or gallic acid. The synthetic studies began with the construction of aryl halide **3.3** from gallic acid.

3.2.1 Construction of C ring moiety from gallic acid

3.2.1.a Demethylation attempts

Control of the regiochemistry during halogenation was to be achieved through selective protection of a single *meta*-hydroxyl group in gallic acid. The initial strategy employed to achieve this desymmetrization was the mono-demethylation of the symmetrically substituted trimethoxy-methyl gallate,[119] **3.12** (Scheme 3.5).

Scheme 3.5. Selective demethylation of trimethoxy-methyl gallate **3.12**.

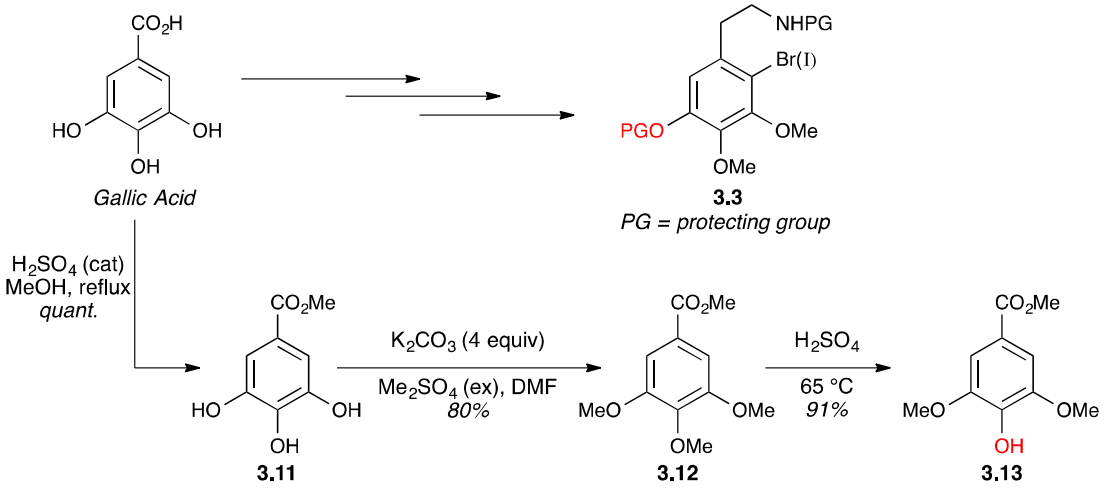

To accomplish this, gallic acid was transesterified to give methyl gallate, **3.11**, which was further treated with an excess of potassium carbonate and dimethyl sulfate to give the trimethylated product, **3.12**. Unfortunately, in our hands, only the *para*-demethylated

product was isolated when **3.12** was treated with sulfuric acid, and we were unable to afford the desired *meta*-demethylation, even upon switching to Lewis acids.[119]

3.2.1.b Mono-benzylated substrate

With the lack of success in the demethylation strategy, our attention turned to the selective protection of methyl gallate (Scheme 3.6). Formation of the orthoformate **3.14**[120] allowed for mono-benzylation of the 5-hydroxyl group which was accomplished through deprotonation of **3.14**, with potassium carbonate followed by treatment with benzyl bromide. Hydrolysis of the orthoformate in **3.15** gave the mono-benzylated methyl gallate, **3.16**. Alternately, we found that methyl gallate could be desymmetrized in a single pot (Pathway B, Scheme 3.6) via catechol boronate[121] formation followed by benzylation and hydrolysis (Scheme 3.6, pathway B), giving **3.16** in a 68 % yield.

Scheme 3.6. Desymmetrization of methyl gallate.

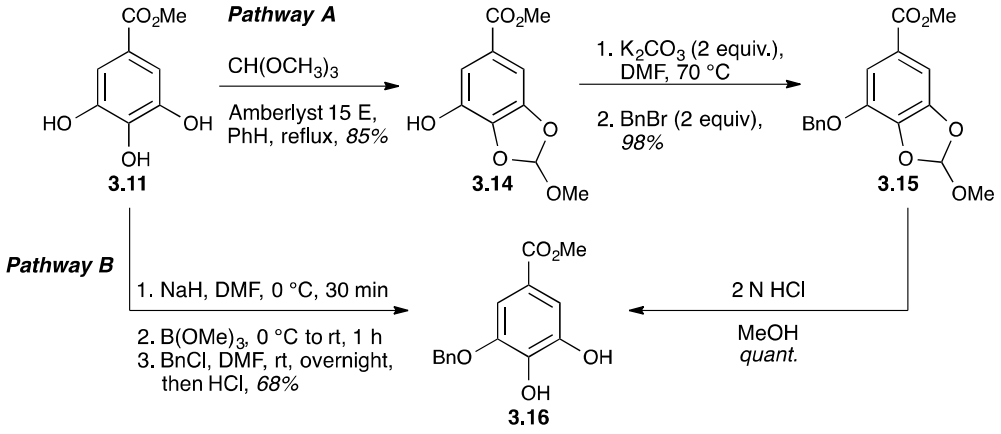

The selective bromination of **3.16** with 1,3-dibromo-5,5-dimethylhydantoin, DBDMH,[122] gave mono-brominated arene **3.17** in an 86 % yield (Scheme 3.7). The

regioselectivity of this bromination was verified by NOE correlations between the aromatic proton and the benzylic protons of the benzyl ether. The hydroxyl groups of **3.17** were then dimethylated in the presence of excess potassium carbonate and dimethyl sulfate to give **3.18**. It should be noted that **3.16** could be methylated prior to bromination, however it was found that the yields were substantially higher if the bromination was performed prior to the methylation.

Scheme 3.7. Regioselective bromination of **3.16**.

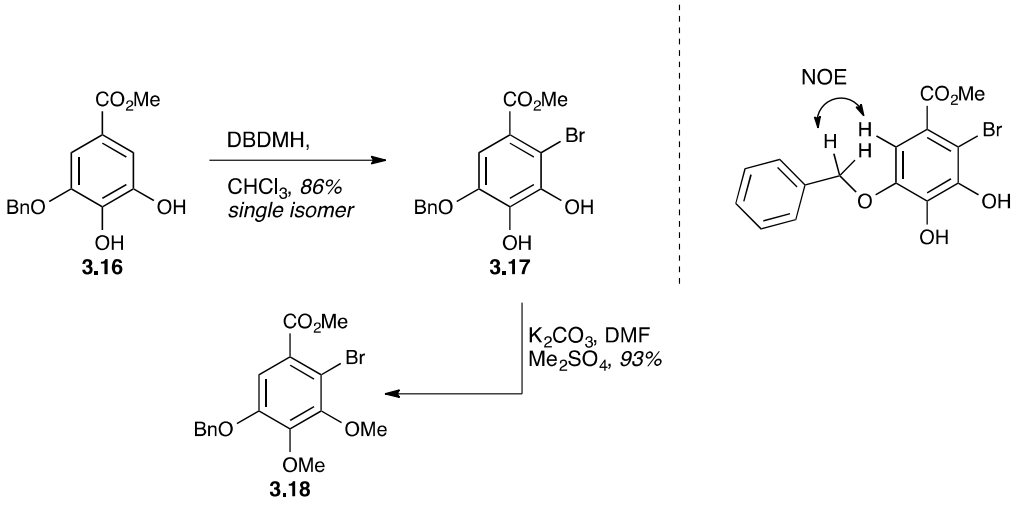

3.2.2 Sonogashira coupling strategy

3.2.2.a Attempted coupling of methyl benzoate derivative

At this point, we were ready to attempt the proposed Sonogashira coupling to connect the A and C ring fragments. A Corey-Fuchs olefination was performed on

commercially available 4-methoxybenzaldehyde to produce the A ring containing alkyne **3.21** (Scheme 3.8).

Scheme 3.8. Corey-Fuchs olefination of 4-methoxybenzaldehyde.

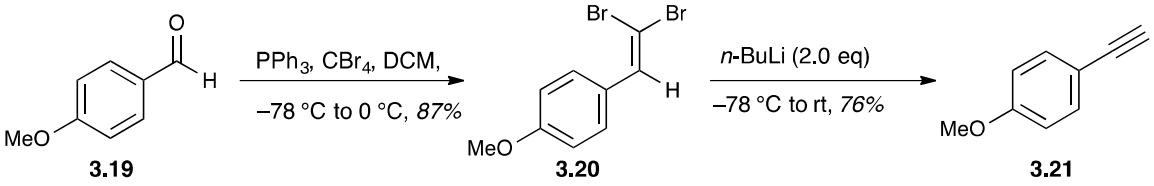

Aware of the potential difficulties associated with oxidative addition to electron rich aryl-halides,[123,124] we were not surprised that our initial conditions led to dimerization of the alkyne (Table 3.1, entry 1).

Table 3.1. Attempts at Sonogashira Coupling.

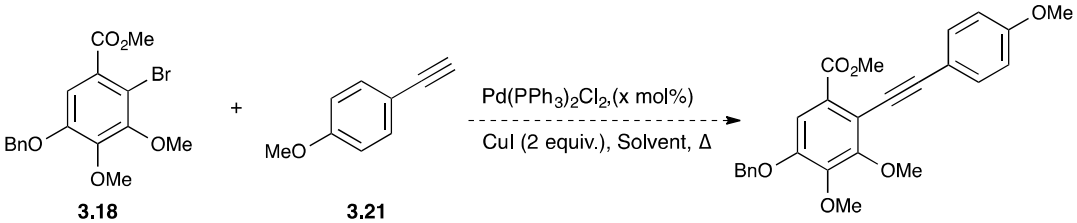

Entry	Catalyst Loading	Solvent	Δ, time
1	2 mol %	Et_2NH	60 °C, 16 h
2	2 mol %	Et_2NH	µW, 60 °C, 10 min
3	5 mol %	Et_2NH	µW, 80 °C, 10 min
4	10 mol %	Et_2NH	µW, 80 °C, 20 min
5	2 mol %	Et_3N	µW, 80 °C, 10 min
6	5 mol %	Et_3N	µW, 100 °C 20 min
7	10 mol %	Et_3N	Reflux, 16 h

However, we were surprised to find that the desired coupling failed regardless of catalyst loading and the use of μW or prolonged heating.[125] The starting material **3.18** and homodimers of alkyne where the only products isolated.

3.2.2.b Attempted coupling of benzylic nitrile derivative

The consistent isolation of the starting material, **3.18**, confirmed our suspensions about the difficult nature of oxidative addition into this electron rich aromatic ring. We sought to perturb the electronics, and reduce some of steric bulk around the Ar–Br bond by converting the ester into a benzylic nitrile (Scheme 3.9). A benzylic nitrile was chosen as it could be readily converted into the ethanamine present in our dearomatization precursor **3.2**.

Scheme 3.9. Attempted Sonogashira coupling of nitrile **3.24.**

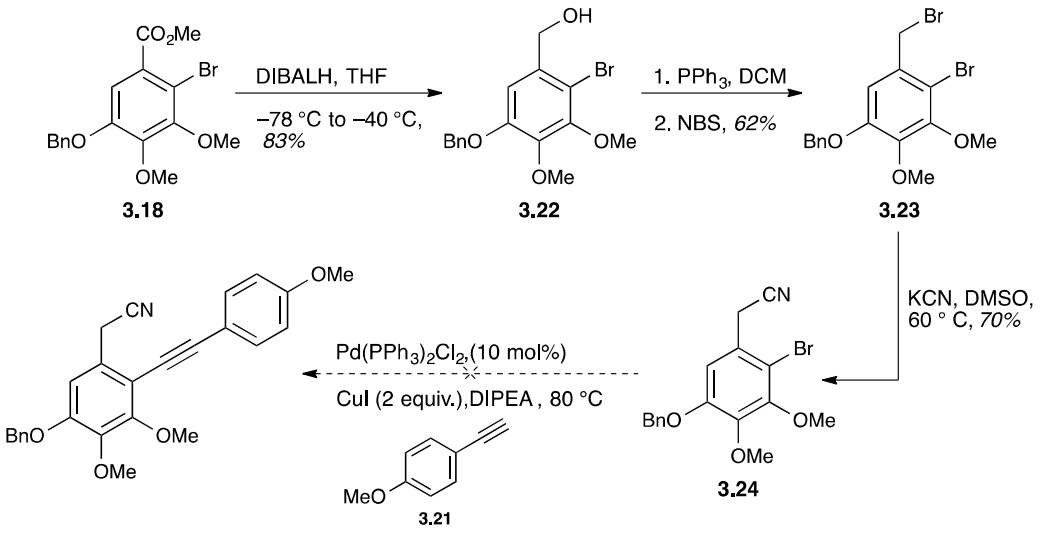

The careful reduction of aryl-bromide **3.18** afforded the benzylic alcohol, **3.22**. Monitoring of the temperature during this reaction was crucial as increased reaction

temperatures led to dehalogenated products. An S_N2 displacement of the intermediate benzylic bromide **3.23**, gave nitrile **3.24**, which unfortunately also proved to be incompatible with Sonogashira coupling.

In additional efforts to increase the efficiency of oxidative addition we exchanged the Ar–Br for a more labile Ar–I bond. Originally a formal Finkelstein reaction, involving bromine-idodine exchange, was proposed for converting aryl bromide **3.18** to an aryl iodide, however, all attempts were unsuccessful in performing this transformation and instead, silver trifluoroacetate was employed to install the Ar–I (Scheme 3.10).

Scheme 3.10. Preparation of aryl iodide **3.26**.

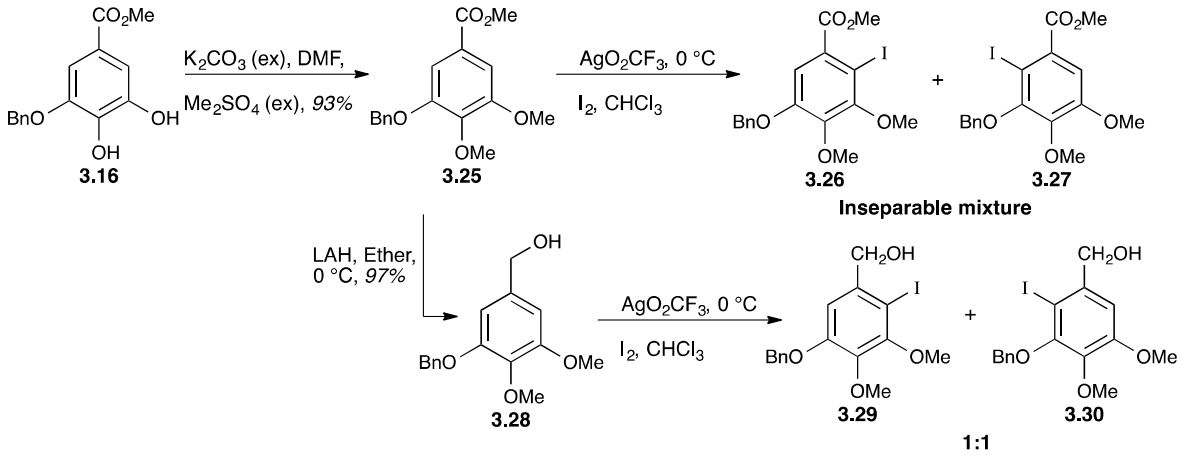

Benzoate **3.16** was dimethylated and treated with silver trifluoroacetate and iodine in chloroform at 0 °C, giving an inseparable mixture of isomers. Fortunately, introduction of the Ar–I on the benzylic alcohol **3.28** yielded a separable mixture, however, no selectivity was observed, with a 1:1 mixture of isomers isolated.

We sought to resolve the regioselectivity issues by employing a bulkier silyl group on the C3-hydroxyl (Scheme 3.11). Methyl gallate was refluxed with triethylorthoacetate,[‡‡] and amberlyst 15E in benzene to give **3.31** in a 76 % yield. The free hydroxyl group of **3.31** was then protected as the TIPS ether; reduction of the benzoate ester with LAH, followed silver trifluoroacetate promoted iodination gave benzylic alcohol **3.34**. Consecutive S_N2 displacements on the benzylic carbon afforded benzylic nitrile **3.35**. Disappointingly though, **3.35**, was also inactive toward Pd oxidative addition.

Scheme 3.11. Preparation of aryl iodide **3.35**.

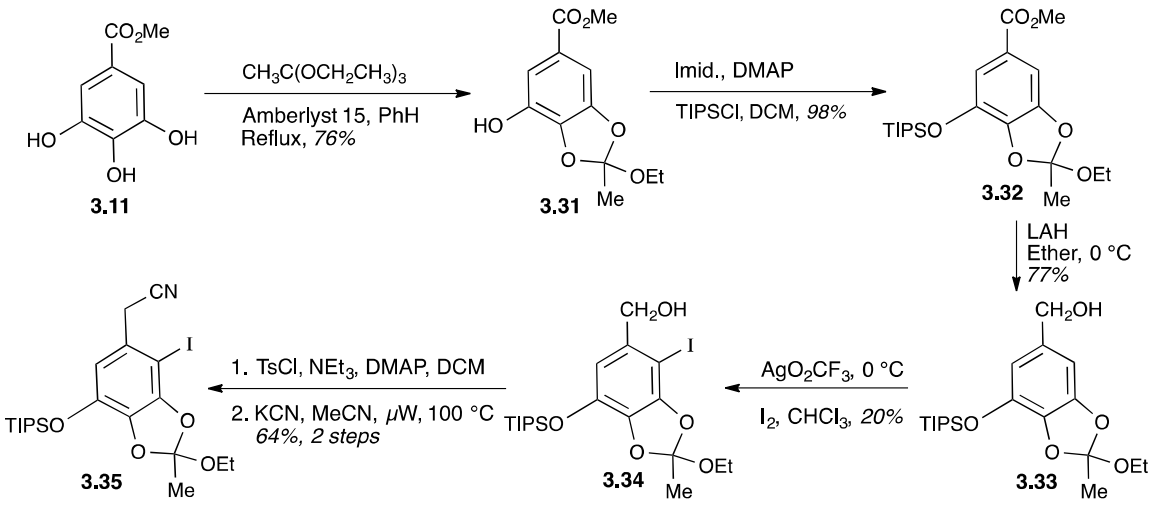

[‡‡] The methyl orthoformate derivative was found to be unstable to iodination conditions and premature removal of the group led to substantial purification issues.

3.2.3 Construction of C ring moiety from isovanillin

At this juncture, we decided to modify our synthetic plan and construct the C ring from isovanillin. The absence of the *ortho*-methoxy group was thought to alleviate the oxidative addition issues associated with the gallic acid substrate. Additionally, isovanillin was substantially easier to manipulate synthetically then gallic acid; being converted into the desired coupling partner in five steps (Scheme 3.12).

Again, we aimed to control the regiochemistry of the halogenation by utilizing a bulky protecting group on the C5 hydroxyl. Therefore isovanillin was converted to the silyl ether, **3.36**. Bromination was carried out by slow addition of bromine in chloroform to the substrate **3.36** suspended in sat'd. aq. sodium bicarbonate. It was found that any build up HBr caused hydrolysis of the TIPS group, which led to inseparable mixtures of mono- and di-brominated products. The regiochemistry of this bromination was confirmed by analysis of the aromatic coupling constants. Reduction of **3.37** with sodium borohydride gave benzylic alcohol **3.38**, which was tosylated prior to µW assisted cyanide displacement to yield benzylic nitrile **3.39**.

Scheme 3.12. Preparation of C ring from isovanillin.

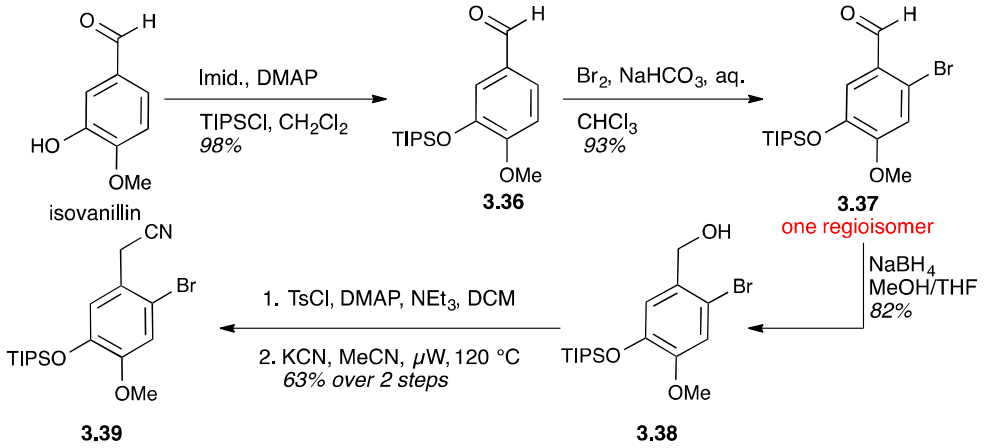

With **3.39** in hand, the Sonogashira reaction was attempted (Scheme 3.13). Yet again it failed, yielding alkyne dimers and starting aryl bromide **3.39**. However, we did find that prolonged reaction times, at high temperatures, yielded some de-halogenated material, leading us to believe that oxidative addition is possible, albeit sluggish, with the isovanillin scaffold. Bolstered by these findings we began to explore other Pd catalyzed cross couplings that may prove more fruitful than the proposed Sonogashira coupling.

Scheme 3.13. Attempted Sonogashira coupling of **3.39** and **3.21**.

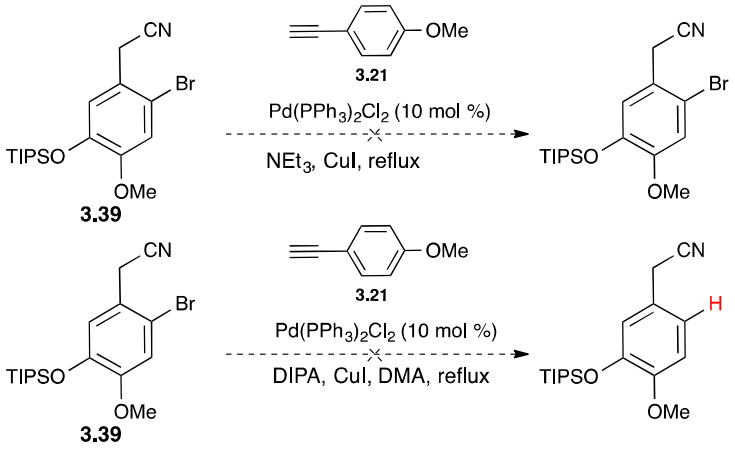

3.2.4 Suzuki-Miyaura coupling strategy.

3.2.4.a Aryl-Potassium trifluoroborate Suzuki coupling

Still weary from our initial foray into Pd catalyzed reactions, we looked toward exploiting a Suzuki-Miyaura cross coupling to afford **3.2**. Since 1998, there has been a myriad of studies on development of phosphine ligands and other catalyst systems for improving oxidative addition in Suzuki couplings.[126–130] Inspired by these studies as well as Molander's success with alkynyl potassium trifluoroborates,[131] we believed that a

carefully designed Suzuki-Miyaura cross coupling could afford our desired Sonogashira adduct.

To this end, alkyne **3.21** was smoothly converted to trifluoroborate **3.40** (Scheme 3.14 (a)) in a two-step process of deprotonation and trapping with trimethyl borate followed by exchange with potassium bifluoride. The recrystallized trifluoroborate was then coupled with aryl-bromide **3.39** in the presence of $Pd(OAc)_2$, K_3PO_4, and the bulky phosphine ligand S-Phos (Scheme 3.14 (b)). To our delight, the Suzuki coupling afforded a very modest yield of our desired adduct **3.41**, however, further optimization efforts failed to increase the yields.

Scheme 3.14. (a) Conversion of alkyne **3.21** to potassium trifluoroborate **3.40**. (b) Suzuki coupling of **3.39** and alkynyl trifluoroborate **3.40**.

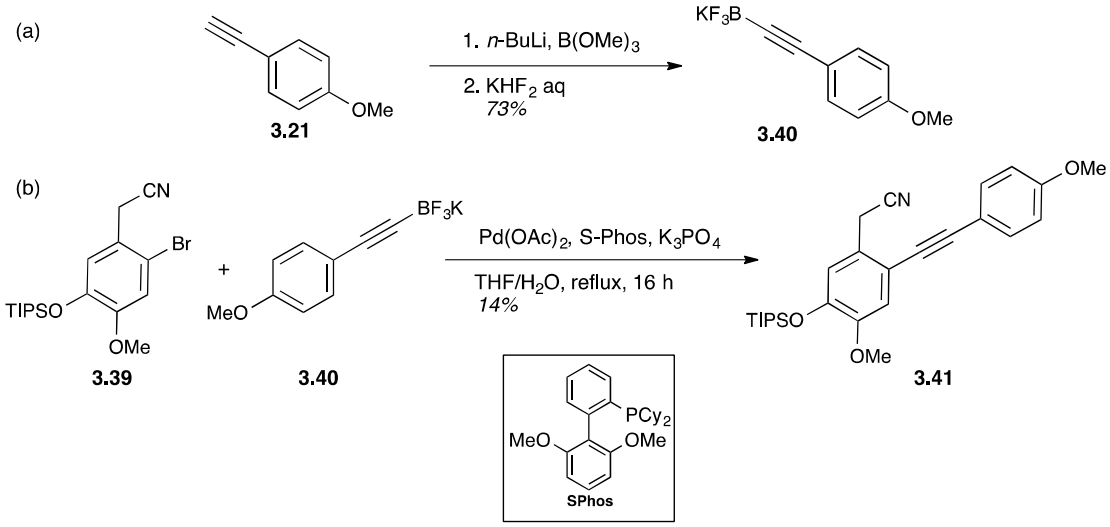

Continuing our misfortune, efforts to reduce the benzylic nitrile in **3.41**[132] to a primary amine were met with substantial decomposition. A cursory NMR analysis of the

decomposition products indicates instability in the alkyne moiety, however a thorough investigation of these products was not conducted.

3.2.4.b Aryl-sp^3 Suzuki coupling

The instability of **3.41** was thought to have played a role in our futile attempts to optimize the yields of the coupling reaction. With this in mind we began looking into the coupling of a completely saturated system, such as the one depicted in Figure 3.1, where an aryl-sp^3 bond is made and the secondary amine is already installed.

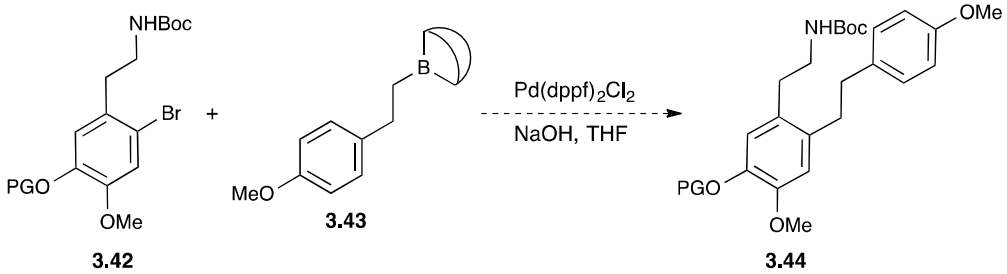

Figure 3.1. Proposed aryl-sp^3 alkyl Suzuki coupling.

Aryl bromide **3.42** would again come from isovanillin. We envisioned installing the secondary amine through a Henry reaction followed by reduction of the nitro olefin and protection. From our previous work with isovanillin, it was known that the TIPS ether was fairly acid labile and it was presumed that a more robust protecting group would be needed for the preparation of **3.42**. After considerable experimentation we determined that benzyl protection of isovanillin would provide the requisite steric bulk for the regioselective bromination while being robust enough to withstand acidic reaction conditions.

Deprotonation of isovanillin with potassium carbonate followed by the addition of benzyl bromide yielded **3.45** (Scheme 3.15). Bromination of **3.45** occurred smoothly giving **3.46** as a single isomer. Henry reaction of **3.46** with ammonium acetate in nitromethane provided nitro olefin **3.47**. Considerable experimentation went into determining optimal nitro olefin reduction conditions. Treatment of **3.47** with LAH and DIBALH afforded a dehalogenated primary amine, while $LiBH_4$ failed to completely reduce the nitro group. Ultimately, it was found that zinc/amalgam in acidic ethanol smoothly reduced the nitro olefin to the primary amine **3.48** in an 85 % yield. The primary amine was immediately protected as the Boc carbamate **3.49**. Borane **3.43** was prepared from the reaction of 4-methoxystyrene with 9-BBN dimer.[133]

Scheme 3.15. Preparation of aryl bromide **3.49** and borane **3.43**.

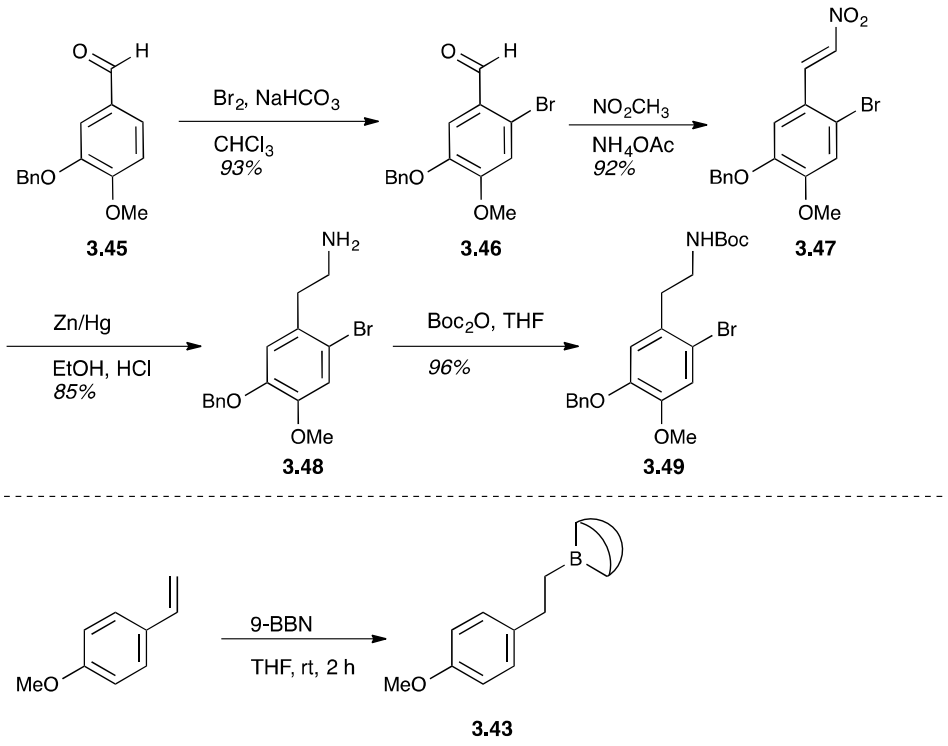

Although the synthesis of the coupling partners was successful, the desired Suzuki coupling was not. Numerous iterations of reaction conditions again failed to produce the desired adduct, a summary of our attempts can be found in the experimental appendix. Including converting the borane **3.43** into a potassium trifluoroborate.[134] Though unlike our previous endeavors we saw substantial dehalogenation of starting material, indicating that the oxidative addition to the benzyl protected isovanillin was more significantly more facile. Our focus continued on the preparation of a more stable coupling adduct with the oxidative addition issues apparently resolved.

3.2.5 Heck coupling strategy

3.2.5.a Initial attempts and optimization

Finding the alkyne containing adduct to be unstable and inability to directly couple the sp^3-ethane bridged A ring to our isovanillin scaffold, led us to consider a Heck coupling[135] between the previously prepared aryl bromide **3.46** and an appropriately substituted styrene (Figure 3.2) to form **3.2**.

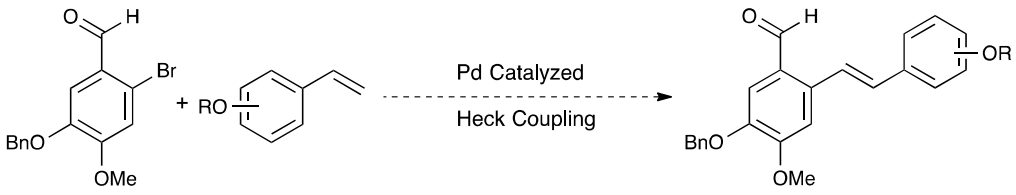

3.46 **3.50**

Figure 3.2. Proposed Heck coupling of styrene and **3.46**.

A model system was developed for the screening of reaction conditions,[136,137] where aryl bromide **3.46** was dissolved in DMA followed by the addition of a palladium

catalyst, styrene, and base. Three different catalyst systems at various loadings were screened: ligand-free $Pd(OAc)_2$, $Pd(OAc)_2$ with a P(*o*-tol)$_3$ ligand, and Pd[PEPPSI] with sodium formate. We also performed a simple screen of bases (Table 3.2). These studies identified ligand-free $Pd(OAc)_2$ conditions that afforded the stable coupling adduct **3.51** in an impressive, un-optimized 65 % yield. Highly encouraged by these results we set out to further optimize the reaction with the styrene.

Table 3.2. Heck reaction conditions.

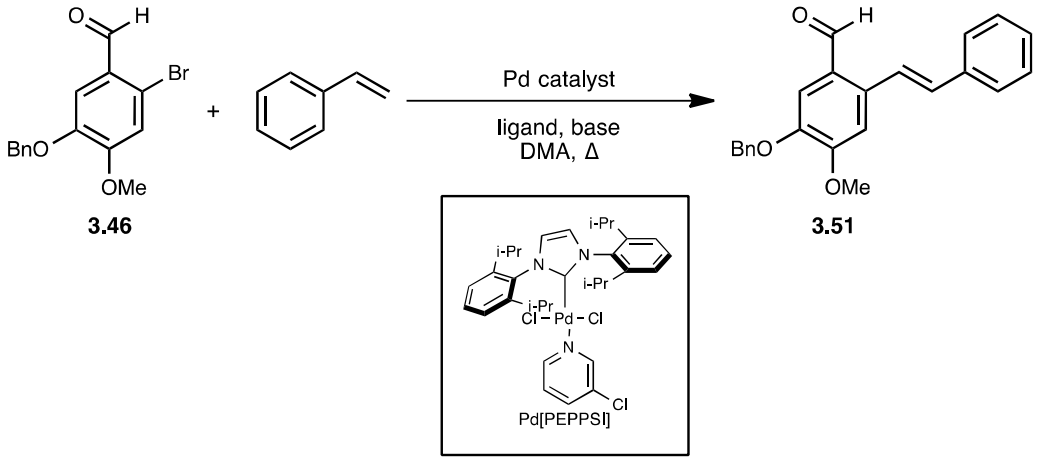

Entry	Pd catalyst	Base[c]	Ligand/additive	Temp	Yield
1	$Pd(OAc)_2$[a]	K_2CO_3	none	125 °C	65 %
2	$Pd(OAc)_2$[a]	K_3PO_4	none	125 °C	23 %
3	$Pd(OAc)_2$[a]	Et_3N	none	125 °C	10 %
4	$Pd(OAc)_2$[a]	Et_3N	P(*o*-tol)$_3$ (10 mol %)	125 °C	43 %
5	Pd[PEPPSI][b]	Et_3N	$NaCO_2H$ (10 mol %)	125 °C	9 %
6	Pd[PEPPSI][b]	Et_3N	$NaCO_2H$ (10 mol %)	80 °C	0 %
7	Pd[PEPPSI][a]	Et_3N	$NaCO_2H$ (10 mol %)	125 °C	50 %

[a] 2 mol % catalyst loading, [b] 5 mol % catalyst loading, [c] 2 equiv of base

The yields were increased, up to 72 % (Scheme 3.16), when the reaction solvent, DMA, was dried over mol sieves and rigorously degassed. Additionally it was found that higher temperatures (>160 °C) and μW heating led to undesirable by-products.

Scheme 3.16. Further optimization of the Heck coupling.

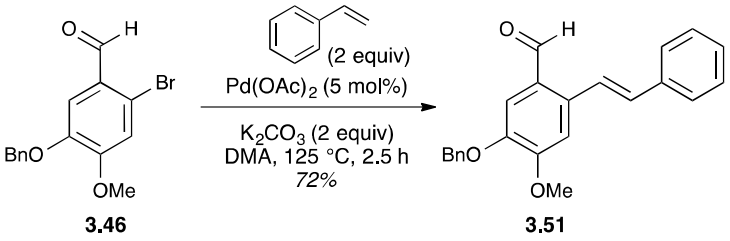

3.46 **3.51**

Next the optimized conditions were used with electron rich styrenes, similar to those found in the A ring of the natural products. The reaction proved compatible with 3,4-dimethoxystryene (**3.54**) and 4-methoxysytrene, giving yields from 65 % to 98 %.

Scheme 3.17. Optimized Heck Couplings with oxygenated styrenes.

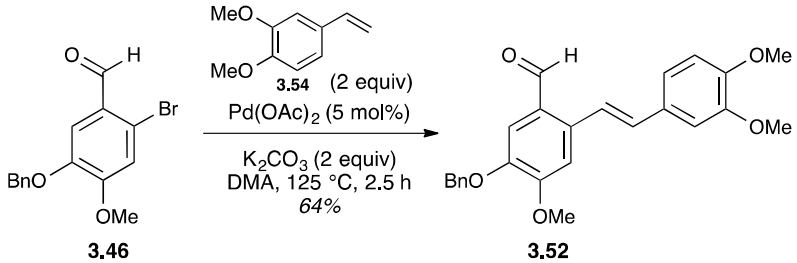

3.46 **3.52**

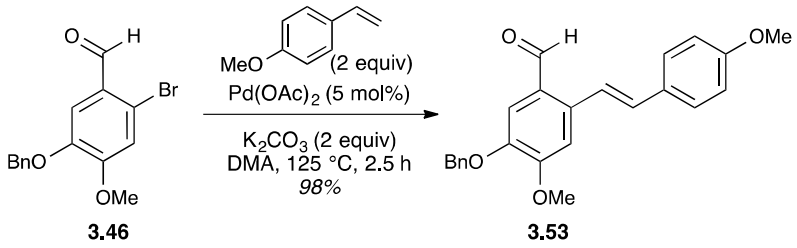

3.46 **3.53**

Emboldened by these positive results, we set out to perform the coupling on the elusive gallic acid derived substrate **3.18**. The initial attempts of direct coupling between

4-methoxystyrene and the methyl benzoate substrate were unsuccessful yielding only dehalogenated starting material. Not easily discouraged, **3.18** was reduced with sodium diisobutyl-*t*-butoxyaluminum hydride[138] to give aldehyde **3.55** in a single step. The aldehyde **3.55** was then subjected to the optimized coupling conditions. Initially the reaction was thought to be a failure with a majority of the aldehyde **3.56** remaining after heating at 125 °C overnight we presumed that this more hindered substrate was again plagued with oxidative addition issues. However, a close examination of the crude ^{1}H NMR revealed that a small amount of **3.56** was produced. Increased temperatures (150 °C) and longer reaction slightly improved the reaction. It should also be noted that our attempts to directly couple nitro olefin **3.47** or an unprotected phenol to 4-methoxystyrene were unsuccessful.

Scheme 3.18. Heck coupling of gallic acid derived substrate **3.18**.

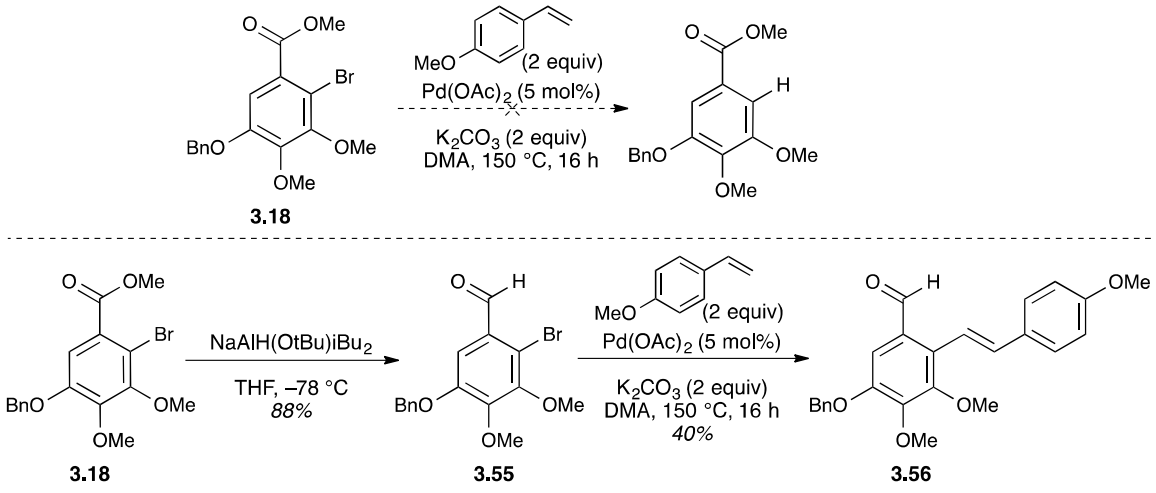

Although the barriers to oxidative addition were not completely removed, this was the first Pd catalyzed reaction to gain access to a gallic acid derived coupling adduct. We

were also pleased to find that these alkene products were considerably more stable then their alkyne counterparts finally allowing us to access our dearomatization precursor.

3.2.6 Completion of Dearomatization Precursor

With the A and C rings coupled together we turned our attention to the installation of the ethylamine moiety. Henry reaction on the coupling adducts cleanly generated the nitro olefins **3.57**, **3.58**, and **3.59** (Scheme 3.19).

Scheme 3.19. Nitro olefin formation.

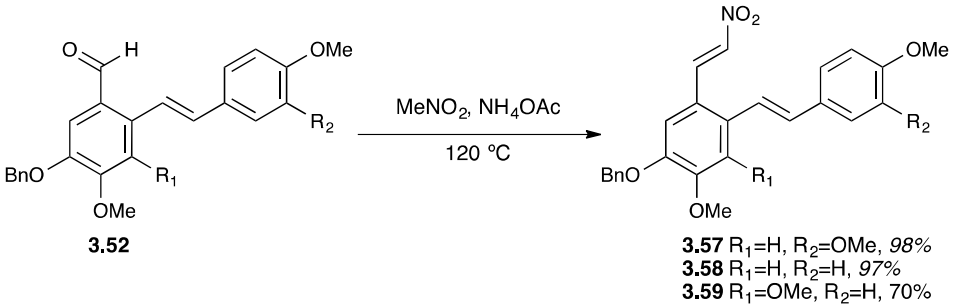

3.2.6.a Global Hydrogenation Strategy

In our previous work, zinc amalgam in acidic ethanol afforded the reduction of the nitro olefin to the ethylamine, **3.48**. It was anticipated that these conditions would not be suitable for these substrates due to the instability of the stilbene in presence of acidic protons.[139] We had also learned from our previous studies that nitro olefins could be reduced under acidic Pd catalyzed hydrogenation conditions. This led to the proposal of a global hydrogenation strategy, where the formation of ethylamine coincides with benzyl ether cleavage and hydrogenation of the stilbene. We believed this reaction sequence

would be feasible, if the stilbene were fully hydrogenated prior to the introduction of acid.

Our initial studies indicated that the stilbene was fully hydrogenated within the first 30 min of reaction time, regardless of solvent choice. Therefore, we devised a system where after 30 mins of reaction time, HCl was added to hopefully drive the reduction of the nitro olefin (Table 3.3).

Table 3.3. Hydrogenation Screening.

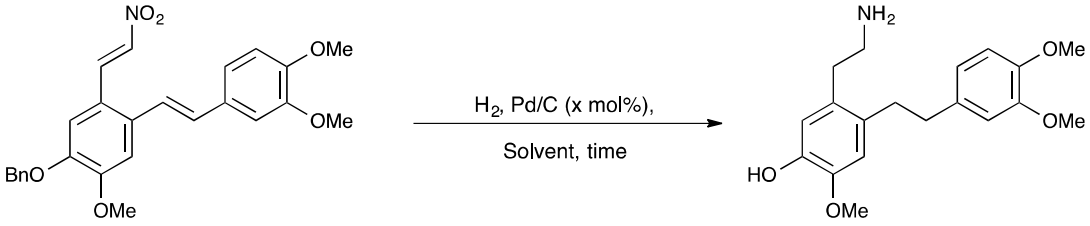

3.57

Entry	Conditions	Result
1	Pd/C (10 mol %), HCl, MeOH	decomp.
2	Pd/C (10 mol %), HCl, THF	decomp.
3	Pd/C (10 mol %), 200 PSI, MeOH/THF	R—NO_2
4	Pd/C (10 mol %), 700 PSI, MeOH/THF	R—NO_2
5	Pd/C (20 mol %), 700 PSI, MeOH/THF	R—NO_2
6	Pd/C (10 mol %), 200 PSI, $Cl^{-+}NHMe_3$	18 %

Contrary to our hypothesis, we found the saturated biaryl product to also be acid sensitive leading to undetermined decomposition products (entries 1 and 2). Because of this acid

sensitivity we attempted to drive the reduction of the vinyl nitro by increasing hydrogenation pressures in a Parr bomb reactor.

Unfortunately reduction of the nitro group was not achieved without some proton source, even with increasing the pressures up to 700 PSI (entries 4-5). The addition of a weak proton source such as trimethyl ammonium chloride afforded the fully reduced amine and the crude NMR indicated that the conversion was clean, however there were significant issues with isolation of the amine product leading us to abandon this route.

3.2.6.b Multi-step strategy

Instead we employed a multi-step strategy, where the nitro olefin is first reduced with LAH and protected, followed by hydrogenation of the double bond and benzyl ether (Scheme 3.20).

Scheme 3.20. Completion of dearomatiztion precursor.

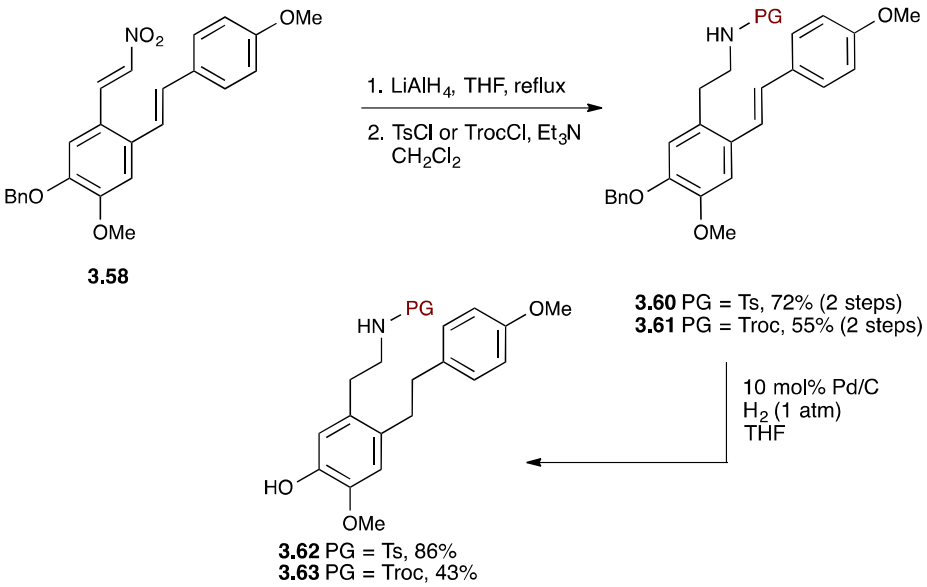

LAH reduction of **3.58**, in refluxing THF afforded a primary amine, which was immediately protected as either: a tosyl-amine, **3.60**, or Troc-carbamate **3.61**. This protection was critical to the success of the subsequent hydrogenation as unprotected amines resulted in poor yields presumably due to catalyst poisoning. Both the Troc-carbamate and tosylamine substrates were hydrogenated to give the biaryl coupling adducts **3.62** and **3.63**. The Heck coupling synthetic route yields the desired dearomatization precursors in 7 steps from isovanillin and 10 steps from gallic acid.

3.3 Dearomatization/Acid Catalyzed Cyclization

3.3.1 Discussion of dearomatization strategy

Finally achieving the synthesis of our precursor we were poised to complete the HB alkaloid core via a hypervalent iodine(III) mediated oxidative dearomatization. As a reminder, we proposed two possible scenarios for this dearomatization: (1) the nitrogen serves as the nucleophile, leading to a fused bicyclic intermediate, and (2) where the aromatic A ring serves as the nucleophile forming a spirocycle intermediate (Scheme 3.21). Spirocyclizations such as the one proposed in our second scenario are well known[140] however, the trapping of the rearrangement product is unprecedented. The formation of the fused bicycle in our first scenario is also unprecedented in the literature.

Scheme 3.21. Possible scenarios for the dearomatization of **3.2**, revisited.

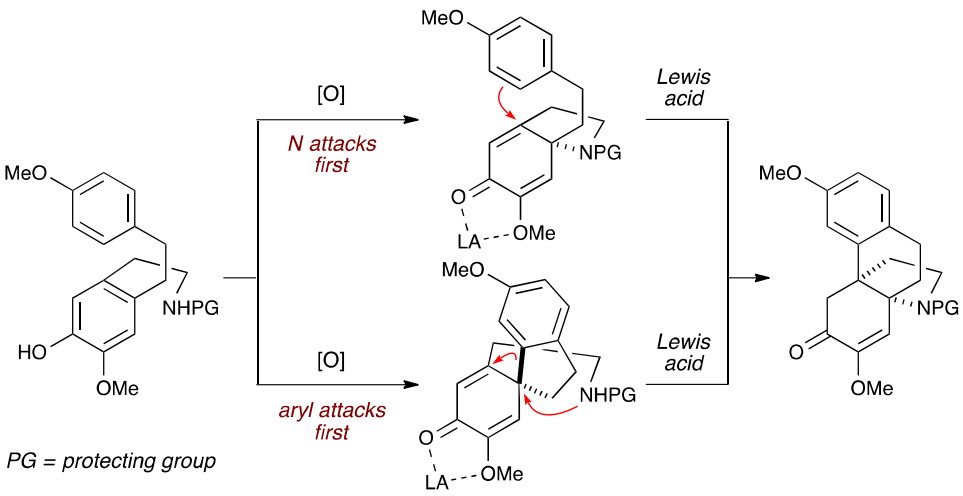

The first example of an iodine(III) mediated C–N bond formation was reported in 2002 by Ciufolini and co-workers (Scheme 3.22).[108] In this example, tosyl-amine **3.64** forms spirocycle **3.65** when treated with PIFA. Other examples of C–N bond forming reactions have been reported,[109] but to date all involve the formation of a spirocycle. The closest example to our proposal was reported by Quideau and co-workers in 2001.[112] Here phenol **3.66** is treated with PIDA to give the stable ketal intermediate **3.67**, removal of the nitrogen protecting group with TBAF leads to bicycle formation followed by rearomatization to give phenol **3.68**. While PIDA is used to form the ketal intermediate the authors observed that the C–N bond formation is ultimately a result of amine deprotection.

Scheme 3.22. Examples of hypervalent iodine(III) mediated C–N bond formation.

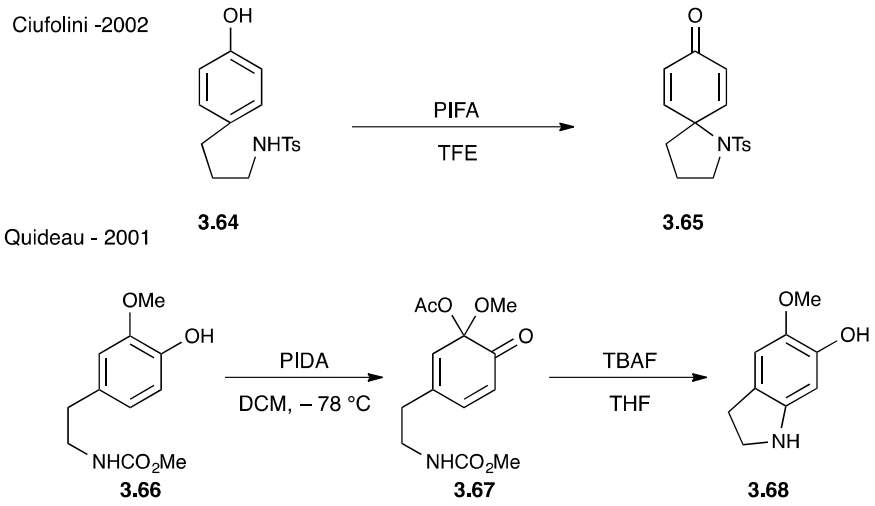

Both a carbamate **3.63** and a tosyl-amine **3.62** protected substrate were prepared. Based on literature reports, **3.62** was expected to be compatible with scenario one. We hoped in lieu of formation of a hindered 4 membered spirocycle the tosyl-amine would attack at the *para* position to yield the fused bicycle.

3.3.2 Results of dearomatization

*3.3.2.a Treatment of tosyl-amine **3.62** with hypervalent iodide(III) reagents*

The traditional hypervalent iodide (III) reagent PIDA, as well as, the more electrophillic μ-oxo-bridged diiodide reagent were used in the dearomatization of tosyl-amine **3.62** (Scheme 3.23). Treatment of **3.62** with PIDA provided the stable, fused bicycle **3.69** confirming that addition of the nitrogen is more facile than spirocyclization of the arene. An identical cyclohexadienone was formed when **3.62** was treated with the diiodide reagent.

Table 3.4. Treatment of tosyl-amine **3.62** with hypervalent iodide(III) reagents.

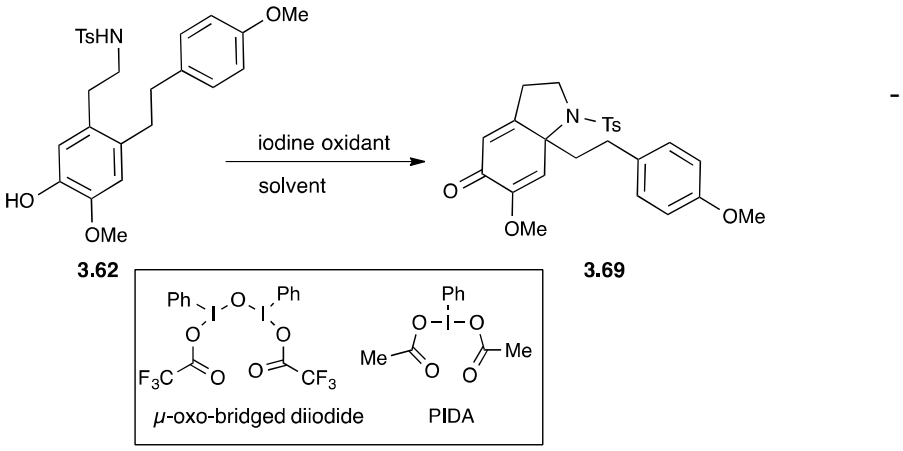

Entry	I(III) reagent	Solvent	Temp/Time	Conversion by TLC
1	PIDA	DCM	0 °C/ 180 min	60 %
2	Diiodide	TFE	–40 °C/ 90 min	100 %
3	Diiodide	TFE	0 °C/ 30 min	100 % (66 % isolated yield)
4	Diiodide	DCM	0 °C/ 30 min	100 % (70 % isolated yield)

The diiodide reagent proved to be more effective at producing the cyclohexadieneone **3.69**, showing 100 % conversion at 0 °C in 30 minutes. Hypervalent iodide(III) reagents like the μ-oxo-bridged diiodide possess a more ionic character than PIDA or PIFA. This increase in electrophilicity at the iodine atom has been shown to improve the rate of dearomatization though acceleration the initial ligand exchange.[140] In addition to our reagent findings, we found that solvent effects do not appear to play an

important role in this transformation as the highly protic trifluoroethanol and DCM provide similar yields and reaction times.

*3.3.2.b Treatment of Troc-carbamate **3.63** with hypervalent iodide(III) reagents*

In stark contrast to tosyl-amine **3.62**, treatment of Troc-carbamate **3.63** with diiodide gives the highly colored, unstable *ortho*-benzoquinone **3.71** (Scheme 3.24). The benzoquinone is thought to arise from an intermediate carbocation such as **3.70**, where loss of the methyl is more facile than attach by the nitrogen nucleophile.

Scheme 3.23. Treatment of Troc-carbamate **3.63** with hypervalent iodide(III) reagents.

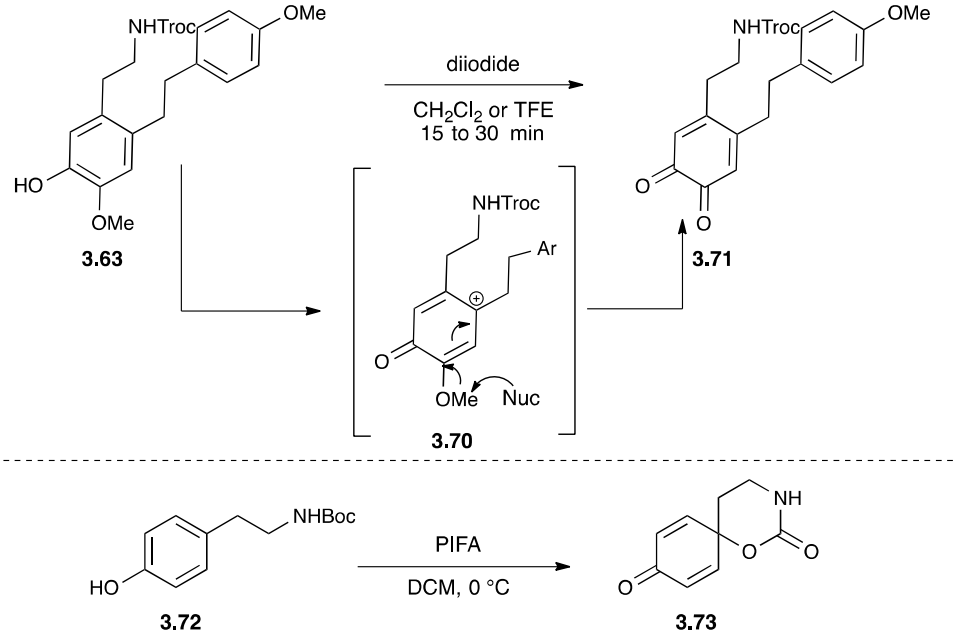

The reluctance of the carbamate to serve as a nucleophile was also observed in related studies, were the oxygen of the carbamate **3.72** was found to cyclize in place of the nitrogen to form a six membered spirocycle **3.73**. Interestingly, a similar methyl ether cleavage occurs when the gallic acid derived tosyl-amine is treated with diiodide

(Scheme 3.25). Unfortunately, the formation of the benzoquinone was persistent in both substrates even with varying the solvent and the hypervalent iodide(III) reagent.

Scheme 3.24. Dearomatization of gallic acid substrate **3.59**.

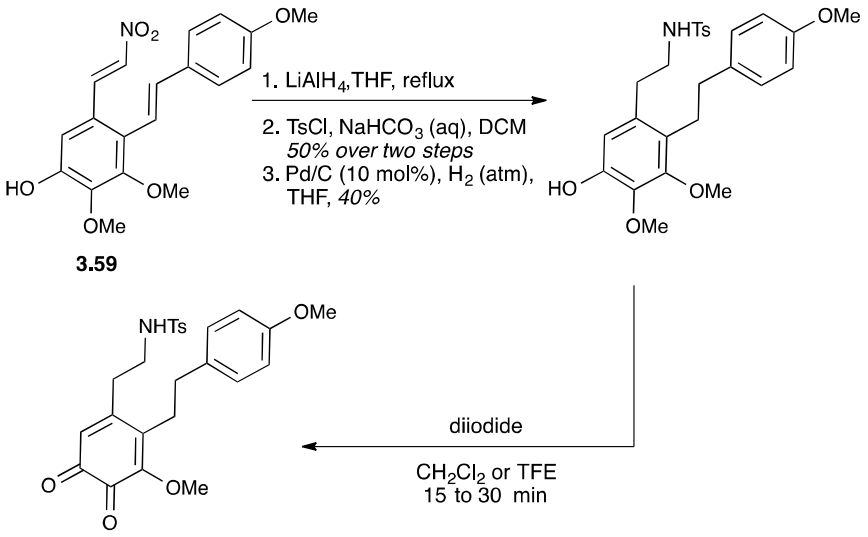

3.3.3 Acid catalyzed conjugate addition

Since the dearomatization cleanly converted tosyl-amine **3.62** to the bicycle **3.69** we were able to attempt the final acid catalyzed conjugate addition. The structure of our fused bicyclic **3.69** bears a striking resemblance to the dihydroindolone prepared in the Reisman synthesis of (–)-demethoxyrunanine (Scheme 2.10). Given these structural similarities we presumed that the treatment of **3.69** with excess TfOH would afford the acid catalyzed conjugate addition. The reaction was carried out in a single pot without purification of the fused bicycle, after the treatment of **3.62** with diiodide, TfOH was added (Scheme 3.26) and the reaction was then immediately quenched. This sequence of events provided interesting results. Analysis of the crude ^{1}H NMR clearly indicated the

presence of a tetracyclic product, however, there appeared to be an additional product. This was also visible as two distinct spots on TLC.

Scheme 3.25. Acid catalyzed conjugate addition.

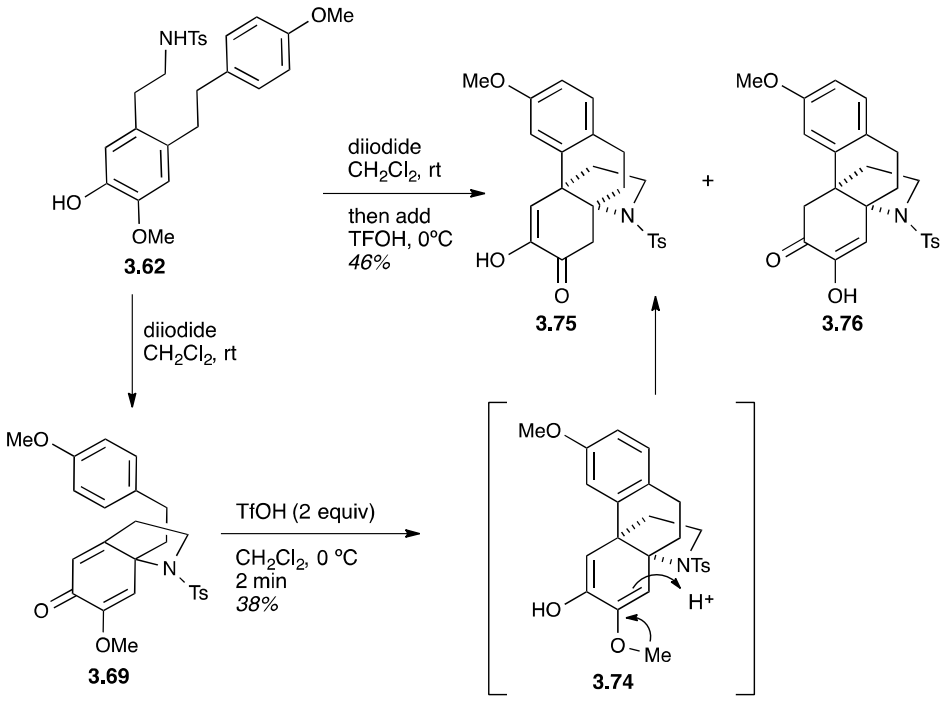

Mass spectrometry of the final product relieved the loss of a methyl group from the tetracycle, presumably through intermediate **3.74**, leading to the formation of isomers **3.75** and **3.76**. Loss of this methyl group is extremely facile, occurring instantaneously upon the addition of Brønsted acid. Our current efforts are focused on screening Lewis acids, which will potentially mitigate the consummate demethylation of intermediate **3.74**.

Although the treatment of **3.62** with the μ-oxo-bridged diiodide unexpectedly yielded isomers **3.75** and **3.76**, the tetracyclic core of the HB alkaloids was nonetheless

constructed in 8 steps from commercially available materials, showcasing our convergent dearomatization strategy.

3.3.4 Future Work

We are currently investigating methods for the selective methylation of **3.76**. As well as, looking into ways to exploit the formation of the *ortho*-quinone **3.71**. Inspired by Matsumoto and co-workers,[141] we envision performing the dearomatization of **3.63** in the presence of methanol producing the simple *ortho*-quinone acetal **3.78** (Scheme 3.27). Treatment with Lewis acid would then lead to the conjugate addition of the aryl ring giving intermediate (**3.78**), followed attack of the nucleophillic nitrogen to eliminate the acetal, affording the tetracyclic core **3.80**.

Scheme 3.26. Trapping of the *ortho*-quinone **3.71**.

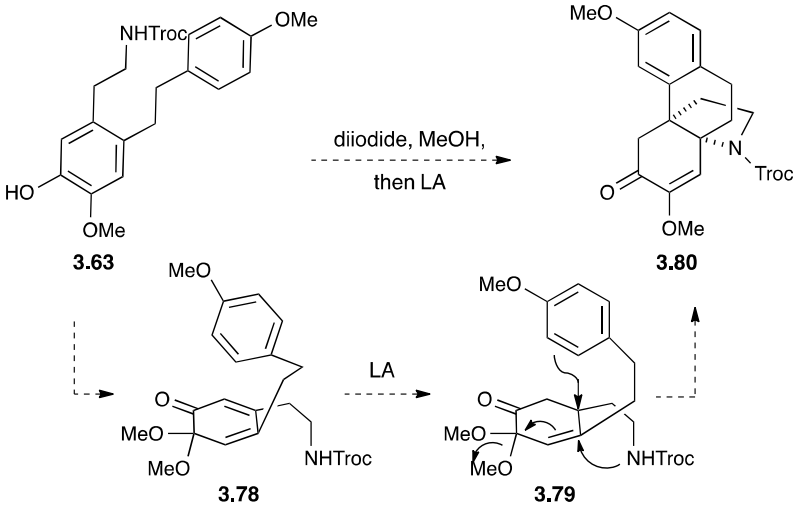

3.3.5 Closing Remarks

Many challenges were endured and overcome during the preparation of the HB alkaloid tetracyclic core. After extensive experimentation, we developed a unique synthetic route, highlighted by the integration of the formation of the C12–C13 and C14–N bonds with the formation of the B and D rings.

This strategy features an unprecedented iodine(III) mediated oxidative dearomatization for the formation of a fused nitrogen bicycle. Most importantly, the simplicity of this route allows for the preparation both natural and unnatural HB alkaloids in less than nine steps from commercially available materials, without the use of expensive or exotic reagents; furthering drug discovery efforts for the treatment of chronic pain.

References

(1) Bonica, J. The Need of a Taxonomy. *Pain* **1979**, *6*, 247–248.

(2) Williams, M.; Kowaluk, E.; Arneric, S. Emerging Molecular Approaches to Pain Therapy. *J. Med. Chem.* **1999**, *42*, 1481–1500.

(3) Harstall, C.; Ospina, M. How Prevalent Is Chronic Pain? *Pain Clin. Updat.* **2003**, *2*, 1–9.

(4) Brownlee, S.; Schrof, J. The Quality of Mercy. *U.S. News and World Report*. 1997, pp. 54–67.

(5) Lussier, D.; Huskey, A.; Portenoy, R. Adjuvant Analgesics in Cancer Pain Management. *Oncologist* **2004**, *9*, 571–591.

(6) Cleeland, C. Recommedations for Pain Management. *J. Am. Med. Assoc.* **1998**, *279*, 1914–1915.

(7) Matsui, M. *The Alkaloids*; Brossi, A., Ed.; Academic Press: New York, 1988; pp. 307–347.

(8) Semwal, D. K.; Badoni, R.; Semwal, R.; Kothiyal, S. K.; Singh, G. J. P.; Rawat, U. The Genus Stephania (Menispermaceae): Chemical and Pharmacological Perspectives. *J. Ethnopharmacol.* **2010**, *132*, 369–383.

(9) Tomita, M.; Ibuka, T.; Inubushi, Y.; Watanabe, Y.; Matsui, M. Structure of Hasubanonine. *Tetrahedron Lett.* **1964**, *5*, 2937–2944.

(10) Carroll, A. R.; Arumugan, T.; Redburn, J.; Ngo, A.; Guymer, G. P.; Forster, P. I.; Quinn, R. J. Hasubanan Alkaloids with ∂-Opioid Binding Affinity from the Aerial Parts of Stephania Japonica. *J. Nat. Prod.* **2010**, *73*, 988–991.

(11) Schultz, A. G.; Wang, A. First Asymmetric Synthesis of a Hasubanan Alkaloid. Total Synthesis of (+)-Cepharamine. *J. Am. Chem. Soc* **1998**, *120*, 8259–8260.

(12) Chuang, K.; Navarro, R.; Reisman, S. Short, Enantioselective Total Syntheses of (−)-8-Demethoxyrunanine and (−)-Cepharatines A, C, and D. *Angew. Chem. Int. Ed.* **2011**, *50*, 9447–9451.

(13) Herzon, S. B.; Calandra, N. A.; King, S. M. Efficient Entry to the Hasubanan Alkaloids: First Enantioselective Total Syntheses of (−)-Hasubanonine, (−)-

Runanine, (−)-Delavayine, and (+)-Periglaucine B. *Angew. Chem. Int. Ed.* **2011**, *50*, 8863–8866.

(14) Jones, S. B.; He, L.; Castle, S. L. Total Synthesis of (±)-Hasubanonine. *Org. Lett.* **2006**, *8*, 3757–3760.

(15) Melinikova, I. Pain Market. *Nat. Rev. Drug Discov.* **2010**, *9*, 589–590.

(16) Pergolizzi, J.; Ahlbeck, K.; Aldington, D.; Alon, E.; Coluzzi, F.; Dahan, A. The Development of Chronic Pain: Physiological Change Necessitates a Multidisciplinary Approach to Treatement. *Curr. Med. Res. Opin.* **2013**, *29*, 1127–1135.

(17) Hardt, J.; Jacobsen, C.; Goldberg, J.; Nickel, R.; Buchwald, D. Prevalence of Chronic Pain in a Representative Sample in the United States. *Pain Med.* **2008**, *9*, 803–912.

(18) Varrassi, G.; Müller-Schwefe, G.; Pergolizzi, J. Pharmacological Treatement of Chronic Pain – The Need for CHANGE. *Curr. Med. Res. Opin.* **2010**, *26*, 1055–1069.

(19) Dubin, A.; Patapoutian, A. Nociceptors: The Sensors of the Pain Pathway. *J. Clin. Investig.* **2010**, *120*, 3760–3772.

(20) Treede, R.; Jensen, T.; Campbell, J.; Cruccu, G.; Dostrovsky, J.; Griffin, J. Neuropathic Pain: Redefinition and a Grading System for Clinical and Research Purposes. *Neurology* **2008**, *70*, 1630–1635.

(21) Chen, H.; Lamer, T.; Rho, R. Contemporary Management of Neuropathic Pain for the Primary Care Physician. *Mayo Clin. Proc.* **2004**, *79*, 1533–1545.

(22) Kroenke, K.; Krebs, E.; Bair, M. Pharmacotherapy of Chronic Pain: A Synthesis of Recommendations from Systematic Reviews. *Gen. Hosp. Psychiatry* **2009**, *31*, 206–219.

(23) Baron, R.; Binder, A.; Wasner, G. Neuropathic Pain: Diagnosis, Pathophysilogical Mechanisms, and Treatment. *The Lancet–neurology* **2010**, *9*, 807–819.

(24) Esin, E.; Yalcin, S. Neuropathic Cancer Pain: What We Are Dealing with? How to Manage It? *Onco. Targets. Ther.* **2014**, *7*, 599–618.

(25) Giustino, V.; Varrassi, G. Severe Chronic Pain – The Reality of Treatment in Europe. *Curr. Med. Res. Opin.* **2011**, *27*, 2063–2064.

(26) World Health Organization. *Cancer Pain Relief*; World Health Organization, Ed.; 2nd ed.; World Health Organization: Geneva, 1996; pp. 1–64.

(27) Vardy, J.; Agar, M. Nonopioid Drugs in the Treatment of Cancer Pain. *J. Clin. Oncol.* **2014**, *32*, 1677–1690.

(28) Warner, T.; JA, M. Cyclooxygenases: New Forms, New Inhibitors, and Lessons from the Clinic. *FASEB J.* **2004**, *18*, 790–804.

(29) Doyle, D.; Hanks, G.; MacDonald, N. *Oxford Textbook of Palliative Medicine*; 2nd ed.; Oxford University Press: New York, 1998; pp. 1–30.

(30) Rollins, D.; Glaumann, H.; Moldeus, P.; Rane, A. Acetaminophen: Potentially Toxic Metabolite Formed by Human Fetal and Liver Microsomes and Isolated Fetal Liver Cells. *Science.* **1979**, *205*, 1414–1416.

(31) Mitchell, J.; Jollow, D.; Potter, W.; Davis, D.; Gillette, J.; Brodie, B. Acetaminophen-Induced Hepatic Necrosis. 1. Role of Druge Metabolism. *J. Pharmacol. Exp. Ther.* **1973**, *187*, 185–194.

(32) Rostom, A.; Muir, K.; Dubé, C. Gastrointestinal Safety of Cyclooxygenase-2 Inhibitors: A Cochrane Collaboration Systematic Review. *Clin. Gastroenterol. Hematology* **2007**, *5*, 818–828.

(33) Baron, J.; Sandler, R.; Bresalier, R. Cardiovascular Evens Associated with Rofecoxib: Final Analysis of APPROVe Trial. *Lancet* **2008**, *372*, 1756–1764.

(34) Lussier, D.; Portenoy, R. Adjuvant Analgesics in Pain Management. In *Oxford Textbook of Palliative Medicine*; Doyle, D.; Hanks, G.; Cherny, N., Eds.; Oxford University Press: Oxford, 2003; pp. 349–377.

(35) Gallagher, R. Management of Neuropathic Pain: Translating Mechanistic Advances and Evidence-Based Research into Clinical Practice. *Clin. J. Pain* **2006**, *22*, 2–8.

(36) Sánchez, C.; Hyttel, J. Comparison of the Effects of Antidepressants and Their Metabolites on Reuptake of Biogenic Amines and on Receptor Binding. *Cell. Mol. Neurobiol.* **1999**, *19*, 467–489.

(37) Sansone, R. A.; Sansone, L. A. Pain, Pain, Go Away: Antidepressants and Pain Management. *Psychiatry* **2008**, *5*, 16.

(38) Beniczky, S.; Tajti, J.; Tímea Varga, E.; Vécsei, L. Evidence-Based Pharmacological Treatment of Neuropathic Pain Syndromes. *J. Neural Transm.* **2005**, *112*, 735–749.

(39) Sultan, A.; Gaskel, H.; Derry, S.; Moore, R. Duloxetine for Painful Diabetic Neuropathy and Fibromyalgia Pain: Systematic Review of Randomized Controlled Trials. *BMC Neurol.* **2008**, *8*, 1–9.

(40) Meldrum, M. L. A Capsule History of Pain Management. *J. Am. Med. Assoc.* **2003**, *290*, 2470–2475.

(41) Rosenblum, A.; Marsch, L.; Joseph, H.; Portenoy, R. Opioids and the Treatment of Chronic Pain: Controversies, Current Status, and Future Directions. *Exp. Clin. Psychopharmacol.* **2008**, *16*, 405–416.

(42) Walker, J. M.; Farney, R. J. Are Opioids Associated with Sleep Apnea? A Review of the Evidence. *Curr. Pain Headache Rep.* **2009**, *13*, 120–126.

(43) Ballantyne, J. C.; Mao, J. Opioid Therapy for Chronic Pain. *N. Engl. J. Med.* **2003**, *349*, 1943–1953.

(44) Hay, J. L.; White, J. M.; Bochner, F.; Somogyi, A. A.; Semple, T. J.; Rounsefell, B. Hyperalgesia in Opioid-Managed Chronic Pain and Opioid-Dependent Patients. *J. Pain* **2009**, *10*, 316–322.

(45) Ballantyne, J. C.; LaForge, K. S. Opioid Dependence and Addiction during Opioid Treatment of Chronic Pain. *Pain* **2007**, *129*, 235–255.

(46) Olsen, Y.; Sharfstein, J. M. Chronic Pain, Addiction, and Zohydro. *N. Engl. J. Med.* **2014**, *370*, 2061–2063.

(47) Meldrum, M. L. A Capsule History of Pain Management. *J. Am. Med. Assoc.* **2003**, *290*, 2470–2475.

(48) Pert, C. B.; Snyder, S. H. Opiate Receptor: Demonstration in Nervous Tissue. *Science.* **1973**, *179*, 1011–1014.

(49) Simon, E. J.; Hiller, J. M.; Edelman, I. Stereospecific Binding of the Potent Narcotic Analgesic [3H]etorphine to Rat Brain Homogenate. *Proc. Natl. Acad. Sci. U. S. A.* **1973**, *70*, 1947–1949.

(50) Terenius, L. Stereospecific Interaction between Narcotic Analgesics and a Synaptic Plasma Membrane Fraction of Rat Cerebral Cortex. *Acta Pharmacol. Toxicol.* **1973**, *32*, 317–319.

(51) Pasternak, G. W. *The Opiate Receptors*; 2011.

(52) Lord, J. A. H.; Waterfield, A. A.; Hughes, J.; Kosterlitz, H. W. Endogenous Opioid Peptides: Multiple Agonists and Receptors. *Nature* **1977**, *267*, 495–499.

(53) Snyder, S. H.; Pasternak, G. W. Historical Review: Opioid Receptors. *Trends Pharmacol. Sci.* **2003**, *24*, 198–205.

(54) Kosterlitz, H. W.; Leslie, F. M. Comparison of the Receptor Binding Characterisitics of Opiate Agonists Interacting with M- or K-Receptors. *Br. J. Pharmacol.* **1978**, *64*, 607–614.

(55) Portoghese, P. S. A New Concept on the Mode of Interaction of Narcotic Analgesics with Receptors. *J. Med. Chem.* **1965**, *8*, 609–613.

(56) Portoghese, P. S. Stereochemical Factors and Receptor Interactions Associated with Narcotic Analgesics. *J. Pharm. Sci.* **1966**, *55*, 865–887.

(57) Beckett, A. H.; Casy, A. F. Synthetic Analgesics: Stereochemical Considerations. *J. Pharm. Pharmacol.* **1954**, *6*, 986–1001.

(58) Kieffer, B. L. Recent Advances in Molecular Recognition and Signal Transduction of Active Peptides: Receptors for Opioid Peptides. *Cell. Mol. Neurobiol.* **1995**, *15*, 615–635.

(59) Kane, B.; Svensson, B.; Ferguson, D. Molecular Recognition of Opioid Receptor Ligands. *AAPS J.* **2006**, *8*, 126–137.

(60) Manglik, A.; Kruse, A. C.; Kobilka, T. S.; Thian, F. S.; Mathiesen, J. M.; Sunahara, R. K.; Pardo, L.; Weis, W. I.; Kobilka, B. K.; Granier, S. Crystal Structure of the M-Opioid Receptor Bound to a Morphinan Antagonist. *Nature* **2012**, *485*, 321–326.

(61) Granier, S.; Manglik, A.; Kruse, A. C.; Kobilka, T. S.; Thian, F. S.; Weis, W. I.; Kobilka, B. K. Structure of the Δ-Opioid Receptor Bound to Naltrindole. *Nature* **2012**, *485*, 400–404.

(62) Wu, H.; Wacker, D.; Mileni, M.; Katritch, V.; Han, G. W.; Vardy, E.; Liu, W.; Thompson, A. A.; Huang, X.; Carroll, F. I.; et al. Structure of the Human K-Opioid Receptor in Complex with JDTic. *Nature* **2012**, *485*, 327–332.

(63) Lagerstrom, M. C.; Schioth, H. B. Structural Diversity of G Protein-Coupled Receptors and Significance for Drug Discovery. *Nat. Rev. Drug Discov.* **2008**, *7*, 339–357.

(64) Knapp, R.; Malatynska, E.; Collins, N.; Fang, L.; Wang, J.; Hruby, V.; Roeske, W.; Yamamura, H. Molecular Biology and Pharmacology of Cloned Opioid Receptors. *FASEB J.* **1995**, *9*, 516–525.

(65) Kieffer, B. L.; Evans, C. J. Opioid Receptors: From Binding Sites to Visible Molecules in Vivo. *Neuropharmacology* **2008**, *56*, 1–8.

(66) Ferguson, S. S. Evolving Concepts in G Protein-Coupled Receptor Endocytosis: The Role in Receptor Desensitization and Signaling. *Pharmacol. Rev.* **2001**, *53*, 1–24.

(67) Molinari, P. Morphine-like Opiates Selectively Antagonize Receptor-Arrestin Interactions. *J. Biol. Chem.* **2010**, *285*, 12522–12535.

(68) Berger, A.; Whistler, J. How to Design an Opioid Drug That Causes Reduced Tolerance and Dependence. *Ann. Neurol.* **2010**, *67*, 559–569.

(69) Martin, M.; Matifas, A.; Maldonado, R.; Kieffer, B. L. Acute Antinociceptive Responses in Single and Combinatorial Opioid Receptor Knockout Mice: Distinct Mu, Delta and Kappa Tones. *Eur. J. Neurosci.* **2003**, *17*.

(70) Wang, Y. H.; Sun, J. F.; Tao, Y. M.; Chi, Z. Q.; Liu, J. G. The Role of K-Opioid Receptor Activation in Mediating Antinociception and Addiction. *Acta Pharmacol. Sin.* **2010**, *31*, 1065–1070.

(71) Filliol, D.; Ghozland, S.; Chluba, J.; Martin, M.; Matthes, H. W.; Simonin, F.; Befort, K.; Kieffer, B. L. Mice Deficient for Delta- and Mu-Opioid Receptors Exhibit Opposing Alterations of Emotional Responses. *Nat. Genet.* **2000**, *25*, 195–200.

(72) Abdelhamid, E. E.; Sultana, M.; Portoghese, P. S.; Takemori, A. E. Selective Blockage of Delta Opioid Receptors Prevents the Development of Morphine Tolerance and Dependence in Mice. *J. Pharmacol. Exp. Ther.* **1991**, *258*, 299–303.

(73) Nadal, X.; Baños, J.-E.; Kieffer, B. L.; Maldonado, R. Neuropathic Pain Is Enhanced in Delta-Opioid Receptor Knockout Mice. *Eur. J. Neurosci.* **2006**, *23*, 830–834.

(74) Kondo, H. M.; Satomi, M.; Odera, T. Alkaloids of Stephania Japonica MIERS. XIV. On Hasubanonine. I (Alkaloids of Menisperrnaceae. LXXXIV.). *Annu. Rep. ITSUU Lab.* **1951**, *2*, 35–43.

(75) Bentley, K. W. The Biogenesis of the Morphine Alkaloids and Related Topics. *Experientia* **1956**, *12*, 251–253.

(76) Okuda, S.; Yamaguchi, S.; Kawazoe, Y.; Tsuda, K. Studies on the Morphine Alkaloids. I. Nuclear Magnetic Resonance Spectral Studies on MOrphine Alkaloids. *Chem. Pharmacol. Bull.* **1964**, *12*, 104–112.

(77) Battersby, A.; Jones, R.; Kazlauskas, R.; Thornber, C.; Ruchirawat, S.; Staunton, J. Biosynthesis. Part 24. Speculative Incorporation Experiments with 1-Benzylisoquinolines and a Logical Approach via C6–C2 and C6–C3 Precursors to the Biosynthesis of Hasubanonine and Protostephanine. *J. Chem. Soc. Perkin Trans. 1* **1981**, 2016.

(78) Battersby, A.; Jones, R.; Minta, A.; Ottridge, A.; Staunton, J. Biosynthesis. Part 25. Proof That Hasubanonine and Protostephanine Are Biosynthesised from the 1-Benzylisoquinoline System. *J. Chem. Soc. Perkin Trans. 1* **1981**, 2030.

(79) Allen, R.; Kirby, G. A Common Aziridinium Ion Intermediate in the Solvolysis of Halogeno-Codeinone and -Neopinone Acetals. *J. Chem. Soc. D Chem. Commun.* **1971**, 1121.

(80) Ibuka, T.; Tanaka, K.; Inubushi, Y. The Total Synthesis of Dl-Hasubanonine. *Tetrahedron Lett.* **1971**, *55*, 4811–4814.

(81) Ibuka, T.; Tanaka, K.; Inubushi, Y. Total Synthesis of the Alkaloid (±)-Metaphanine. *Chem. Pharm. Bull. (Tokyo).* **1974**, *22*, 907–921.

(82) Ibuka, T.; Tanaka, K.; Inubushi, Y. Total Synthesis of Dl-Metaphanine. *Tetrahedron Lett.* **2001**, *15*, 1393–1396.

(83) Keely, S.; Martinez, A.; Tahk, F. The 3-Arylpyrrolidine Alkaloid Synthon: A Formal Total Synthesis of Cepharamine Utilizing and Endocyclic Enamine. *Tetrahedron* **2001**, *26*, 4729–4742.

(84) Inubushi, Y.; Kitano, M.; Ibuka, T. Total Synthesis of Dl-Cepharamine. *Chem. Pharm. Bull. (Tokyo).* **1971**, *19*, 1820–1841.

(85) Magnus, P.; Seipp, C. Concise Synthesis of the Hasubanan Alkaloid (±)-Cepharatine A Using a Suzuki Coupling Reaction To Effect O, P-Phenolic Coupling. *Org. Lett.* **2013**, *15*, 4870–4871.

(86) Kametani, T.; Kobari, T.; Fukumoto, K. Synthesis of the Hasubanan Ring System from the Alkaloid Reticuline. *J. Chem. Soc. Chem. Commun.* **1972**, 288.

(87) Belleau, B.; Wong, H.; Monkovi, I.; Perron, Y. Total Synthesis of 3,14-Dihydroxyisomophinans and 9-Hydroxy-3-Methoxyhasubanans. *J. Chem. Soc. Chem. Commun.* **1974**, 603.

(88) Schwarta, M. A.; Wallance, R. A. Synthesis of Morphine Alkaloid Analogs. Hasubanans and 9,17-Secomorphinans. *Tetrahedron Lett.* **2001**, *35*, 3257–3260.

(89) Shiotani, S.; Kometani, T. A Novel Synthesis of Hasubanan Skeleton. *Tetrahedron Lett.* **2001**, *10*, 767–770.

(90) Kametani, T.; Kobari, T.; Shishido, K.; Fukumoto, K. Studies on the Syntheses of Heterocyclic compounds–DXLVII. Synthesis of a Hasubanan Ring System from Benylisoquinline Reticuline. *Tetrahedron* **2001**, *30*, 1059–1064.

(91) Evans, D. A.; Bryan, C.; Sims, C. The Complementarity of (4+2) Cycloaddition Reactions and [2,3] Sigmatropic Rearrangments in Synthesis. A New Synthesis of Functionalized Hasubanan Derivatives. *J. Am. Chem. Soc.* **2001**, *94*, 2891–2892.

(92) Evans, D. An Approach to the Synthesis of the Hasbanan Carbocyclic System. *Tetrahedron Lett.* **2001**, *20*, 1573–1576.

(93) Evans, D. A.; Bryan, C.; Wahl, G. M. Total Synthesis of Naturally Occurring Substances. II. The Synthesis of the Hasubanan Carbocyclic System. *J. Org. Chem.* **2003**, *35*, 4122–4127.

(94) Jones, S. B.; He, L.; Castle, S. L. Total Synthesis of (±)-Hasubanonine. *Org. Lett.* **2006**, *8*, 3757–3760.

(95) Nguyen, T. X.; Kobayashi, Y. Synthesis of the Common Propellane Core Structure of the Hasubanan Alkaloids. *J. Org. Chem.* **2008**, *73*, 5536–5541.

(96) Nielsen, D. K.; Nielsen, L. L.; Jones, S. B.; Toll, L.; Asplund, M. C.; Castle, S. L. Synthesis of Isohasubanan Alkaloids via Enantioselective Ketone Allylation and Discovery of an Unexpected Rearrangement. *J. Org. Chem.* **2008**, *74*, 1187–1199.

(97) Chuang, K.; Navarro, R.; Reisman, S. Benzoquinone-Derived Sulfinyl Imines as Versatile Intermediates for Alkaloid Synthesis: Total Synthesis of (–)-3-Demethoxyerythratidinone. *Chem. Sci.* **2011**, *2*, 1086.

(98) Calandra, N. A.; King, S. M.; Herzon, S. B. Development of Enantioselective Synthetic Routes to the Hasubanan and Acutumine Alkaloids. *J. Org. Chem.* **2013**, *78*, 10031–10057.

(99) Jacquet, Y. F.; Klee, W. A.; Rice, K. C.; Iijima, I.; Minamikawa, J. Stereospecific and Nonstereospecific Effects of (+)- and (–)-Morphine: Evidence for a New Class of Receptors? *Science.* **1977**, *198*, 842–845.

(100) Iijima, I.; Minamikawa, J.-J.; Jacobson, A. E.; Brossi, A.; Rice, K. C. Studies in the (+)-Morphinan Series 4. A Markedly Improved Synthesis of (+)-Morphine. *J. Org. Chem.* **1978**, *43*, 1492–1493.

(101) Hsin, L.-W.; Chang, L.-T.; Rothman, R. B.; Dersch, C. M.; Fishback, J. A.; Mastumoto, R. R. Synthesis and Opioid Activity of Enantiomeric N-Substituted 2,3,4,4a,5,6,7,7a-Octahydro-1H-benzofuro[3,2-E]isoquinolines. *J. Med. Chem.* **2010**, *53*, 1392–1396.

(102) Ananthan, S.; Saini, S. K.; Dersch, C. M.; Xu, H.; McGlinchey, N.; Giuvelis, D.; Bilsky, E. J.; Rothman, R. B. 14-Alkoxy-and 14-Acyloxypyridomorphinans: M Agonist/δ Antagonist Opioid Analgesics with Diminished Tolerance and Dependence Side Effects. *J. Med. Chem.* **2012**, *55*, 8350–8363.

(103) Schmidhammer, H. Opioid Receptor Antagonists. *Prog. Med. Chem.* **1998**, *35*, 83–132.

(104) Takemori, A. E.; Portoghese, P. S. Selective Naltrexone-Derived Opioid Receptor Antagonists. *Annu. Rev. Pharmacol. Toxicol.* **1992**, *32*, 239–269.

(105) Dondio, G.; Ronzoni, S.; Petrillo, P. Non-Peptide Δ Opioid Agonists and Antagonists. *Expert Opin. Ther. Patents* **1997**, *7*.

(106) Chen, Y.; Mestek, A.; Liu, J.; Yu, L. Molecular Cloning of a Rat K Opioid Reveals Sequence Similarities to the M and Δ Opioid Receptors. *Biochem. J.* **1993**, *295*, 625–628.

(107) Canesi, S.; Belmont, P.; Bouchu, D.; Rousset, L.; Ciufolini, M. A. Efficient Oxidative Spirocyclization of Phenolic Sulfonamides. *Tetrahedron Lett.* **2002**, *43*, 5193–5195.

(108) Dohi, T.; Maruyama, A.; Minamitsuji, Y.; Takenaga, N.; Kita, Y. First Hypervalent Iodine(III)-Catalyzed C–N Bond Forming Reaction: Catalytic Spirocyclization of Amides to N-Fused Spirolactams. *Chem. Commun.* **2007**, *12*, 1224.

(109) Liang, H.; Ciufolini, M. A. Synthetic Aspects of the Oxidative Amidation of Phenols. *Tetrahedron* **2010**, *66*, 5884–5892.

(110) Liang, H.; Ciufolini, M. A. Improved Procedure for the Bimolecular Oxidative Amidation of Phenols. *J. Org. Chem.* **2008**, *73*, 4299–4301.

(111) Liang, J.; Chen, J.; Du, F.; Zeng, X.; Li, L.; Zhang, H. Oxidative Carbon-Carbon Bond Formation in the Synthesis of Bioactive Spiro Beta-Lactams. *Org. Lett.* **2009**, *11*, 2820–2823.

(112) Quideau, S. P.; Pouysegu, L.; Avellan, A. V; Whelligan, D. K.; Looney, M. A. Hypervalent Iodine(III)-Mediated Oxidative Acetoxylation of 2-Methoxyphenols for Regiocontrolled Nitrogen Benzannulation. *Tetrahedron Lett.* **2001**, *42*, 7393–7396.

(113) Liu, H.; Tran, D. D. Intramolecular Friedel-Crafts Alkylation Promoted by the Cross Conjugated B-Keto Ester System. An Efficient Approach to Highly Functionalized Hydrophenanthrenes and Hydrochrysenes. *Tetrahedron Lett.* **1999**, *40*, 3827–3830.

(114) Ueno, A.; Kitawaki, T.; Chida, N. Total Synthesis of (±)-Murrayazoline. *Org. Lett.* **2008**, *10*, 1999–2002.

(115) Taber, D. F.; Sheth, R. B. A Three-Step Route to a Tricyclic Steroid Precursor. *J. Org. Chem.* **2008**, *73*, 8030–8032.

(116) Kodama, S.; Takita, H.; Kajimoto, T.; Nishide, K.; Node, M. Synthesis Of *Amaryllidaceae* Alkaloids, Siculine, Oxocrinine, Epicrinine, and Buflavine. *Tetrahedron* **2004**, *60*, 4901–4907.

(117) Bru, C.; Guillou, C. Total Syntheses of Crinine and Related Alkaloids. *Tetrahedron* **2006**, *62*, 9043–9048.

(118) Ward, R. S.; Hughes, D. D. Oxidative Cyclisation of *Cis*-and *Trans*-2, 3-Dibenzylbutyrolactones Using Phenyl Iodonium Bis (trifluoroacetate) and 2, 3-Dichloro-5, 6-Dicyano-1, 4-Benzoquinone. *Tetrahedron* **2001**, *57*, 5633–5639.

(119) Prager, R. H.; Tan, Y. T. Selective Demethylation of 3,4-Dimethoxybenzaldehyde. *Tetrahedron Lett.* **1967**, *38*, 3661–3664.

(120) Alam, A.; Takaguchi, Y.; Ito, H.; Yoshida, T.; Tsuboi, S. Multi-Functionalization of Gallic Acid towards Improved Synthesis of A- and B-DDB. *Tetrahedron* **2005**, *61*, 1909–1918.

(121) Zhang, W.; Zhao, R.; Ren, J.; Ren, L.; Lin, J.; Liu, D.; Wu, Y.; Yao, X. Synthesis and Anti-Proliferative in-Vitro Activity of Two Natural Dihydrostilbenes and Their Analogues. *Arch. Pharm. Chem* **2007**, *340*, 244–250.

(122) Wu, G.; Guo, H.; Gao, K.; Liu, Y.; Bastow, K.; Morris-Natschke, S.; Lee, K.; Xie, L. Synthesis of Unsymmetrical Biphenyls as Potent Cytotoxic Agents. *Bioorg. Med. Chem. Lett.* **2008**, *18*, 5272–5276.

(123) Amatore, C.; Pfluger, F. Mechanism of Oxidative Addition of Palladium (0) with Aromatic Iodides in Toluene, Monitored at Ultramicroelectrodes. *Organometallics* **1990**, *9*, 2276–2282.

(124) Stille, J. K.; Lau, K. S. Mechanisms of Oxidative Addition of Organic Halides to Group 8 Transition-Metal Complexes. *Acc. Chem. Res.* **1977**, *10*, 434–442.

(125) Rudyanto, M.; Kobayashi, K.; Honda, T. Synthetic Studies on Natural Isocoumarins and Isocarbostyril Derivatives Having an Alkyl Substituent at the 3-Position: Total Synthesis of Scoparines A and B, and Ruprechstyril. *Heterocycles* **2009**, *79*, 753–764.

(126) Dreher, S.; Lim, S.; Sandrock, D.; Molander, G. Suzuki− Miyaura Cross-Coupling Reactions of Primary Alkyltrifluoroborates with Aryl Chlorides. *J. Org. Chem.* **2009**, *74*, 3626–3631.

(127) Littke, A. F.; Fu, G. C. A Convenient and General Method for Pd□catalyzed Suzuki Cross□couplings of Aryl Chlorides and Arylboronic Acids. *Angew. Chem. Int. Ed.* **1998**, *37*, 3387–3388.

(128) Littke, A. F.; Dai, C.; Fu, G. C. Versatile Catalysts for the Suzuki Cross-Coupling of Arylboronic Acids with Aryl and Vinyl Halides and Triflates under Mild Conditions. *J. Am. Chem. Soc.* **2000**, *122*, 4020–4028.

(129) Wolfe, J.; Singer, R. A.; Yang, B. H.; Buchwald, S. L. Highly Active Palladium Catalysts for Suzuki Coupling Reactions. *J. Am. Chem. Soc.* **1999**, *121*, 9550–9561.

(130) Old, D. W.; Wolfe, J.; Buchwald, S. L. A Highly Active Catalyst for Palladium-Catalyzed Cross-Coupling Reactions: Room-Temperature Suzuki Couplings and Amination of Unactivated Aryl Chlorides. *J. Am. Chem. Soc.* **1998**, *120*, 9722–9723.

(131) Molander, G.; Katona, B.; Machrouhi, F. Development of the Suzuki-Miyaura Cross-Coupling Reaction: Use of Air-Stable Potassium Alkynyltrifluoroborates in Aryl Alkynylations. *J. Org. Chem.* **2002**, *67*, 8416–8423.

(132) Brown, H.; Choi, Y.; Narasimhan, S. Improved Prodedure for Borane-Dimethyl Sulfide Reduction of Nitriles. *Syntheis* **1981**, 605–606.

(133) Soderqust, J.; Negron, A. 9-Borabicyclo[3.3.1]nonane Dimer. *Org. Synth.* **2006**, *70*, 169.

(134) Kalinin, A.; Scherer, S.; Snieckus, V. Di(isopropylprenyl)borane: A New Hydroboration Reagent for the Synthesis of Alkyl and Alkenyl Boronic Acids. *Angew. Chem. Int. Ed.* **2003**, *42*, 3399–3404.

(135) Beletskaya, I. P.; Cheprakov, A. V. The Heck Reaction as a Sharpening Stone of Palladium Catalysis. *Chem. Rev.* **2000**, *100*, 3009–3066.

(136) Reddy, M. A.; Jain, N.; Yada, D.; Kishore, C.; Vangala, J. R.; P. Surendra, R.; Addlagatta, A.; Kalivendi, S. V; Sreedhar, B. Design and Synthesis of Resveratrol-Based Nitrovinylstilbenes as Antimitotic Agents. *J. Med. Chem.* **2011**, *54*, 6751–6760.

(137) Valente, C.; Çalimsiz, S.; Hoi, K.; Mallik, D.; Sayah, M.; Organ, M. The Development of Bulky Palladium NHC Complexes for the Most-Challenging Cross-Coupling Reactions. *Angew. Chem. Int. Ed.* **2012**, *51*, 3314–3332.

(138) Song, J. I.; An, D. K. New Method for Synthesis of Aldehydes from Esters by Sodium Diisobutyl-T-Butoxyaluminum Hydride. *Chem. Lett.* **2007**, *36*, 886–887.

(139) Hansen, H. C.; Chiacchia, F. S.; Patel, R.; Wong, N. C.; Khlebnikov, V.; Jankowska, R.; Patel, K.; Reddy, M. M. Stilbene Analogs as Inducers of Apolipoprotein-I Transcription. *Eur. J. Med. Chem.* **2012**, *45*, 2018–2023.

(140) Dohi, T.; Uchiyama, T.; Yamashita, D.; Washimi, N.; Kita, Y. Efficient Phenolic Oxidations Using I M-Oxo-Bridged Phenyliodine Trifluoroacetate. *Tetrahedron Lett.* **2011**, *52*, 2212–2215.

(141) Yasui, Y.; Koga, Y.; Suzuki, K.; Matsumoto, T. A Novel Approach to Erythrinan Alkaloids by Utilizing Substituted Biphenyl as Building Block. *Synlett* **2004**, 615–618.

EXPERIMENTAL APPENDIX

Materials and Methods

Unless otherwise stated, reactions were performed in flame- or oven-dried glassware under an argon or nitrogen atmosphere using anhydrous solvents. Acetic acid was distilled from acetic anhydride with CrO_3 or $KMnO_4$. Acetonitrile, CH_2Cl_2, and toluene were dried by passage through an activated alumina column under nitrogen. Dimethyl sulfoxide (DMSO) was placed over activated alumina overnight, and then distilled from CaH_2 and stored over 4Å molecular sieves. Methanol was dried over 3Å molecular sieves. 1,4-Dioxane and tetrahydrofuran (THF) were distilled from sodium/benzophenone. Powdered 4Å molecular sieves were activated by heating under vacuum and stored at 90 ºC until use. $Pd(OAc)_2$ was purchased from Strem Chemicals. Unless otherwise stated, reactions were monitored using thin-layer chromatography (TLC) using plates precoated with silica gel XHL w/ UV254 (250 μm) and visualized by UV light or $KMnO_4$, phosphomolybdic acid, or anisaldehyde stains, followed by heating. Silica gel (particle size 32–63 μm) was used for flash column chromatography. ^1H and ^{13}C NMR spectra are reported relative to the residual solvent peak (δ 7.26 and δ 77.2 for ^1H and ^{13}C in $CDCl_3$, δ 7.16 and δ 128.0 for ^1H and ^{13}C in C_6D_6, respectively), or tetramethylsilane (δ 0.00 for ^1H) when the residual solvent peak is obscured. Data for ^1H NMR spectra are reported as follows: chemical shift (ppm) (multiplicity, coupling constant (Hz), integration). Multiplicity is described using the following abbreviations: s

= singlet, d = doublet, t = triplet, q = quartet, hept = heptet, m = multiplet, bs = broad singlet. IR samples were prepared on NaCl plates either neat or by evaporation from $CHCl_3$ or CH_2Cl_2.

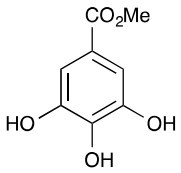

methyl 3,4,5-trihydroxybenzoate (3.11)

Into a round-bottom flask equipped with a stir bar was placed gallic acid (5.0 g, 0.29 mol), sulfuric acid (10 mL) and methanol (200 mL). The flask was fitted with a reflux condenser and slowly warmed to reflux. After refluxing overnight, the reaction was cooled to room temperature and concentrated by rotary evaporation. The crude product was recrystallized from ethanol and water (90:10) to afford a transparent crystalline product (5.41 g, quant.). Identity was verified by comparison of ^{1}H NMR spectrum with literature data[1]

---

[1] Alam, A.; Takaguchi, Y.; Ito, H.; Yoshida, T.; Tsuboi, S. Multi-functionalization of gallic acid towards improved synthesis of α- and β-DDB. *Tetrahedron* **2005**, *61*, 1909–1918.

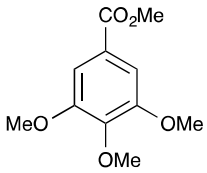

methyl 3,4,5-trimethoxybenzoate (3.12)

Into a round-bottom flask equipped with a stir bar was placed methyl 3,4,5-trihydroxybenzoate (**3.11**) (500 mg, 2.7 mmol), potassium carbonate (1.87 g, 13.57 mmol), and DMF (20.0 mL). The flask was stirred at room temperature for 1 hour. At this time, dimethylsulfate (3.0 g, 8.10 mmol) was added to the mixture. After stirring overnight, the mixture was then quenched with H_2O (60 mL) and extracted with EtOAc (3 x 100 mL). The combined organic extracts were washed with brine (100 mL), dried with Na_2SO_4, filtered, and concentrated. The resulting oil was purified by flash chromatography (SiO_2, 10:1 hexane:EtOAc) to afford a white solid (488.6 mg, 80 %). Identity was verified by comparison of ^1H NMR spectrum with literature data.[2]

---

[2] Brossi, A.; Guien, H.; Rachlin, A. I.; Teitel, S. Selective Demethylation of 3,4-Dimethoxy- Substituted Aromatic Aldehydes and Ketones. *J. Org. Chem.* **1967**, *32*, 1269–1270.

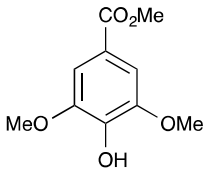

methyl 4-hydroxy-3,5-dimethoxybenzoate (3.13)

Into a round-bottom flask equipped with a stir bar was placed methyl 3,4,5-trimethoxybenzoate (**3.12**) (400 mg, 1.7 mmol) and sulfuric acid (10 mL). The flask was fitted with a reflux condenser and slowly warmed to 80 °C. After stirring overnight, the mixture was then cooled to room temperature and quenched with sat'ed $NaHCO_3$ (30 mL) and extracted with EtOAc (3 x 100 mL). The combined organic extracts were washed with brine (100 mL), dried with Na_2SO_4, filtered, and concentrated. The resulting powder was purified by flash chromatography (SiO_2, 8:1 hexane:EtOAc) to afford an amorphous white solid (328.2 mg, 91 %). Identity was verified by comparison of ^1H NMR spectrum with literature data.[3]

---

[3] Prager, R. H.; Tan, Y. T. Selective Demethylation of 3,4-Dimethoxybenzaldehyde. *Tetrahedron Lett.* **1967**, *38*, 3661–3664.

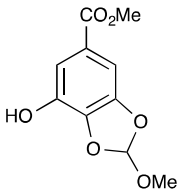

methyl-7-hydroxy-2-methoxybenzo[*d*][1,3]dioxole-5-carboxylate (3.14)

Into a round-bottom flask equipped with a stir bar was placed methyl gallate (**3.11**) (5.0 g, 0.3 mol), Amberlyst 15E (1.5g, 15 mg/mL), methyl orthoformate (9.54 g, 0.9 mol) and Benzene (150 mL). The flask was fitted with a reflux condenser and slowly warmed to reflux. After refluxing for 4 hours, the reaction was cooled to room temperature, filtered and concentrated by rotary evaporation. The residue extracted with EtOAc (3 x 100 mL). The combined organic extracts were washed with brine (100 mL), dried with Na_2SO_4, filtered, and concentrated. The resulting powder was purified by flash chromatography (SiO_2, 6:1 hexane:EtOAc) to afford an amorphous white solid (5.76 g, 85 %).

^{1}H NMR (300 MHz, $CDCl_3$) δ 7.45 (d, 1H, *J*= 1.5), 7.21 (d, 1H, *J*=1.5), 6.95 (s, 1H), 3.89 (s, 3H), 3.44 (s, 3H)

^{13}C NMR (75 MHz, $CDCl_3$) δ 167.4, 147.9, 139.2, 137.7, 124.9, 121.0, 114.6, 103.4, 53.1, 50.9

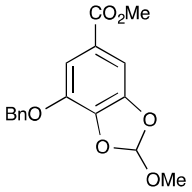

methyl-7-(benzyloxy)-2-methoxybenzo[*d*][1,3]dioxole-5 –carboxylate (3.15)

Into a round-bottom flask equipped with a stir bar was placed methyl benzoate (**3.14**) (618 mg, 2.73 mmol), potassium carbonate (755.5 mg, 5.46 mmol), and DMF (27.3 mL). The flask was fitted with a reflux condenser and slowly warmed to 60 °C. At this time, benzyl bromide (0.65 mL, 5.46 mmol) was added and the mixture warmed to 80 °C. After stirring overnight, the mixture was then cooled to room temperature and quenched with H_2O (30 mL) and extracted with EtOAc (3 x 100 mL). The combined organic extracts were washed with brine (100 mL), dried with Na_2SO_4, filtered, and concentrated. The resulting oil was purified by flash chromatography (SiO_2, 100 % hexane until removal of benzyl bromide, then 6:1 hexane:EtOAc) to afford an amorphous white solid (845.6 mg, 98 %).

^{1}H NMR (300 MHz, $CDCl_3$) δ 7.44-7.42 (m, 5H), 7.35 (s, 1H), 7.32 (s, 1H), 6.94 (s, 1H), 5.22 (s, 1H), 3.88 (s, 3H), 3.40 (s, 3H)

^{13}C NMR (75 MHz, $CDCl_3$) δ 147.9, 139.1, 136.8, 134.3, 129.3, 128.9, 128.3, 125.0, 120.9, 112.6, 104.2, 72.2, 52.9, 50.8

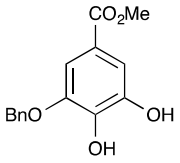

methyl 3-(benzyloxy)-4,5-dihydroxybenzoate (3.16)

Into a round-bottom flask equipped with a stir bar was placed methyl-7-(benzyloxy)-2-methoxybenzocarboxylate **(3.15)** (824.6 mg, 2.60 mmol), hydrochloric acid (2.5 mL, 2N) and MeOH (50.0 mL). After stirring at room temperature for 2 hours, the mixture was quenched with sat'd $NaHCO_3$ (50 mL) concentrated by rotary evaporation. The resulting residue was extracted with EtOAc (3 x 100 mL). The combined organic extracts were washed with brine (100 mL), dried with Na_2SO_4, filtered, and concentrated. The resulting residue was purified by flash chromatography (SiO_2, 100 % 1:1 hexane:EtOAc) to afford an amorphous white solid (684.6 mg, 96 %).

^{1}H NMR (300 MHz, $CDCl_3$) δ 7.44-7.42 (m, 5H), 7.26 (s, 2H), 7.32 (s, 1H), 5.79 (s, 1H), 5.33 (s, 1H), 5.12 (s, 2H) 3.88 (s, 3H)

^{13}C NMR (75 MHz, $CDCl_3$) δ 155.7, 137.6, 134.7, 129.5, 129.4, 128.9, 111.8, 109.3, 107.6, 100.9, 72.2, 52.8

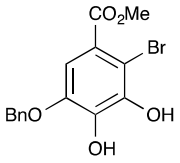

methyl 5-(benzyloxy)-2-bromo-3,4-dihydroxybenzoate (3.17)[4]

Into a round-bottom flask equipped with a stir bar and covered with foil was placed methyl 3-(benzyloxy)-4,5-dihydroxybenzoate (**3.16**) (684.6 mg, 2.40 mmol), and chloroform (7.0 mL). At this time, DBDMH (356.8 mg, 1.26 mmol) was added to the mixture After stirring at room temperature overnight, the mixture was quenched with sat'd Na_2SO_3 (10 mL) extracted with DCM (3 x 10 mL). The combined organic extracts were washed with brine (10 mL), dried with Na_2SO_4, filtered, and concentrated. The resulting residue was purified by flash chromatography (SiO_2, 4:1 hexane:EtOAc) to afford an amorphous white solid (653 mg, 75 %).

^{1}H NMR (300 MHz, $CDCl_3$) δ 7.44-7.42 (m, 5H), 7.28 (s, 1H), 5.94 (s, 1H), 5.91 (s, 1H) 5.14 (s, 2H), 3.88 (s, 3H)

[4] Alam, A.; Takaguchi, Y.; Ito, H.; Yoshida, T.; Tsuboi, S. Multi-functionalization of gallic acid towards improved synthesis of α- and β-DDB. *Tetrahedron* **2005**, *61*, 1909–1918.

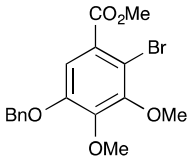

methyl 5-(benzyloxy)-2-bromo-3,4-dimethoxybenzoate (3.18)

Into a round-bottom flask equipped with a stir bar was placed methyl 5-(benzyloxy)-2-bromo-3,4-dihydroxybenzoate (**3.17**) (690.1 mg, 1.95 mmol), potassium carbonate (674.46 mg, 4.88 mmol), and DMF (10.0 mL). The flask was stirred at room temperature for 1 hour. At this time, dimethylsulfate (0.388 mL, 4.095 mmol) was added and the mixture. After stirring overnight, the mixture was then quenched with H_2O (30 mL) and extracted with EtOAc (3 x 100 mL). The combined organic extracts were washed with brine (100 mL), dried with Na_2SO_4, filtered, and concentrated. The resulting oil was purified by flash chromatography (SiO_2, 6:1 hexane:EtOAc) to afford a white solid (691.3 mg, 93 %).

^{1}H NMR (300 MHz, $CDCl_3$) δ 7.44-7.42 (m, 5H), 7.24 (s, 1H), 5.06 (s, 1H), 3.89 (s, 3H), 3.85 (s, 6H)

^{13}C NMR (75 MHz, $CDCl_3$) δ 166.0, 151.2, 146.3, 135.8, 128.4, 127.9, 127.2, 127.1, 111.7, 109.6, 70.9, 60.9, 60.8, 52.2

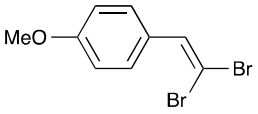

1-(2,2-dibromovinyl)-4-methoxybenzene (3.20)

A 1.7 M solution of PPh_3 (21.6 g, 0.8 mol) in dry DCM was added dropwise to a 0.7 M solution of CBr_4 (12.1 g, 0.36 mol) in dry DCM at 0 °C, under a nitrogen atmosphere, over 30 minutes. The reaction was stirred at 0 °C for 30 min to develop a red slurry, before adding the 4-methoxybenzaldehyde (2.23 mL, 0.18 mmol) dropwise. The reaction was left stirring at 0 °C for 1 h. The reaction was diluted with 100 mL of DCM, which was followed by addition of 50 mL of petroleum ether, used to precipitate the triphenylphopshine oxide. The supernatant liquid was decanted and then a further 100 mL of DCM as well as 50 mL of petroleum ether were added to the precipitate. This procedure was repeated once more, before drying the combined supernatant fractions over Na_2SO_4, filtering, and concentrating them under reduced pressure. The crude product was then dry loaded onto a silica gel column and purified by flash chromatography (SiO_2, 20:1 hexane:EtOAc) to afford a cream yellow solid (21.0 g, 40 %). Identity was verified by comparison of ^{1}H NMR spectrum with literature data.[5]

---

5 Michaelides, I. N.; Darses, B.; Dixon, D. J. Acid-catalyzed Synthesis of Bicyclo[3.n.1]alkenediones. *Org. Lett.* **2011**, *13*, 664–667.

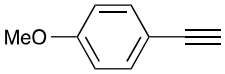

1-ethynyl-4-methoxybenzene (3.21)

To a 0.07 M solution of the 1-(2,2-dibromovinyl)-4-methoxybenzene **(3.20)** (2.00 g, 6.85 mmol) in anhydrous THF at –78 °C, under a nitrogen atmosphere, *n*-BuLi (2.4 equiv.) was added dropwise. The reaction mixture was left stirring for 1h at –78 °C before allowing the flask to warm to room temperature for 1 h. The reaction was then cooled down to 0 °C and H_2O (10 mL) was added in one portion. The reaction was then allowed to reach room temperature over 4 h. The reaction was quenched using sat'ed NH_4Cl (aq) and extracted with EtOAc (3 x 250 mL). The combined organic extracts were dried over Na_2SO_4, filtered, and concentrated under reduced pressure. The crude product was purified by flash chromatography (SiO_2, 20:1 hexane:EtOAc) to afford a yellow oil (688.02 mg, 76 %). Identity was verified by comparison of ^1H NMR spectrum with literature data.[6]

---

6 Michaelides, I. N.; Darses, B.; Dixon, D. J. Acid-catalyzed Synthesis of Bicyclo[3.n.1]alkenediones. *Org. Lett.* **2011**, *13*, 664–667.

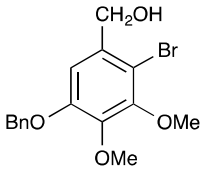

(5-(benzyloxy)-2-bromo-3,4-dimethoxyphenyl)methanol (3.22)

To a solution of methyl 5-(benzyloxy)-2-bromo-3,4-dimethoxybenzoate **(3.18)** (150.0 mg, 0.39 mmol) in anhydrous THF at –78 °C, under a nitrogen atmosphere, DIBALH (117.3 mg, 0.83 mmol) was added dropwise. The reaction mixture was left stirring for 3h at –78 °C before allowing the flask to warm to room temperature for 1 h. The reaction was quenched with Rochelle's salt (10 mL) and was stirred for 1 H. At this time, the reaction was filtered over celite and concentrated by rotary evaporation. The crude product was purified by flash chromatography (SiO_2, 20:1 hexane:EtOAc) to afford a cream solid (115 mg, 83 %).

^{1}H NMR (300 MHz, $CDCl_3$) δ 7.44-7.42 (m, 5H), 6.95 (s, 1H), 5.12 (s, 2H), 4.65 (s, 2H), 3.90 (s, 6H)

^{13}C NMR (75 MHz, $CDCl_3$) δ 151.8, 150.7, 142.6, 136.3, 135.1, 128.4, 127.6, 127.1, 109.2, 108.4, 70.8, 64.7, 60.9, 60.8

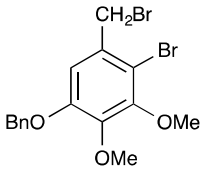

1-(benzyloxy)-4-bromo-5-(bromomethyl)-2,3-dimethoxybenzene (3.23)

Into a round-bottom flask equipped with a stir bar was placed (5-(benzyloxy)-2-bromo-3,4-dimethoxyphenyl)methanol **(3.22)** (115 mg, 0.33 mmol), PPh_3 (128.6 mg, 0.49 mmol), and DCM (7.0 mL). The mixture was stirred at room temperature for 30 min. At this time, *N*-bromosuccinimide (87.2 mg, 0.49 mmol) was added. After stirring overnight, the reaction was quenched with sat'ed $NaHCO_3$ (10 mL) and extracted with DCM (3 x 10 mL). The combined organic extracts were washed with brine (100 mL), dried with Na_2SO_4, filtered, and concentrated. The resulting oil was purified by flash chromatography (SiO_2, 100 % 20:1 hexane:EtOAc) to afford an yellow oil (85.1 mg, 62 %).

^{1}H NMR (300 MHz, $CDCl_3$) δ 7.44-7.42 (m, 5H), 6.88 (s, 1H), 5.12 (s, 2H), 4.57 (s, 2H), 3.91 (s, 6H)

^{13}C NMR (75 MHz, $CDCl_3$) δ 151.7, 150.5, 146.1, 143.8, 136.0, 131.9, 128.4, 127.9, 127.2, 111.5, 70.9, 60.9, 60.8, 33.9

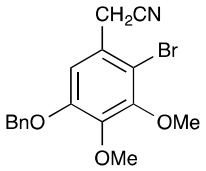

2-(5-(benzyloxy)-2-bromo-3,4-dimethoxyphenyl)acetonitrile (3.24)

Into a round-bottom flask equipped with a stir bar was placed 1-(benzyloxy)-4-bromo-5-(bromomethyl)-2,3-dimethoxybenzene **(3.23)** (85.8 mg, 0.206 mmol), KCN (20.1 mg, 0.31 mmol), and DMSO (2.0 mL). The mixture was stirred at 60 °C for 1 hr. At this time, the reaction was quenched with H_2O (10 mL) and extracted with EtOAc (3 x 10 mL). The combined organic extracts were washed with brine (100 mL), dried with Na_2SO_4, filtered, and concentrated. The resulting oil was purified by flash chromatography (SiO_2, 100 % 20:1 hexane:EtOAc) to afford an yellow oil (52.6 mg, 70 %).

^{1}H NMR (300 MHz, $CDCl_3$) δ 7.44-7.42 (m, 5H), 6.95 (s, 1H), 5.12 (s, 2H), 3.91 (s, 6H), 3.78 (s 2H)

^{13}C NMR (75 MHz, $CDCl_3$) δ 151.7, 150.5, 146.1, 143.8, 136.0, 131.9, 128.4, 127.9, 127.2, 111.5, 70.9, 60.9, 60.8, 33.9

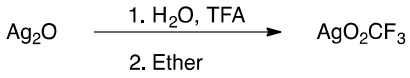

silver trifluoroacetate

A literature procedure was adapted.[7] To a suspension of 1.45 g. (6.25 mol) of silver oxide in 200 mL of water was added trifluoroacetic acid (1.36 g, 12.5 mol). The resulting solution was filtered, and evaporated to dryness under rotary evaporation. The dry silver trifluoroacetate was purified by dissolution in diethyl ether, filtering through activated carbon, and concentrating. Affording a colorless crystalline salt (1.18 g, 90 %).

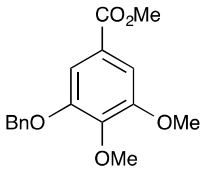

methyl 3-(benzyloxy)-4,5-dimethoxybenzoate (3.25)

Into a round-bottom flask equipped with a stir bar was placed methyl 3-(benzyloxy)-4,5-dihydroxybenzoate (**3.16**) (596.7 mg, 2.17 mmol), potassium carbonate (899.7 mg, 6.51 mmol), and DMF (10.0 mL). The flask was stirred at room temperature for 1 hour. At this time, dimethylsulfate (0.451 mL, 4.77 mmol) was added and the mixture. After stirring overnight, the mixture was then quenched with H_2O (30 mL) and extracted with

---

7 Janssen, D. E.; Wilson, C. 4□Iodoveratrole. *Org. Synth.* **1963**, *4*, 547–549.

EtOAc (3 x 100 mL). The combined organic extracts were washed with brine (100 mL), dried with Na_2SO_4, filtered, and concentrated. The resulting oil was purified by flash chromatography (SiO_2, 15:1 hexane:EtOAc) to afford a white solid (609.1 mg, 93 %).

^{1}H NMR (300 MHz, $CDCl_3$) δ 7.44-7.42 (m, 5H), 7.38 (d, 1H, *J* = 1.2 Hz), 5.16 (s, 2H), 3.93 (s, 3H), 3.91 (s, 3H), 3.90 (s, 3H)

^{13}C NMR (75 MHz, $CDCl_3$) δ 152.8, 142.6, 142.5, 136.4, 128.3, 127.8, 125.6, 124.8, 108.6, 106.8, 70.9, 60.7, 56.0, 51.9

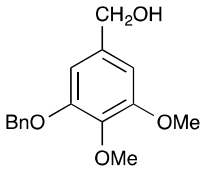

(3-(benzyloxy)-4,5-dimethoxyphenyl)methanol (3.28)

To a solution of methyl 3-(benzyloxy)-4,5-dimethoxybenzoate (**3.25**) (803.4 mg, 2.65 mmol) in anhydrous diethyl ether (10 mL) at 0 °C, under a nitrogen atmosphere, LAH (151.27 mg, 3.98 mmol) was added. The reaction mixture was left stirring for 3 h at 0 °C before allowing the flask to warm to room temperature for 1 h. The reaction was quenched with Feiser method and was stirred for 1 h. At this time, the reaction was filtered over celite and concentrated by rotary evaporation. The crude product was purified by flash chromatography (SiO_2, 20:1 hexane:EtOAc) to afford a white solid (705.1 mg, 97 %).

^{1}H NMR (300 MHz, $CDCl_3$) δ 7.44-7.42 (m, 5H), 6.63 (d, 1H, *J* = 1.2 Hz), 6.61 (d, 1H, *J* = 1.2 Hz), 5.13 (s, 2H), 4.59 (d, 2H, *J* = 4.2 Hz), 3.87 (s, 6H), 3.82 (brs, 1H)

^{13}C NMR (75 MHz, $CDCl_3$) δ 153.3, 136.8, 136.2, 128.3, 128.2, 127.9, 127.6, 127.0, 105.7, 103.9, 70.7, 65.2, 60.7, 55.9

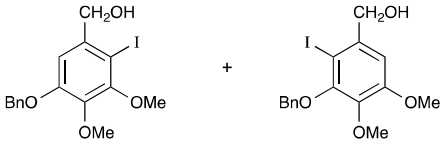

(5-(benzyloxy)-2-iodo-3,4-dimethoxyphenyl)methanol (3.29), (3.30)

Into a round-bottom flask equipped with a stir bar was placed (3-(benzyloxy)-4,5-dimethoxyphenyl)methanol (**3.28**) (369.3 mg, 1.34 mmol), dry silver trifluoroacetate (356.8 mg, 1.62 mmol), and DCM (10.0 mL). Iodine (357.09 mg, 1.41 mmol) was added portionwise. After iodine addition, the flask was stirred at room temperature for 1 h. At this time the mixture was filtered over celite and concentrated. The crude residue was extracted with DCM (3 x 50 mL). The combined organic extracts were washed with brine (50 mL), dried with Na_2SO_4, filtered, and concentrated. The resulting oil was purified by flash chromatography (SiO_2, 4:1 hexane:EtOAc) to afford a white solid (**3.29**, 59 %, **3.30**, 41 %).

3.29: ^{1}**H NMR** (300 MHz, $CDCl_3$) δ 7.44-7.42 (m, 5H), 6.98 (s, 1H), 5.13 (s, 2H), 4.61(s, 2H), 3.88 (s, 6H)

^{13}**C NMR** (75 MHz, $CDCl_3$) δ 152.9, 141.7, 138.0, 137.3, 136.3, 128.4, 127.8, 127.1, 109.5, 84.8, 70.8, 69.1, 60.9, 60.7

3.30: ^{1}**H NMR** (300 MHz, $CDCl_3$) δ 7.61 (apt d, 2H, J = 6 Hz) 7.44-7.42 (m, 5H), 5.03 (s, 2H), 4.64(s, 2H), 3.88 (s, 6H)

^{13}**C NMR** (75 MHz, $CDCl_3$) δ 152.8, 143.5, 141.6, 138.1, 136.3, 129.4, 128.3, 128.1, 127.8, 127.1, 109.4, 84.7, 70.8, 69.0, 60.7

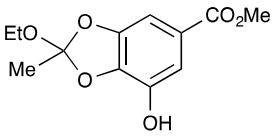

methyl 2-ethoxy-7-hydroxy-2-methylbenzo[*d*][1,3]dioxole-5-carboxylate (3.31)

Into a round-bottom flask equipped with a stir bar was placed methyl gallate (**3.11**) (1.78 g, 0.09 mol), Amberlyst 15E (48.3 mg, 15 mg/mL), trimethyl orthoacetal (4.71 g, 0.3 mol) and Benzene (100 mL). The flask was fitted with a reflux condenser and slowly warmed to reflux. After refluxing for 8 h, the reaction was cooled to room temperature, filtered and concentrated by rotary evaporation. The residue extracted with EtOAc (3 x 100 mL). The combined organic extracts were washed with brine (100 mL), dried with Na_2SO_4, filtered, and concentrated. The resulting powder was purified by flash chromatography (SiO_2, 15:1 hexane:EtOAc) to afford an amorphous white solid (1.86 g, 76 %).

^{1}H NMR (300 MHz, $CDCl_3$) δ 7.44 (dd, 1H, *J* = 1.5, 1.5 Hz), 7.12 (dd, 1H, *J* = 1.5, 1.5 Hz), 6.42 (s, 1H), 3.88 (s, 3H), 3.61 (q, 2H *J* = 7.2, 14.4 Hz), 1.83 (s, 3H), 1.18 (t, 3H, *J* = 7.2 Hz)

^{13}C NMR (75 MHz, $CDCl_3$) δ 167.8, 148.3, 139.0, 130.1, 124.1, 114.3, 102.9, 62.1, 59.1, 53.1, 25.3, 15.4

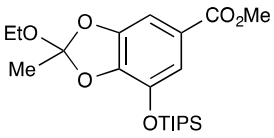

methyl-2-ethoxy-2-methyl-7-((triisopropylsilyl)oxy)benzo[*d*][1,3]dioxole-5 carboxylate (3.32)

Into a round-bottom flask equipped with a stir bar was placed methyl 2-ethoxy-7-hydroxy-2-methylbenzo[*d*][1,3]dioxole-5-carboxylate (**3.31**) (1.84 g, 7.2 mmol), imidazole (1.96 g, 28.9 mmol), DMAP (44.16 mg, 0.36 mmol) and DCM (24.0 mL). The mixture was stirred at room temperature for 10 min. At this time, TIPSCl (1.86 mL, 8.67 mmol) was added and the mixture was stirred overnight. After stirring overnight, the mixture was then quenched with H_2O (30 mL) and extracted with DCM (3 x 100 mL). The combined organic extracts were washed with brine (100 mL), dried with Na_2SO_4, filtered, and concentrated. The resulting oil was purified by flash chromatography (SiO_2, then 20:1 hexane:EtOAc) to afford yellow oil (2.89 g, 98 %).

^{1}H NMR (300 MHz, $CDCl_3$) δ 7.20 (s, 1H), 7.14 (s 1H), 3.86 (s, 3H), 3.59 (q, 2H *J* = 7.2, 12 Hz), 1.79 (s, 3H), 1.26 (t, 3H, *J* = 7.0 Hz), 1.20 (t, 3H, *J* = 7.2 Hz) 1.12 (d, 18 H, *J* = 7.0 Hz)

^{13}C NMR (75 MHz, $CDCl_3$) δ 166.3, 147.5, 140.4, 137.9, 128.6, 123.1, 117.3, 102.5, 58.1, 51.9, 24.4, 17.5, 14.6, 12.5

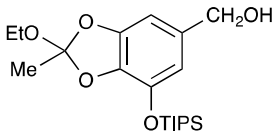

(2-ethoxy-2-methyl-7-((triisopropylsilyl)oxy)benzo[*d*][1,3]dioxol-5-yl)-methanol (3.33)

To a solution of methyl 3-(benzyloxy)-4,5-dimethoxybenzoate (**3.25**) (7.23 g, 17.6 mmol) in anhydrous diethyl ether (100 mL) at 0 °C, under a nitrogen atmosphere, LAH (1.00 g, 26.4 mmol) was added. The reaction mixture was left stirring for 4 h at 0 °C before allowing the flask to warm to room temperature for 1 h. The reaction was quenched with Feiser method and was stirred for 1 h. At this time, the reaction was filtered over celite and concentrated by rotary evaporation. The crude product was purified by flash chromatography (SiO_2, 20:1 hexane:EtOAc) to afford a white solid (1.87 g, 77 %).

^{1}H NMR (300 MHz, $CDCl_3$) δ 6.49 (d, 1H, *J* = 1.5 Hz), 6.47 (d, 1H, *J* = 1.5 Hz), 4.53 (d, 2H, *J* = 6 Hz), 3.61 (q, 2H *J* = 7.0, 14.0 Hz), 1.76 (s, 3H), 1.25 (t, 3H, *J* = 7.0 Hz), 1.19 (t, 3H, *J* = 7.2 Hz) 1.11 (d, 18 H, *J* = 7.2 Hz)

^{13}C NMR (75 MHz, $CDCl_3$) δ 148.7, 139.4, 136.7, 135.1, 128.8, 114.3, 101.1, 66.1, 58.7, 25.3, 18.5, 15.6, 13.4

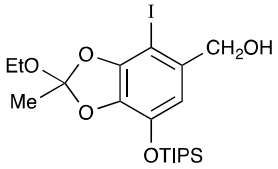

(2-ethoxy-4-iodo-2-methyl-7-((triisopropylsilyl)oxy)benzo[*d*][1,3]dioxol-5-yl)methanol (3.34)

Into a round-bottom flask equipped with a stir bar was placed (2-ethoxy-2-methyl-7-((triisopropylsilyl)oxy)benzo[*d*][1,3]dioxol-5-yl)methanol (**3.33**) (58.2 mg, 0.15 mmol), dry silver trifluoroacetate (40.2 mg, 0.18 mmol), and DCM (5.0 mL). Iodine (40.5 mg, 0.16 mmol) was added portionwise. After iodine addition, the flask was stirred at room temperature for 1 h. At this time the mixture was filtered over celite and concentrated. The crude residue was extracted with DCM (3 x 10 mL). The combined organic extracts were washed with brine (50 mL), dried with Na_2SO_4, filtered, and concentrated. The resulting oil was purified by flash chromatography (SiO_2, 10:1 hexane:EtOAc) to afford a white solid (15.2 mg, 20 %).

^{1}H NMR (300 MHz, $CDCl_3$) δ 6.27 (s, 1H), 4.51 (d, 2H, *J* = 6 Hz), 3.61 (q, 2H *J* = 7.0, 14.0 Hz), 1.77 (s, 3H), 1.25 (t, 3H, *J* = 7.0 Hz), 1.22 (t, 3H, *J* = 7.0 Hz) 1.11 (d, 18 H, *J* = 7.0 Hz)

^{13}C NMR (75 MHz, $CDCl_3$) δ 148.8, 139.1, 136.7, 135.1, 128.8, 114.3, 101.1, 66.1, 58.8, 25.2, 18.5, 15.6, 13.4

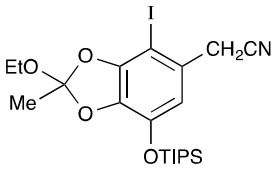

2-(2-ethoxy-4-iodo-2-methyl-7-((triisopropylsilyl)oxy)benzo[*d*][1,3]dioxol-5-yl)acetonitrile (3.35)

Into a round-bottom flask equipped with a stir bar was placed 2-(2-ethoxy-2-methyl-7-((triisopropylsilyl)oxy)benzo[d][1,3]dioxol-5-yl)acetonitrile (23.7 mg, 0.06 mmol), dry silver trifluoroacetate (14.5 mg, 0.07 mmol), and DCM (2.0 mL). Iodine (16.8 mg, 0.07 mmol) was added portionwise. After iodine addition, the flask was stirred at room temperature for 1 h. At this time the mixture was filtered over celite and concentrated. The crude residue was extracted with DCM (3 x 5 mL). The combined organic extracts were washed with brine (50 mL), dried with Na_2SO_4, filtered, and concentrated. The resulting oil was purified by flash chromatography (SiO_2, 10:1 hexane:EtOAc) to afford a white solid (19.8 mg, 64 %).

^{1}H NMR (300 MHz, $CDCl_3$) δ 6.15 (s, 1H), 4.33 (s, 2H), 3.88 (q, 2H *J* = 7.0, 12.0 Hz), 2.05 (s, 3H), 1.21 (t, 3H, *J* = 7.0 Hz), 1.18 (t, 3H, *J* = 7.0 Hz) 1.11 (d, 18 H, *J* = 7.0 Hz)

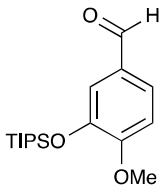

4-methoxy-3-((triisopropylsilyl)oxy)benzaldehyde (3.36)

Into a round-bottom flask equipped with a stir bar was placed isovanillin (2.27 g, 14.9 mmol), imidazole (4.10 g, 60.0 mmol), DMAP (91.0 mg, 0.75 mmol) and DCM (20.0 mL). The mixture was stirred at room temperature for 10 min. At this time, TIPSCl (3.83 mL, 17.88 mmol) was added and the mixture was stirred overnight. After stirring overnight, the mixture was then quenched with H_2O (30 mL) and extracted with DCM (3 x 100 mL). The combined organic extracts were washed with brine (100 mL), dried with Na_2SO_4, filtered, and concentrated. The resulting oil was purified by flash chromatography (SiO_2, 20:1 hexane:EtOAc) to afford white solid (4.48 g, 98 %).

^{1}H NMR (300 MHz, $CDCl_3$) δ 9.81 (s, 1H), 7.44 (dd 1H, *J* = 2.0, 8.0 Hz), 7.38 (d, 1H, *J* = 2.0 Hz), 6.95 (d, 1H, *J* = 8.0 Hz), 3.89 (s, 3H), 1.24 (t, 3H, *J* = 7.0 Hz), 1.10 (d, 18 H, *J* = 7.0 Hz)

^{13}C NMR (75 MHz, $CDCl_3$) δ 191.6, 157.2, 146.7, 130.7, 126.8, 119.9, 111.7, 56.2, 18.5, 13.5

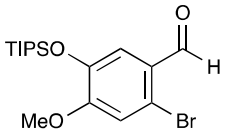

2-bromo-4-methoxy-5-((triisopropylsilyl)oxy)benzaldehyde (3.37)

Into a round-bottom flask equipped with a stir bar was placed 4-methoxy-3-((triisopropylsilyl)oxy)benzaldehyde (**3.36**) (2.30 g, 7.46 mmol), sat'ed $NaHCO_3$ (aq) (10 mL) and DCM (10.0 mL). The mixture was stirred at room temperature for 10 min. At this time, Br_2 (0.497 mL, 9.70 mmol) in DCM (10 mL) was added dropwise to the mixture and was stirred overnight. After stirring overnight, the mixture was then quenched with 10 % aq Na_2SO_3 (30 mL) and extracted with DCM (3 x 100 mL). The combined organic extracts were washed with brine (100 mL), dried with Na_2SO_4, filtered, and concentrated. The resulting oil was purified by flash chromatography (SiO_2, 20:1 hexane:EtOAc) to afford white solid (2.68 g, 93 %).

^{1}H NMR (300 MHz, $CDCl_3$) δ 10.14 (s, 1H), 7.41 (s, 1H), 7.02 (s, 1H), 3.89 (s, 3H), 1.25 (t, 3H, *J* = 7.0 Hz), 1.09 (d, 18 H, *J* = 7.0 Hz)

^{13}C NMR (75 MHz, $CDCl_3$) δ 191.3, 157.3, 146.1, 127.2, 120.4, 120.3, 116.6, 56.6, 32.7, 18.5, 13.4

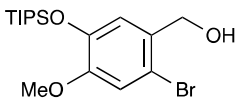

(2-bromo-4-methoxy-5-((triisopropylsilyl)oxy)phenyl)methanol (3.38)

To a solution of 2-bromo-4-methoxy-5-((triisopropylsilyl)oxy)benzaldehyde (**3.37**) (1.21 g, 3.1 mmol) in methanol (20 mL) at 0 °C, under a nitrogen atmosphere, $NaBH_4$ (141.3 mg, 3.73 mmol) was added. The reaction mixture was left stirring for 4 h at 0 °C before allowing the flask to warm to room temperature for 1 h. The reaction was quenched with 10 % aq $NaHCO_3$ (10 mL), and was stirred for 1 h. At this time, the reaction was filtered over celite and concentrated by rotary evaporation. The crude product was purified by flash chromatography (SiO_2, 4:1 hexane:EtOAc) to afford a white solid (1.10 g, 91 %).

^{1}H NMR (300 MHz, $CDCl_3$) δ 6.98 (apt d, 2H, *J* = 2.4 Hz)), 4.61 (s, 2H), 3.79 (s, 3H), 1.24 (t, 3H, *J* = 7.0 Hz), 1.09 (d, 18H, *J* = 7.0 Hz)

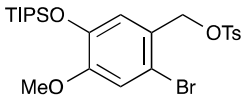

2-bromo-4-methoxy-5-((triisopropylsilyl)oxy)benzyl 4-methylbenzenesulfonate

To a solution of (2-bromo-4-methoxy-5-((triisopropylsilyl)oxy)phenyl)methanol (**3.38**) (1.10 g, 2.8 mmol), NEt_3 (0.597 mL, 4.25 mmol), DMAP (17.2 mg, 0.14 mmol) in DCM (15 mL) at room temperature TsCl (647.4 mg, 3.40 mmol) was added. The reaction mixture was left stirring overnight. The reaction was quenched with H_2O (10 mL), and extracted with DCM (3 x 10 mL). The combined organic extracts were washed with brine

(100 mL), dried with Na_2SO_4, filtered, and concentrated. The resulting oil was taken on crude.

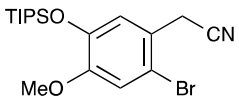

2-(2-bromo-4-methoxy-5-((triisopropylsilyl)oxy)phenyl)acetonitrile (3.39)

Into a μW vial equipped with a stir bar was placed 2-bromo-4-methoxy-5-((triisopropylsilyl)oxy)benzyl 4-methylbenzenesulfonate (1.42 g, 2.6 mmol), and KCN (424.6 mg, 6.52 mmol) in ACN (10 mL). The reaction mixture was μW at 100 °C for 30 min. At this time, the reaction transferred into a round bottom flask and concentrated by rotary evaporation. The residue was extracted into DCM (3 x 10 mL). The combined organic extracts were washed with brine (100 mL), dried with Na_2SO_4, filtered, and concentrated. The crude product was purified by flash chromatography (SiO_2, 4:1 hexane:EtOAc) to afford a yellow solid (652.6 mg, 63 %).

^{1}H NMR (300 MHz, $CDCl_3$) δ 6.99 (s, 1H), 6.95 (s, 1H), 4.60 (s, 2H), 3.79 (s, 3H), 1.19 (t, 3H, *J* = 7.0 Hz), 1.09 (d, 18 H, *J* = 7.0 Hz)

^{13}C NMR (75 MHz, $CDCl_3$) δ 152.3, 145.8, 129.2, 122.9, 116.7, 115.4, 116.7, 115.4, 56.3, 46.9, 32.7, 18.5, 13.5

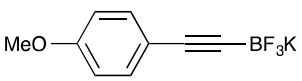

trifluoro((4-methoxyphenyl)ethynyl)-λ^4-borane, potassium salt (3.40)

To a 0.5 M solution of the 1-ethynyl-4-methoxybenzene (**3.21**) (960.2 mg, 7.26 mmol) in anhydrous THF at –78 °C, under a nitrogen atmosphere, *n*-BuLi (2.90 mL, 1.0 equiv.) was added dropwise. The reaction mixture was left stirring for 1h at –78 °C. At this time, trimethyl borate (1.21 mL, 10.89 mmol) was added and the mixture was stirred at –78 °C for an additional 1 h. The reaction was then allowed to reach –20 °C and sat'ed aq KHF_2 (12 mL) was added and the mixture was stirred for 1 h. After 1 h the reaction was concentrated and placed on a high vac to remove the water. The residue was taken up in acetone and filtered. The filtrate was washed with hot acetone and precipitated with diethyl ether. The white solid was filtered and washed with diethyl ether and dried (1.23 g, 70 %). Identity was verified by comparison of ^{1}H NMR spectrum with literature data.[8]

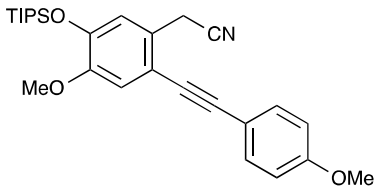

[8] Molander, G.; Katona, B.; Machrouhi, F. *J. Org. Chem.* **2002**, *67*, 8416–8423.

2-(4-methoxy-2-((4-methoxyphenyl)ethynyl)-5-((triisopropylsilyl)oxy)phenyl)acetonitrile (3.41)

Into a round-bottom flask equipped with a stir bar was placed 2-(2-bromo-4-methoxy-5-((triisopropylsilyl)oxy)phenyl)acetonitrile (**3.39**) (50.0 mg, 0.125 mmol), tri-potassium phosphate (106.13 mg, 0.5 mmol), SPhos (10.26 mg, 0.025 mmol), trifluoro((4-methoxyphenyl)ethynyl)-borane, potassium salt (**3.40**) (44.80, 0.18 mmol), $Pd(OAc)_2$ (2.84 mg, 0.0125 mmol) and THF (1.0 mL). The flask was fitted with a reflux condenser and slowly warmed to reflux. After refluxing for 4 hours, the reaction was cooled to room temperature, filter through silica and concentrated by rotary evaporation. The resulting oil was purified by flash chromatography (SiO_2, 10:1 hexane:EtOAc) to afford a white solid (16.5 mg, 28 %).

^{1}H NMR (300 MHz, $CDCl_3$) δ 7.33 (d, 2H, *J* = 2.0, 9.0 Hz), 7.23 (s, 1H), 6.98 (s, 1H), 6.84 (d, 2H, *J* = 2.0, 9.0 Hz), 3.95 (s, 2H), 3.83 (s, 3H), 3.82 (s, 3H) 1.23 (t, 3H, *J* = 7.0 Hz), 1.09 (d, 18 H, *J* = 7.0 Hz)

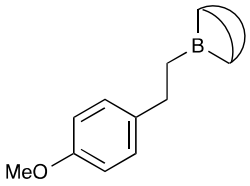

(4-methoxyphenethyl) 9-borabicyclo[3.3.1]nonane (3.43)

To a 0.5 M solution of 9-BBN dimer (180.0 mg, 0.74 mmol), in anhydrous THF, under a nitrogen atmosphere, 4-methoxystyrene (198.1 mg, 1.47 mmol) was added dropwise. The reaction was monitored by GC for the disappearance of 4-methoxystyrene. Once the starting material was consumed the product was taken on crude.

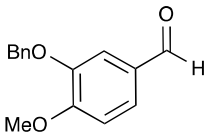

3-(benzyloxy)-4-methoxybenzaldehyde (3.45)

Into a round-bottom flask equipped with a stir bar was placed isovanillin (3.0 g, 19.7 mmol), potassium carbonate (8.17 g, 59.15 mmol), and ethanol (50.0 mL). The flask was fitted with a reflux condenser and slowly warmed to 60 °C. At this time, benzyl bromide (2.82 mL, 23.64 mmol) was added and the mixture warmed to 75 °C. After refluxing overnight, the mixture was then cooled to room temperature, filtered, and concentrated by rotary evaporation. The residue was extracted with EtOAc (3 x 100 mL). The combined organic extracts were washed with brine (100 mL), dried with Na_2SO_4, filtered, and concentrated. The resulting oil was purified by flash chromatography (SiO_2, 100 % hexane until removal of benzyl bromide, then 5:1 hexane:EtOAc) to afford an amorphous white solid (4.50 g, 94 %).

^{1}H NMR (500 MHz, $CDCl_3$) δ 9.82 (s, 1H), 7.48 (apt t, 1H, *J* = 3.0 Hz), 7.45 (s, 1H), 7.42-7.32 (m, 5H), 7.01 (d, 1H, *J* = 14.0 Hz), 5.19 (s, 2H), 3.96 (s, 3H)

^{13}C NMR (75 MHz, $CDCl_3$) δ 191.5, 149.3, 136.9, 136.6, 129.3, 128.8, 128.2, 127.6, 111.9, 111.4, 71.5, 56.9

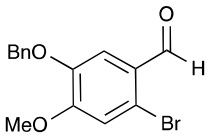

5-(benzyloxy)-2-bromo-4-methoxybenzaldehyde (3.46)

Into a round-bottom flask equipped with a stir bar was placed 3-(benzyloxy)-4-methoxybenzaldehyde (**3.45**) (15.9 g, 0.065 mol), sat'ed $NaHCO_3$ (aq) (30.0 mL) and DCM (30.0 mL). The mixture was stirred at room temperature for 10 min. At this time, Br_2 (8.4 mL, 0.16 mol) in DCM (20 mL) was added dropwise to the mixture and was stirred overnight. After stirring overnight, the mixture was then quenched with 10 % aq Na_2SO_3 (30 mL) and extracted with DCM (3 x 100 mL). The combined organic extracts were washed with brine (100 mL), dried with Na_2SO_4, filtered, and concentrated. The resulting solid was recrystallized from 90: 10 EtOAc:hexanes to afford clear crystalline solid (19.6 g, 93 %).

^{1}H NMR (500 MHz, $CDCl_3$) δ 10.15 (s, 1H), 7.47 (s, 1H), 7.42-7.32 (m, 5H), 7.07 (s, 1H), 5.15 (s, 2H), 3.95 (s, 3H)

^{13}C NMR (75 MHz, $CDCl_3$) δ 190.6, 155.1, 147.9, 135.8, 128.7, 128.2, 127.5, 126.4, 120.6, 115.7, 112.4, 70.9, 56.5

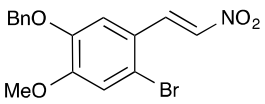

(*E*)-1-(benzyloxy)-4-bromo-2-methoxy-5-(2-nitrovinyl)benzene (3.47)

Into a round-bottom flask equipped with a stir bar was placed 5-(benzyloxy)-2-bromo-4-methoxybenzaldehyde (**3.46**) (280.6 mg, 0.873 mmol), nitromethane (5.0 mL) and ammonium acetate (336.6 mg, 4.36 mmol). The flask was fitted with a reflux condenser and slowly warmed to 120 °C. After stirring overnight, the reaction was concentrated by rotary evaporation. The residue was extracted with EtOAc (3 x 10 mL). The combined organic extracts were washed with brine (10 mL), dried with Na_2SO_4, filtered, and concentrated. The resulting brown solid was purified by flash chromatography (SiO_2, 1:1 hexane:EtOAc) to afford an amorphous orange solid (300.5 mg, 94 %).

^{1}H NMR (500 MHz, $CDCl_3$) δ 8.35 (d, 1H, *J* = 14.0 Hz), 7.52 (d, 1H, *J* = 14.0 Hz), 7.42-7.32 (m, 5H), 7.16 (s, 1H), 7.00 (s, 1H), 5.16 (s, 2H), 3.91 (s, 3H)

^{13}C NMR (75 MHz, $CDCl_3$) δ 152.2, 149.4, 137.8, 137.1, 135.5, 128.9, 128.6, 127.5, 122.4, 119.1, 117.9, 110.1, 71.3, 56.4

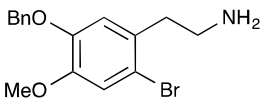

2-(5-(benzyloxy)-2-bromo-4-methoxyphenyl)ethan-1-amine (3.48)

Into a round-bottom flask equipped with a stir bar was placed Zinc (0) metal (155.4 mg, 2.37 mmol), 5 % aq HCl (5.0 mL) and $HgCl_2$ (15.5 mg, 0.1 equiv to Zn (0)). The mixture cooled to 0 °C and stirred for 30 min. At this time the 5 % aq HCl was decanted and replaced with ethanol (10 mL). A solution of (*E*)-1-(benzyloxy)-4-bromo-2-methoxy-5-(2-nitrovinyl)benzene (**3.47**) (34.6 mg, 0.09 mmol) in ethanol (5 mL) was then added along with conc. HCl (2-5 drops). The reaction was stirred allowing warmed to room temperature overnight. After stirring overnight, the reaction was filtered over celite and concentrated. The yellow residue was taken on crude (25.7 mg, 85 %).

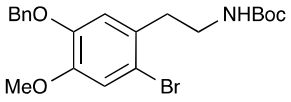

***tert*-butyl (5-(benzyloxy)-2-bromo-4-methoxyphenethyl)carbamate (3.49)**

Into a round-bottom flask equipped with a stir bar was placed 2-(5-(benzyloxy)-2-bromo-4-methoxyphenyl)ethan-1-amine (**3.48**) (389.0 mg, 1.51 mmol), Boc_2O (362.5 mg, 1.66 mmol) and THF (10 mL). After stirring overnight, the reaction was concentrated by rotary evaporation. The residue was extracted with EtOAc (3 x 10 mL). The combined organic extracts were washed with brine (10 mL), dried with Na_2SO_4, filtered, and

concentrated. The resulting brown solid was purified by flash chromatography (SiO_2, 4:1 hexane:EtOAc) to afford an amorphous white solid (632.5 mg, 96 %).

^{1}H NMR (300 MHz, $CDCl_3$) δ 7.42-7.32 (m, 5H), 7.02 (s, 1H), 6.77 (s, 1H), 5.09 (s, 2H), 4.20 (q, 1H, *J* = 3.0, 6.0 Hz), 3.85 (s, 3H), 3.34 (q, 2H, *J* = 7.0, 12.0 Hz), 2.81 (t, 2H, *J* = 7 Hz), 1.44 (s, 9H)

Experimental Table 1.1. Suzuki Coupling Attempts.

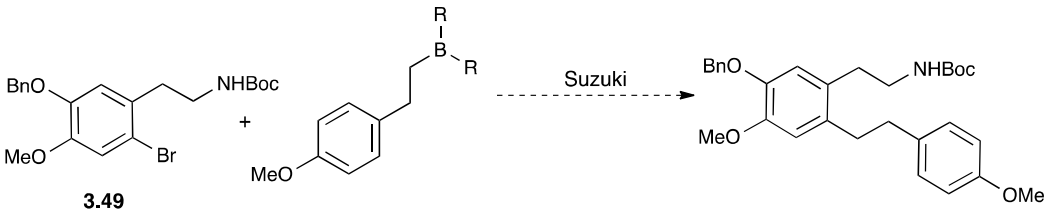

Entry	Borane/Borate[a]	Pd catalyst[b]/base	Ligand[c]
1	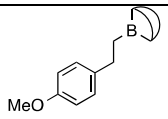	$Pd(dppf)_2Cl_2$ NaOH	P(*t*-Bu)$_3$
2	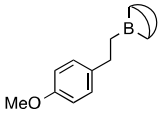	$Pd(dppf)_2Cl_2$ NaOH	P(*o*-tol)$_3$
3	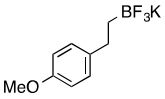	$Pd(OAc)_2$ K_3PO_4	SPhos
4	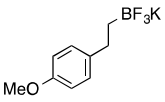	$Pd(OAc)_2$ K_3PO_4	XPhos
5	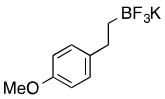	$Pd(OAc)_2$ K_3PO_4	DavePhos

[a] 1.1 equiv, THF/H_2O (10:1), [b] 10 mol %, [c] 25 mol %

General Ligand-Free Heck Coupling Conditions

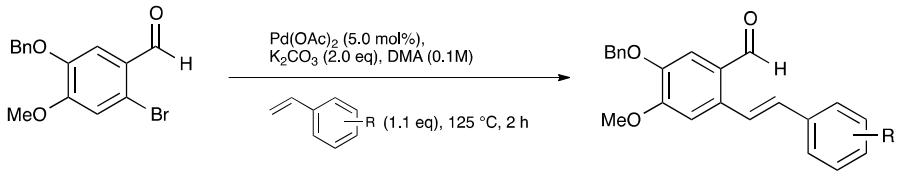

A literature procedure was adapted.[9] Aryl bromide (110.6 mg, 0.344 mmol), K_2CO_3 (95.0 mg, 0.688 mmol) and $Pd(OAc)_2$ (3.8 mg, 0.017 mmol) were combined in a 25 mL rb flask. The flask was evacuated and then refilled with N_2 (3×). Dimethylacetamide[10] was added followed by the styrene (67.8 mg, 0.413 mmol). The reaction mixture was then heated to 125 °C. After 2 h the reaction mixture was cooled to rt and quenched with sat. aq. NH_4Cl (10 mL). The aqueous layer was extracted with EtOAc (3 × 10 mL) and the combined organic layers were washed with brine, dried (Na_2SO_4), filtered, and concentrated under reduced pressure. The residue was purified by flash column chromatography (4:1 hexanes/EtOAc) to afford the coupled product in 65–98 % yield.

---

9 Reddy, M. A.; Jain, N.; Yada, D.; Kishore, C.; Vangala, J. R.; P. Surendra, R.; Addlagatta, A.; Kalivendi, S. V; Sreedhar, B. Design and synthesis of resveratrol-based nitrovinylstilbenes as antimitotic agents. *J. Med. Chem.* **2011**, *54*, 6751–6760.

10 DMA was degassed prior to use via 3 cycles of freeze-pump-thawing.

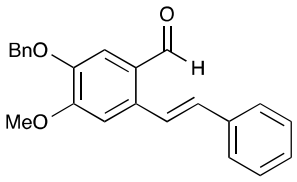

(*E*)-5-(benzyloxy)-4-methoxy-2-styrylbenzaldehyde (3.51)

Using general ligand-free Heck coupling conditions, aryl bromide (**3.46**) was converted into stilbene **3.51** in 72 % yield after flash-column chromatography (1:0→4:1 hexanes/EtOAc).

^{1}H NMR (500 MHz, $CDCl_3$) δ 10.26 (s, 1H), 7.91 (d, 1H, *J* = 16.0 Hz), 7.55 (d, 2H, *J* = 8.0 Hz), 7.48 (d, 2H, *J* = 8.0 Hz), 7.43 (d, 1H, *J* = 16.0 Hz), 7.39 (t, 4H, *J* = 7.0 Hz), 7.34 (dd, 2H, *J* = 7.0, 16 Hz), 7.12 (s, 1H), 6.98 (d, 1H, *J* =16 Hz), 5.21 (s, 2H), 4.02 (s, 3H)

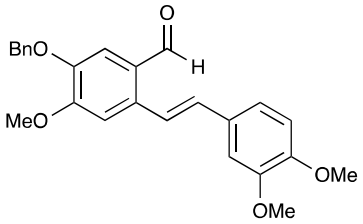

(*E*)-5-(benzyloxy)-2-(3,4-dimethoxystyryl)-4-methoxybenzaldehyde (3.52)

Using general ligand-free Heck coupling conditions, aryl bromide (**3.46**) was converted into stilbene **3.52** in 64 % yield after flash-column chromatography (1:0→4:1 hexanes/EtOAc).

^{1}H NMR (500 MHz, $CDCl_3$) δ 10.25 (s, 1H), 7.77 (d, 1H, *J* = 16.0 Hz), 7.47 (d, 2H, *J* = 8.0 Hz), 7.40 (dd, 2H, *J* = 4.0, 8.0 Hz), 7.33 (d, 2H, *J* = 8.0 Hz), 7.09 (d, 3H, *J* = 8.0 Hz), 6.92 (d, 1H, *J* = 16.0 Hz), 6.88 (d, 1H, *J* = 8.0 Hz), 5.20 (s, 2H), 4.01 (s, 3H), 3.94 (s, 3H), 3.92 (s, 3H)

^{13}C NMR (75 MHz, $CDCl_3$) δ 190.1, 154.3, 149.4, 149.2, 147.8, 136.3, 136.1, 133.1, 129.9, 128.6, 128.1, 127.5, 126.2, 121.7, 120.2, 113.6, 111.2, 109.1, 109.0, 70.9, 56.1, 55.9, 55.8

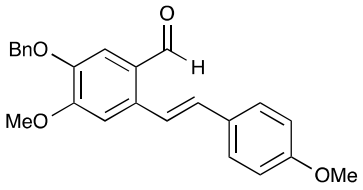

(*E*)-5-(benzyloxy)-4-methoxy-2-(4-methoxystyryl)benzaldehyde (3.53)

Using general ligand-free Heck coupling conditions, aryl bromide (**3.46**) was converted into stilbene **3.53** in 98 % yield after flash-column chromatography (1:0→4:1 hexanes/EtOAc).

^{1}H NMR (500 MHz, $CDCl_3$) δ 10.25 (s, 1H), 7.70 (d, 1H, *J* = 16.0 Hz), 7.47 (t, 4H, *J* = 8.0 Hz), 7.42 (d, 1H, *J* = 16.0 Hz), 7.38 (t, 2H, *J* = 7.0 Hz), 7.33 (d, 1H, *J* = 7.0 Hz), 7.09 (s, 1H), 6.93 (s, 1H), 6.91 (d, 2H, *J* = 4.0 Hz), 5.20 (s, 2H), 4.01 (s, 3H), 3.94 (s, 3H), 3.92 (s, 3H)

^{13}C NMR (75 MHz, $CDCl_3$) δ 190.1, 159.7, 154.3, 147.7, 136.3, 136.2, 129.6, 128.7, 128.6, 128.1, 128.0, 127.5, 126.2, 121.4, 114.2, 113.4, 108.9, 70.9, 56.1, 55.3

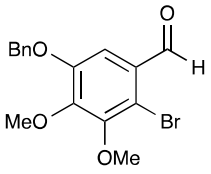

5-(benzyloxy)-2-bromo-3,4-dimethoxybenzaldehyde (3.55)

Into a round-bottom flask equipped with a stir bar was placed sodium *tert*-butoxide (634.6 mg, 6.6 mmol) and THF (10 mL) and the mixture was cooled to 0 °C and

DIBALH (1.17 mL, 6.6 mmol) was added. After stirred at 0 °C for 2 h the mixture was further cooled to –40 °C and a solution of methyl 5-(benzyloxy)-2-bromo-3,4-dimethoxybenzoate (**3.18**) (1.66 g, 5.5 mmol) in THF (10 mL) was added. After stirring 2 h, the reaction was quenched with 10 % aq HCl (10 mL), extracted into EtOAc (3 x 50 mL). The combined extracts were washed with Brine (50 mL), dried with Na_2SO_4, filtered and concentrated. The resulting white solid was purified by flash chromatography (SiO_2, 4:1 hexane:EtOAc) to afford an amorphous white solid (1.33 g, 88 %).

^{1}H NMR (500 MHz, $CDCl_3$) δ 10.30 (s, 1H), 7.54 (t, 3H, *J* = 7.0 Hz), 7.47 (d, 2H, *J* = 7.0 Hz), 7.42 (s, 1H), 5.14 (s, 2H), 4.02 (s, 3H), 4.00 (s, 3H), 3.95 (s, 3H)

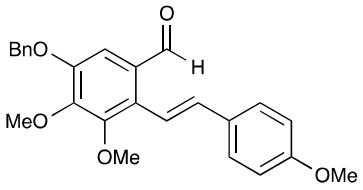

(*E*)-5-(benzyloxy)-3,4-dimethoxy-2-(4-methoxystyryl)benzaldehyde (3.56)

Using general ligand-free Heck coupling conditions, aryl bromide (**3.55**) was converted into stilbene **3.56** in 40 % yield after flash-column chromatography (1:0→4:1 hexanes/EtOAc).

^{1}H NMR (500 MHz, $CDCl_3$) δ 10.15 (s, 1H), 7.52 (d, 2H, *J* = 8 Hz), 7.50 (d, 2H, *J* = 7.0 Hz), 7.43 (t, 3H, *J* = 7.0 Hz), 7.37 (s, 1H), 7.32 (d, 1H, *J* = 16 Hz), 6.96 (d, 2H, *J* = 8.0 Hz), 6.63 (d, 1H, *J* = 16 Hz), 5.21 (s, 2H), 4.03 (s, 3H), 3.91 (s, 3H), 3.86 (s, 3H)

^{13}C NMR (75 MHz, $CDCl_3$) δ 191.0, 159.8, 151.7, 147.5, 137.9, 136.3, 131.2, 129.9, 129.7, 128.6, 128.2, 128.1, 127.5, 117.1, 114.2, 108.2, 70.8, 61.2, 61.1, 55.4

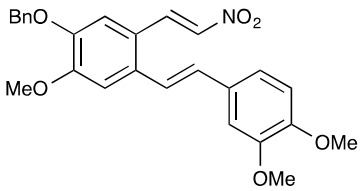

1-(benzyloxy)-4-((*E*)-3,4-dimethoxystyryl)-2-methoxy-5-((*E*)-2-nitrovinyl)benzene (3.57)

Into a round-bottom flask equipped with a stir bar was placed (*E*)-5-(benzyloxy)-2-(3,4-dimethoxystyryl)-4-methoxybenzaldehyde (**3.52**) (101.5 mg, 0.25 mmol), nitromethane

(5.0 mL) and ammonium acetate (38.6 mg, 0.50 mmol). The flask was fitted with a reflux condenser and slowly warmed to 120 °C. After stirring overnight, the reaction was concentrated by rotary evaporation. The residue was extracted with EtOAc (3 x 10 mL). The combined organic extracts were washed with brine (10 mL), dried with Na_2SO_4, filtered, and concentrated. The resulting brown solid was purified by flash chromatography (SiO_2, 1:1 hexane:EtOAc) to afford an amorphous orange solid (300.5 mg, 94 %).

^{1}H NMR (500 MHz, $CDCl_3$) δ 8.39 (d, 1H, *J* = 14.0 Hz), 7.46 (d, 2H, *J* = 7.0 Hz), 7.45 (t, 2H, *J* = 7.0 Hz), 7.36 (d, 2H, *J* = 7.0 Hz), 7.22 (d, 1H, *J* = 16.0 Hz), 7.10 (d, 2H, *J* = 7.0 Hz), 7.08 (s, 1H), 6.98 (s, 1H), 6.89 (d, 1H, *J* = 16 Hz) 6.86 (d, 1H, *J* = 14 Hz), 5.18 (s, 2H), 3.99 (s, 3H), 3.95 (s, 3H), 3.91 (s, 3H)

^{13}C NMR (75 MHz, $CDCl_3$) δ 153.2, 149.6, 149.1, 147.7, 136.6, 136.2, 135.9, 134.8, 133.1, 129.8, 128.6, 128.2, 127.3, 122.3, 120.1, 120.0, 112.1, 111.1, 109.8, 109.2, 71.2, 56.1, 56.0, 55.9

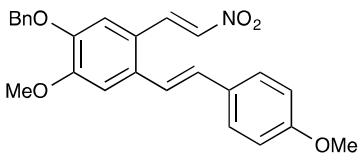

1-(benzyloxy)-2-methoxy-4-((*E*)-4-methoxystyryl)-5-((*E*)-2-nitrovinyl)benzene (3.58)

Into a round-bottom flask equipped with a stir bar was placed (*E*)-5-(benzyloxy)-3,4-dimethoxy-2-(4-methoxystyryl)benzaldehyde (**3.56**) (2.70 g, 7.20 mmol), nitromethane (50.0 mL) and ammonium acetate (2.59 g, 36.0 mmol). The flask was fitted with a reflux condenser and slowly warmed to 120 °C. After stirring overnight, the reaction was concentrated by rotary evaporation. The residue was extracted with EtOAc (3 x 100 mL). The combined organic extracts were washed with brine (100 mL), dried with Na_2SO_4, filtered, and concentrated. The resulting brown solid was purified by flash chromatography (SiO_2, 1:1 hexane:EtOAc) to afford an amorphous orange solid (2.90 g, 97 %).

^{1}H NMR (500 MHz, $CDCl_3$) δ 8.43 (d, 1H, *J* = 14.0 Hz), 7.49 (apt t, 4H, *J* = 7.0 Hz), 7.43 (t, 2H, *J* = 7.0 Hz), 7.38 (d, 2H, *J* = 14.0 Hz), 7.25 (d, 1H, *J* = 16.0 Hz), 7.11 (s, 1H), 7.00 (s, 1H), 6.96 (d, 2H, *J* = 8.0 Hz), 6.90 (d, 1H, *J* = 16 Hz) 5.18 (s, 2H), 4.02 (s, 3H), 3.87 (s, 3H)

^{13}C NMR (75 MHz, $CDCl_3$) δ 159.9, 153.3, 147.7, 136.7, 136.2, 135.7, 134.9, 132.8, 129.4, 128.8, 128.3, 128.1, 127.4, 122.0, 120.1, 114.3, 111.9, 109.6, 71.2, 56.1, 55.3

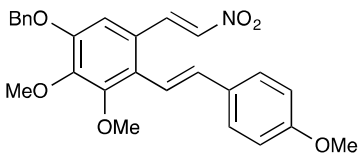

1-(benzyloxy)-2,3-dimethoxy-4-((*E*)-4-methoxystyryl)-5-((*E*)-2-nitrovinyl)benzene (3.59)

Into a round-bottom flask equipped with a stir bar was placed (*E*)-5-(benzyloxy)-3,4-dimethoxy-2-(4-methoxystyryl)benzaldehyde (**3.56**) (135.3 mg, 0.329 mmol), nitromethane (10.0 mL) and ammonium acetate (118.5 mg, 1.6 mmol). The flask was fitted with a reflux condenser and slowly warmed to 120 °C. After stirring overnight, the reaction was concentrated by rotary evaporation. The residue was extracted with EtOAc (3 x 10.0 mL). The combined organic extracts were washed with brine (10.0 mL), dried with Na_2SO_4, filtered, and concentrated. The resulting brown solid was purified by flash chromatography (SiO_2, 1:1 hexane:EtOAc) to afford an amorphous orange solid (125.8 mg, 86 %).

^{1}H NMR (500 MHz, $CDCl_3$) δ 8.37 (d, 1H, *J* = 14.0 Hz), 7.52-7.48 (m, 5H), 7.46 (d, 2H, *J* = 7.0 Hz), 7.43 (s, 1H), 7.36 (d, 2H, *J* = 14.0 Hz), 7.18 (d, 1H, *J* = 16.0 Hz), 6.92 (d, 2H, *J* = 7.0 Hz), 6.90 (d, 1H, *J* = 16.0 Hz) 5.19 (s, 2H), 4.01 (s, 3H), 3.89 (s, 3H), 3.86 (s, 3H)

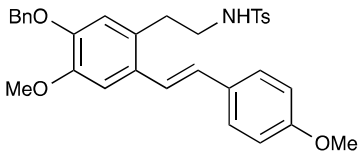

(*E*)-*N*-(5-(benzyloxy)-4-methoxy-2-(4-methoxystyryl)phenethyl)-4-methylbenzene-sulfonamide (3.60)

To a solution of 1-(benzyloxy)-2-methoxy-4-((*E*)-4-methoxystyryl)-5-((*E*)-2-nitrovinyl)benzene (**3.58**) (442.5 mg, 1.06 mmol) in anhydrous THF (15.0 mL) at 0 °C, under a nitrogen atmosphere, LAH (200.0 mg, 5.3 mmol) was added. The reaction flask was fitted with a reflux condenser and the reaction was slowly warmed to reflux. After 4 h the reaction was quenched with Feiser method and was stirred for 1 h. At this time, the reaction was filtered over celite and concentrated by rotary evaporation. The crude product was purified by flash chromatography (SiO_2, 20:1 hexane:EtOAc) to afford a white solid which was immediately dissolved in DCM (5.0 mL). To this solution was added sat'd aq. Na_2CO_3 (2 mL) and TsCl (53.5 mg, 0.280 mmol). The reaction was stirred overnight at room temperature. After stirring overnight, the reaction was extracted into DCM (3 x 10 mL). The combined extracts were and washed with Brine (10.0 mL), dried with Na_2SO_4, filtered and concentrated. The resulting yellow solid was purified by flash chromatography (SiO_2, 4:1 hexane:EtOAc) to afford an amorphous yellow solid (82.0 mg, 72.0 % over 2 steps).

^{1}H NMR (500 MHz, $CDCl_3$) δ 7.64 (d, 2H, *J* = 8.0 Hz), 7.45 (dd, 4H, *J* = 4.0, 8.0 Hz), 7.40 (t, 3H, *J* = 7.0 Hz), 7.36 (d, 1H, *J* = 7.0 Hz), 7.19 (d, 2H, *J* = 8.0 Hz), 7.09 (s, 1H),

7.06 (d, 1H, *J* = 16.0 Hz), 6.94 (d, 2H, *J* = 8.0 Hz), 6.84 (d, 1H, *J* = 16.0 Hz), 6.64 (s, 1H), 5.14 (s, 2H), 4.49 (t, N–H), 3.95 (s, 3H), 3.86 (s, 3H), 3.12 (q, 2H, *J* = 7.0, 14.0 Hz), 2.87 (t, 2H, *J* = 7.0 Hz), 2.37 (s, 3H)

^{13}C NMR (75 MHz, $CDCl_3$) δ 159.3, 148.8, 147.7, 143.3, 136.9, 136.8, 130.2, 129.7, 129.6, 128.9, 128.6, 127.8, 127.7, 127.4, 127.0, 123.1, 115.7, 114.2, 109.3, 71.1, 56.2, 55.4, 43.9, 33.3, 21.5

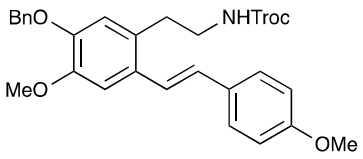

2,2,2-trichloroethyl (*E*)-(5-(benzyloxy)-4-methoxy-2-(4-methoxystyryl)phenethyl)-carbamate (3.61)

To a solution of 1-(benzyloxy)-2-methoxy-4-((*E*)-4-methoxystyryl)-5-((*E*)-2-nitrovinyl)benzene (**3.58**) (626.2 mg, 1.50 mmol) in anhydrous THF (25.0 mL) at 0 °C, under a nitrogen atmosphere, LAH (569.3 mg, 15.0 mmol) was added. The reaction flask was fitted with a reflux condenser and the reaction was slowly warmed to reflux. After 4 h the reaction was quenched with Feiser method and was stirred for 1 h. At this time, the reaction was filtered over celite and concentrated by rotary evaporation. The crude product was purified by flash chromatography (SiO_2, 20:1 hexane:EtOAc) to afford a white solid which was immediately dissolved in DCM (15.0 mL). To this solution was added sat'd aq. Na_2CO_3 (5.0 mL) and TsCl (210.6 mg, 0.994 mmol). The reaction was

stirred overnight at room temperature. After stirring overnight, the reaction was extracted into DCM (3 x 20 mL). The combined extracts were and washed with Brine (20.0 mL), dried with Na_2SO_4, filtered and concentrated. The resulting yellow solid was purified by flash chromatography (SiO_2, 4:1 hexane:EtOAc) to afford an amorphous yellow solid (312.0 mg, 55.0 % over 2 steps).

^{1}H NMR (500 MHz, $CDCl_3$) δ 7.49 (d, 2H, *J* = 8.0 Hz), 7.47 (d, 2H, *J* = 7.0 Hz), 7.40 (t, 3H, *J* = 7.0 Hz), 7.20 (d, 1H, *J* = 16.0 Hz), 7.16 (s, 1H), 6.94 (d, 2H, *J* = 8.0 Hz), 6.87 (d, 1H, *J* = 16.0 Hz), 6.72 (s, 1H), 5.17 (s, 2H), 4.63 (s, 2H), 3.97 (s, 3H), 3.86 (s, 3H), 3.42 (q, 2H, *J* = 7.0, 14.0 Hz), 2.94 (t, 2H, *J* = 7.0 Hz)

^{13}C NMR (75 MHz, $CDCl_3$) δ 159.3, 154.5, 148.8, 147.8, 136.9, 130.4, 129.9, 128.8, 128.7, 128.6, 128.5, 128.0, 127.9, 127.7, 127.4, 123.3, 115.9, 114.3, 114.2, 109.3, 99.4, 95.5, 77.3, 76.3, 74.4, 71.2, 56.2, 55.3, 42.3, 33.7

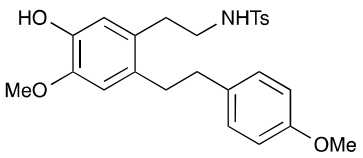

***N*-(5-hydroxy-4-methoxy-2-(4-methoxyphenethyl)phenethyl)-4-methylbenzene-sulfonamide (3.62)**

To a solution of (*E*)-*N*-(5-(benzyloxy)-4-methoxy-2-(4-methoxystyryl)phenethyl)-4-methylbenzene-sulfonamide (**3.60**) (47.0 mg, 0.08 mmol) in anhydrous THF (2.0 mL), 10 % Pd/C (9.10 mg, 0.008 mmol) was added. The reaction flask was fitted with a hydrogen balloon and was stirred at room temperature 8 h. After 8 h the reaction was filtered over celite and concentrated by rotary evaporation. The crude product was purified by flash chromatography (SiO_2, 25:1 hexane:EtOAc) to afford a brown solid (31.3 mg, 86 %)

^{1}H NMR (500 MHz, $CDCl_3$) δ 7.72 (d, 2H, *J* = 8.0 Hz), 7.27 (d, 1H, *J* = 8.0 Hz), 7.06 (d, 2H, *J* = 8.0 Hz), 6.85 (d, 2H, *J* = 8.0 Hz), 6.58 (s, 1H), 6.55(s, 1H), 4.53 (br s, N–H), 3.81 (s, 6H), 3.10 (q, 2H, *J* = 7.0, 14.0 Hz), 2.73 (apt s, 4H), 2.68 (t, 2H, *J* = 7.0 Hz), 2.42 (s, 3H)

^{13}C NMR (75 MHz, $CDCl_3$) δ 157.9, 145.2, 143.7, 143.4, 136.8, 133.5, 131.6, 129.7, 129.4, 127.9, 127.0, 115.2, 113.8, 112.3, 55.9, 55.3, 43.9, 37.1, 34.1, 31.9, 21.5

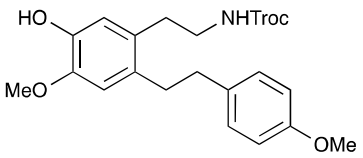

2,2,2-trichloroethyl-(5-hydroxy-4-methoxy-2-(4-methoxyphenethyl)phenethyl)-carbamate (3.63)

To a solution of 2,2,2-trichloroethyl (*E*)-(5-(benzyloxy)-4-methoxy-2-(4-methoxystyryl)phenethyl)-carbamate (**3.61**) (288.8 mg, 0.511 mmol) in anhydrous THF (10.0 mL), 10 % Pd/C (54.2 mg, 0.051 mmol) was added. The reaction flask was fitted with a hydrogen balloon and was stirred at room temperature 5 h. After 5 h the reaction was filtered over celite and concentrated by rotary evaporation. The crude product was purified by flash chromatography (SiO_2, 15:1 hexane:EtOAc) to afford a white solid (105.1 mg, 43 %)

^{1}H NMR (500 MHz, $CDCl_3$) δ 7.10 (d, 2H, *J* = 8.0 Hz), 6.86 (d, 2H, *J* = 8.0 Hz), 6.73 (s, 1H), 6.61 (s, 1H), 5.56 (br s, N–H), 4.74 (s, 2H), 3.83 (s, 3H), 3.82 (s, 3H), 3.41 (q, 2H, *J* = 7.0, 14.0 Hz), 2.83 (dd, 4H, *J* = 7.0 Hz), 2.76 (t, 2H, *J* = 7.0 Hz)

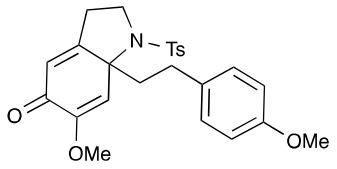

6-methoxy-7a-(4-methoxyphenethyl)-1-tosyl-1,2,3,7a-tetrahydro-5*H*-indol-5-one (3.69)

To a solution of *N*-(5-hydroxy-4-methoxy-2-(4-methoxyphenethyl)phenethyl)-4-methylbenzene- sulfonamide (**3.62**) (22.7 mg, 0.05 mmol) in DCM (1.0 mL), μ-oxo-bridged iodide (17.3 mg, 0.03 mmol) was added. The reaction was stirred for 30 min before being concentrated by rotary evaporation. The crude product was purified by flash chromatography (SiO_2, 5:1 hexane:EtOAc) to afford a white solid (15.9 mg, 70 %)

^{1}H NMR (500 MHz, $CDCl_3$) δ 7.65 (d, 2H, *J* = 7.0 Hz), 7.26 (d, 1H, *J* = 7.0 Hz), 7.03 (d, 2H, *J* = 8.0 Hz), 6.83 (d, 2H, *J* = 8.0 Hz), 6.51 (s, 1H), 6.09 (s, 1H), 3.90 (td, 1H, *J* = 3.0, 7.0 Hz), 3.80 (s, 3H), 3.66 (s, 3H), 3.62 (t, 1H, *J* =7.0 Hz), 2.95 (m, 1H), 2.63 (m, 1H) 2.56 (m, 1H), 2.46 (m, 2H), 2.41 (s, 3H), 2.37 (m, 1H)

^{13}C NMR (75 MHz, $CDCl_3$) δ 180.1, 161.8, 158.0, 151.4, 143.8, 137.2, 132.3, 129.6, 129.1, 126.9, 122.7, 113.9, 112.4, 67.8, 55.3, 47.5, 42.6, 29.4, 28.3, 21.5

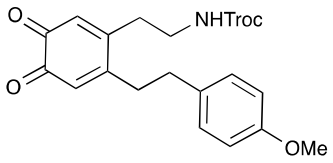

2,2,2-trichloroethyl-(2-(6-(4-methoxyphenethyl)-3,4-dioxocyclohexa-1,5-dien-1-yl)ethyl-carbamate (3.71)

To a solution of 2,2,2-trichloroethyl-(5-hydroxy-4-methoxy-2-(4-methoxyphenethyl)phenethyl)-carbamate (**3.63**) (60.0 mg, 0.13 mmol) in TFE (2.0 mL), μ-oxo-bridged iodide (40.9 mg, 0.062 mmol) was added. The reaction was stirred for 30 min before being concentrated by rotary evaporation. The crude product was bright orange and was analyzed immediately without purification.

^{1}H NMR (500 MHz, $CDCl_3$) δ 7.14 (d, 2H, *J* = 8.0 Hz), 6.88 (d, 2H, *J* = 8.0 Hz), 6.24 (s, 1H), 6.22 (s, 1H), 5.33 (apt t, N–H), 4.73 (s, 2H), 3.81 (s, 3H), 3.50 (q, 2H, *J* = 7.0, 14.0 Hz), 2.86 (t, 2H, *J* =7.0 Hz), 2.74 (t, 2H, *J* =7.0 Hz), 2.67 (t, 2H, *J* =7.0 Hz)

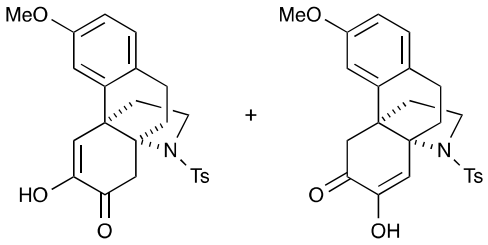

7-hydroxy-3-methoxy-11-tosyl-9,10-dihydro-8a,4b-(epiminoethano)phenanthren-6(5*H*)-one (3.75 & 3.76)

To a solution of 6-methoxy-7a-(4-methoxyphenethyl)-1-tosyl-1,2,3,7a-tetrahydro-5*H*-indol-5-one (**3.69**) (11.0 mg, 0.02 mmol) in DCM (0.10 mL), cooled to 0 °C, TfOH (2.1 mg, 0.02 mmol) was added. The reaction was stirred for 1 min before being concentrated by rotary evaporation. The crude product was purified by flash chromatography (SiO_2, 5:1 hexane:EtOAc) to afford a white solid (3.8 mg, 36 %)

^{1}H NMR (500 MHz, $CDCl_3$) δ 7.84 (dd, 2H, *J* = 2.0, 8.0 Hz), 7.36 (ddd, 2H, *J* = 2.0, 8.0, 8.0 Hz), 6.75 (dd, 3H, *J* = 2.0, 8.0 Hz), 6.72 (d, 1H, *J* = 8.0 Hz), 3.79 (apt d, 1H, *J* = 4.0, 6.0 Hz), 3.23 (d, 1H, *J* = 16.0 Hz), 2.79 (d, 1H, *J* = 16.0 Hz), 2.43 (apt d, 1H, *J* = 4.0, 6.0 Hz), 2.30 (t, 2H, *J* = 7.0 Hz), 2.20 (m, 1H) 2.07 (dd, 1H, *J* = 6.0 Hz), 2.00 (m, 1H), 1.52 (m, 1H), 1.40 (dd, 1H *J* = 6.0 Hz) 1.27 (s, 1H)

HRMS (ESI+) *m/z* calcd for $C_{24}H_{25}NO_5SNa$ $[M + Na]^+$ 462.1351, found 462.133

SPECTRAL APPENDIX

SPECTRA APPENDIX

SPECTRA APPENDIX

SPECTRA APPENDIX

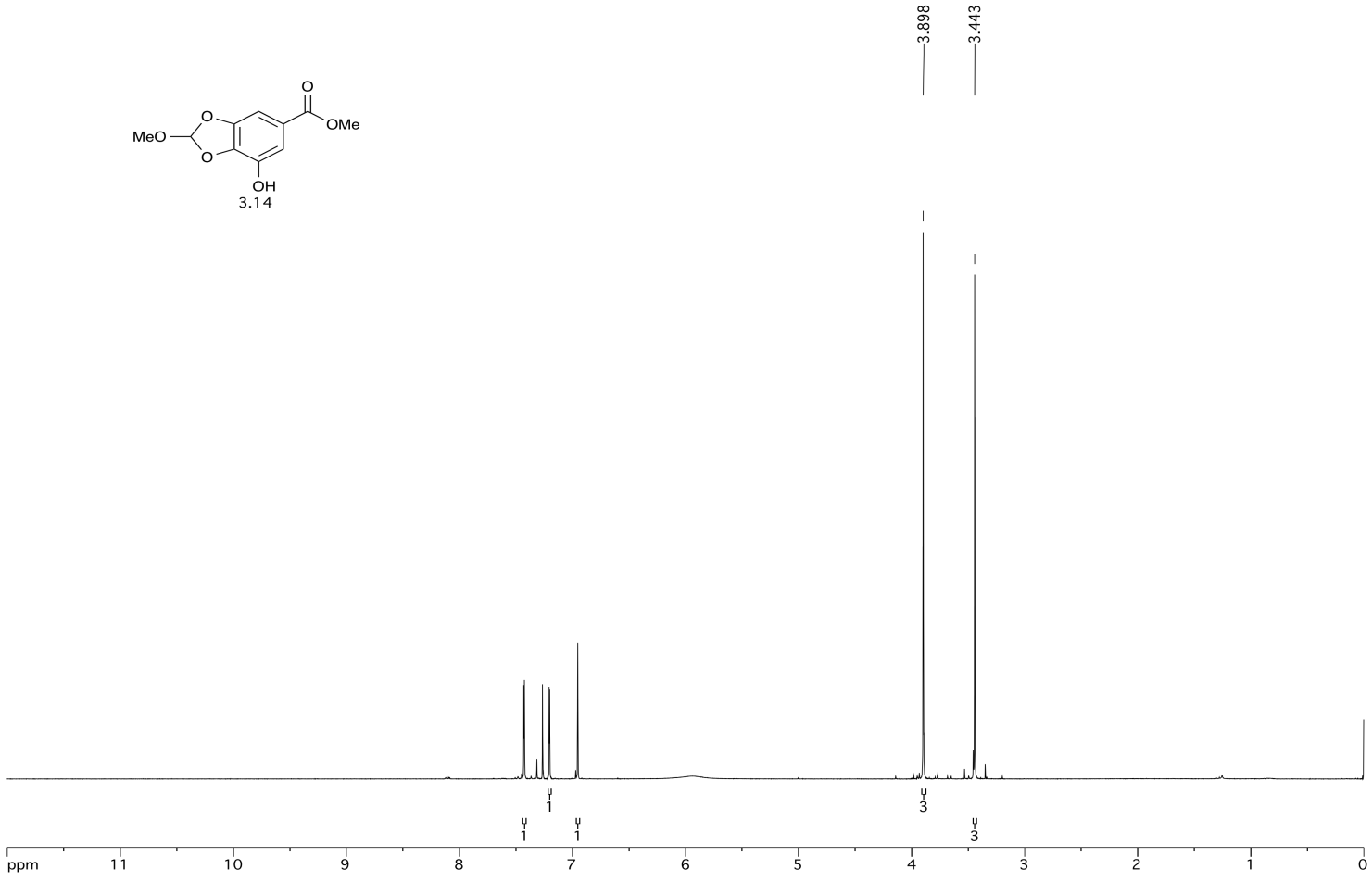
3.898
3.443
O
MeO
O
O
OMe
OH
3.14
1
1
3
1
1
3
ppm
11
10
9
8
7
6
5
4
3
2
1
0

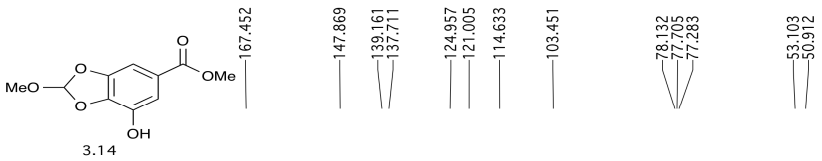
MeO
O
O
O
OMe
OH
167.452
147.869
139.161
137.711
124.957
121.005
114.633
103.451
78.132
77.705
77.283
53.103
50.912

3.14

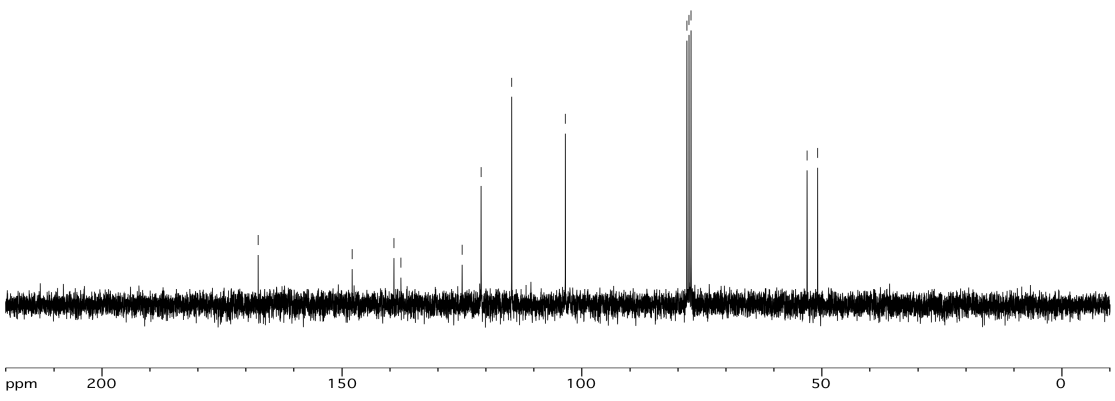
ppm
200
150
100
50
0

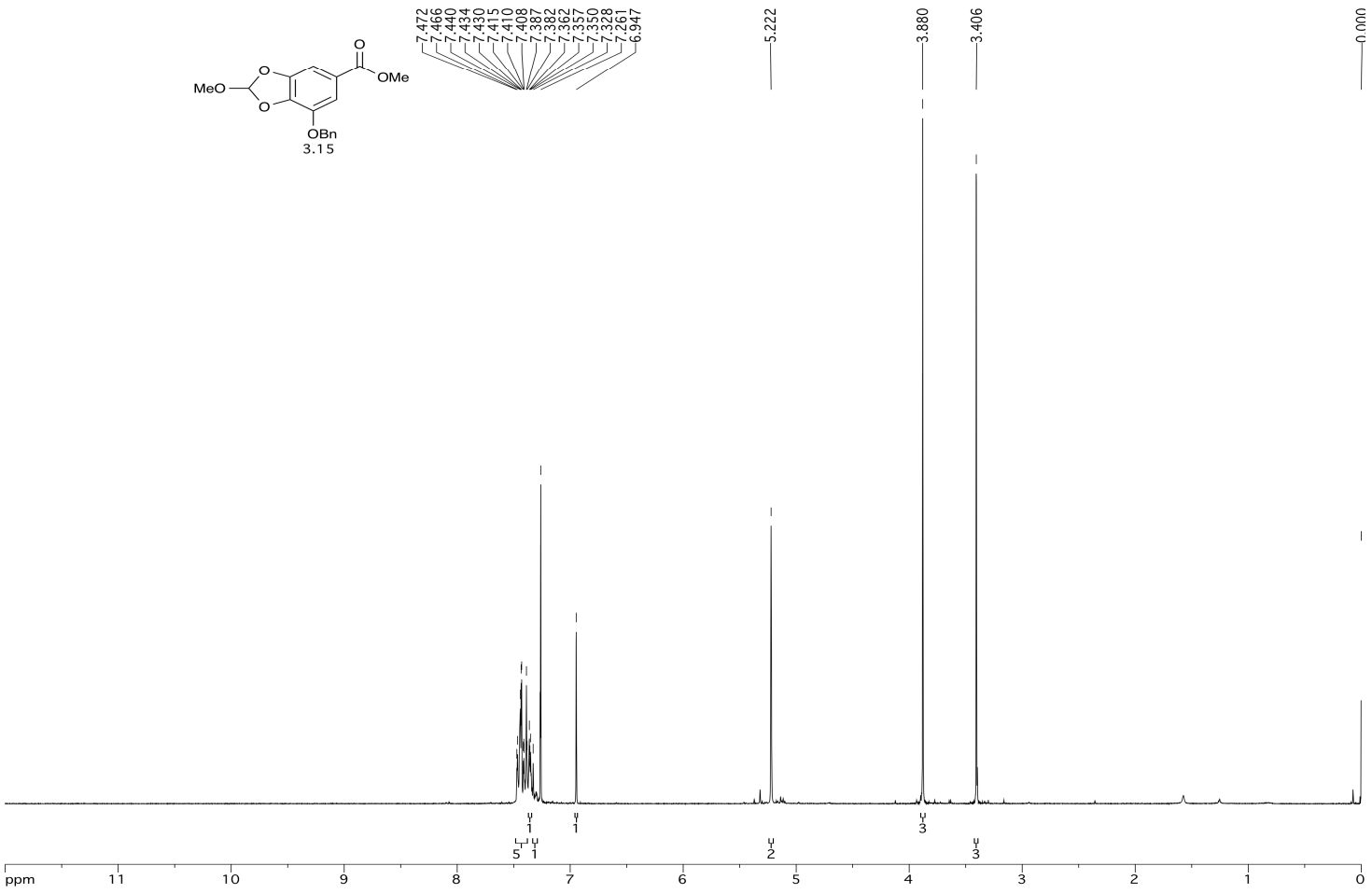
7.472
7.466
7.440
7.434
7.430
7.415
7.410
7.408
7.387
7.382
7.362
7.357
7.350
7.328
7.261
6.947
5.222
3.880
3.406
0.000
MeO
OMe
OBn
3.15
ppm
11
10
9
8
7
6
5
4
3
2
1
0

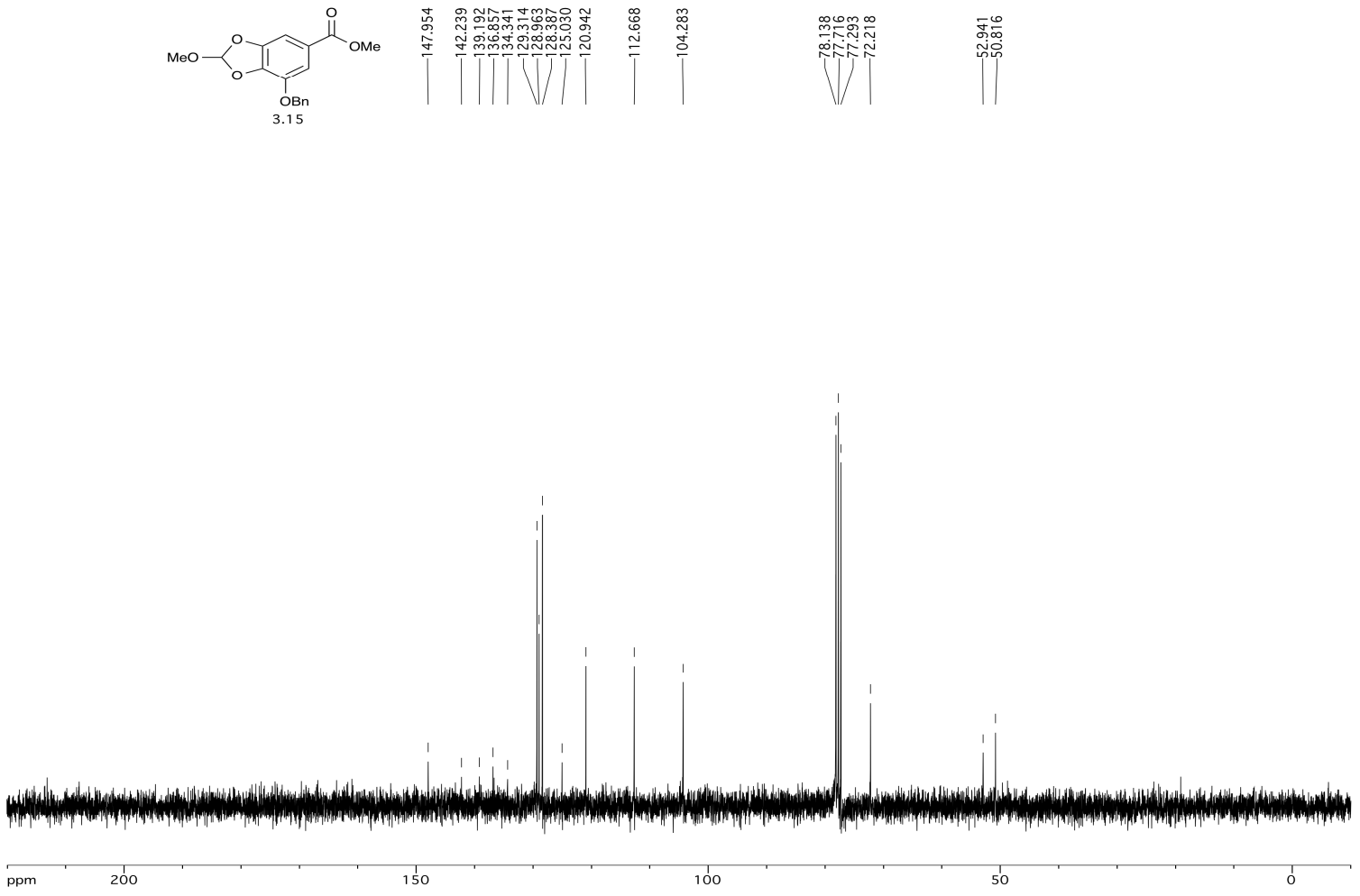
MeO
OMe
OBn
3.15
147.954
142.239
139.192
136.857
134.341
129.314
128.963
128.387
125.030
120.942
112.668
104.283
78.138
77.716
77.293
72.218
52.941
50.816
ppm
200
150
100
50
0


HO
HO
O
OMe
OBn
7.422
7.355
7.321
7.319
7.261
5.799
5.333
5.139
3.882

3.16

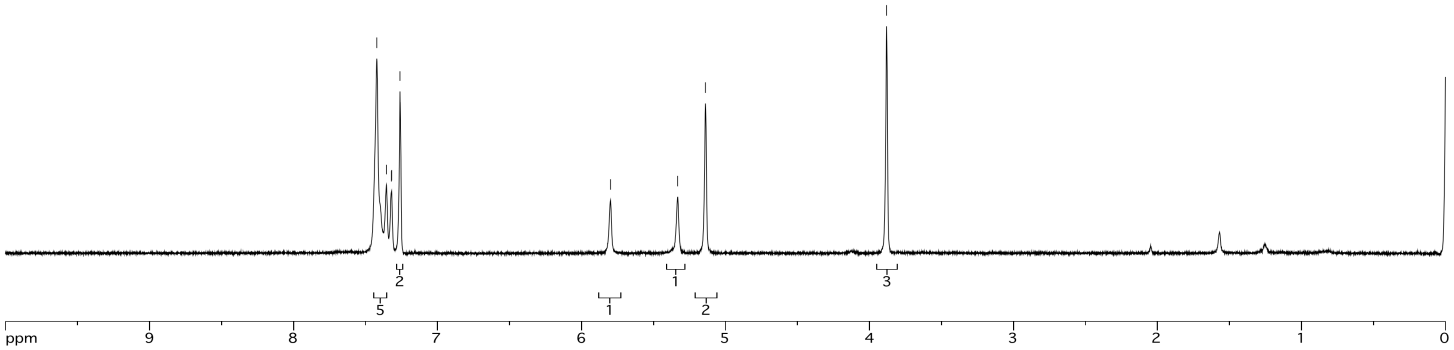
5
2
1
2
1
3
ppm
9
8
7
6
5
4
3
2
1
0

SPECTRA APPENDIX

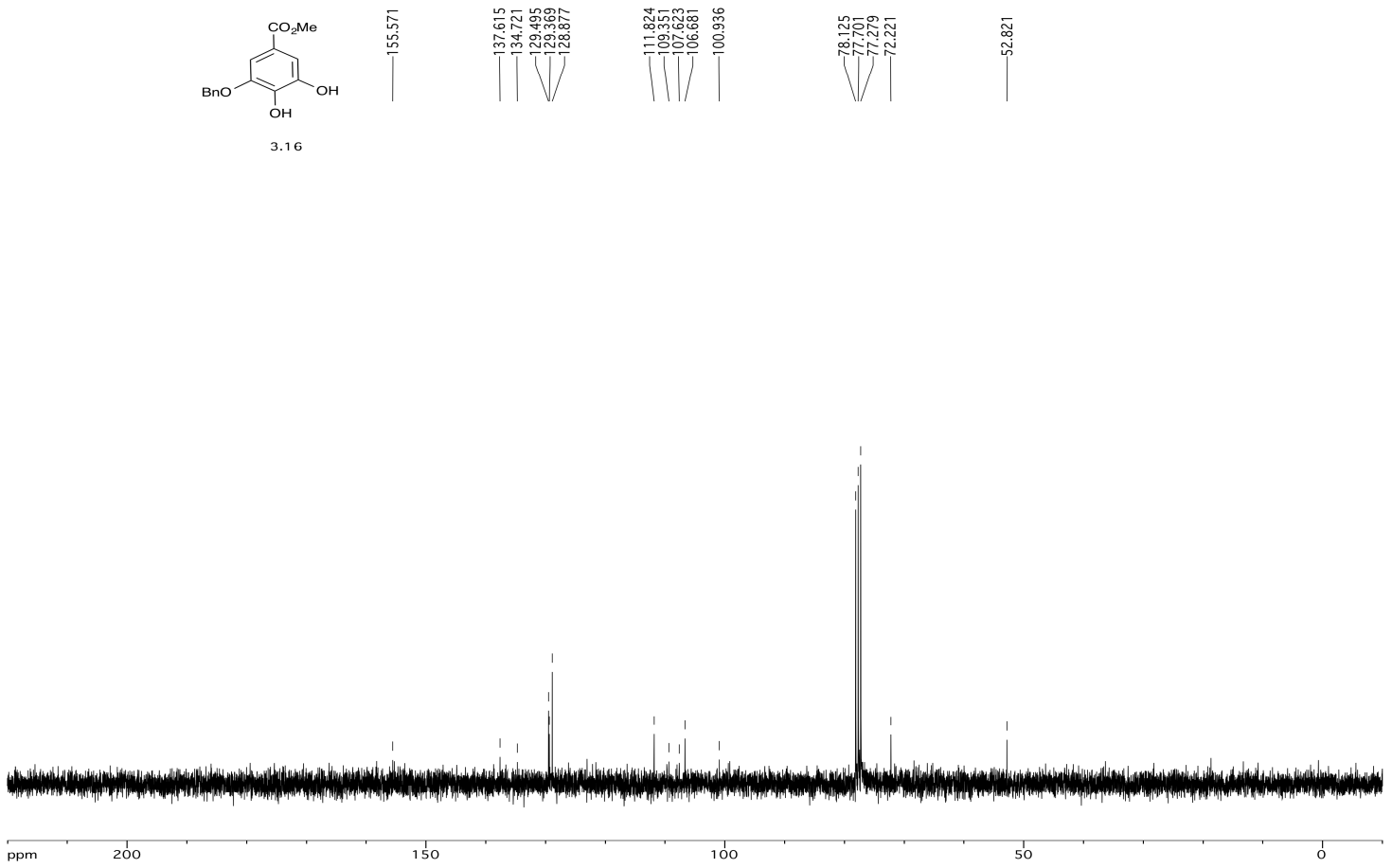
CO2Me
BnO
OH
OH
3.16
155.571
137.615
134.721
129.495
129.369
128.877
111.824
109.351
107.623
106.681
100.936
78.125
77.701
77.279
72.221
52.821
ppm
200
150
100
50
0

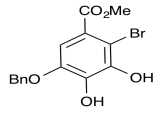
CO2Me
Br
BnO
OH
OH

3.17

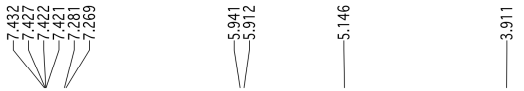
7.432
7.427
7.422
7.421
7.281
7.269
5.941
5.912
5.146
3.911

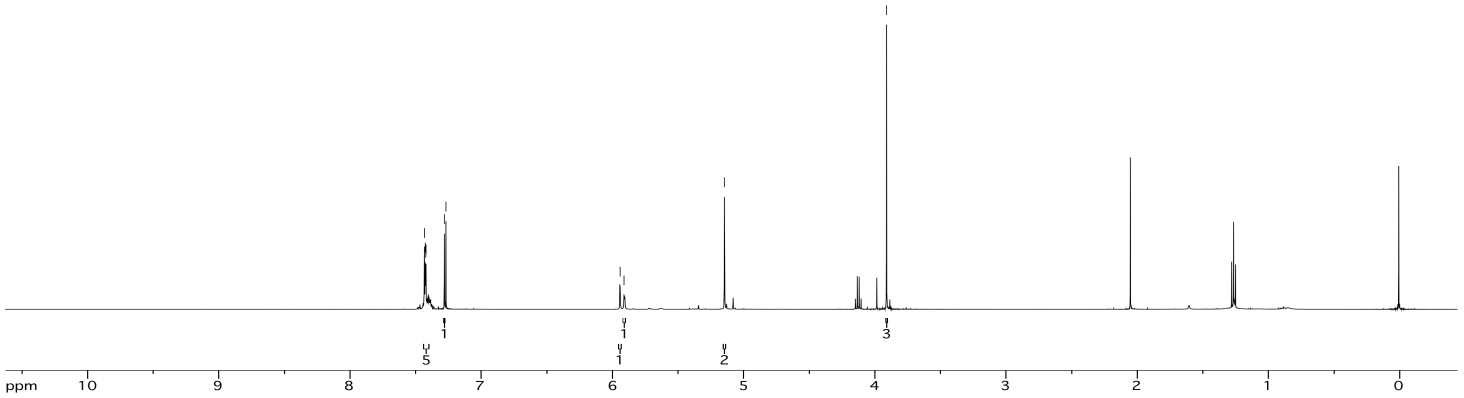
1
1
3
5
1
2
ppm
10
9
8
7
6
5
4
3
2
1
0

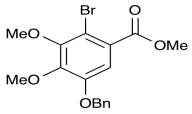
Br
O
MeO
OMe
MeO
OBn

3.18

7.388
7.346
7.316
7.241
5.063
3.899
3.853
1
5
2
3
6
ppm
9
8
7
6
5
4
3
2
1
0

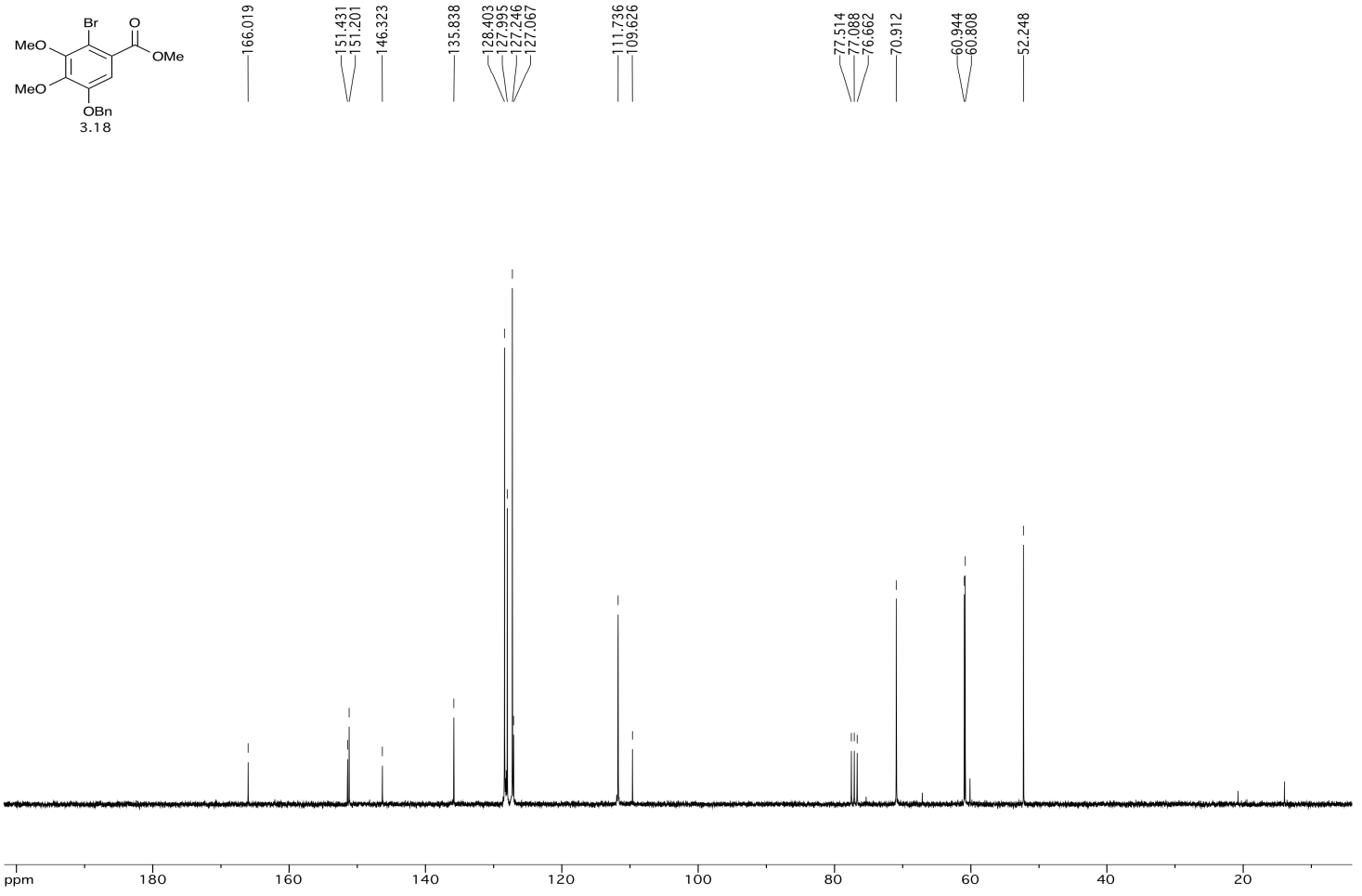
Br
O
MeO
OMe
MeO
OBn
3.18
166.019
151.431
151.201
146.323
135.838
128.403
127.995
127.246
127.067
111.736
109.626
77.514
77.088
76.662
70.912
60.944
60.808
52.248
ppm
180
160
140
120
100
80
60
40
20

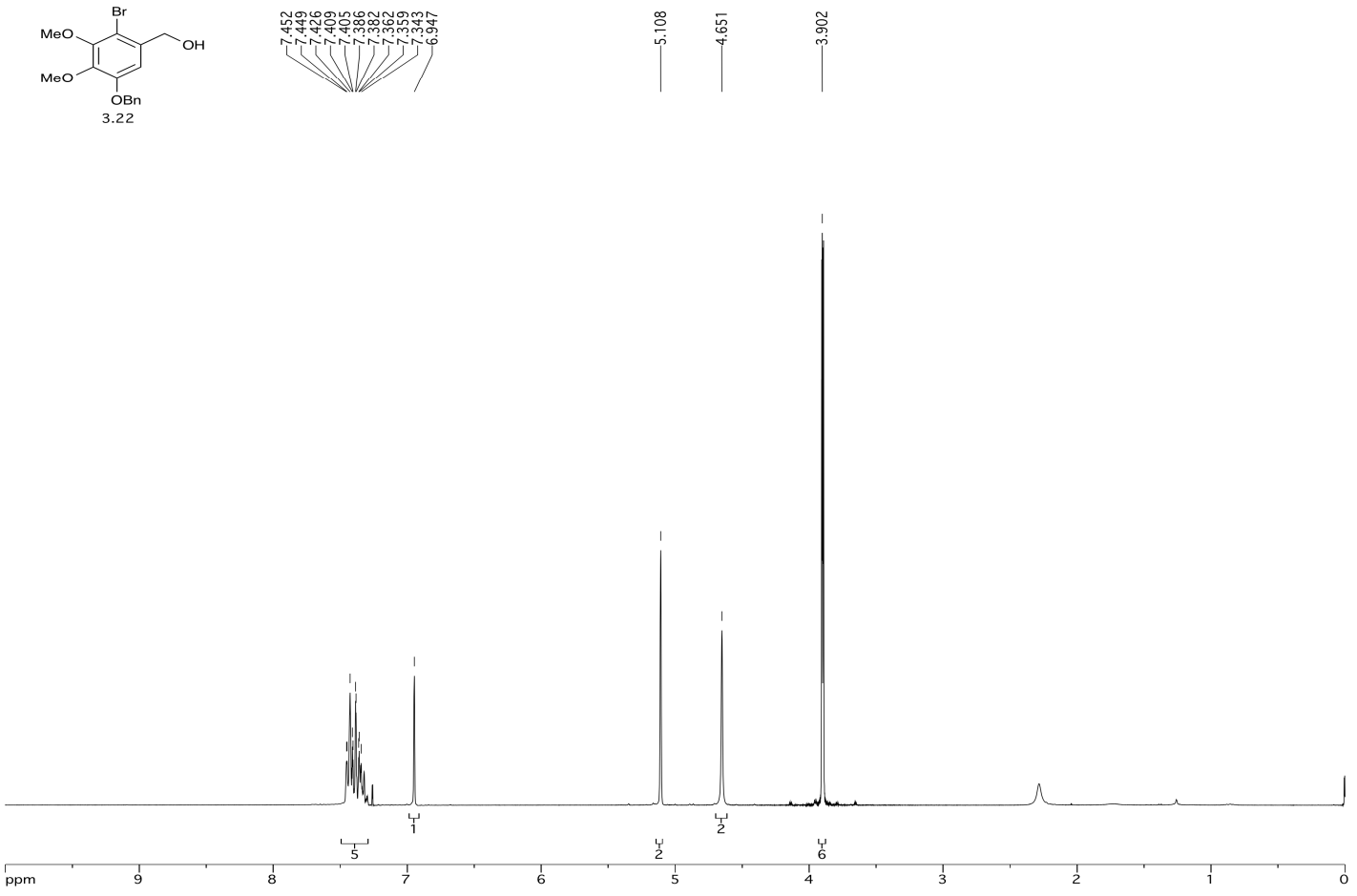
Br
MeO
OH
MeO
OBn
3.22
7.452
7.449
7.426
7.409
7.405
7.386
7.382
7.362
7.359
7.343
6.947
5.108
4.651
3.902
1
2
5
2
6
ppm
9
8
7
6
5
4
3
2
1
0

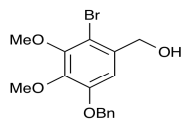

3.22

151.808
150.701
142.609
136.325
135.134
128.391
127.855
127.116
109.163
108.421
77.267
76.842
76.417
70.785
64.744
60.989
60.899

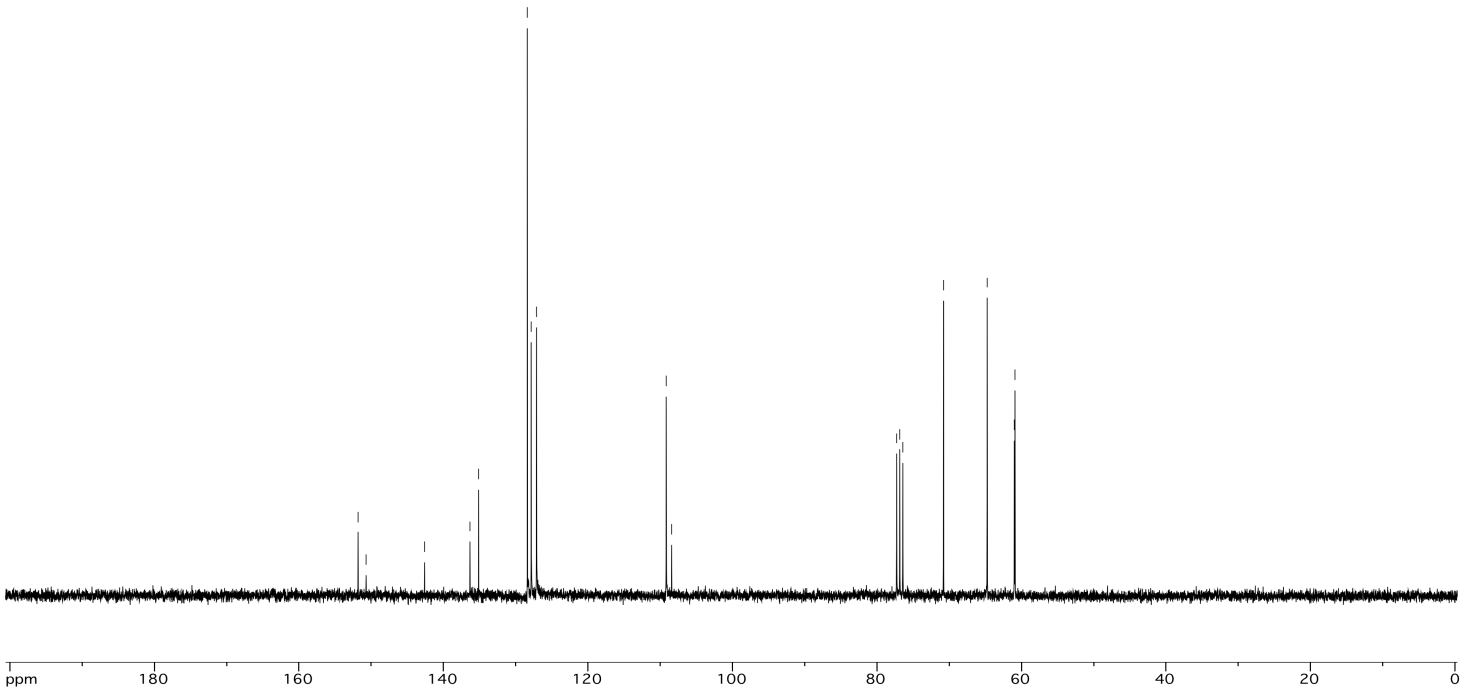

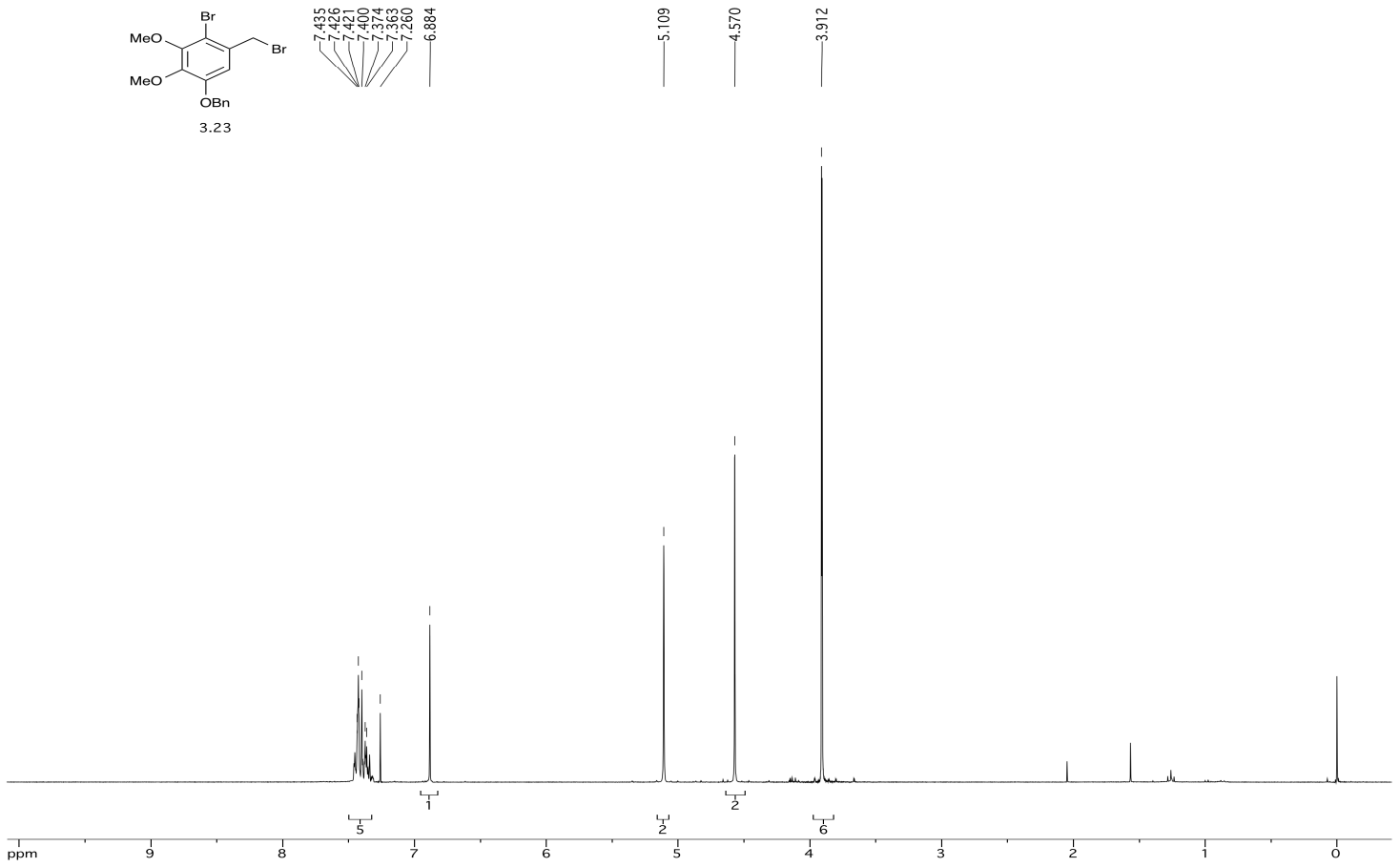
Br
MeO
Br
MeO
OBn
3.23
7.435
7.426
7.421
7.400
7.374
7.363
7.260
6.884
5.109
4.570
3.912
5
1
2
2
6
ppm
9
8
7
6
5
4
3
2
1
0

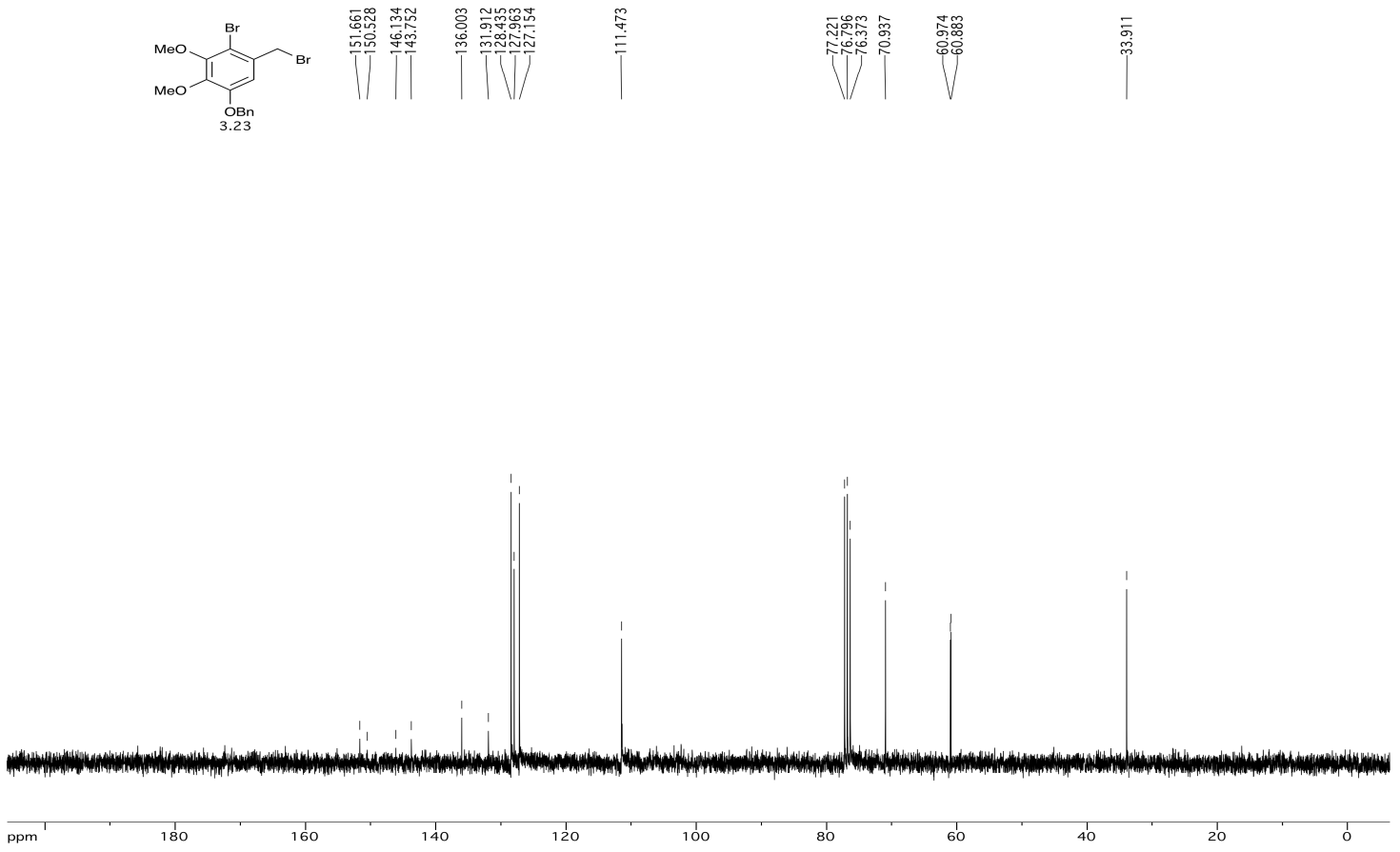
Br
MeO
Br
MeO
OBn
3.23
151.661
150.528
146.134
143.752
136.003
131.912
128.435
127.963
127.154
111.473
77.221
76.796
76.373
70.937
60.974
60.883
33.911
ppm
180
160
140
120
100
80
60
40
20
0

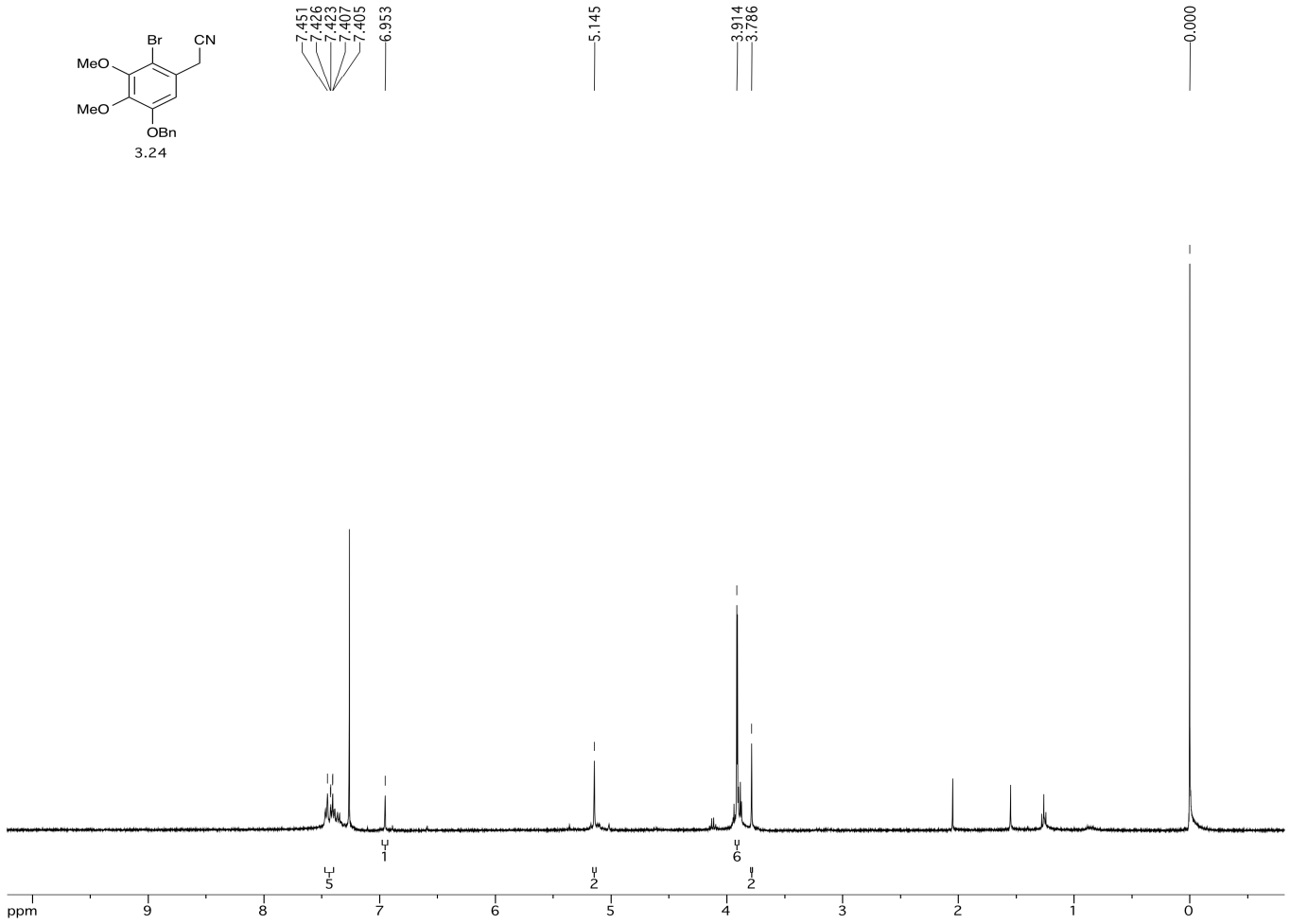
Br
CN
MeO
MeO
OBn
3.24
7.451
7.426
7.423
7.407
7.405
6.953
5.145
3.914
3.786
0.000
1
2
6
5
2
2
ppm
9
8
7
6
5
4
3
2
1
0

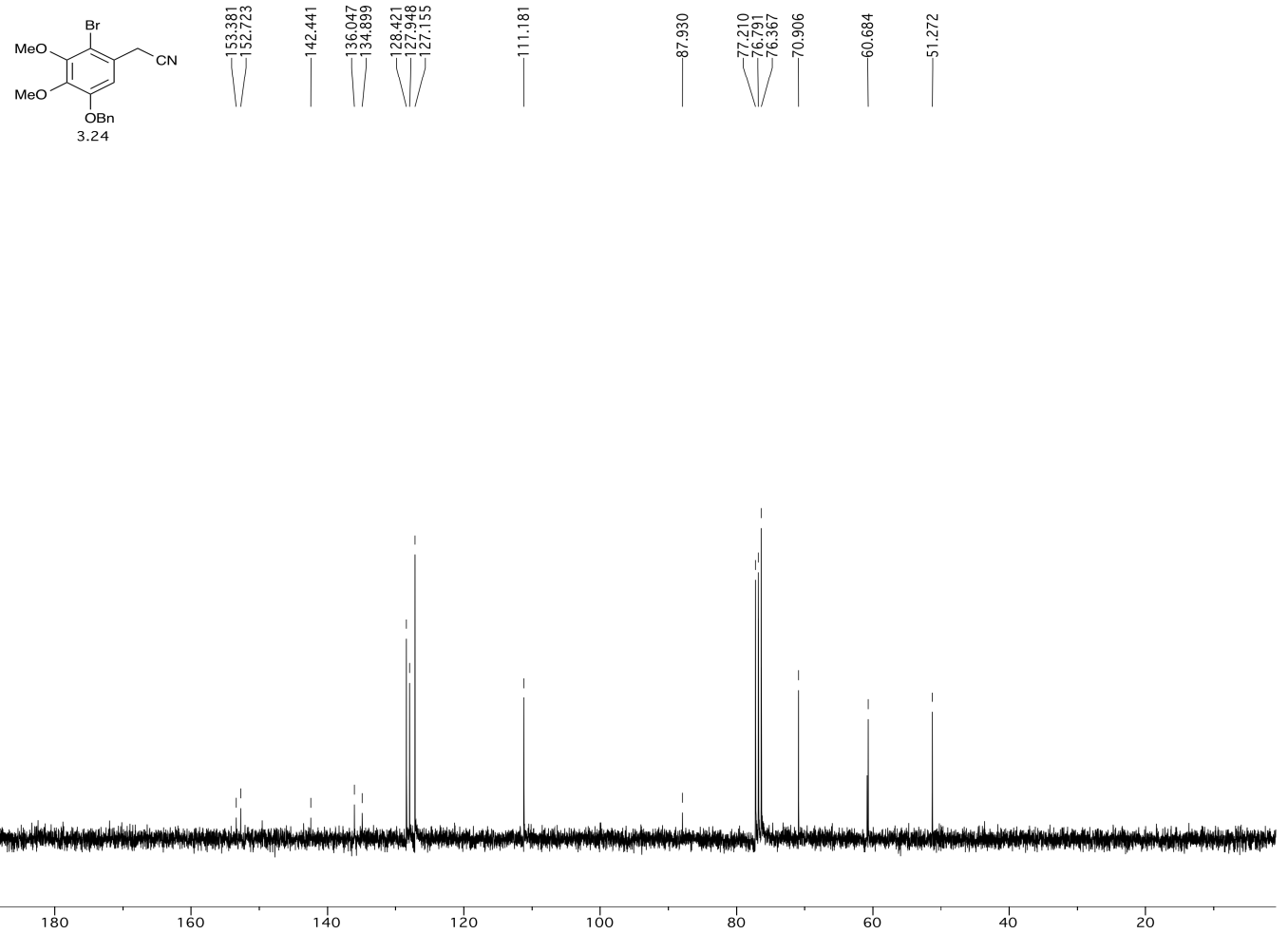
Br
MeO
MeO
CN
OBn
3.24
153.381
152.723
142.441
136.047
134.899
128.421
127.948
127.155
111.181
87.930
77.210
76.791
76.367
70.906
60.684
51.272
ppm
180
160
140
120
100
80
60
40
20

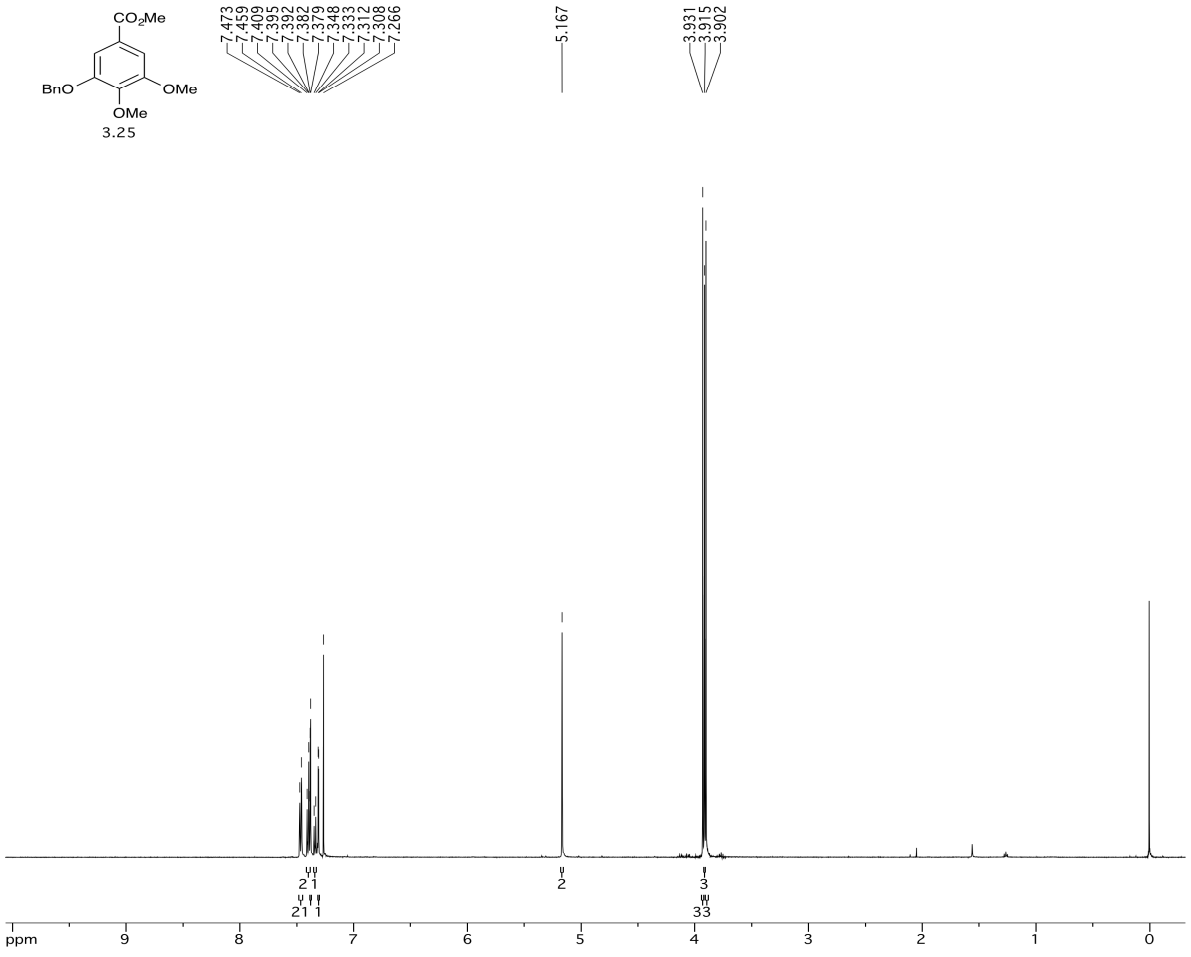
CO2Me
BnO
OMe
OMe
3.25
7.473
7.459
7.409
7.395
7.392
7.382
7.379
7.348
7.333
7.312
7.308
7.266
5.167
3.931
3.915
3.902
2
1
2
1
1
2
3
3
3
ppm
9
8
7
6
5
4
3
2
1
0

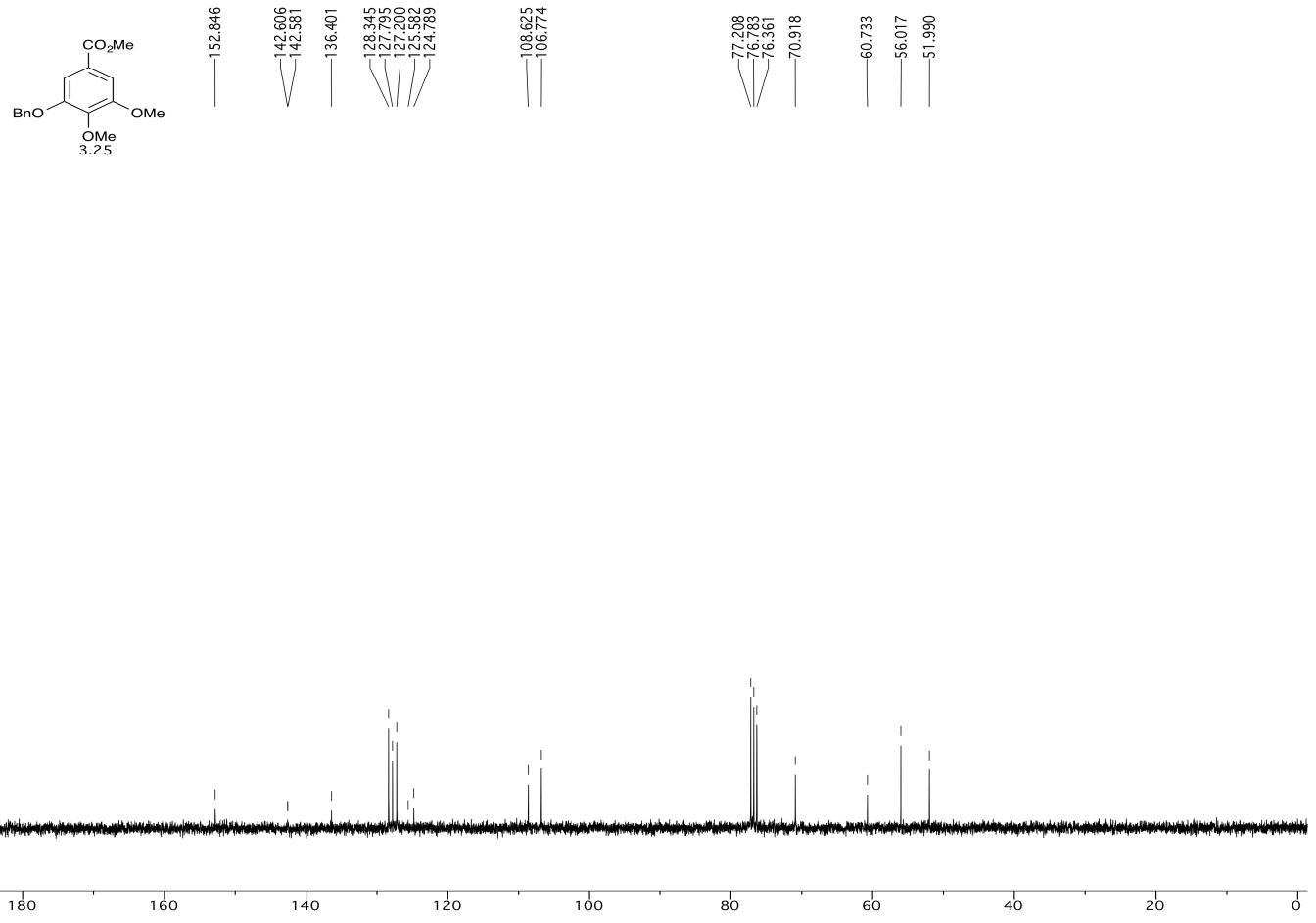
CO2Me
BnO
OMe
OMe
3.25
152.846
142.606
142.581
136.401
128.345
127.795
127.200
125.582
124.789
108.625
106.774
77.208
76.783
76.361
70.918
60.733
56.017
51.990
ppm
180
160
140
120
100
80
60
40
20
0

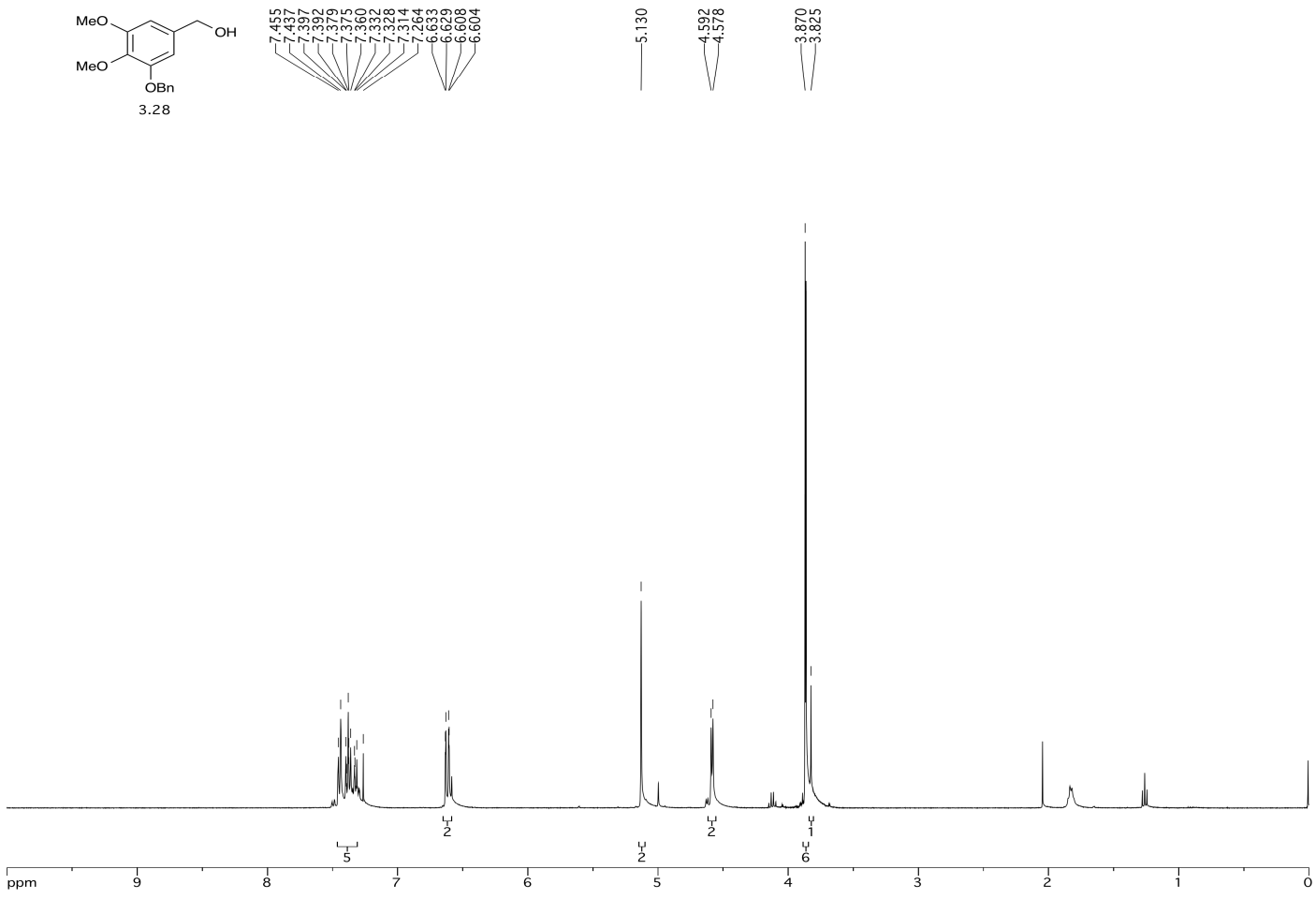
MeO
MeO
OBn
OH
3.28
7.455
7.437
7.397
7.392
7.379
7.375
7.360
7.332
7.328
7.314
7.264
6.633
6.629
6.608
6.604
5.130
4.592
4.578
3.870
3.825
5
2
2
2
1
6
ppm
9
8
7
6
5
4
3
2
1
0

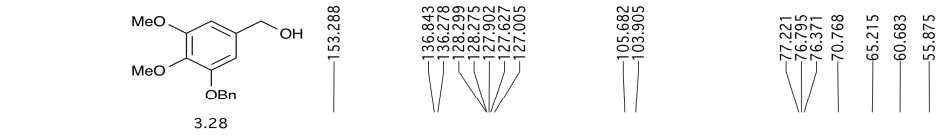
MeO
MeO
OBn
OH
153.288
136.843
136.278
128.299
128.275
127.902
127.627
127.005
105.682
103.905
77.221
76.795
76.371
70.768
65.215
60.683
55.875

3.28

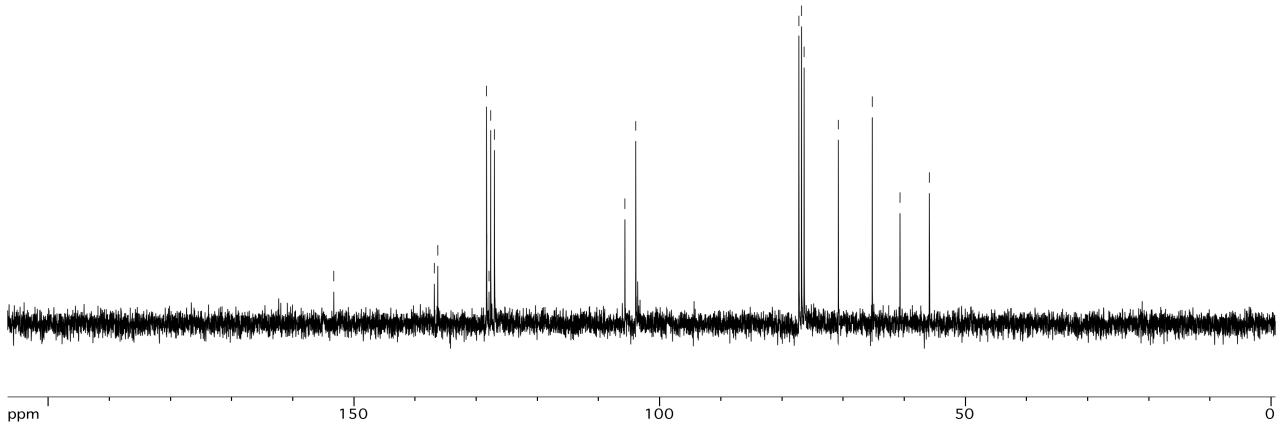
ppm
150
100
50
0

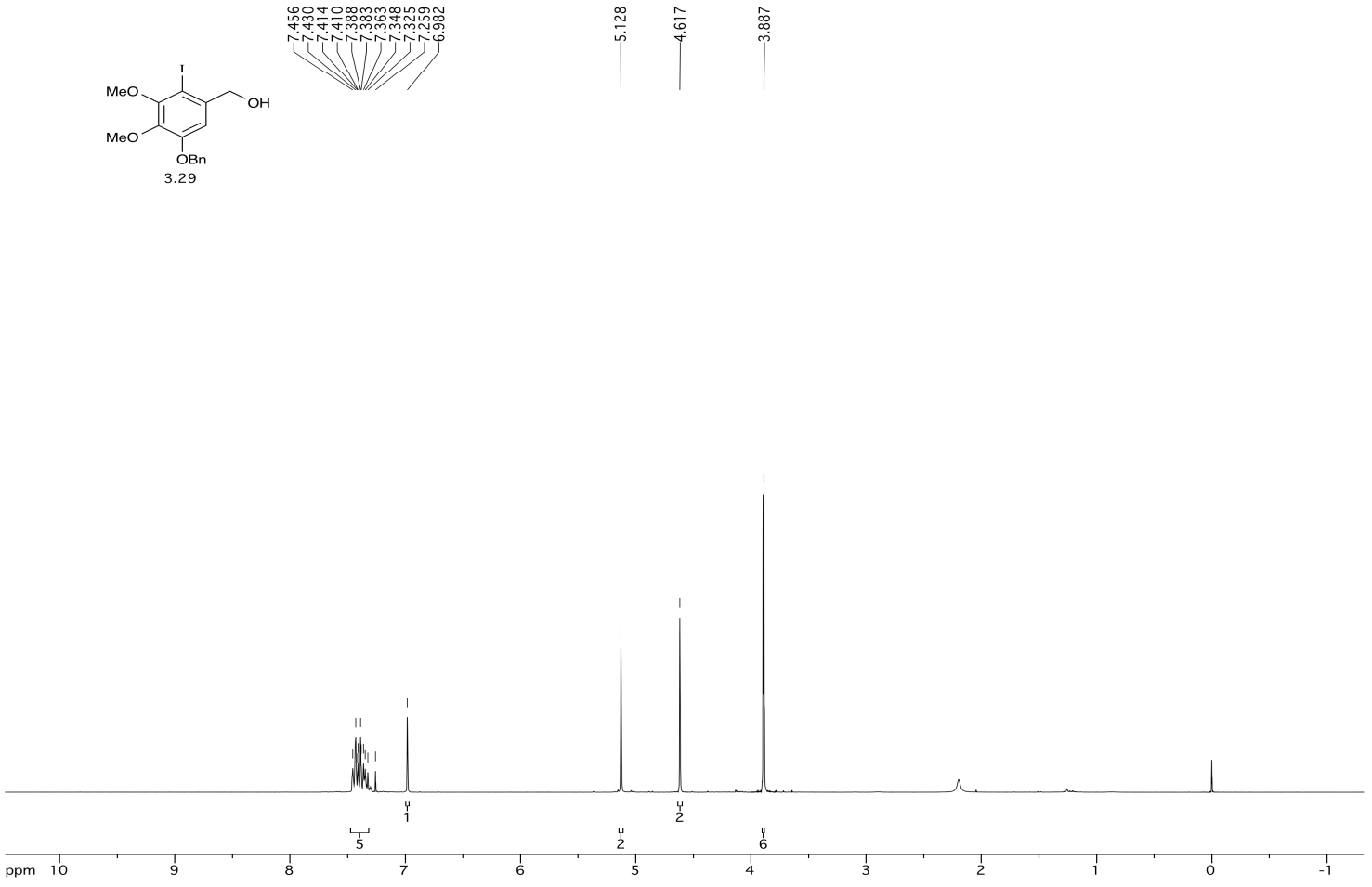
7.456
7.430
7.414
7.410
7.388
7.383
7.363
7.348
7.325
7.259
6.982
5.128
4.617
3.887
I
MeO
MeO
OH
OBn
3.29
1
2
5
2
6
ppm 10 9 8 7 6 5 4 3 2 1 0 -1

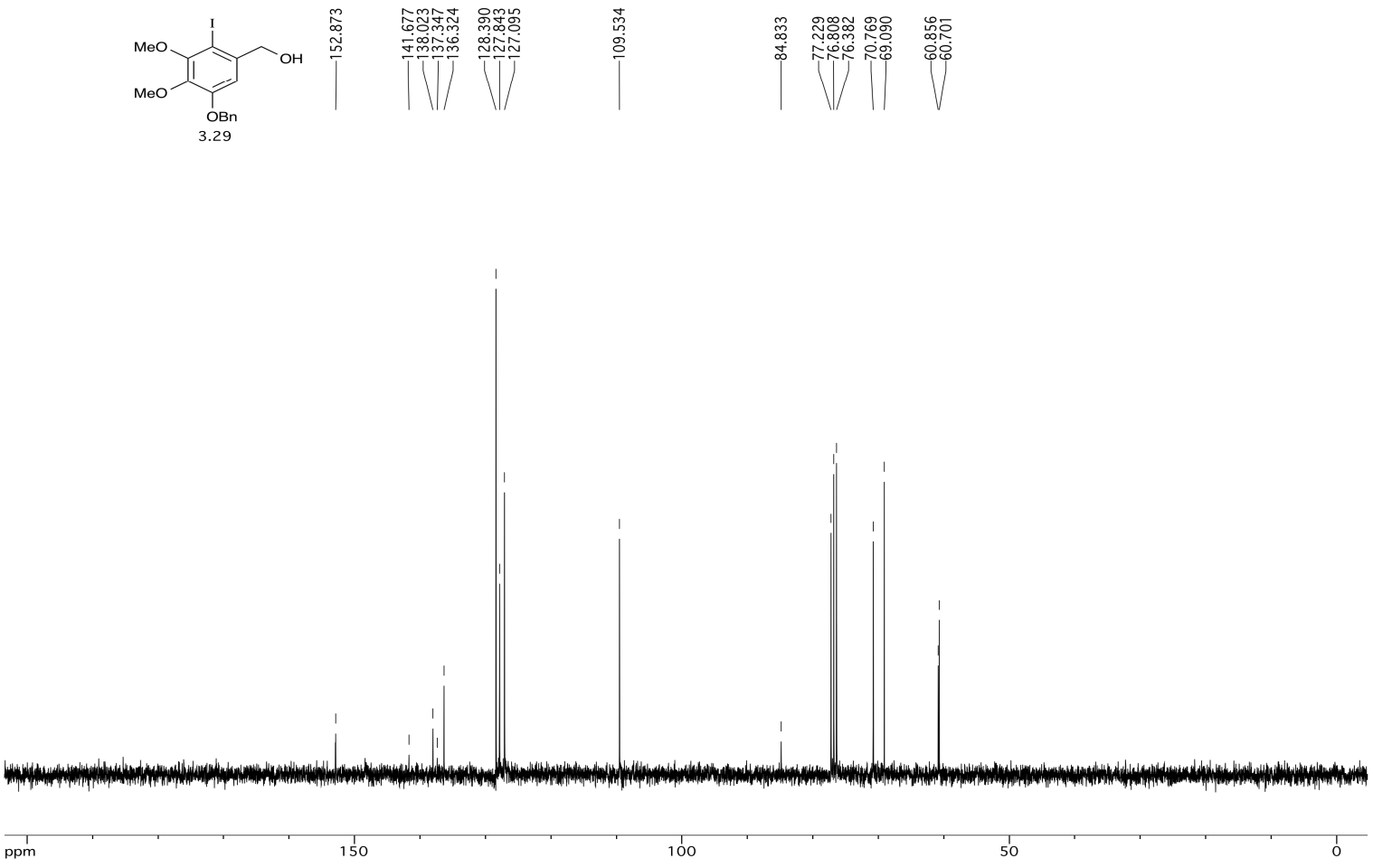
I
MeO
MeO
OBn
OH
3.29
152.873
141.677
138.023
137.347
136.324
128.390
127.843
127.095
109.534
84.833
77.229
76.808
76.382
70.769
69.090
60.856
60.701
ppm
150
100
50
0

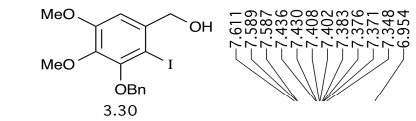
MeO
MeO
OBn
OH
I

3.30

7.611
7.589
7.587
7.436
7.430
7.408
7.402
7.383
7.376
7.371
7.348
6.954

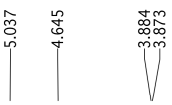
5.037
4.645
3.884
3.873

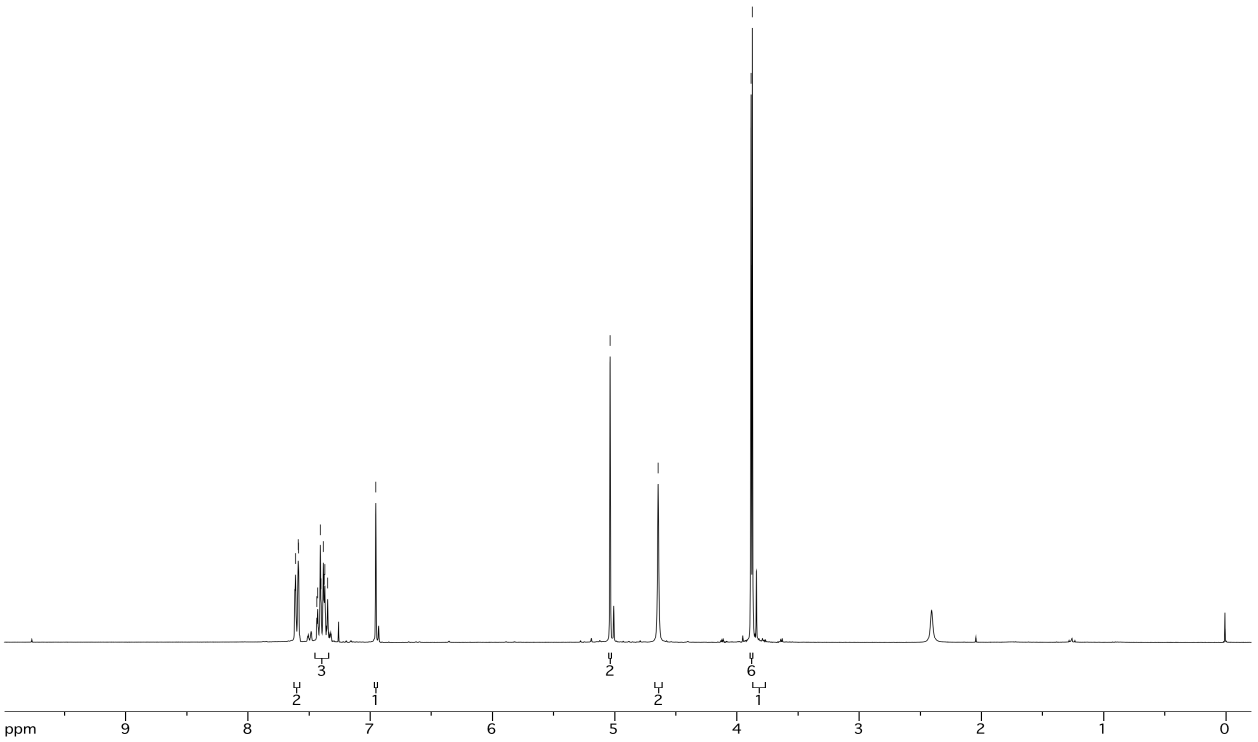
3
2
6
2
1
2
1
ppm
9
8
7
6
5
4
3
2
1
0

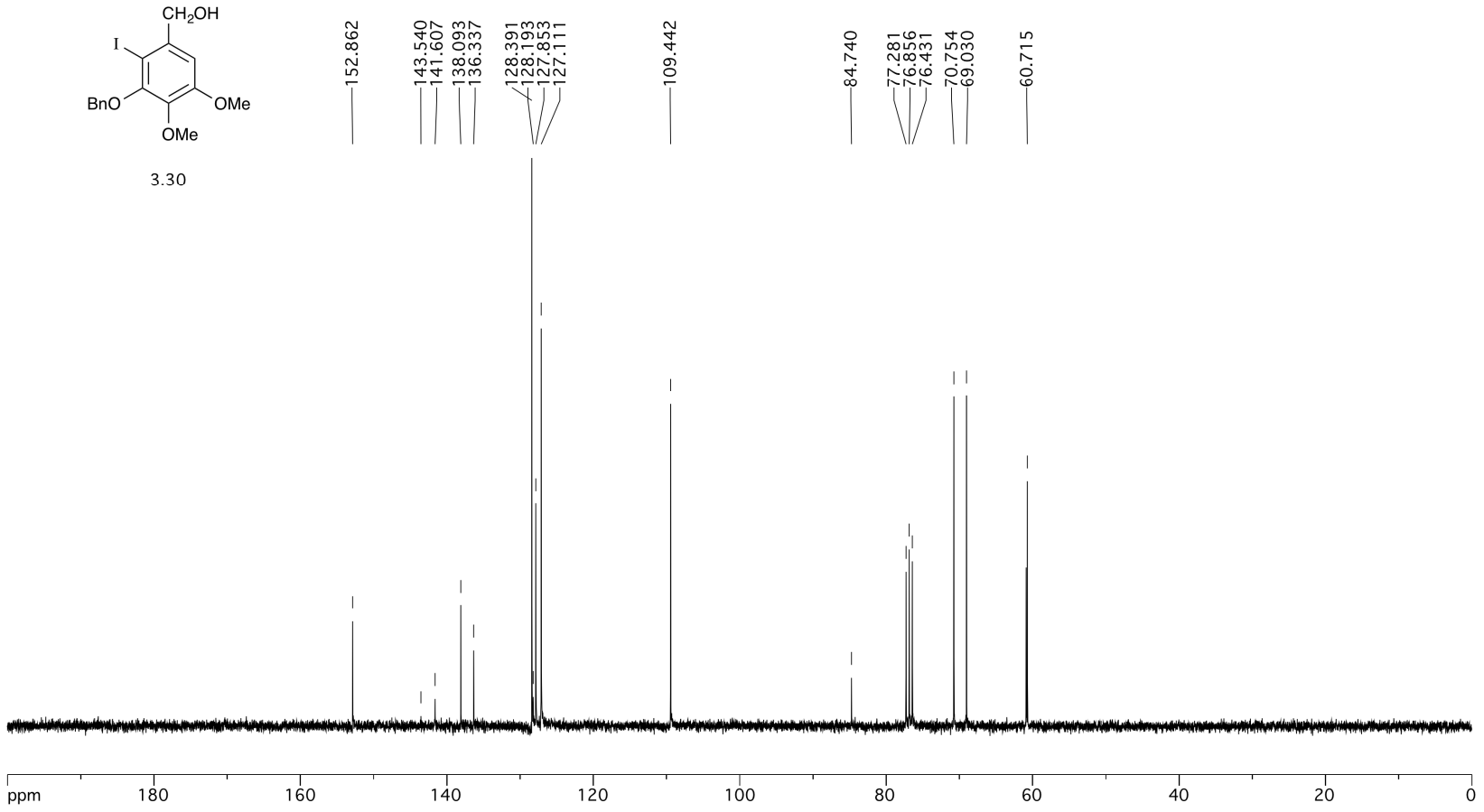
CH2OH
I
BnO
OMe
OMe
3.30
152.862
143.540
141.607
138.093
136.337
128.391
128.193
127.853
127.111
109.442
84.740
77.281
76.856
76.431
70.754
69.030
60.715
ppm
180
160
140
120
100
80
60
40
20
0

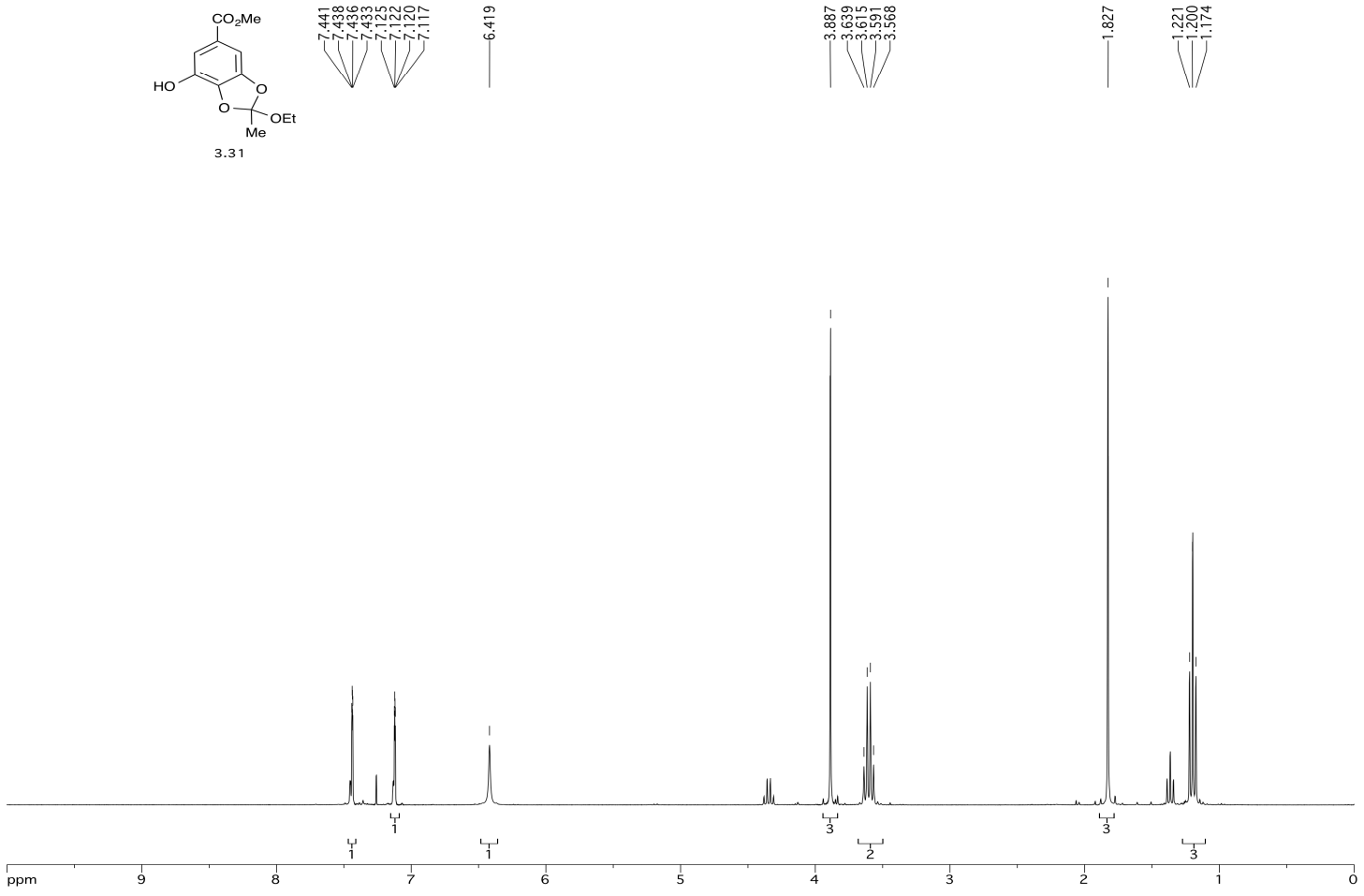
CO2Me
HO
O
O
OEt
Me
3.31
7.441
7.438
7.436
7.433
7.125
7.122
7.120
7.117
6.419
3.887
3.639
3.615
3.591
3.568
1.827
1.221
1.200
1.174
1
1
1
3
2
3
3
ppm
9
8
7
6
5
4
3
2
1
0

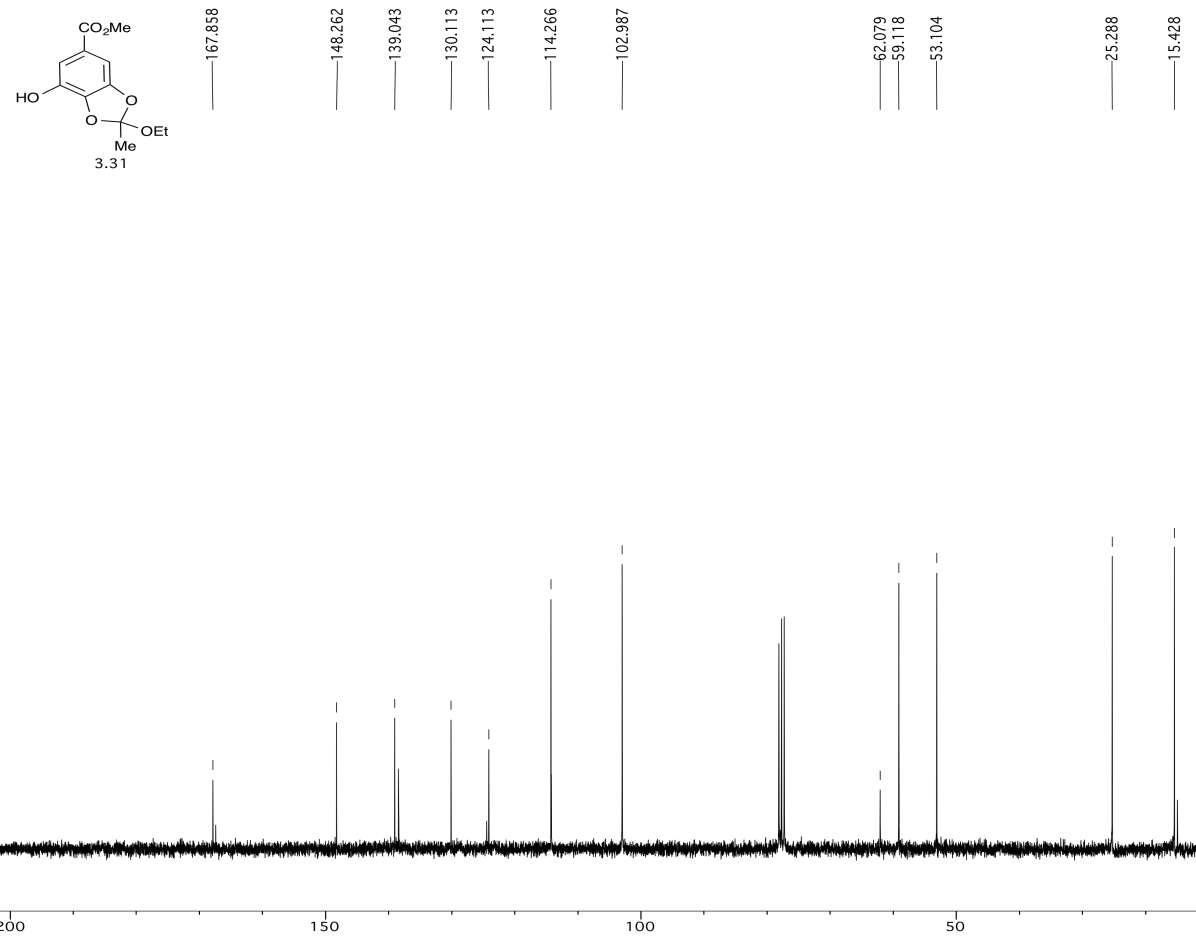
CO2Me
HO
O
O
OEt
Me
3.31
167.858
148.262
139.043
130.113
124.113
114.266
102.987
62.079
59.118
53.104
25.288
15.428
ppm
200
150
100
50
0

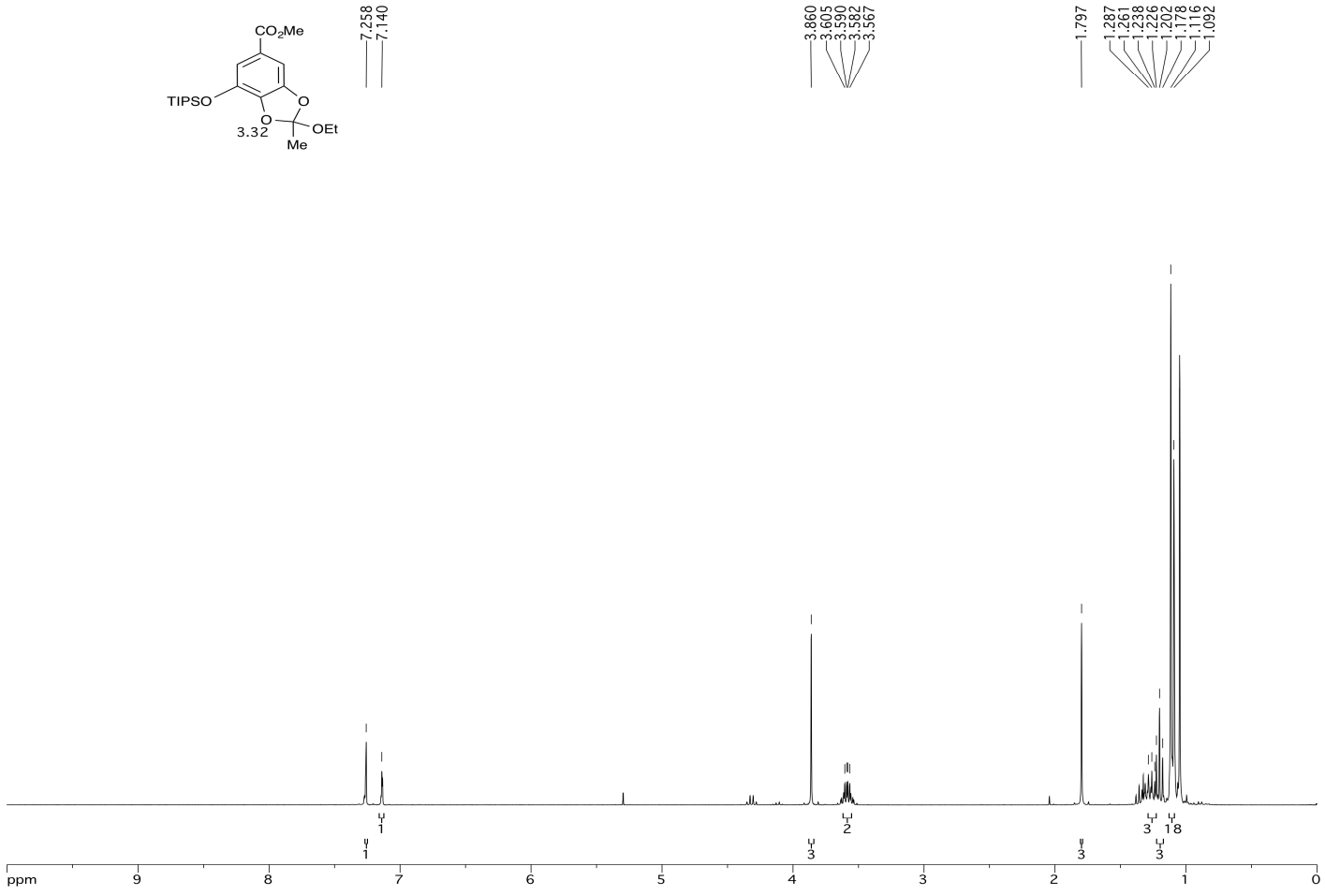
CO2Me
TIPSO
O
O
3.32
OEt
Me
7.258
7.140
3.860
3.605
3.590
3.582
3.567
1.797
1.287
1.261
1.238
1.226
1.202
1.178
1.116
1.092
1
1
3
2
3
3
18
3
ppm
9
8
7
6
5
4
3
2
1
0

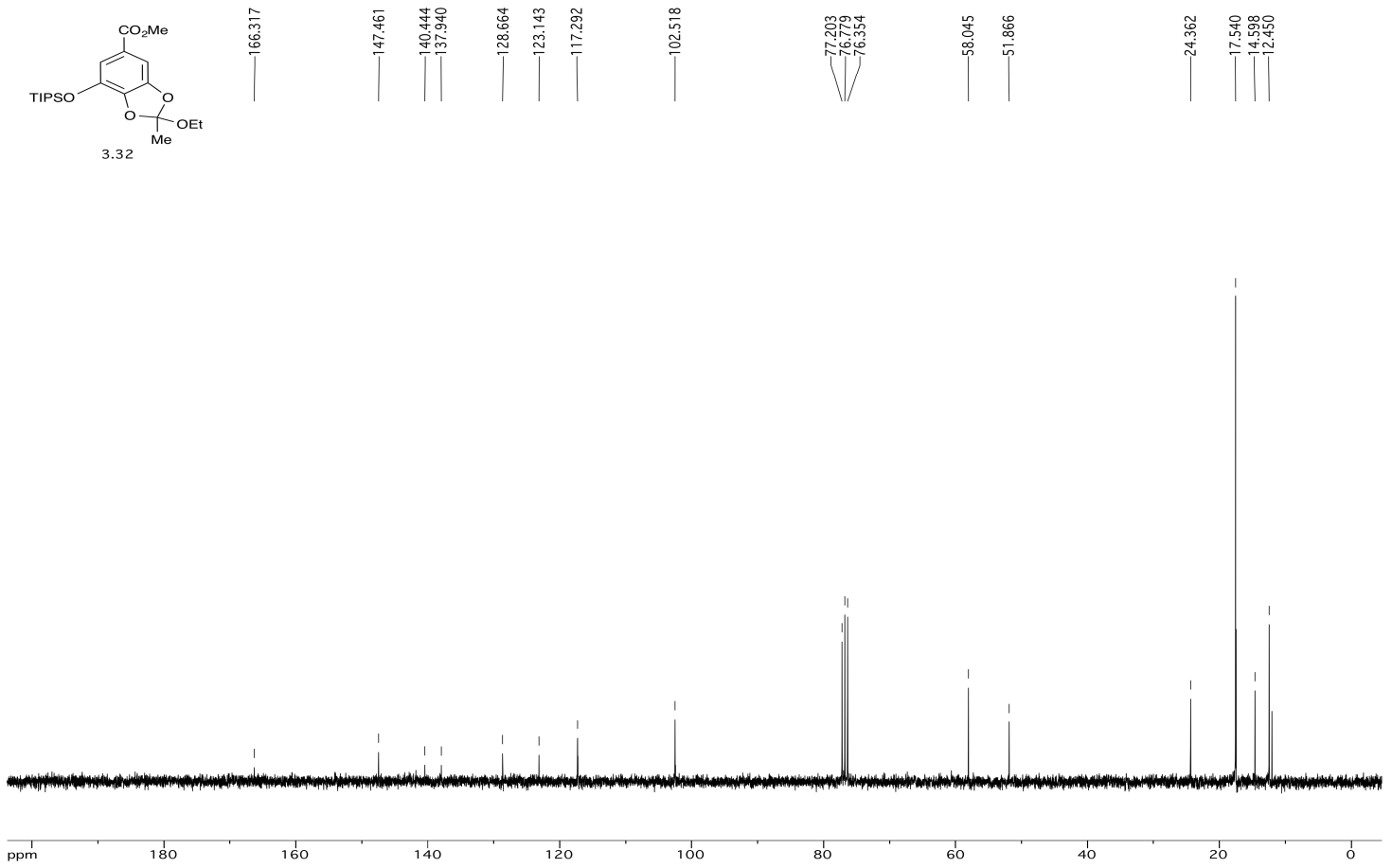
CO2Me
TIPSO
O
O
OEt
Me
3.32
166.317
147.461
140.444
137.940
128.664
123.143
117.292
102.518
77.203
76.779
76.354
58.045
51.866
24.362
17.540
14.598
12.450
ppm
180
160
140
120
100
80
60
40
20
0

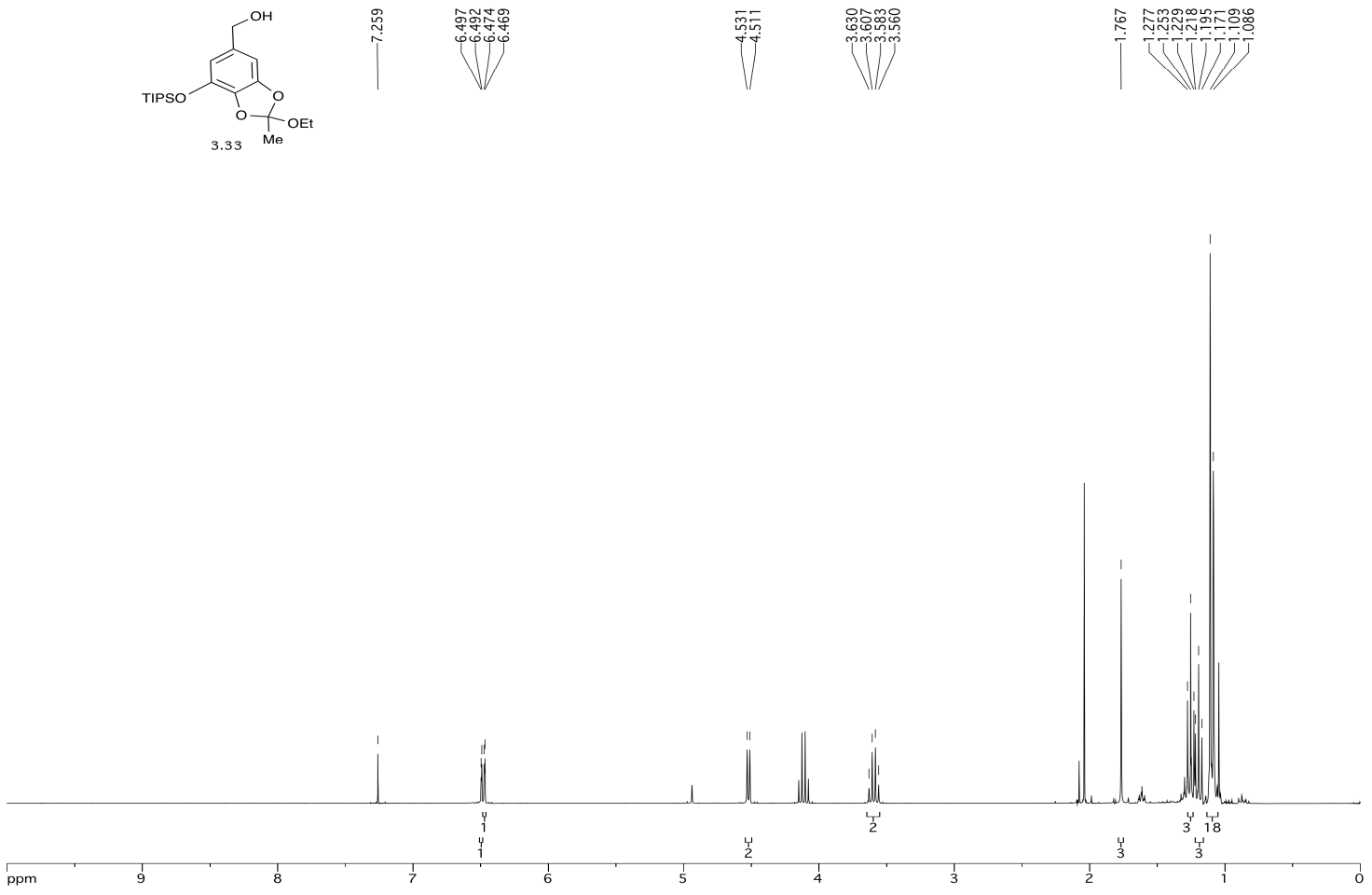
OH
TIPSO
O
O
OEt
Me
3.33
7.259
6.497
6.492
6.474
6.469
4.531
4.511
3.630
3.607
3.583
3.560
1.767
1.277
1.253
1.229
1.218
1.195
1.171
1.109
1.086
ppm

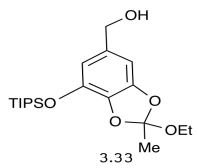
OH
TIPSO
O
O
OEt
Me
3.33

148.755
139.076
136.675
135.067
128.807
114.323
101.105
78.123
77.701
77.278
66.110
58.751
25.258
18.503
15.582
13.434
ppm
160
140
120
100
80
60
40
20
0

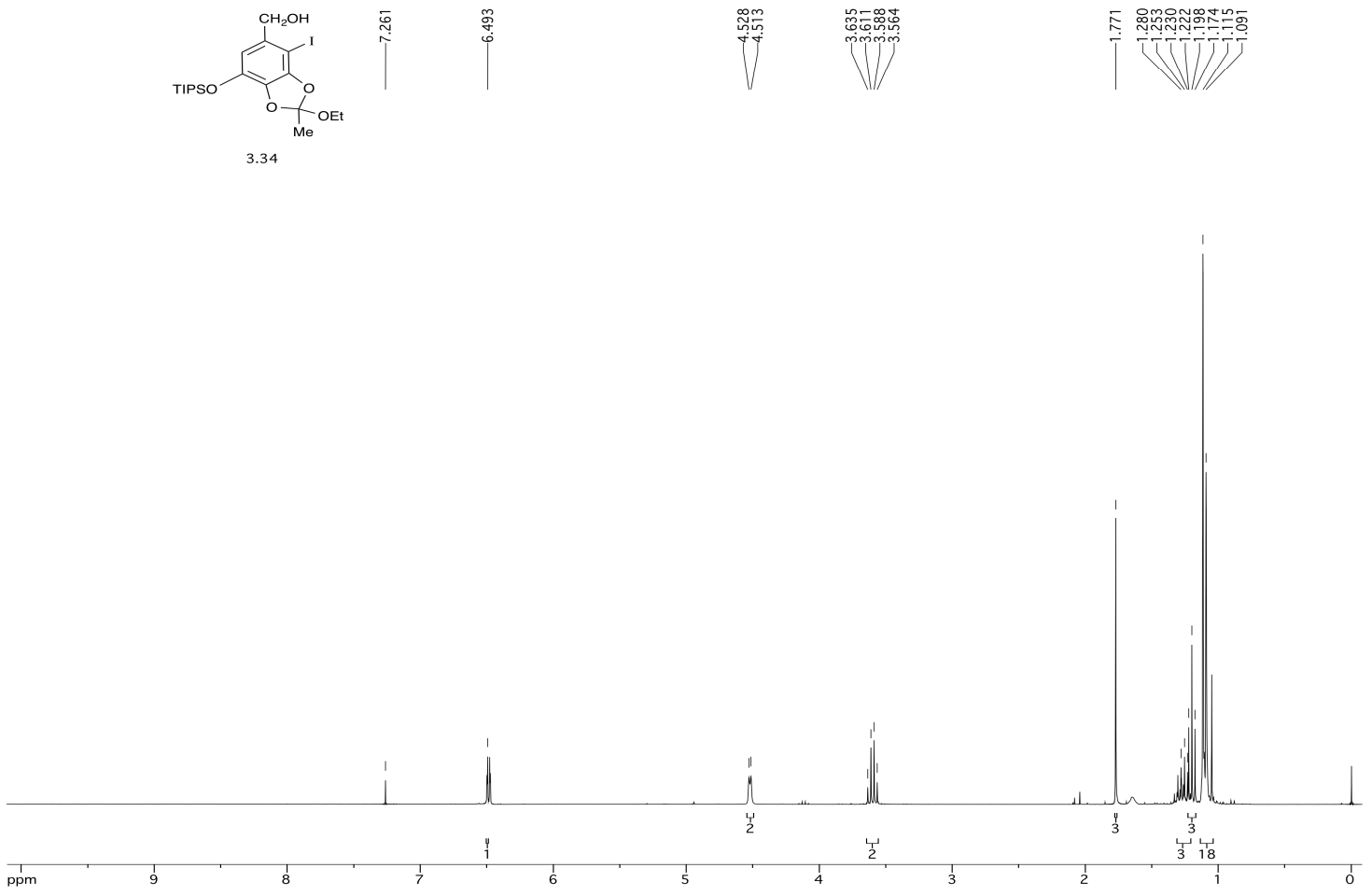
CH2OH
I
TIPSO
O
O
OEt
Me
3.34
7.261
6.493
4.528
4.513
3.635
3.611
3.588
3.564
1.771
1.280
1.253
1.230
1.222
1.198
1.174
1.115
1.091
2
3
3
1
2
3
18
ppm
9
8
7
6
5
4
3
2
1
0

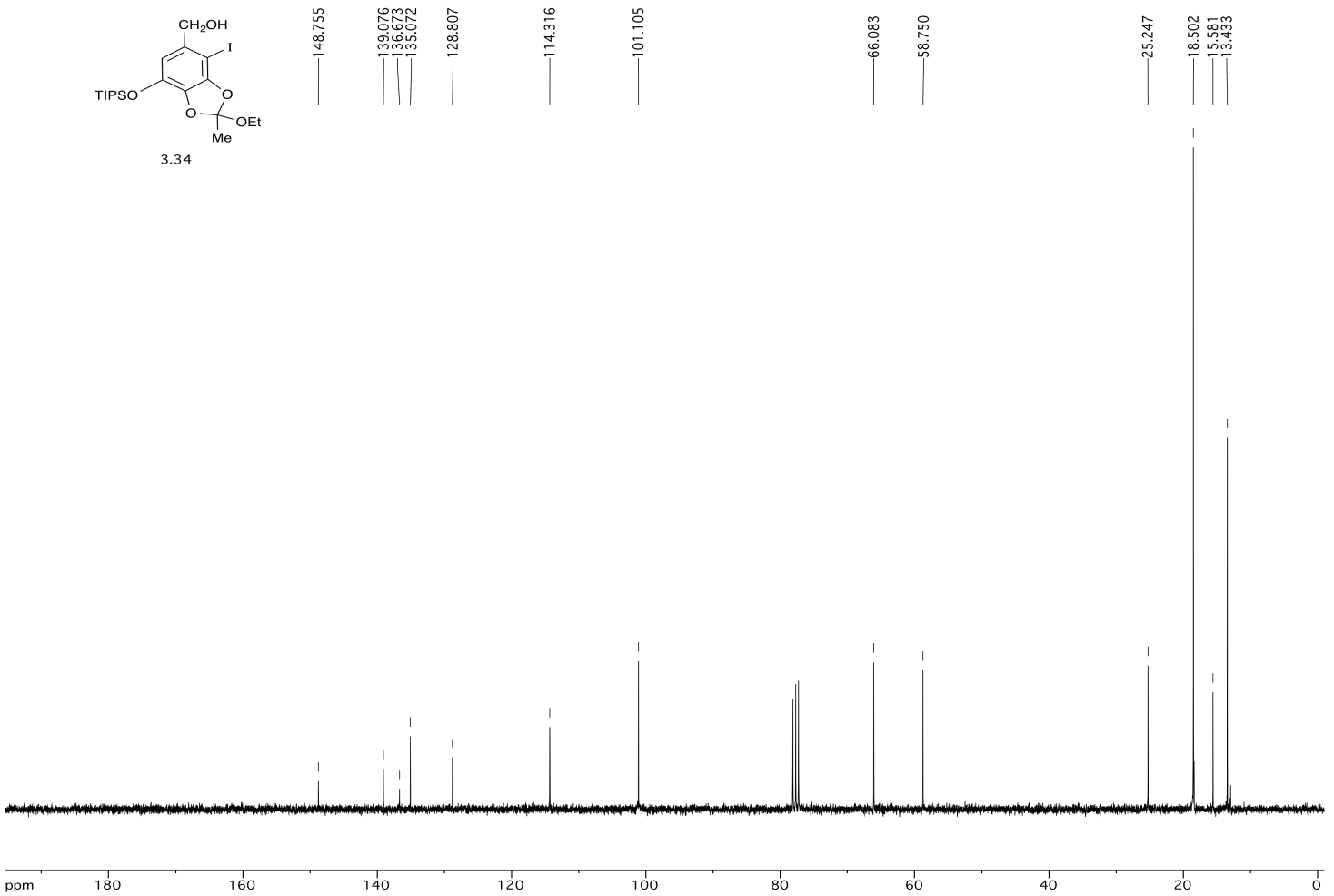
CH2OH
I
TIPSO
O
O
OEt
Me
3.34
148.755
139.076
136.673
135.072
128.807
114.316
101.105
66.083
58.750
25.247
18.502
15.581
13.433
ppm
180
160
140
120
100
80
60
40
20
0

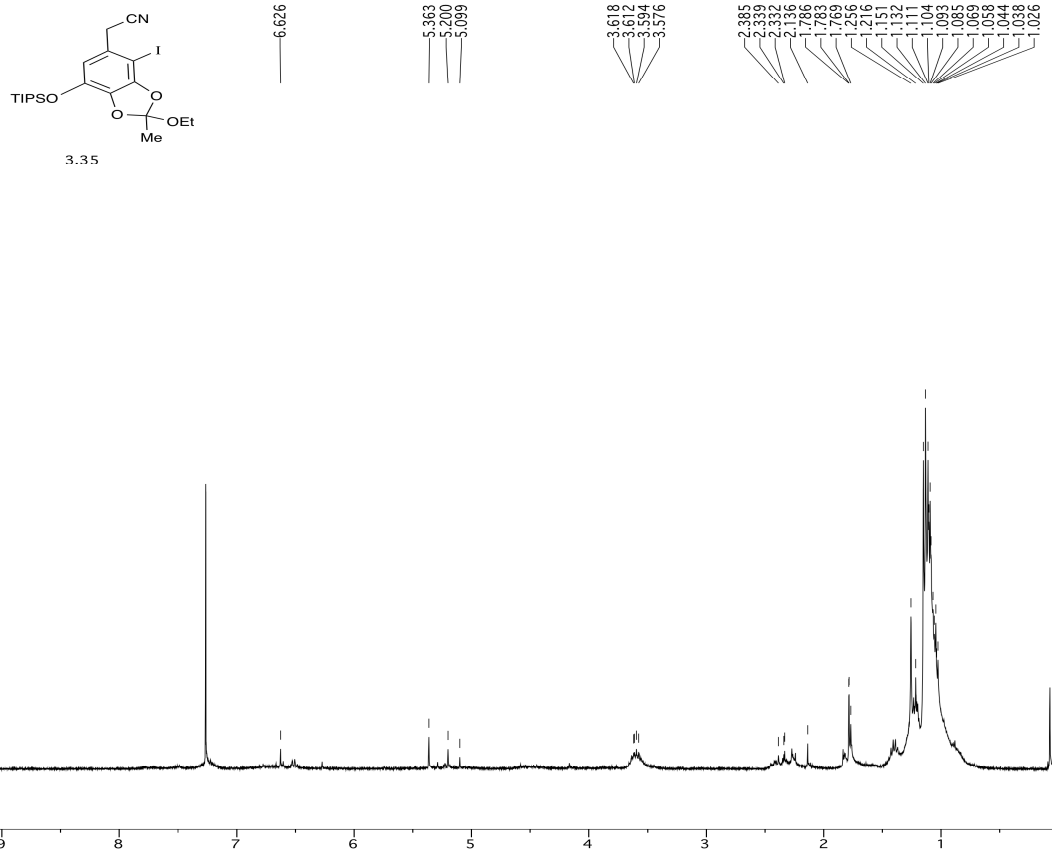
CN
I
TIPSO
O
O
OEt
Me
3.35
6.626
5.363
5.200
5.099
3.618
3.612
3.594
3.576
2.385
2.339
2.332
2.136
1.786
1.783
1.769
1.256
1.216
1.151
1.132
1.111
1.104
1.093
1.085
1.069
1.058
1.044
1.038
1.026
ppm
9
8
7
6
5
4
3
2
1
0

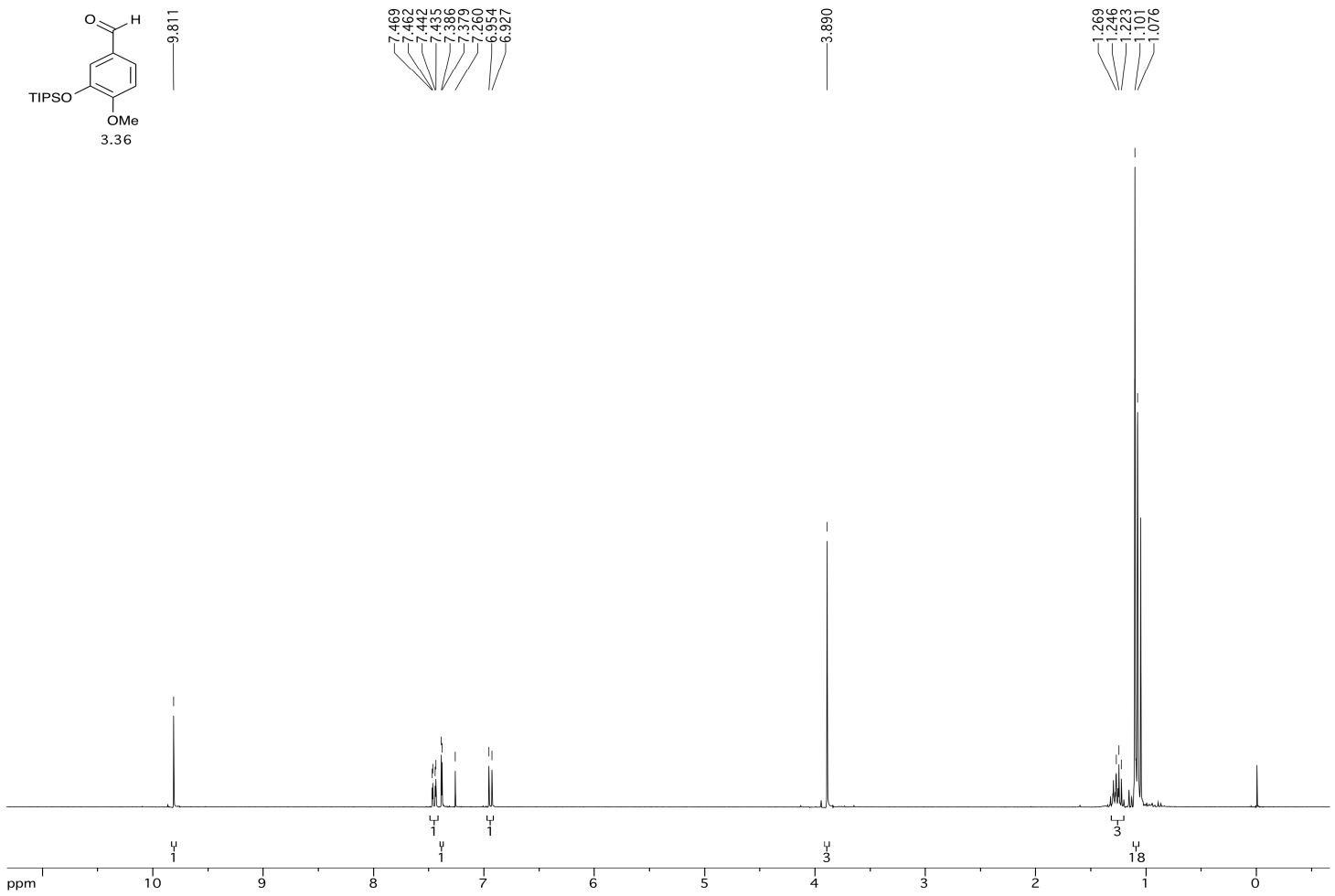
O
H
TIPSO
OMe
3.36
9.811
7.469
7.462
7.442
7.435
7.386
7.379
7.260
6.954
6.927
3.890
1.269
1.246
1.223
1.101
1.076
1
1
1
1
3
3
18
ppm
10
9
8
7
6
5
4
3
2
1
0

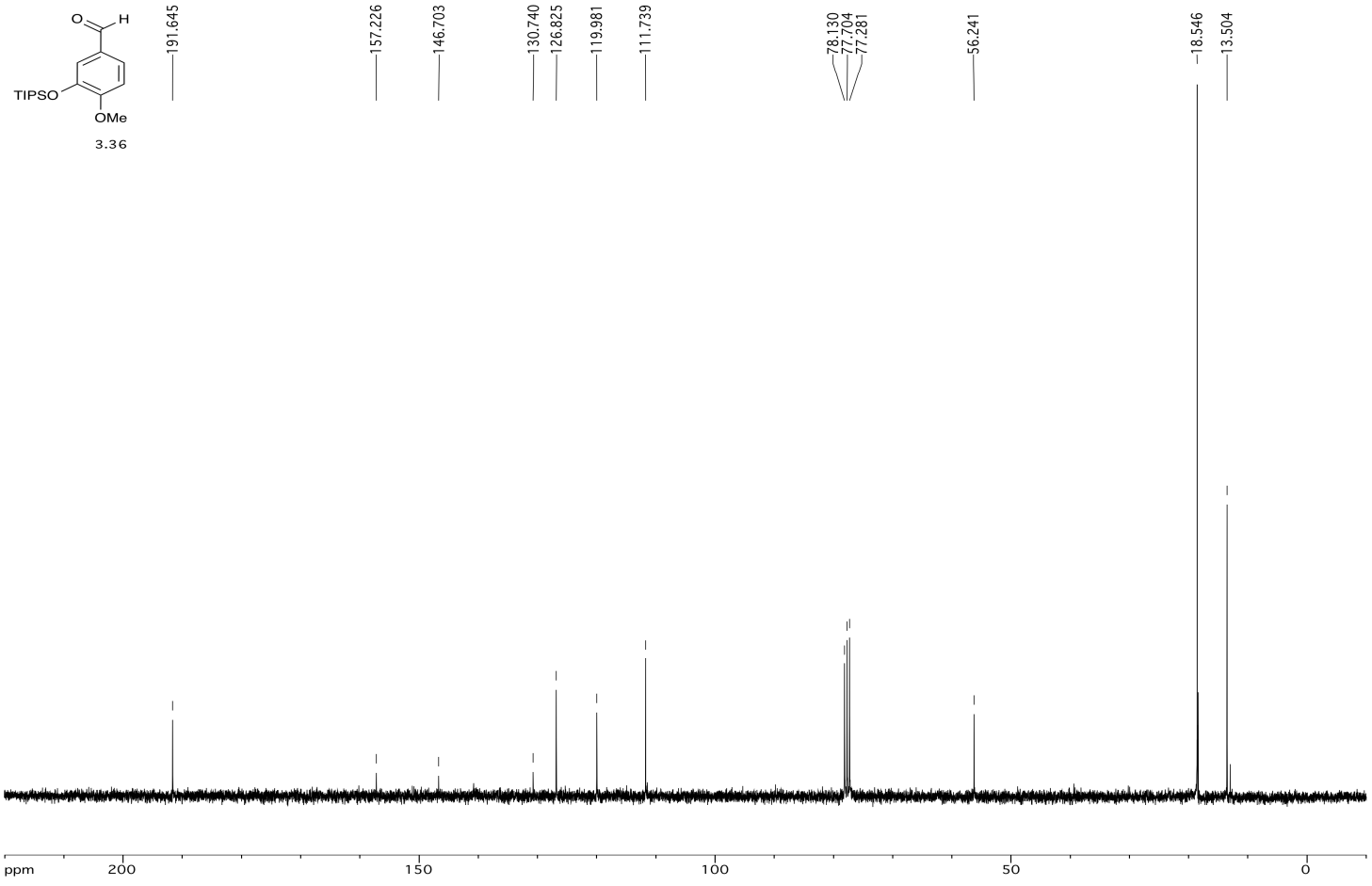
O
H
TIPSO
OMe
3.36
191.645
157.226
146.703
130.740
126.825
119.981
111.739
78.130
77.704
77.281
56.241
18.546
13.504
ppm
200
150
100
50
0

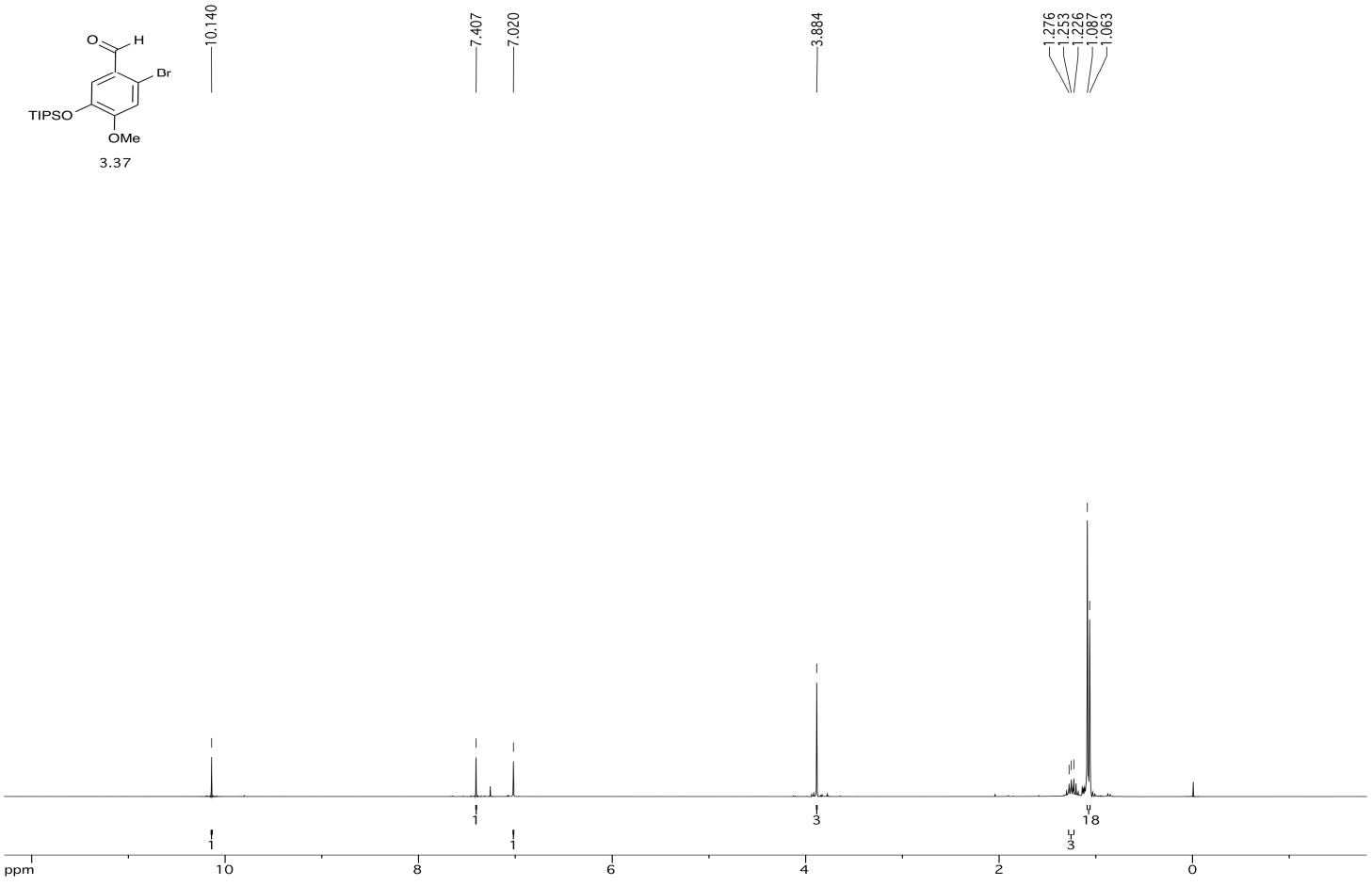
O
H
Br
TIPSO
OMe
3.37
10.140
7.407
7.020
3.884
1.276
1.253
1.226
1.087
1.063
1
1
3
18
1
1
3
ppm
10
8
6
4
2
0

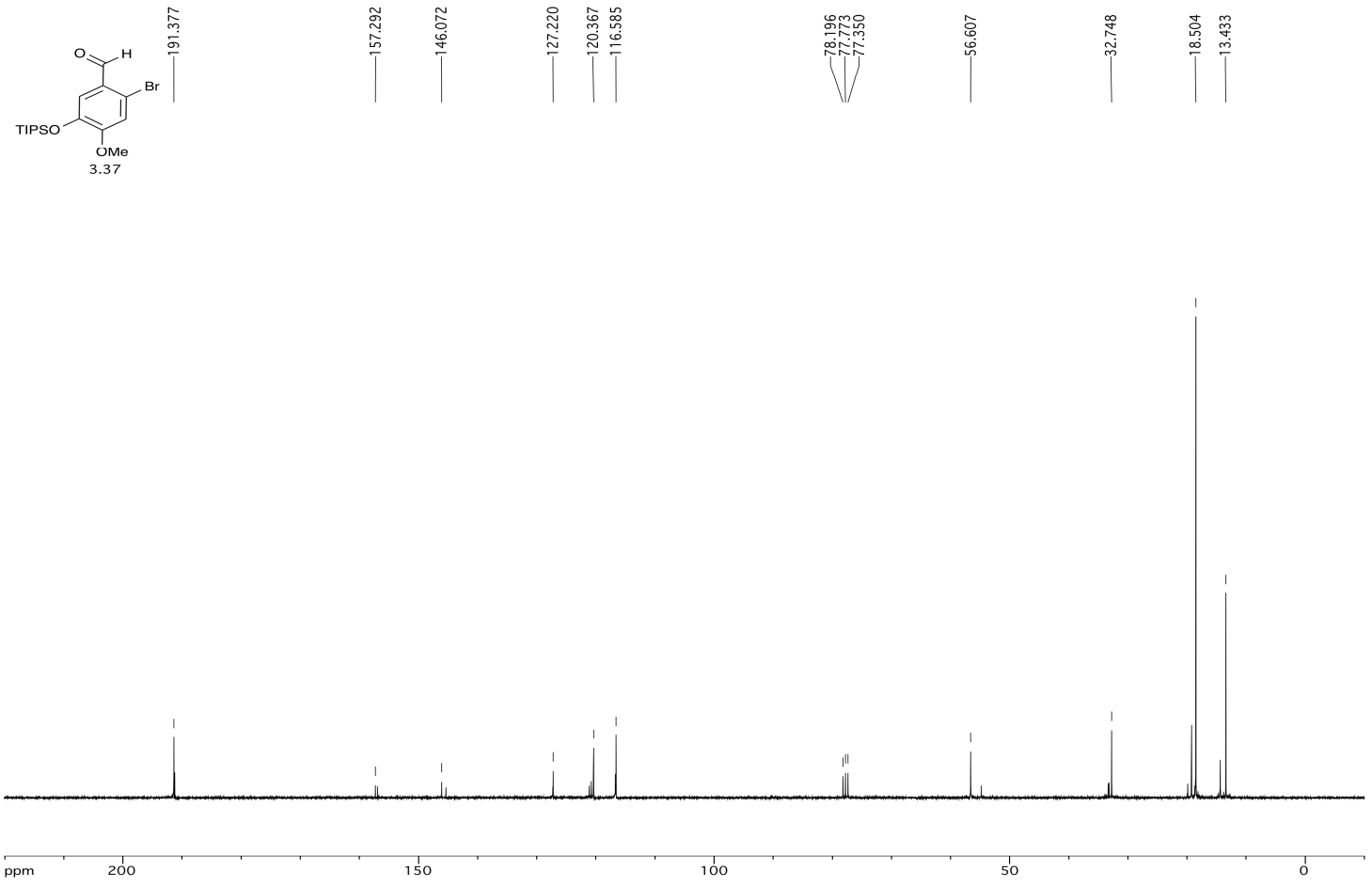
O
H
Br
TIPSO
OMe
3.37
191.377
157.292
146.072
127.220
120.367
116.585
78.196
77.773
77.350
56.607
32.748
18.504
13.433
ppm
200
150
100
50
0

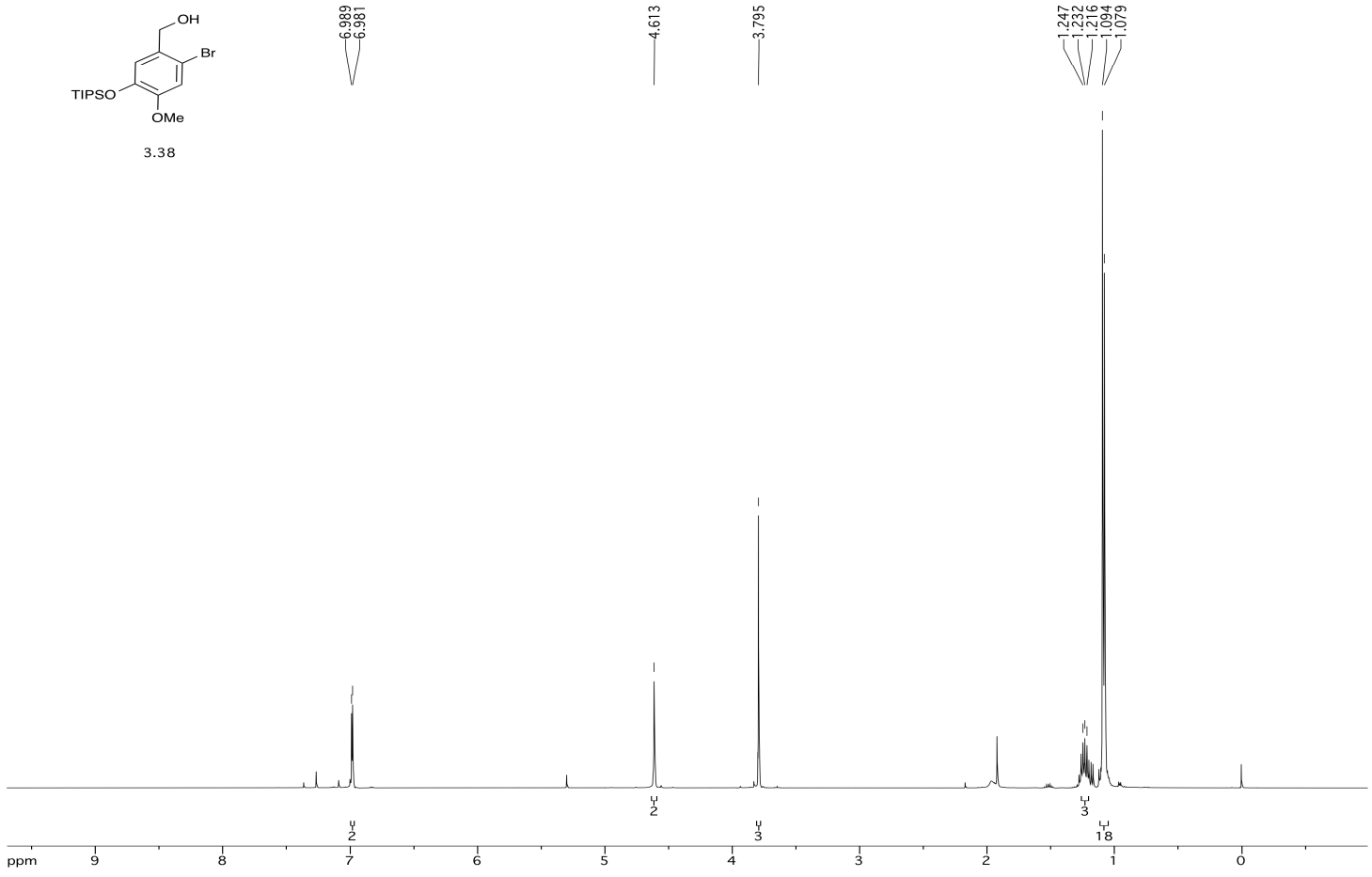
OH
Br
TIPSO
OMe
3.38
6.989
6.981
4.613
3.795
1.247
1.232
1.216
1.094
1.079
2
2
3
3
2
18
ppm
9
8
7
6
5
4
3
2
1
0

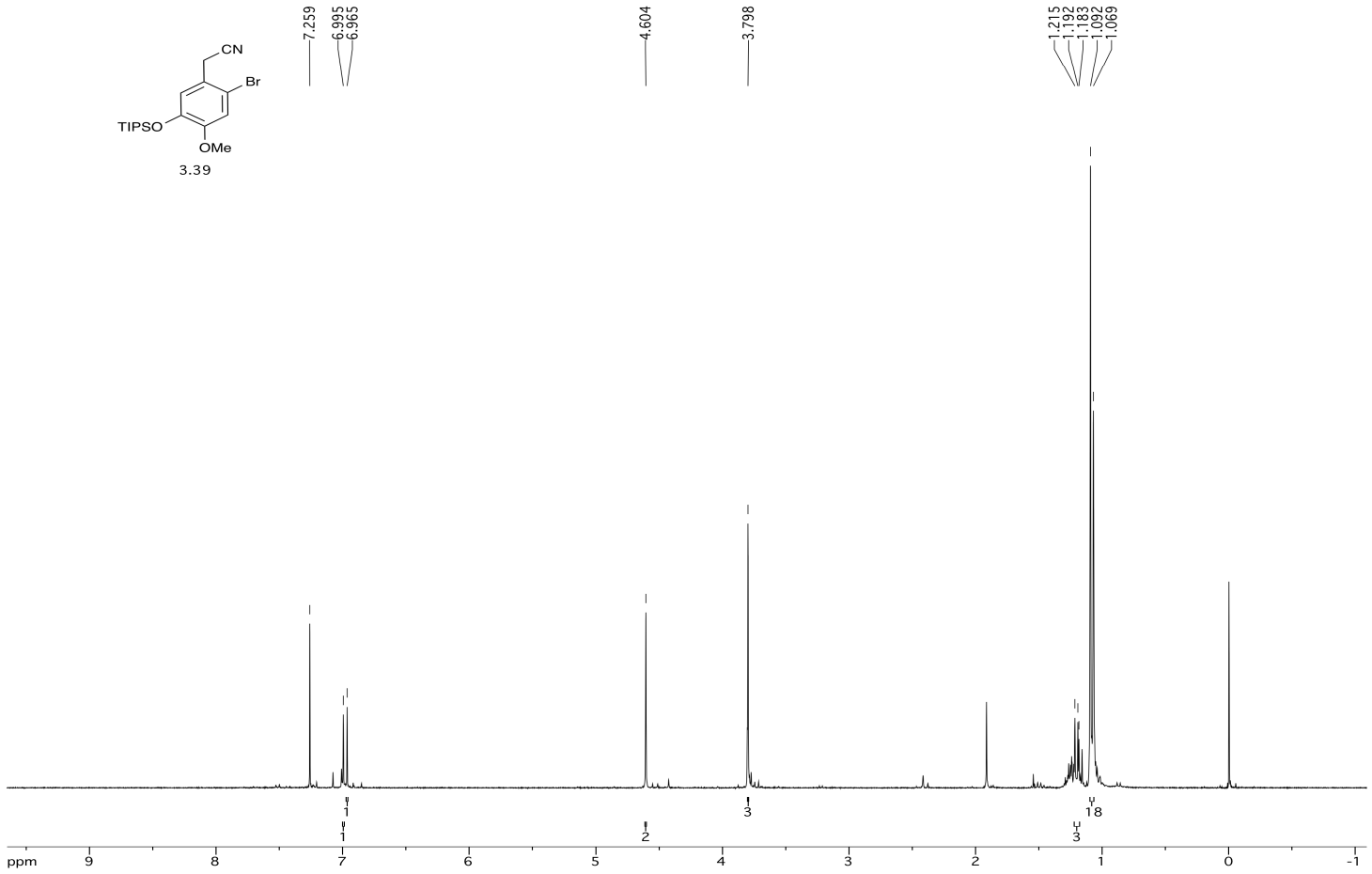
CN
Br
TIPSO
OMe
3.39
7.259
6.995
6.965
4.604
3.798
1.215
1.192
1.183
1.092
1.069
1
1
2
3
18
3
ppm
9
8
7
6
5
4
3
2
1
0
-1

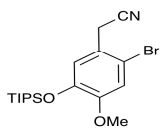
CN
Br
TIPSO
OMe

3.39

152.373
145.763
129.256
122.976
116.753
115.405
56.351
46.974
32.778
18.546
13.526
ppm
200
150
100
50
0

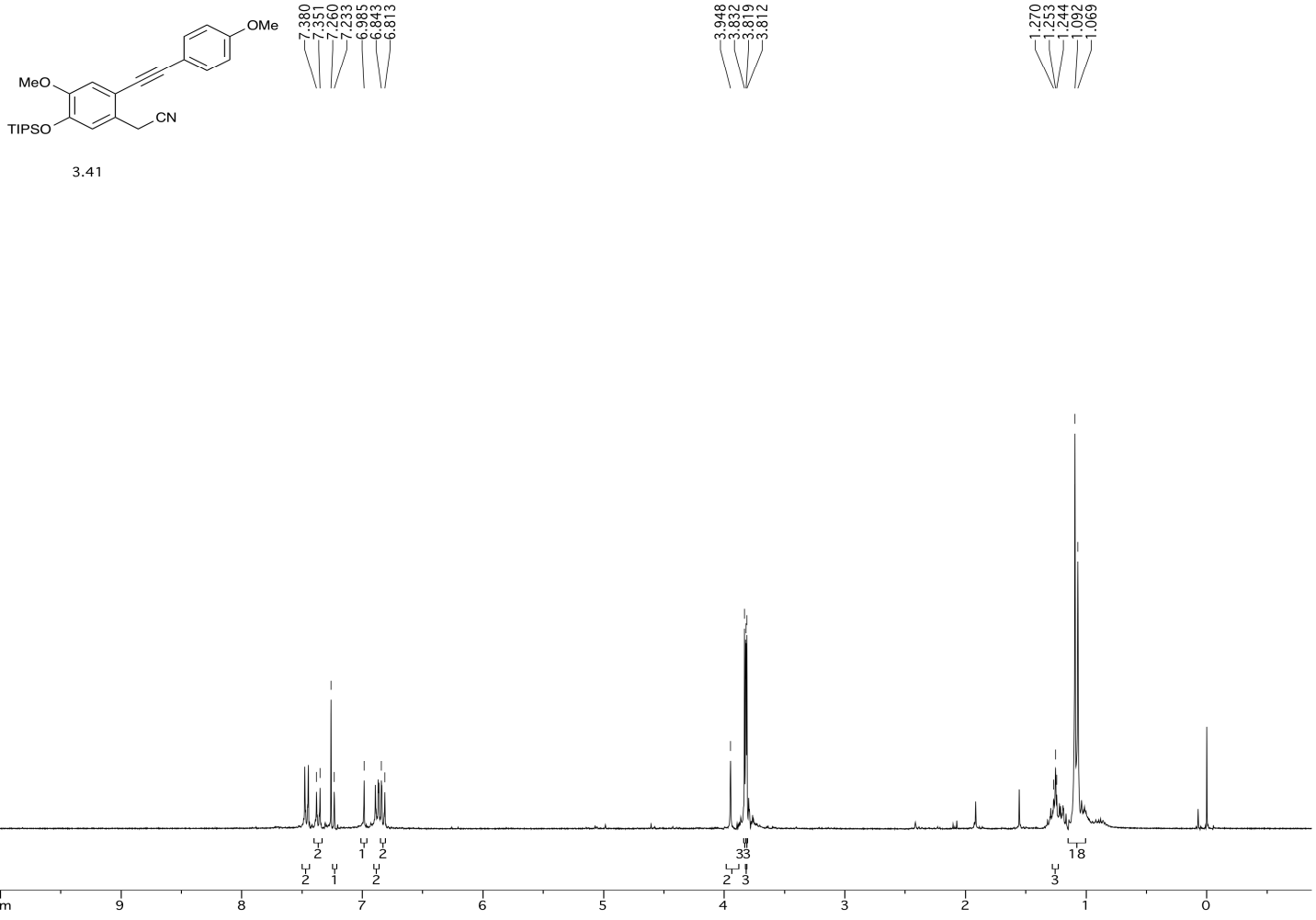
OMe
MeO
TIPSO
CN
7.380
7.351
7.260
7.233
6.985
6.843
6.813
3.948
3.832
3.819
3.812
1.270
1.253
1.244
1.092
1.069
2
1
2
2
1
2
33
2
3
18
3
ppm
9
8
7
6
5
4
3
2
1
0

3.41

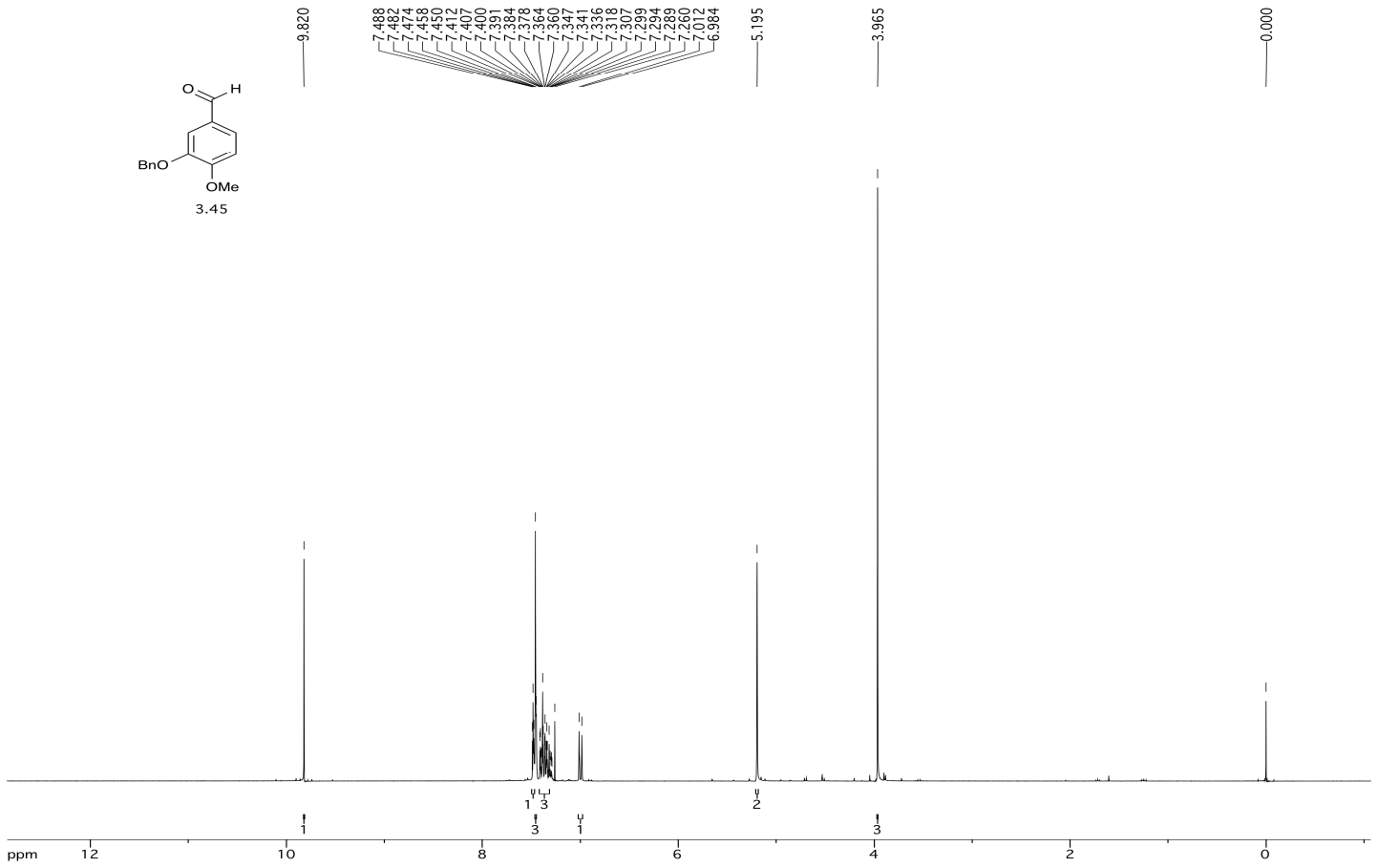
9.820
7.488
7.482
7.474
7.458
7.450
7.412
7.407
7.400
7.391
7.384
7.378
7.364
7.360
7.347
7.341
7.336
7.318
7.307
7.299
7.294
7.289
7.260
7.012
6.984
5.195
3.965
0.000
O
H
BnO
OMe
3.45
1
3
1
2
3
ppm
12
10
8
6
4
2
0

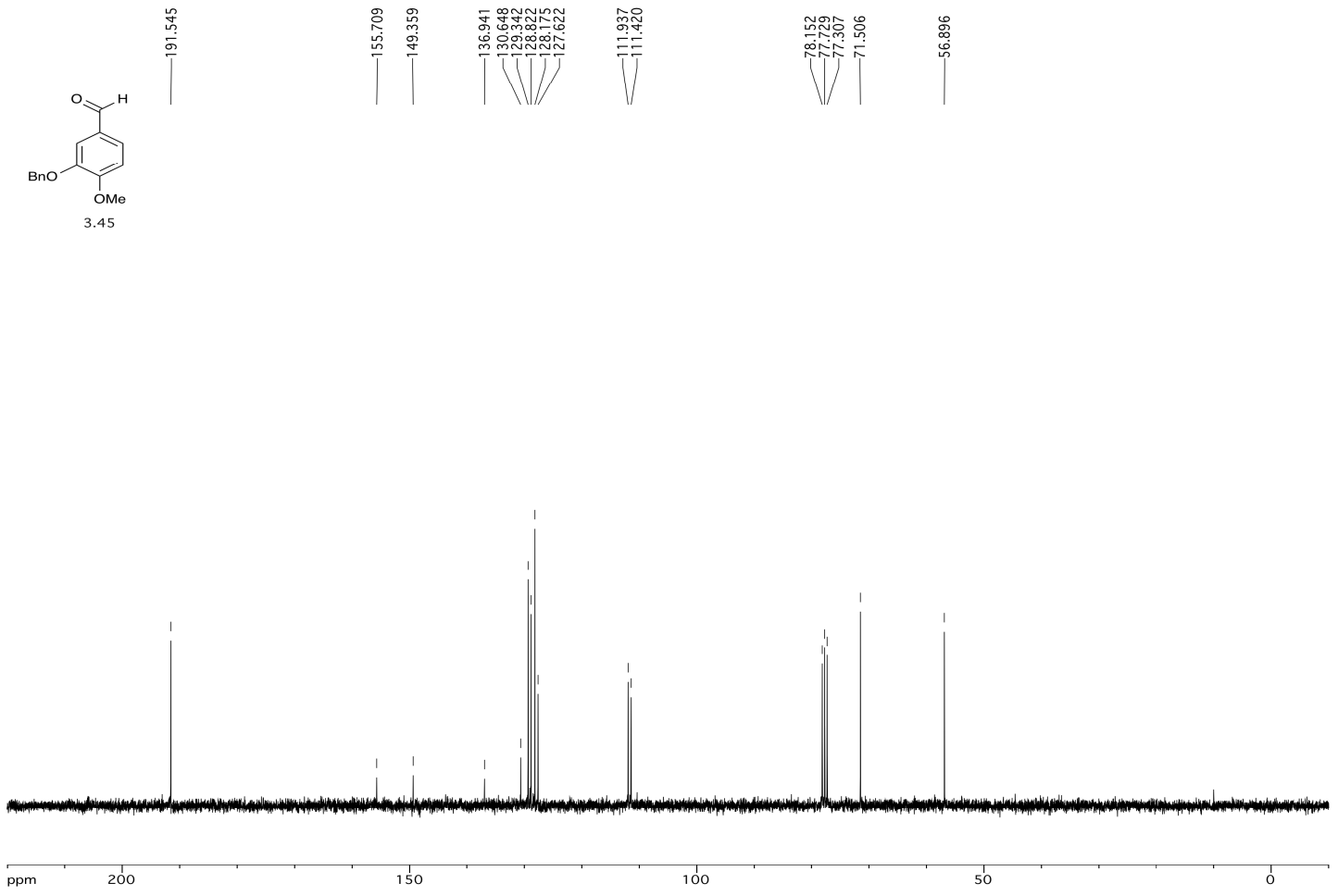
191.545
155.709
149.359
136.941
130.648
129.342
128.822
128.175
127.622
111.937
111.420
78.152
77.729
77.307
71.506
56.896
O
H
BnO
OMe
3.45
ppm
200
150
100
50
0

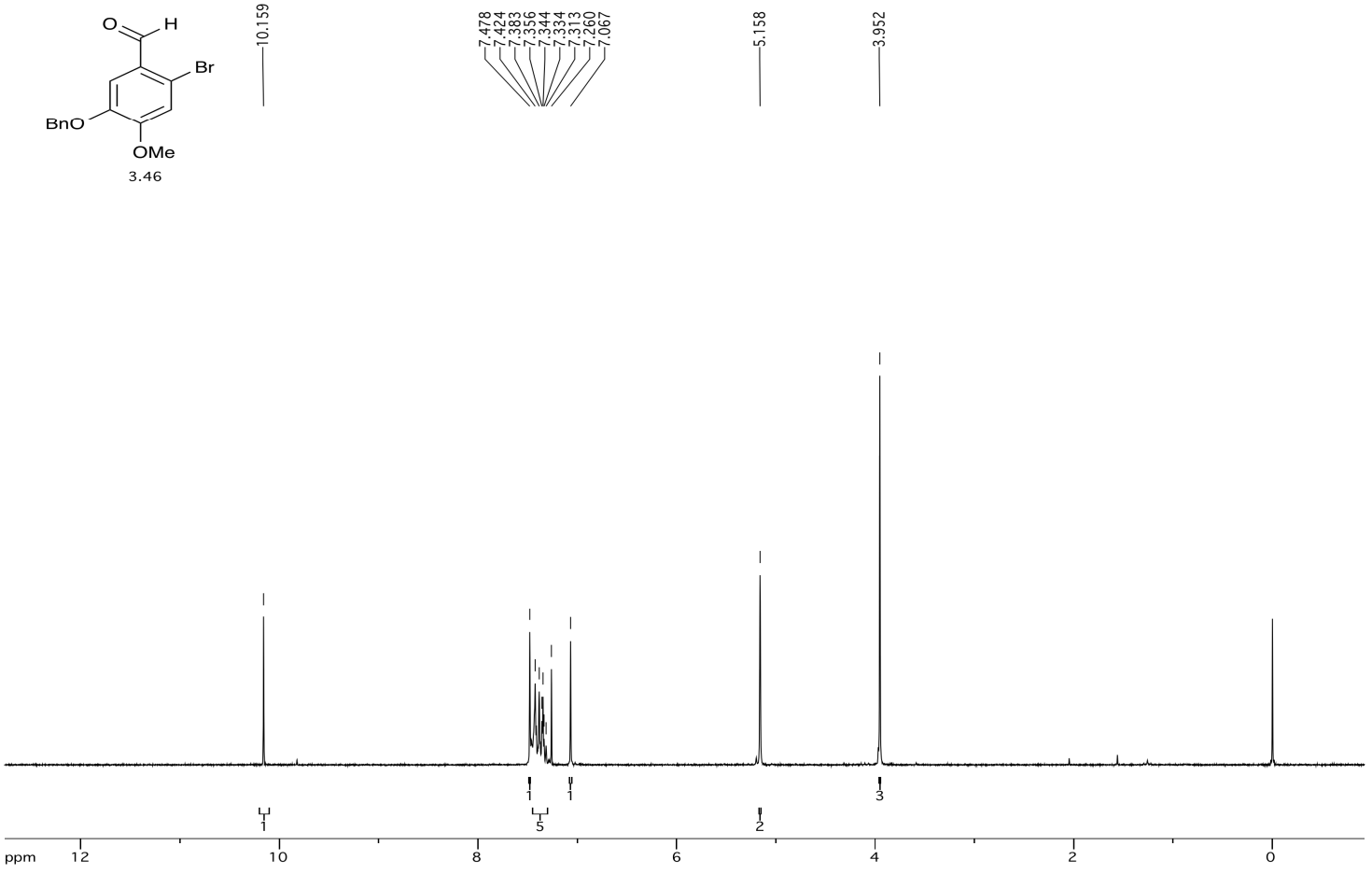
O
H
Br
BnO
OMe
3.46
10.159
7.478
7.424
7.383
7.356
7.344
7.334
7.313
7.260
7.067
5.158
3.952
1
1
1
5
2
3
ppm
12
10
8
6
4
2
0

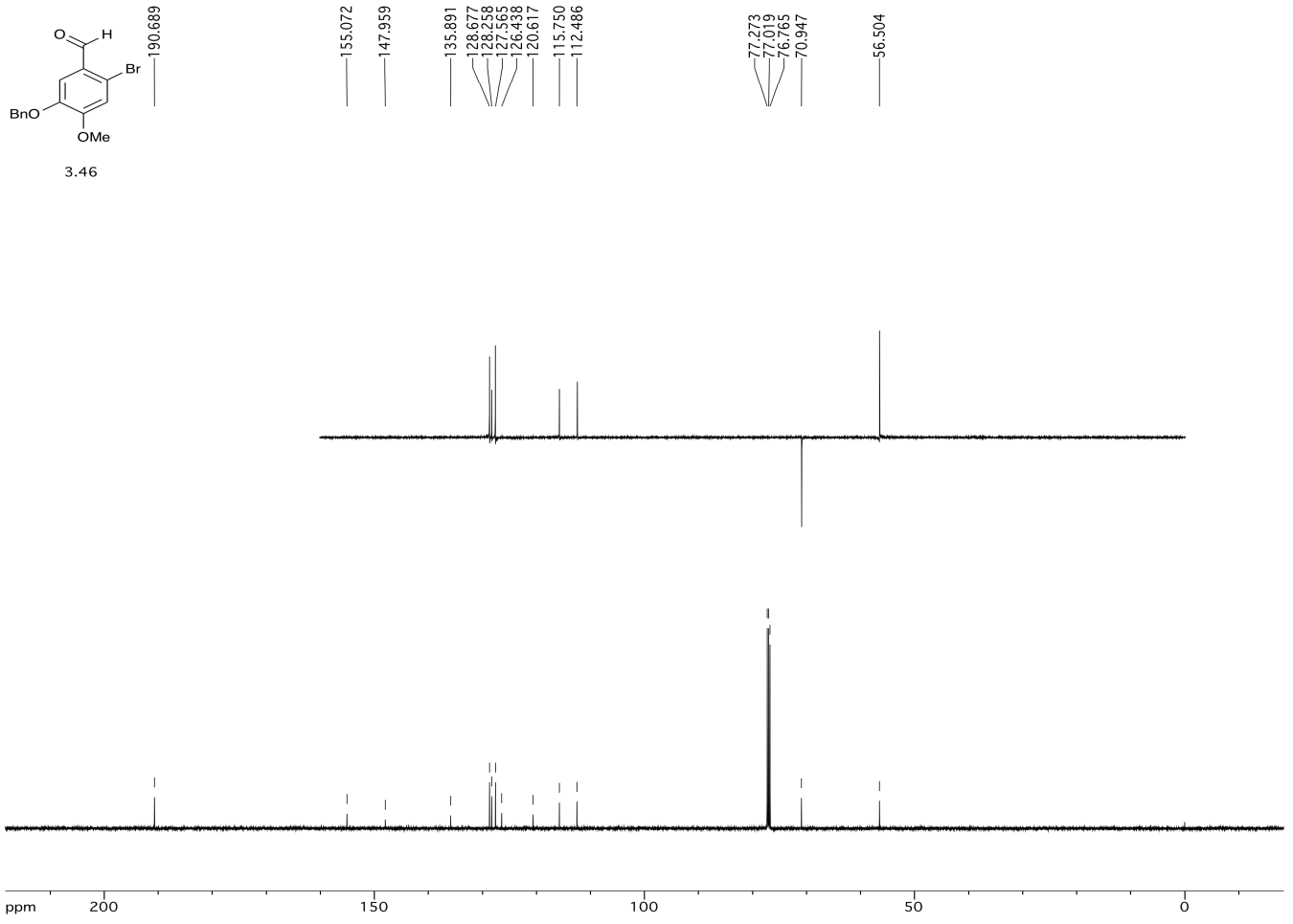
O
H
Br
BnO
OMe
3.46
190.689
155.072
147.959
135.891
128.677
128.258
127.565
126.438
120.617
115.750
112.486
77.273
77.019
76.765
70.947
56.504
ppm
200
150
100
50
0

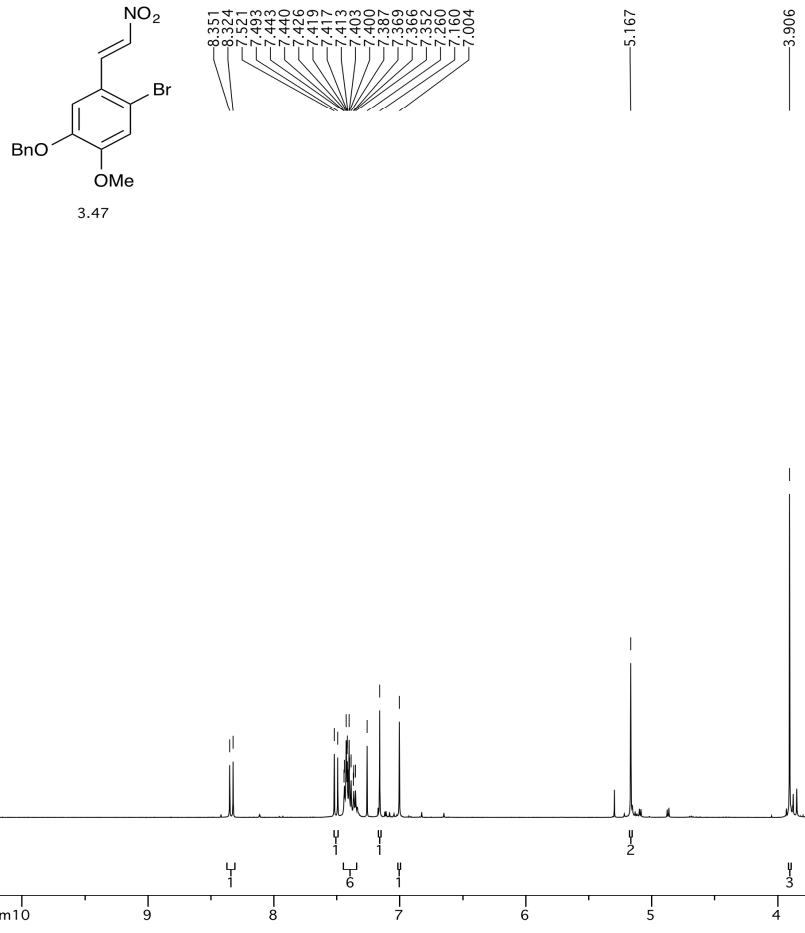
NO2
Br
BnO
OMe
3.47
8.351
8.324
7.521
7.493
7.443
7.440
7.426
7.419
7.417
7.413
7.403
7.400
7.387
7.369
7.366
7.352
7.260
7.160
7.004
5.167
3.906
1
1
2
1
6
1
3
ppm10
9
8
7
6
5
4
3
2
1
0
-1

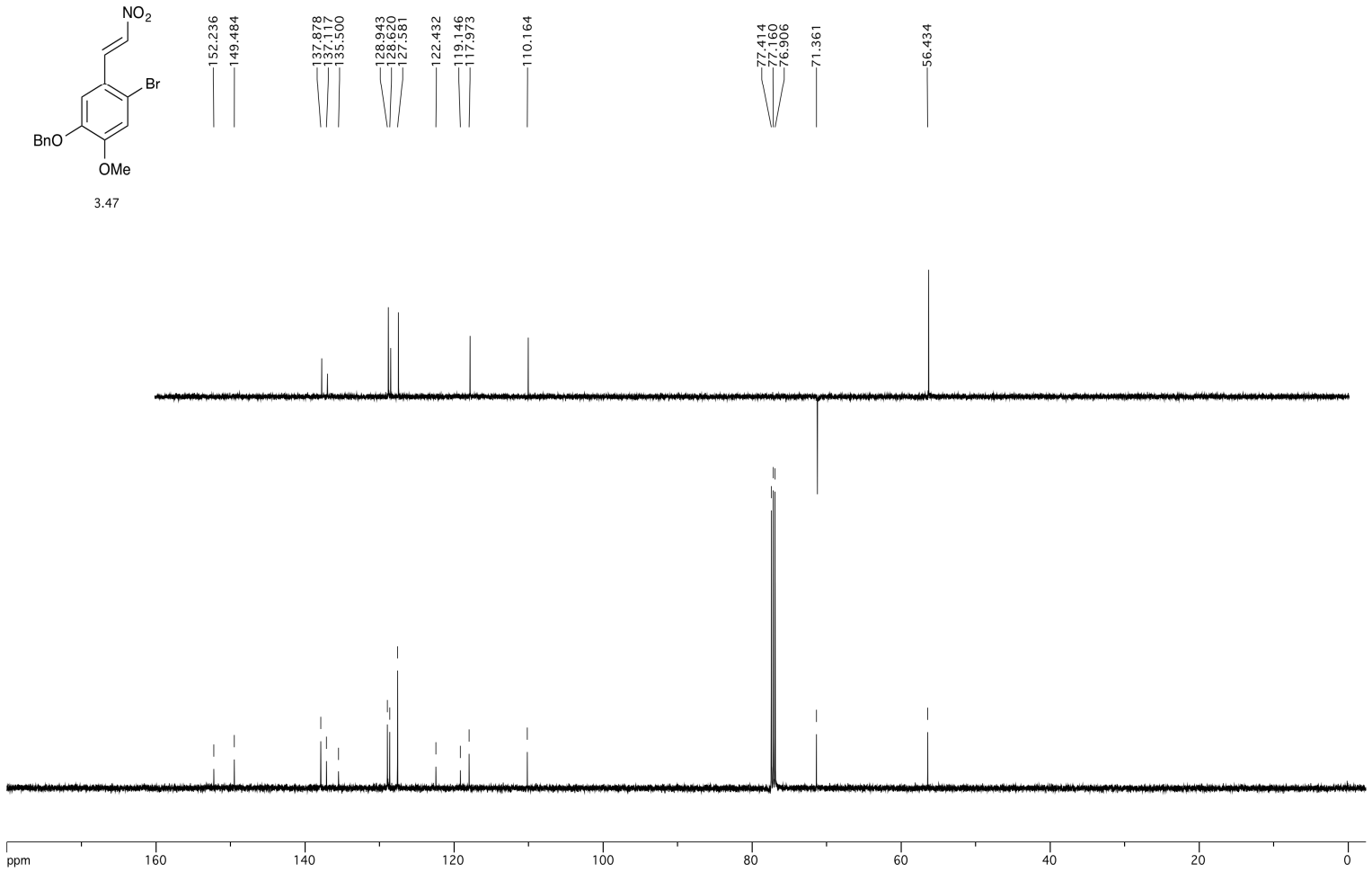
NO2
Br
BnO
OMe
3.47
152.236
149.484
137.878
137.117
135.500
128.943
128.620
127.581
122.432
119.146
117.973
110.164
77.414
77.160
76.906
71.361
56.434
ppm
160
140
120
100
80
60
40
20
0

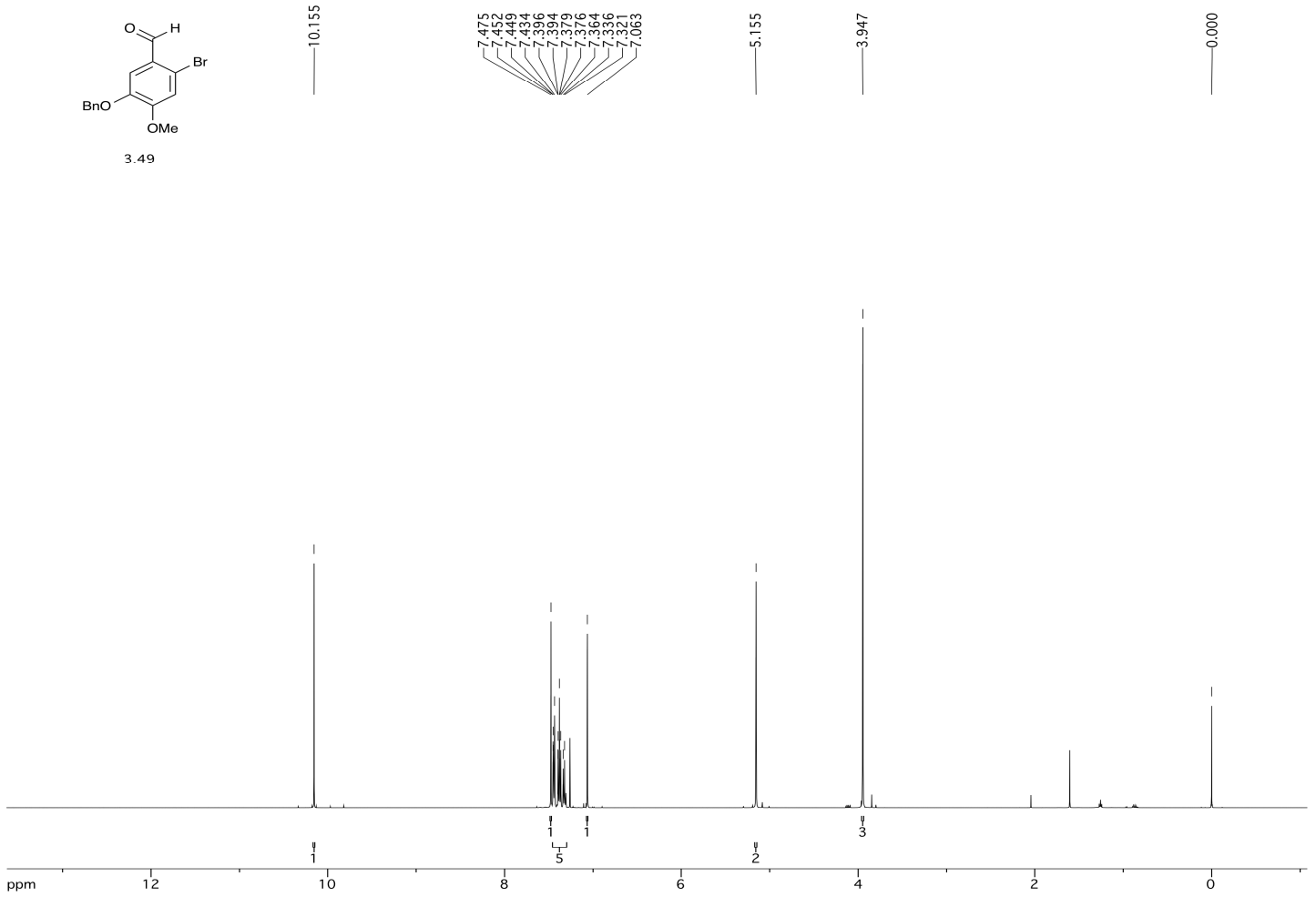
O
H
Br
BnO
OMe
3.49
10.155
7.475
7.452
7.449
7.434
7.396
7.394
7.379
7.376
7.364
7.336
7.321
7.063
5.155
3.947
0.000
1
1
5
1
2
3
ppm
12
10
8
6
4
2
0

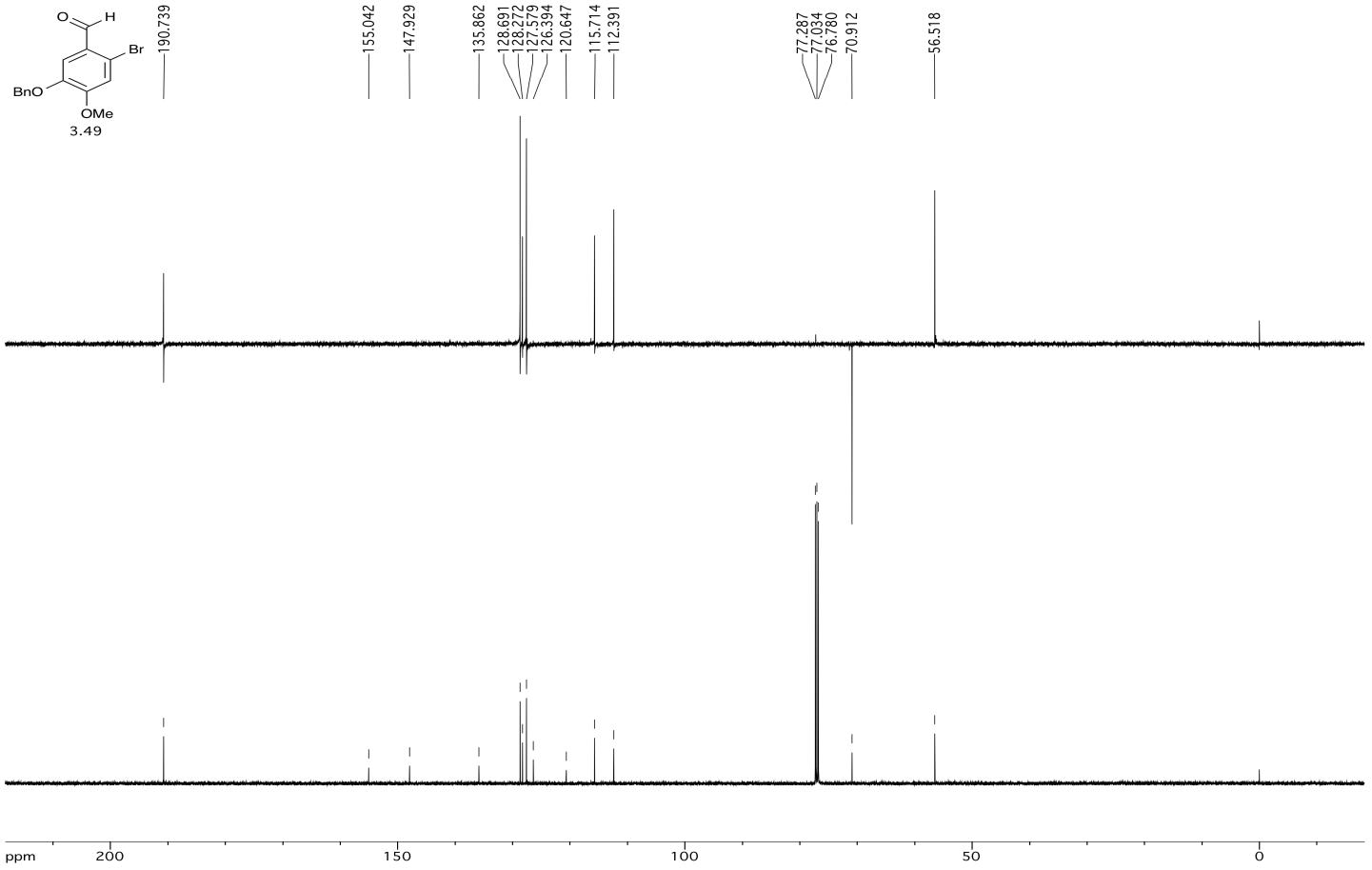
O
H
Br
BnO
OMe
3.49
190.739
155.042
147.929
135.862
128.691
128.272
127.579
126.394
120.647
115.714
112.391
77.287
77.034
76.780
70.912
56.518
ppm
200
150
100
50
0

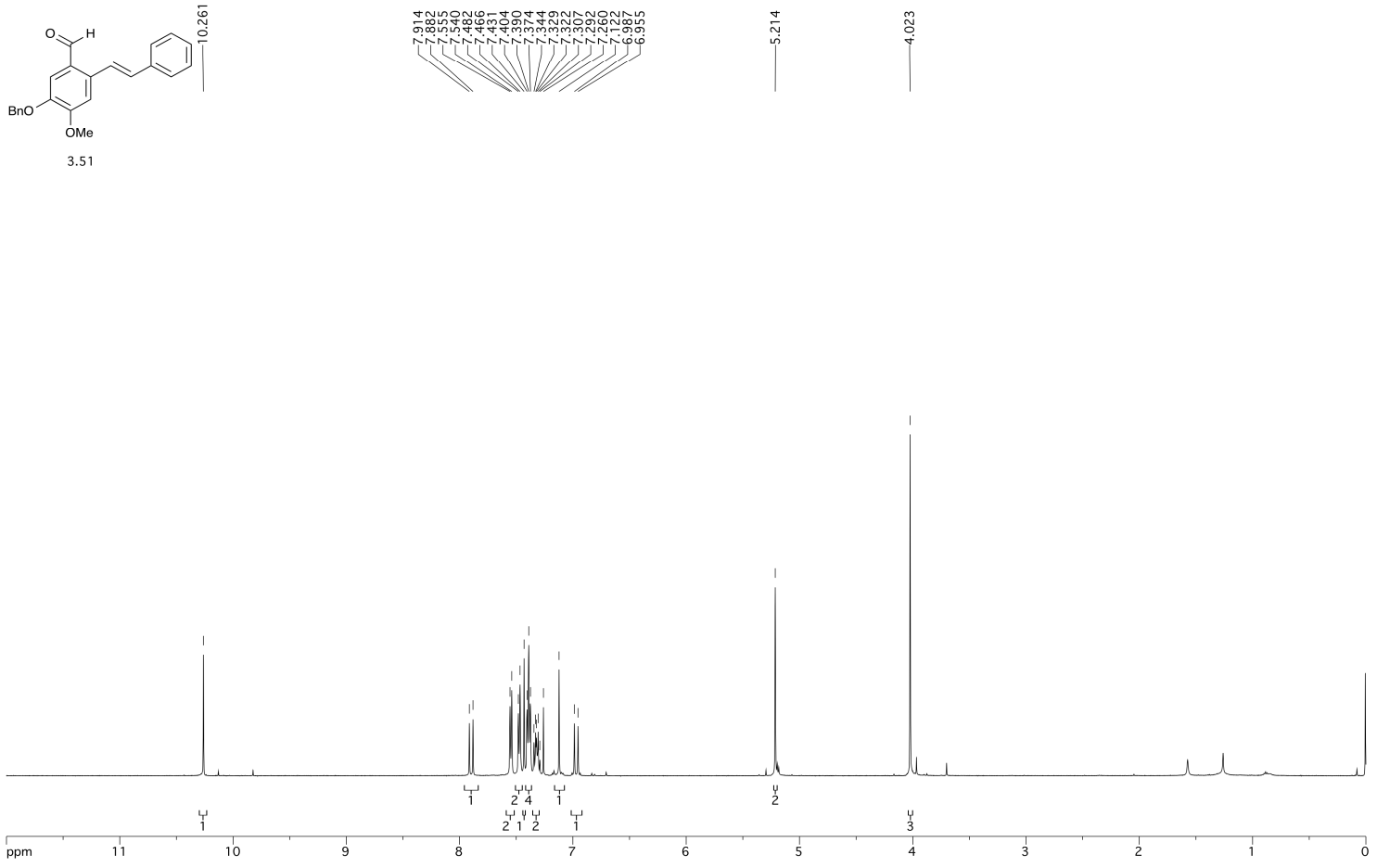
O
H
BnO
OMe
3.51
10.261
7.914
7.882
7.555
7.540
7.482
7.466
7.431
7.404
7.390
7.374
7.344
7.329
7.322
7.307
7.292
7.260
7.122
6.987
6.955
5.214
4.023
1
2
4
1
2
1
2
1
2
1
3
ppm
11
10
9
8
7
6
5
4
3
2
1
0

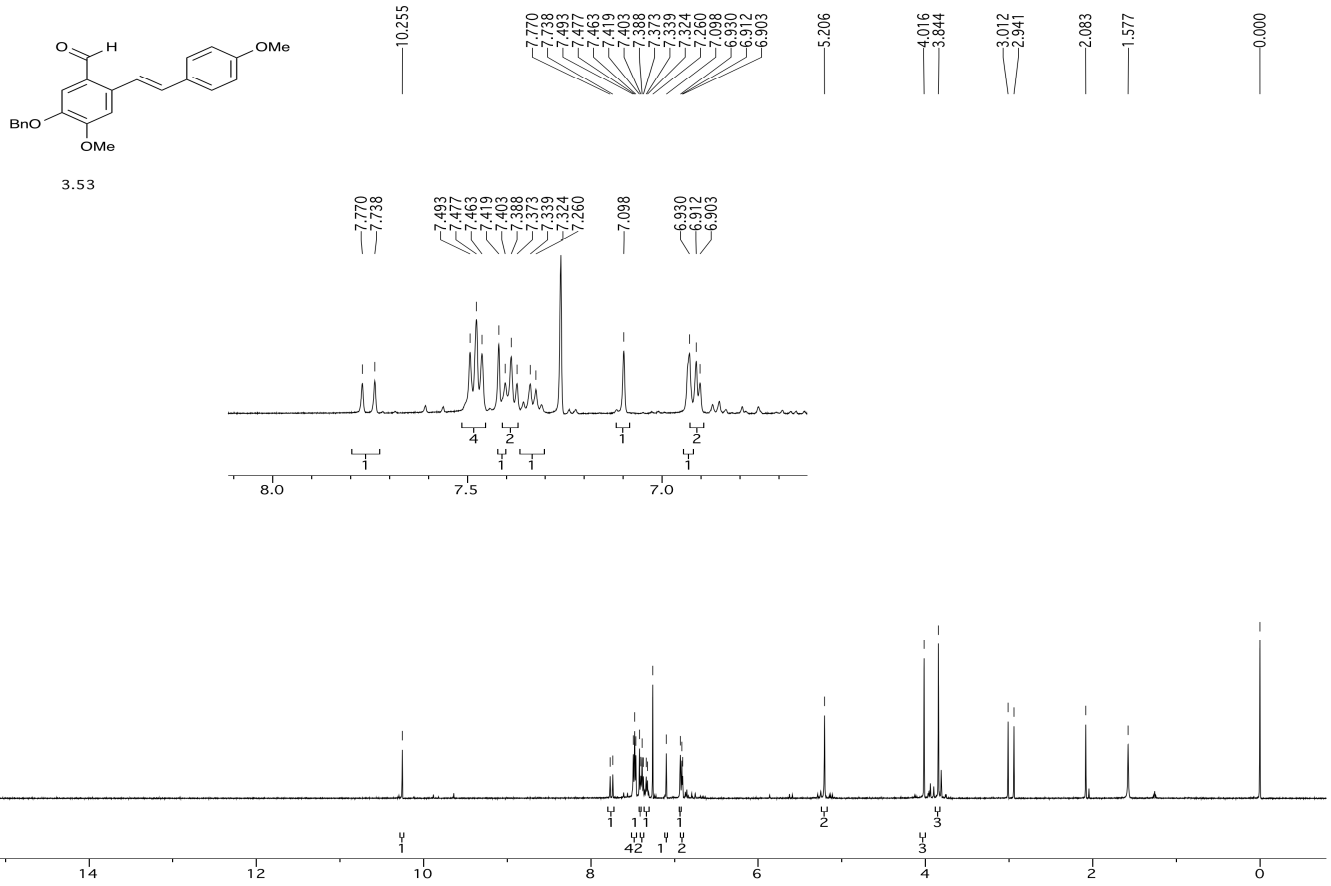
O
H
OMe
BnO
OMe
3.53
10.255
7.770
7.738
7.493
7.477
7.463
7.419
7.403
7.388
7.373
7.339
7.324
7.260
7.098
6.930
6.912
6.903
5.206
4.016
3.844
3.012
2.941
2.083
1.577
0.000
ppm

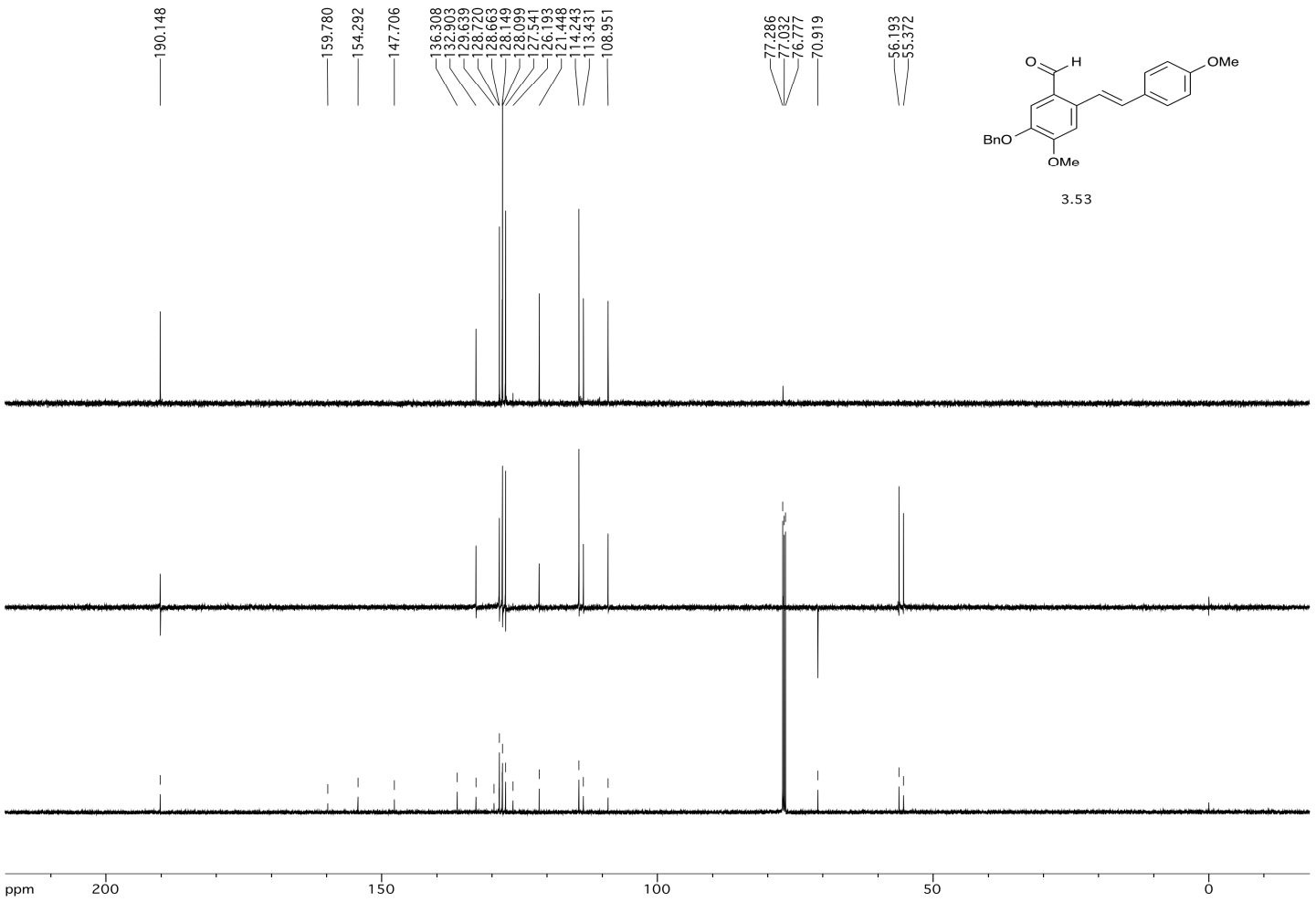
190.148
159.780
154.292
147.706
136.308
132.903
129.639
128.720
128.663
128.149
128.099
127.541
126.193
121.448
114.243
113.431
108.951
77.286
77.032
76.777
70.919
56.193
55.372
O
H
OMe
BnO
OMe
3.53
ppm
200
150
100
50
0

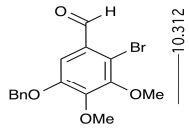
O
H
Br
BnO
OMe
OMe

3.55

10.312
7.556
7.541
7.479
7.465
7.439
7.424
5.174
4.018
4.000
3.951
3
1
3
3
1
2
2
3
ppm
11
10
9
8
7
6
5
4
3
2
1
0

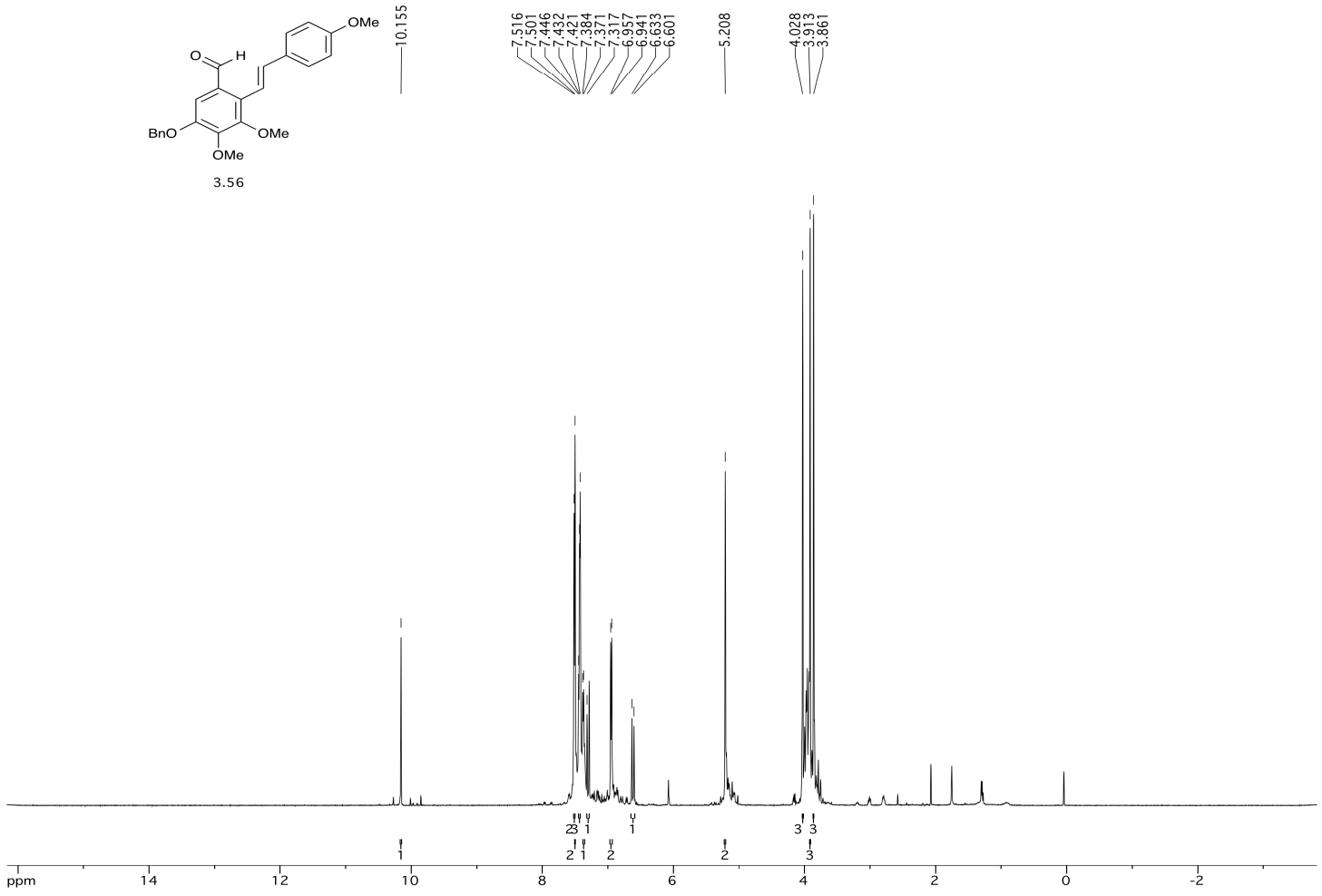
OMe
O
H
BnO
OMe
OMe
3.56
10.155
7.516
7.501
7.446
7.432
7.421
7.384
7.371
7.317
6.957
6.941
6.633
6.601
5.208
4.028
3.913
3.861
ppm
14
12
10
8
6
4
2
0
-2

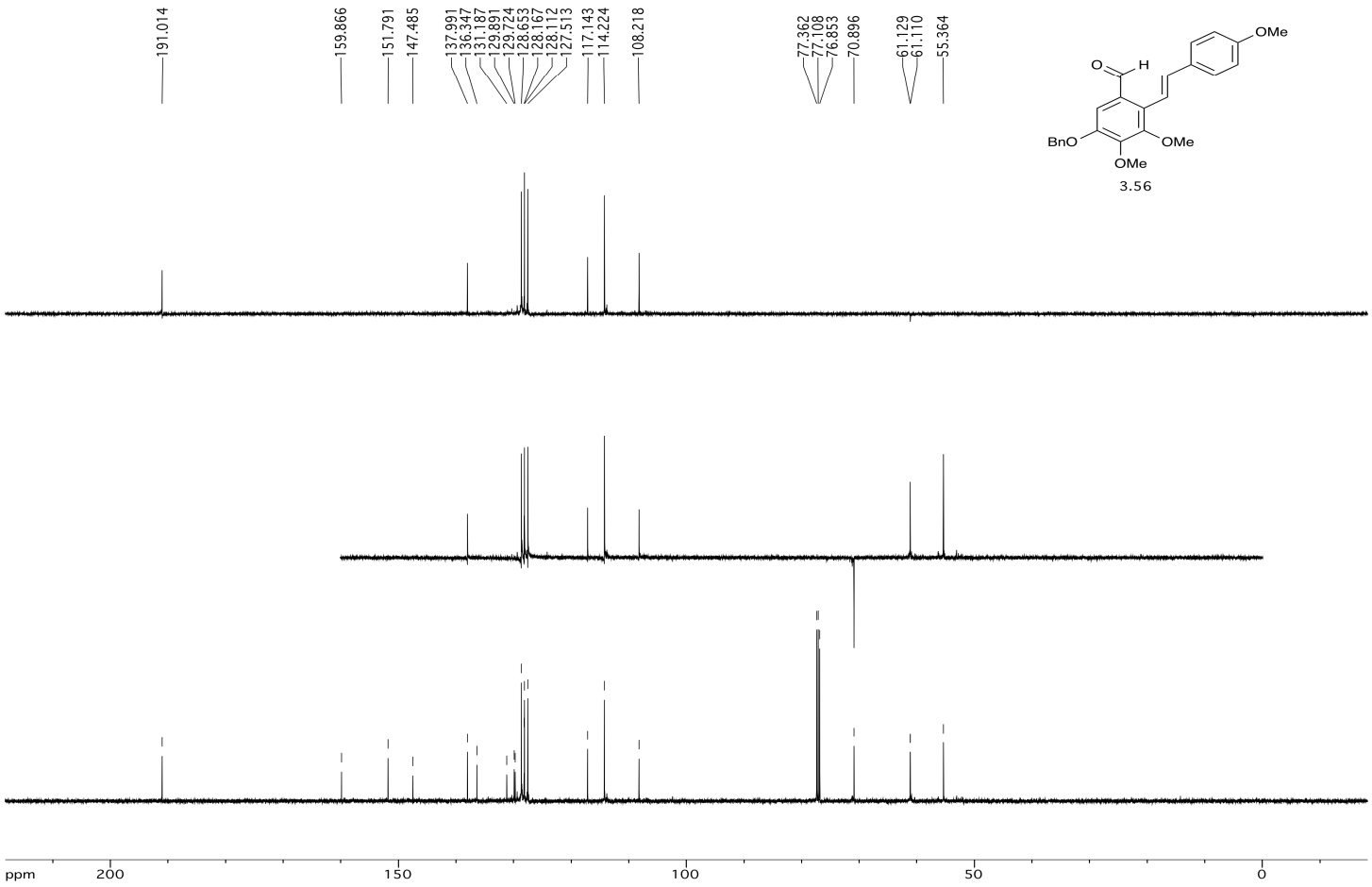
191.014
159.866
151.791
147.485
137.991
136.347
131.187
129.891
129.724
128.653
128.167
128.112
127.513
117.143
114.224
108.218
77.362
77.108
76.853
70.896
61.129
61.110
55.364
O
H
OMe
BnO
OMe
OMe
3.56
ppm
200
150
100
50
0

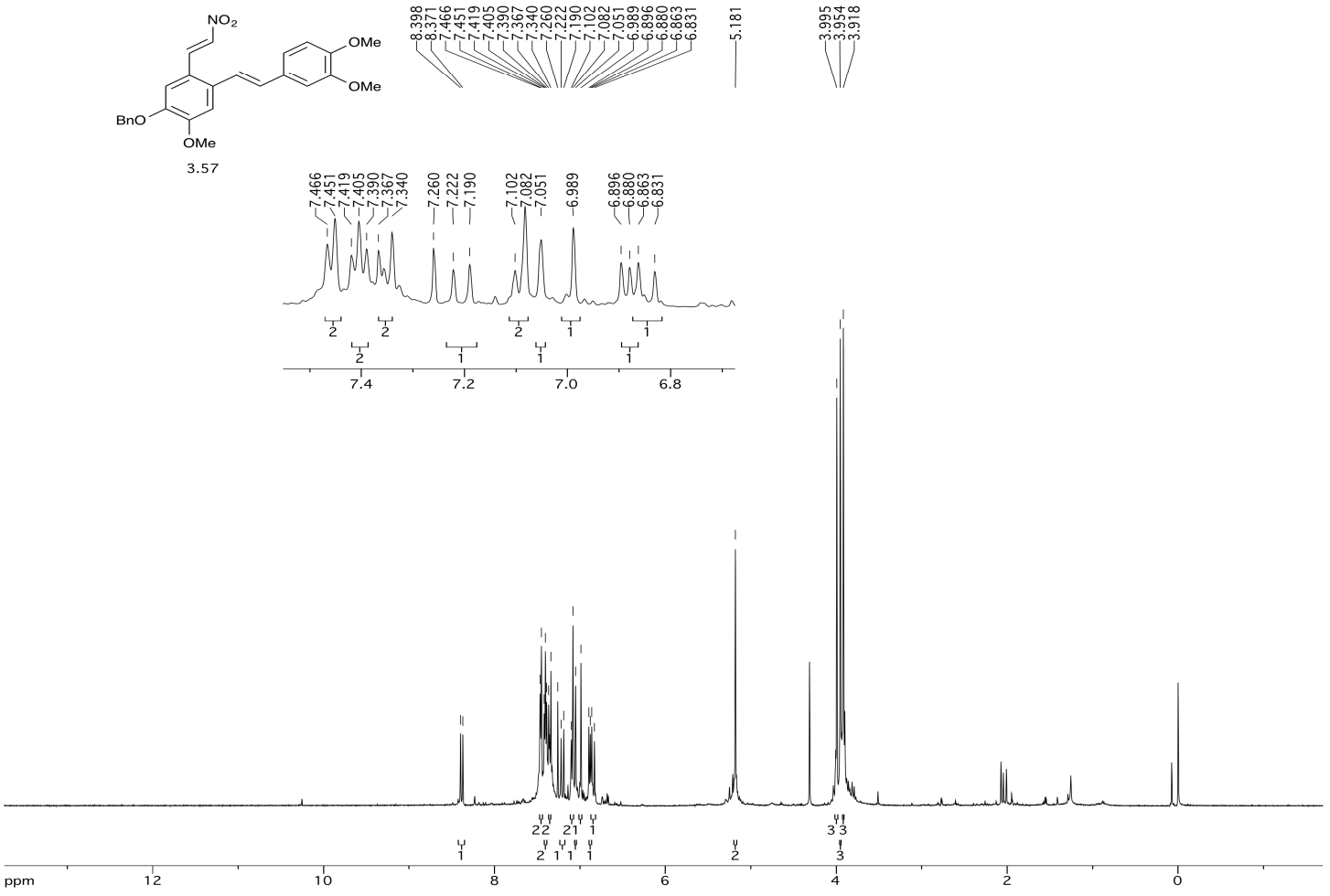
NO2
OMe
OMe
BnO
OMe
3.57
8.398
8.371
7.466
7.451
7.419
7.405
7.390
7.367
7.340
7.260
7.222
7.190
7.102
7.082
7.051
6.989
6.896
6.880
6.863
6.831
5.181
3.995
3.954
3.918
7.4
7.2
7.0
6.8
ppm
12
10
8
6
4
2
0

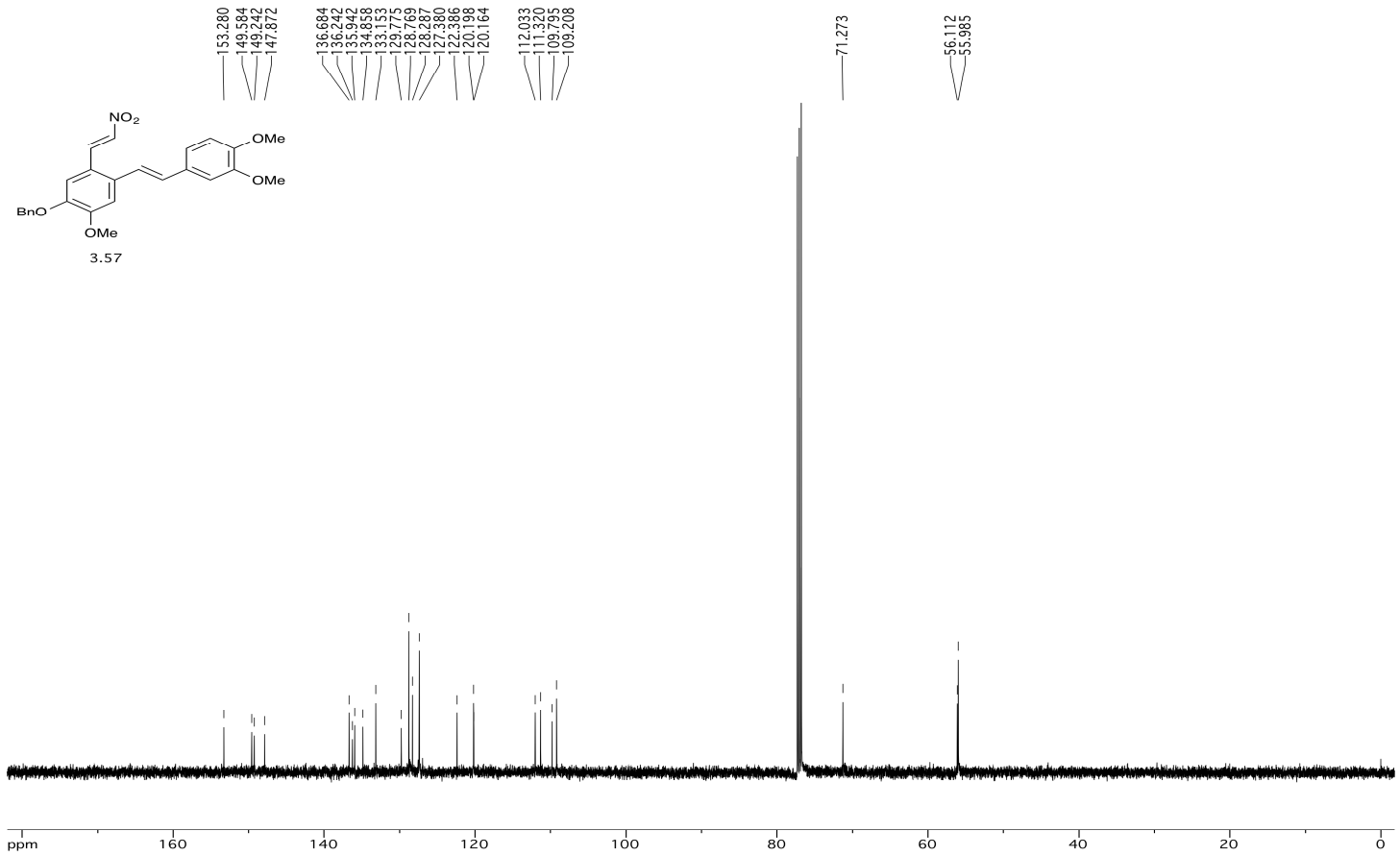
153.280
149.584
149.242
147.872
136.684
136.242
135.942
134.858
133.153
129.775
128.769
128.287
127.380
122.386
120.198
120.164
112.033
111.320
109.795
109.208
71.273
56.112
55.985
NO2
OMe
OMe
BnO
OMe
3.57
ppm
160
140
120
100
80
60
40
20
0

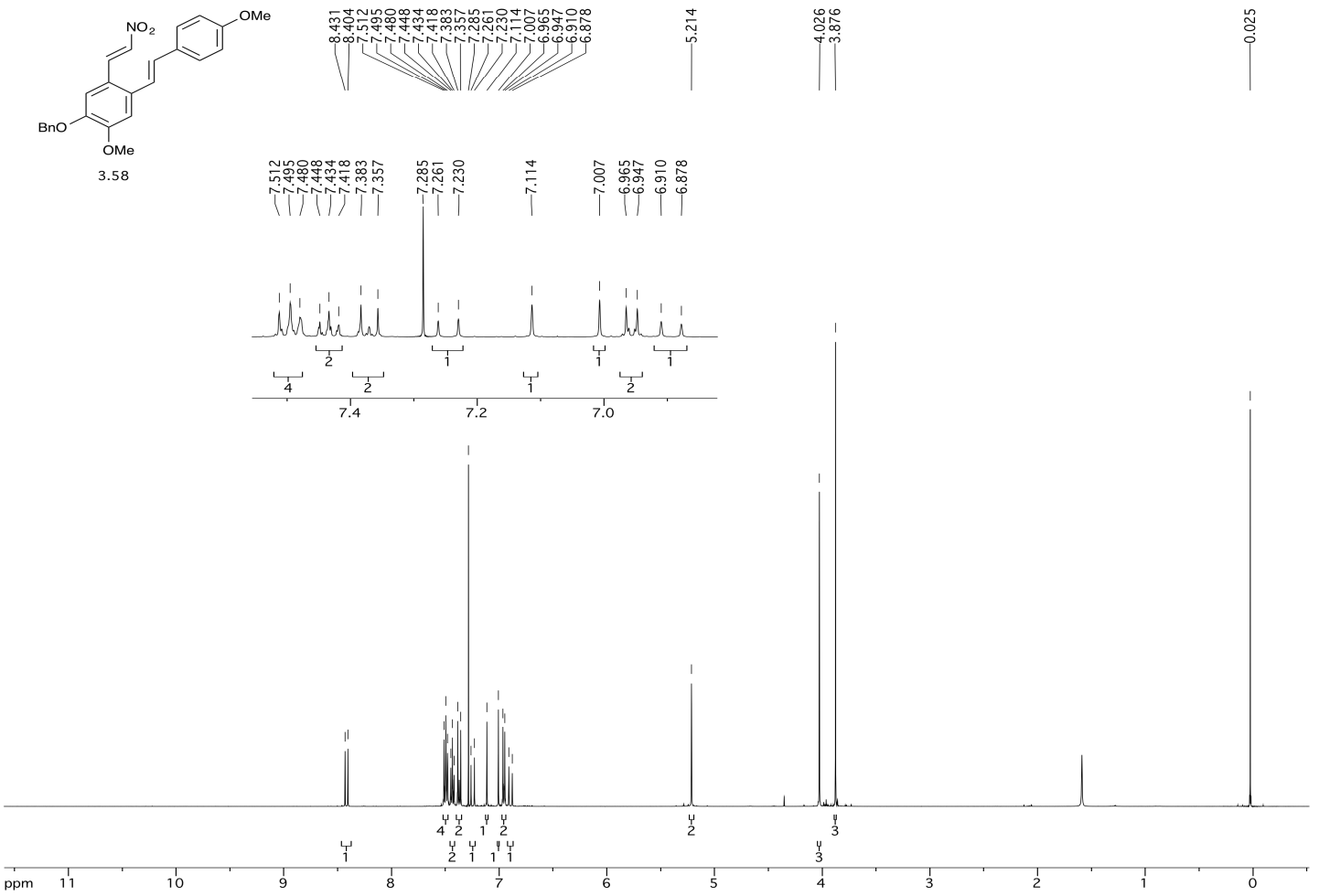
NO2
OMe
BnO
OMe
3.58
8.431
8.404
7.512
7.495
7.480
7.448
7.434
7.418
7.383
7.357
7.285
7.261
7.230
7.114
7.007
6.965
6.947
6.910
6.878
5.214
4.026
3.876
0.025
7.4
7.2
7.0
ppm

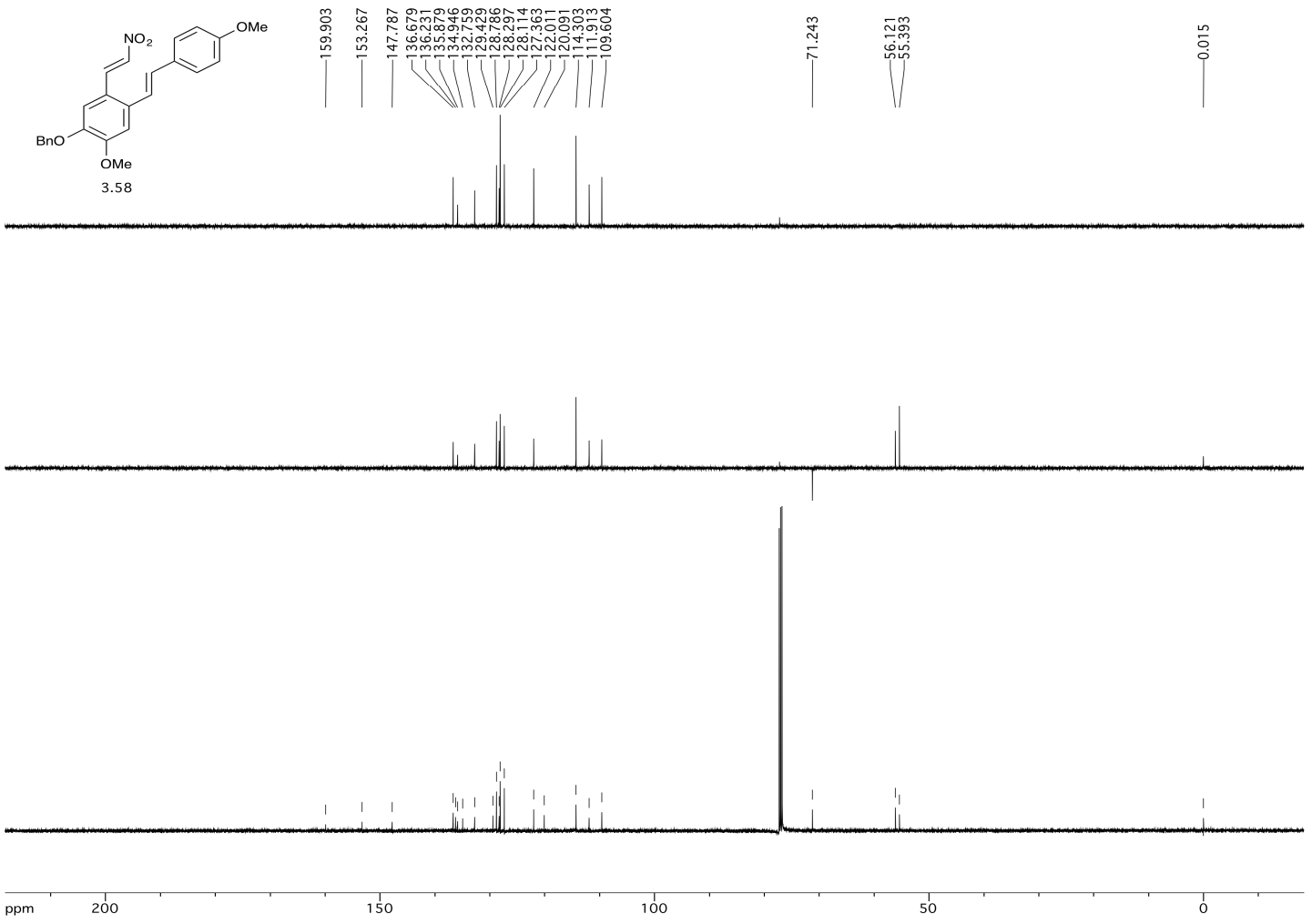
NO2
OMe
BnO
OMe
3.58
159.903
153.267
147.787
136.679
136.231
135.879
134.946
132.759
129.429
128.786
128.297
128.114
127.363
122.011
120.091
114.303
111.913
109.604
71.243
56.121
55.393
0.015
ppm
200
150
100
50
0

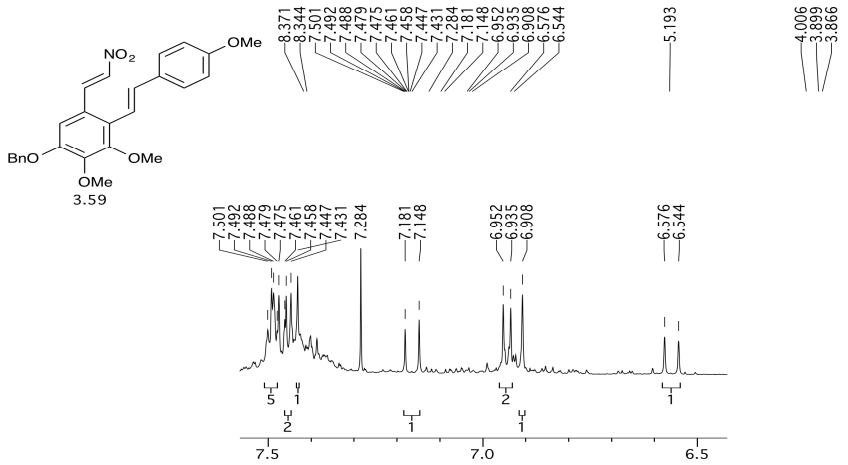
NO2
OMe
BnO
OMe
OMe
3.59
8.371
8.344
7.501
7.492
7.488
7.479
7.475
7.461
7.458
7.447
7.431
7.284
7.181
7.148
6.952
6.935
6.908
6.576
6.544
5.193
4.006
3.899
3.866
7.5
7.0
6.5

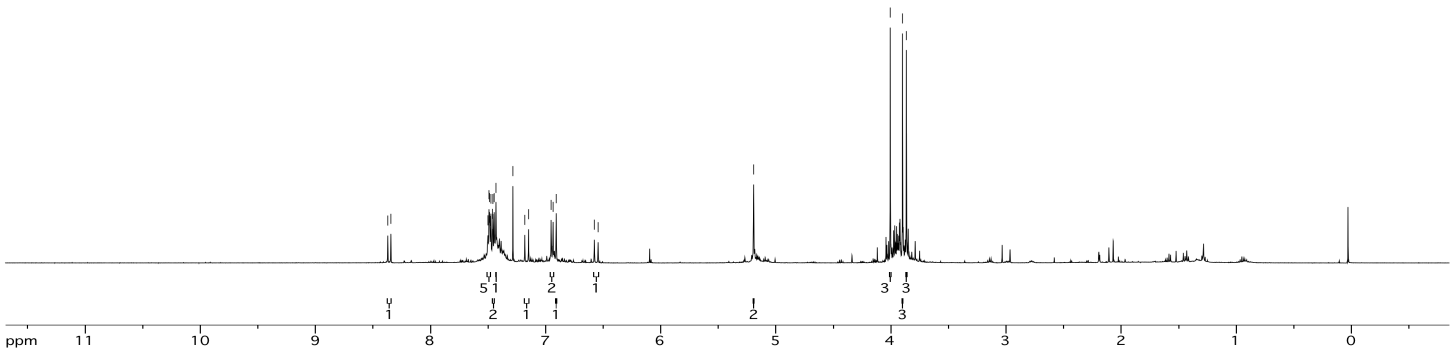
ppm
11
10
9
8
7
6
5
4
3
2
1
0

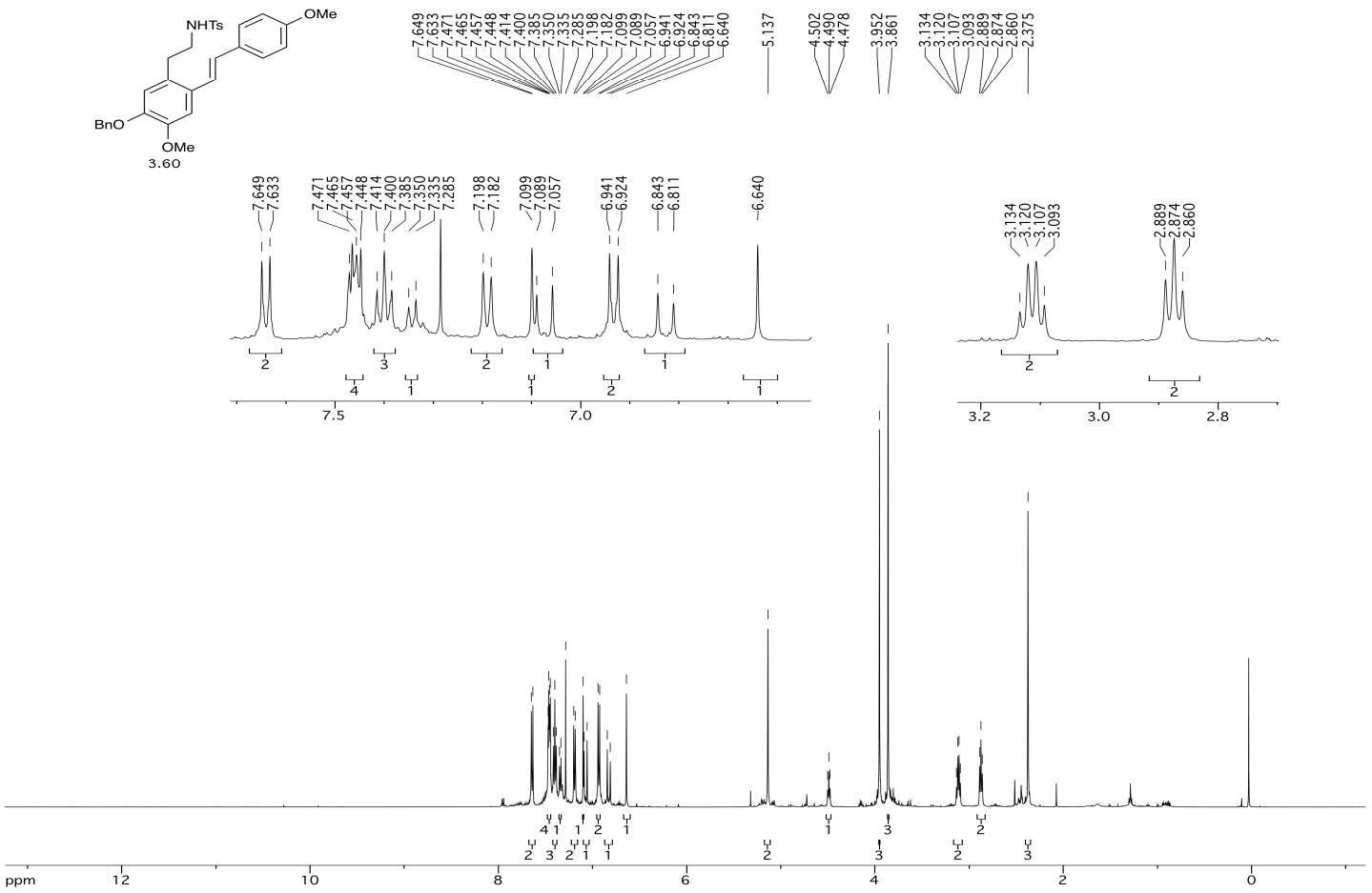
NHTs
OMe
BnO
OMe
3.60
7.649
7.633
7.471
7.465
7.457
7.448
7.414
7.400
7.385
7.350
7.335
7.285
7.198
7.182
7.099
7.089
7.057
6.941
6.924
6.843
6.811
6.640
5.137
4.502
4.490
4.478
3.952
3.861
3.134
3.120
3.107
3.093
2.889
2.874
2.860
2.375
ppm

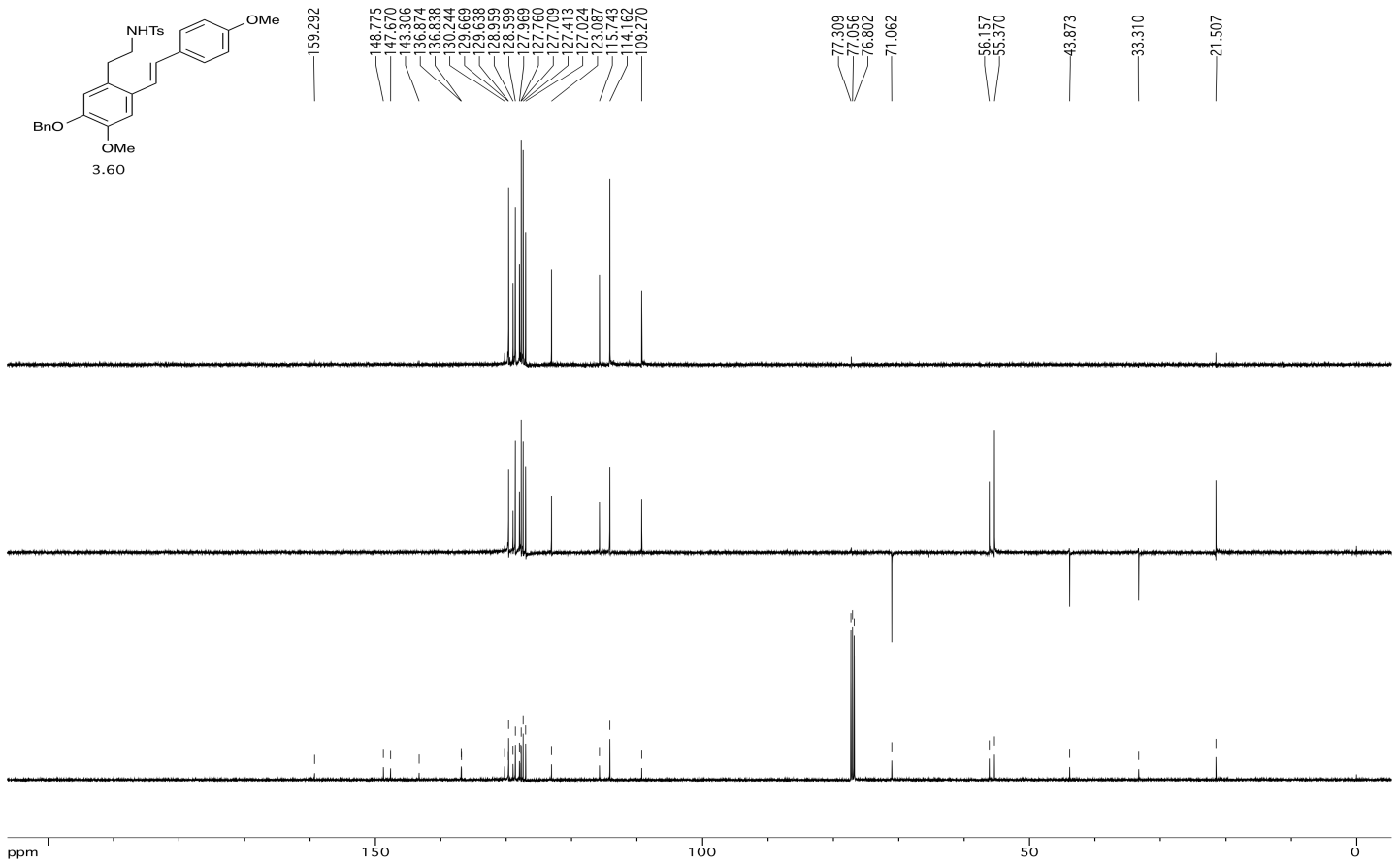
NHTs
OMe
BnO
OMe
3.60
159.292
148.775
147.670
143.306
136.874
136.838
130.244
129.669
129.638
128.959
128.599
127.969
127.760
127.709
127.413
127.024
123.087
115.743
114.162
109.270
77.309
77.056
76.802
71.062
56.157
55.370
43.873
33.310
21.507
ppm
150
100
50
0

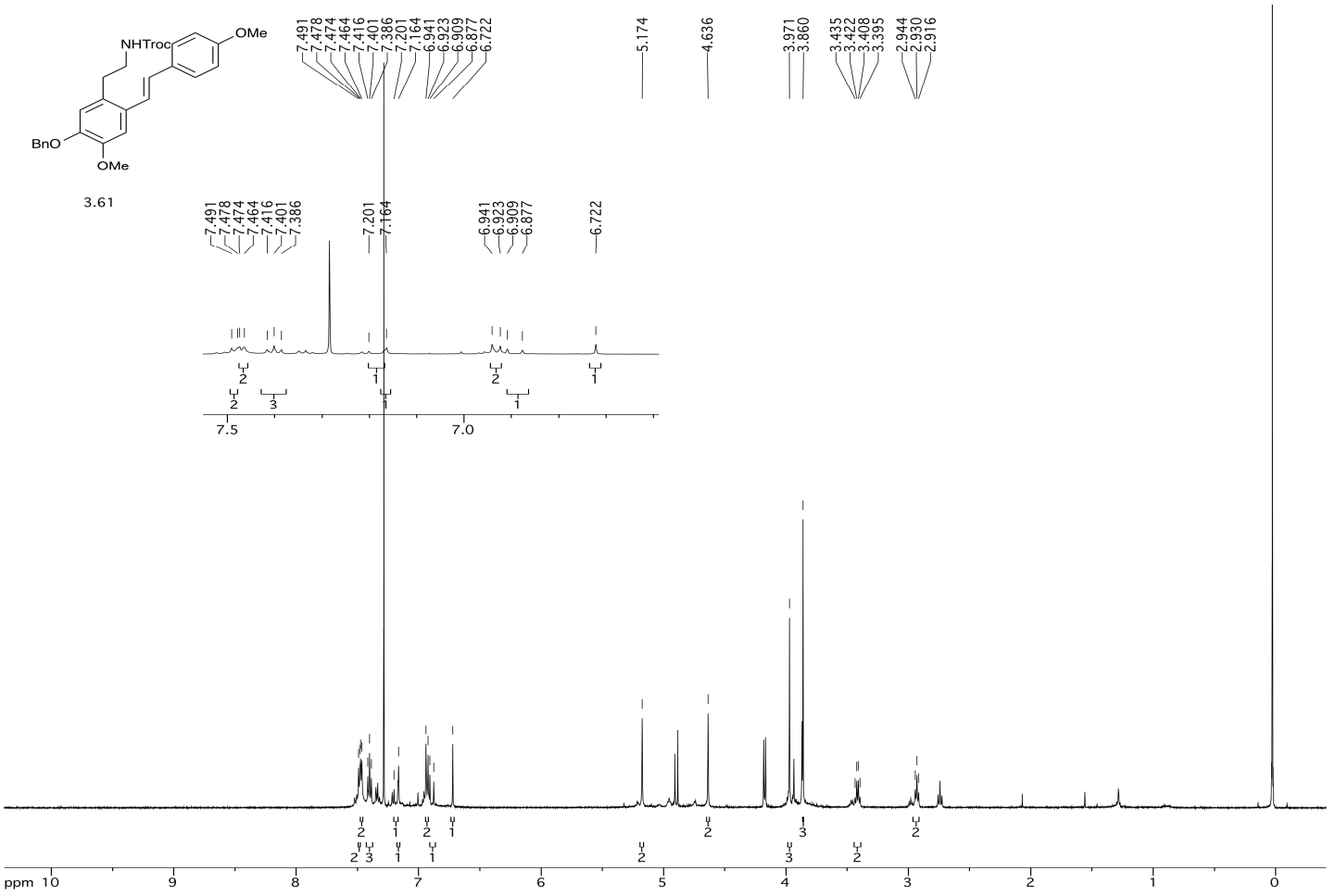
NHTroc
OMe
BnO
OMe
3.61
7.491
7.478
7.474
7.464
7.416
7.401
7.386
7.201
7.164
6.941
6.923
6.909
6.877
6.722
5.174
4.636
3.971
3.860
3.435
3.422
3.408
3.395
2.944
2.930
2.916
7.5
7.0
ppm 10
9
8
7
6
5
4
3
2
1
0

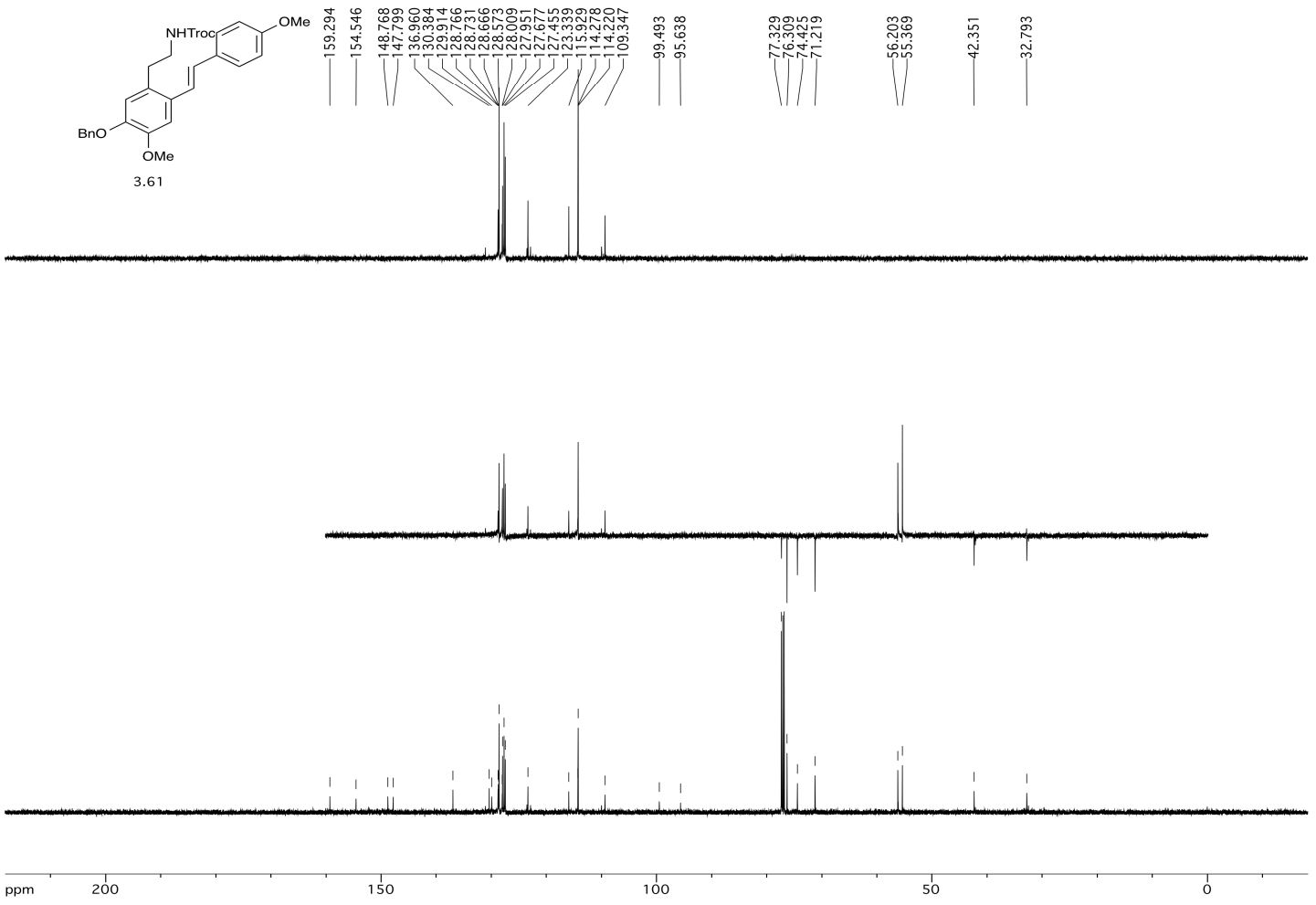
NHTroc
OMe
BnO
OMe
3.61
159.294
154.546
148.768
147.799
136.960
130.384
129.914
128.766
128.731
128.666
128.573
128.009
127.951
127.677
127.455
123.339
115.929
114.278
114.220
109.347
99.493
95.638
77.329
76.309
74.425
71.219
56.203
55.369
42.351
32.793
ppm
200
150
100
50
0

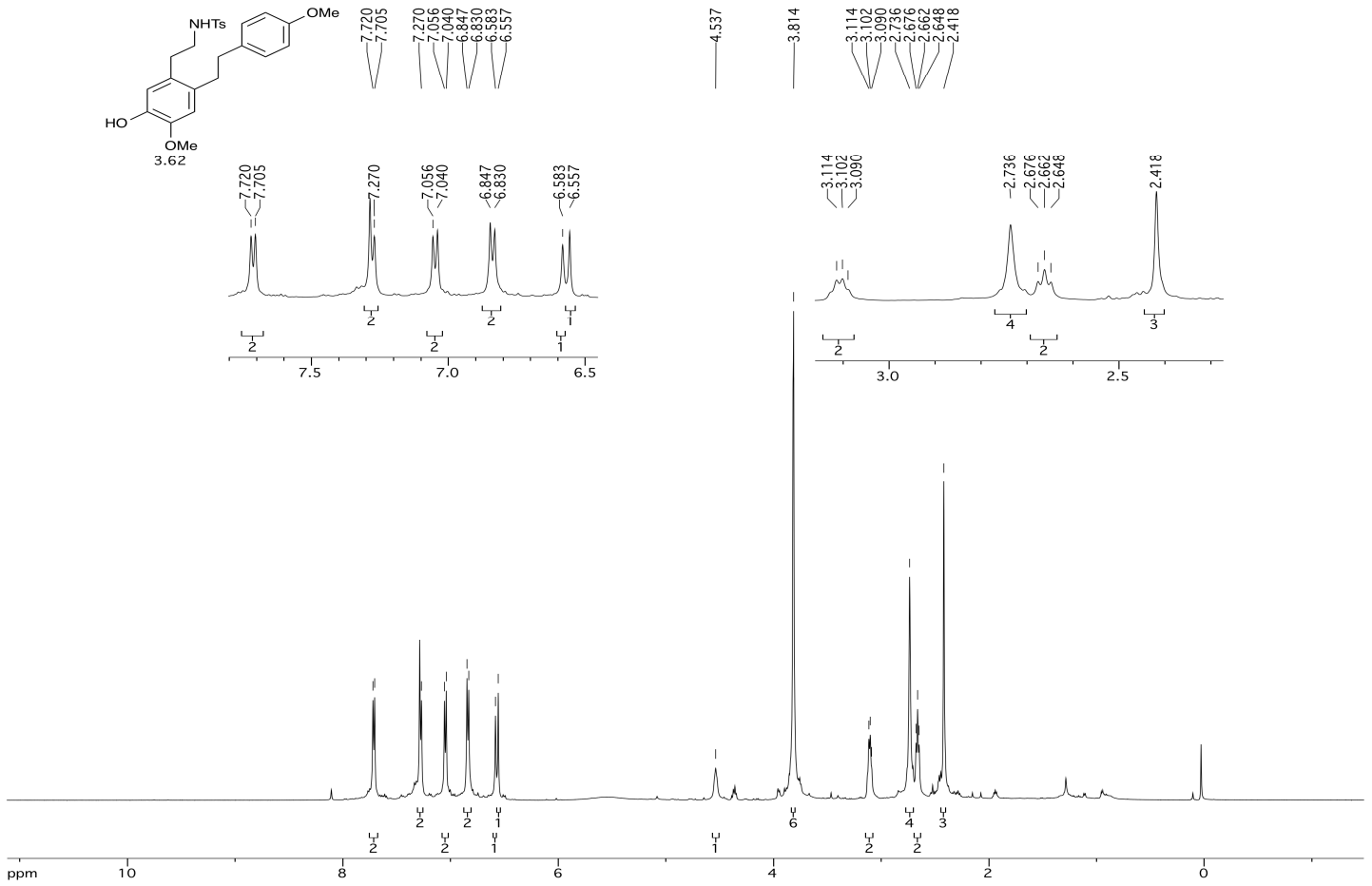
NHTs
OMe
HO
OMe
3.62
7.720
7.705
7.270
7.056
7.040
6.847
6.830
6.583
6.557
4.537
3.814
3.114
3.102
3.090
2.736
2.676
2.662
2.648
2.418
ppm

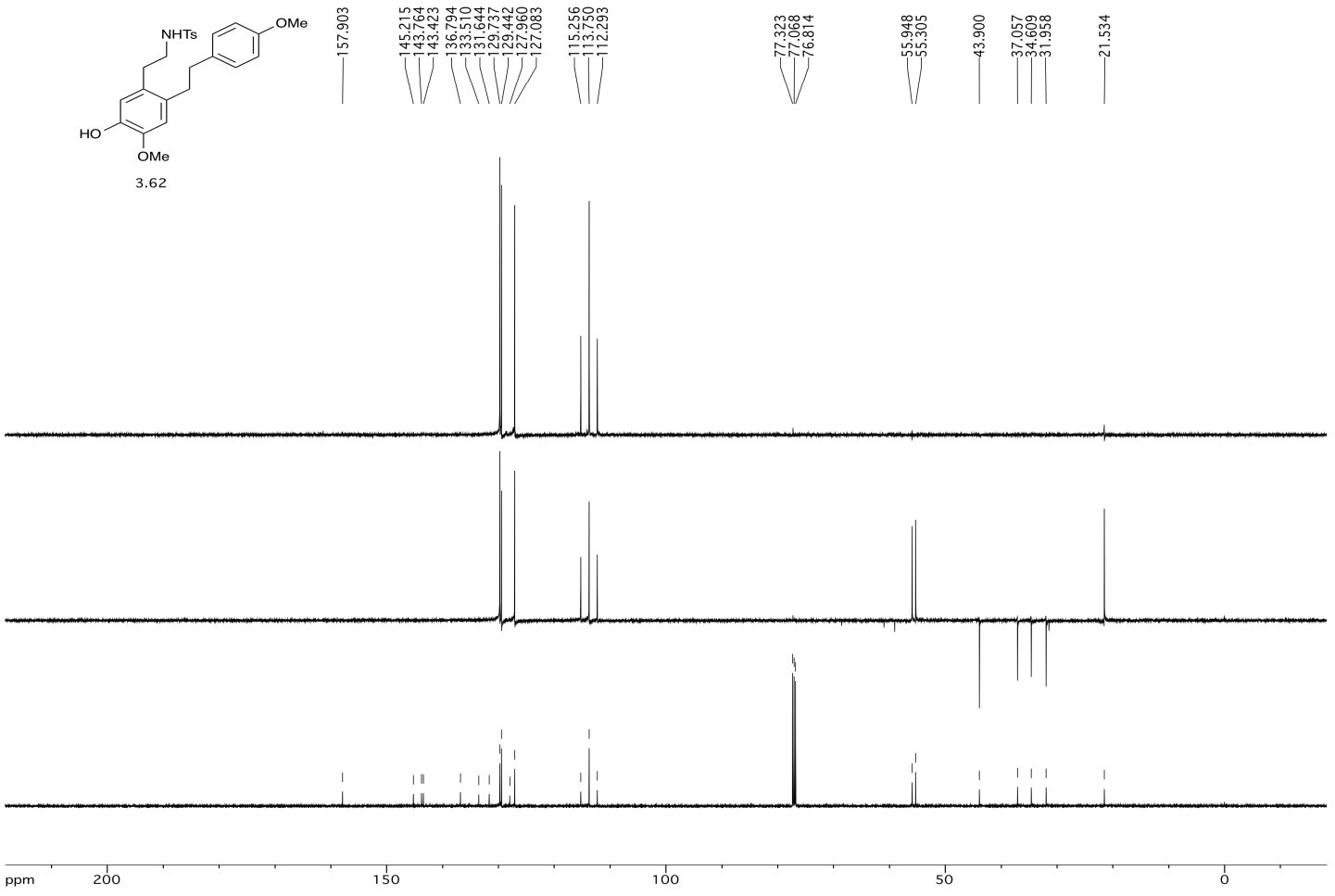
NHTs
OMe
HO
OMe
3.62
157.903
145.215
143.764
143.423
136.794
133.510
131.644
129.737
129.442
127.960
127.083
115.256
113.750
112.293
77.323
77.068
76.814
55.948
55.305
43.900
37.057
34.609
31.958
21.534
ppm
200
150
100
50
0

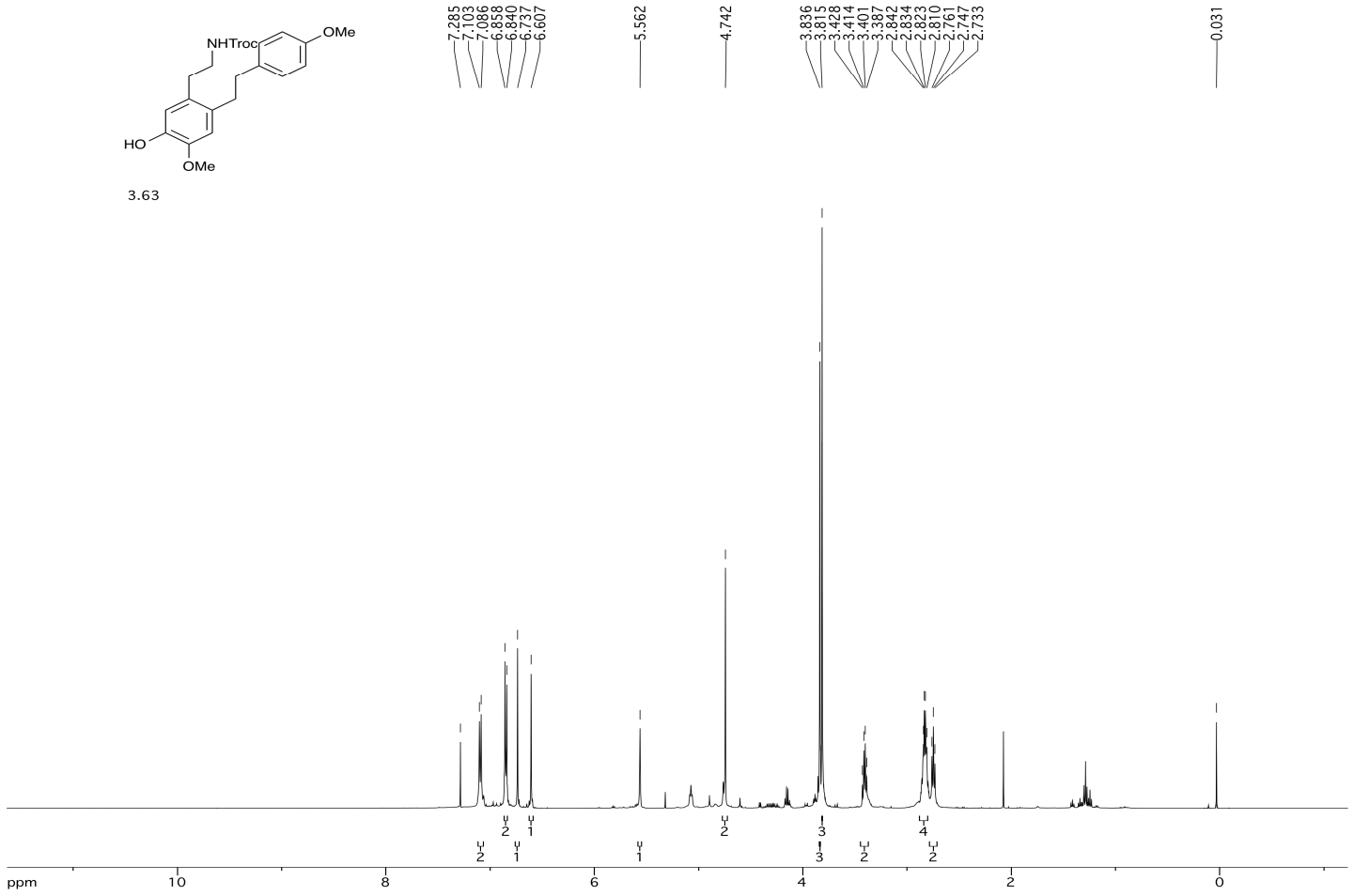
NHTroc
OMe
HO
OMe
3.63
7.285
7.103
7.086
6.838
6.840
6.737
6.607
5.562
4.742
3.836
3.815
3.428
3.414
3.401
3.387
2.842
2.834
2.823
2.810
2.761
2.747
2.733
0.031
ppm
10
8
6
4
2
0

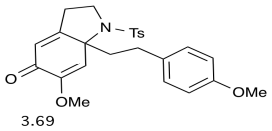
N
Ts
O
OMe
OMe

3.69

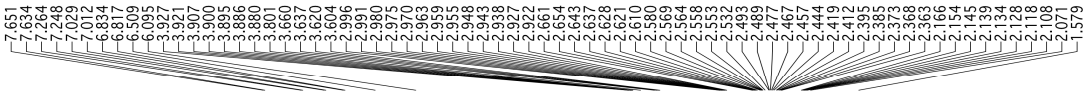
7.651
7.634
7.264
7.248
7.029
7.012
6.834
6.817
6.509
6.095
3.927
3.921
3.907
3.900
3.895
3.886
3.880
3.801
3.660
3.637
3.620
3.604
2.996
2.991
2.980
2.975
2.970
2.963
2.959
2.955
2.948
2.943
2.938
2.927
2.922
2.661
2.654
2.643
2.637
2.628
2.621
2.610
2.580
2.569
2.564
2.558
2.553
2.532
2.493
2.489
2.477
2.467
2.457
2.444
2.419
2.412
2.395
2.385
2.373
2.368
2.363
2.166
2.154
2.145
2.139
2.134
2.128
2.118
2.108
2.071
1.579

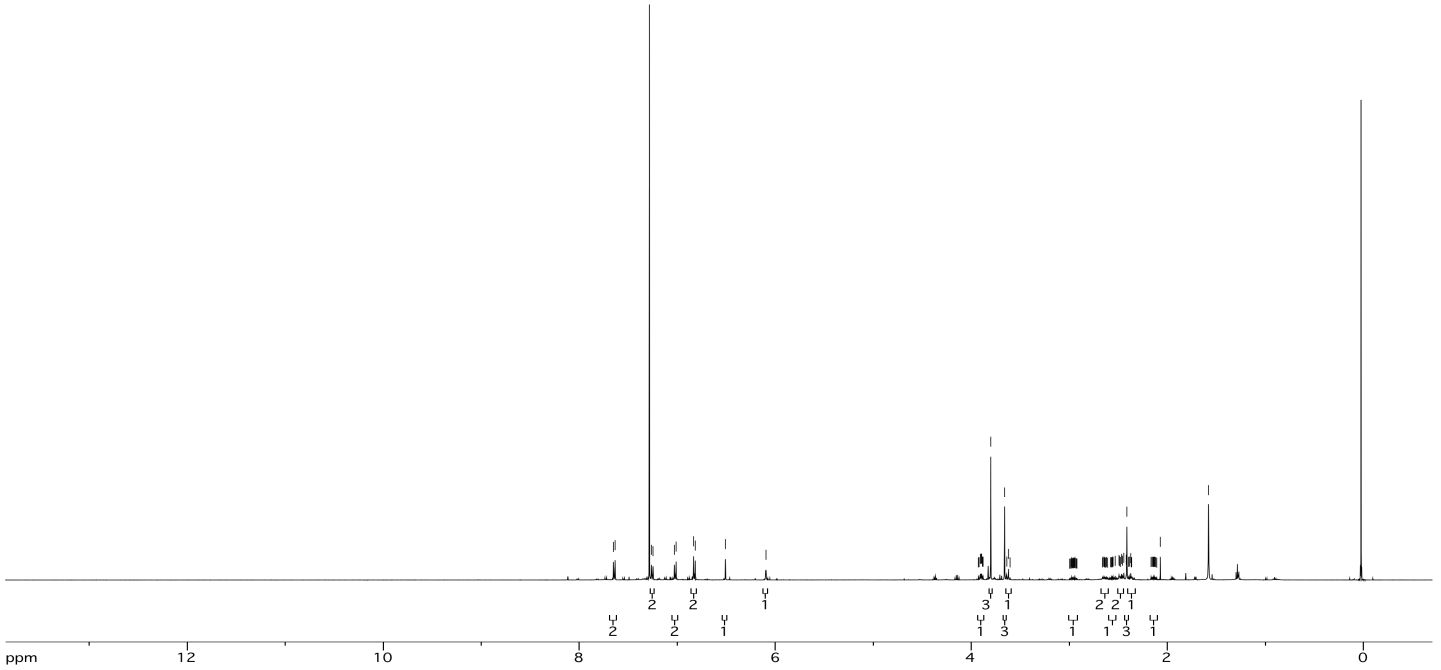
2
2
1
3
1
2
2
1
2
2
1
1
3
1
1
3
1
1
3
1
ppm
12
10
8
6
4
2
0

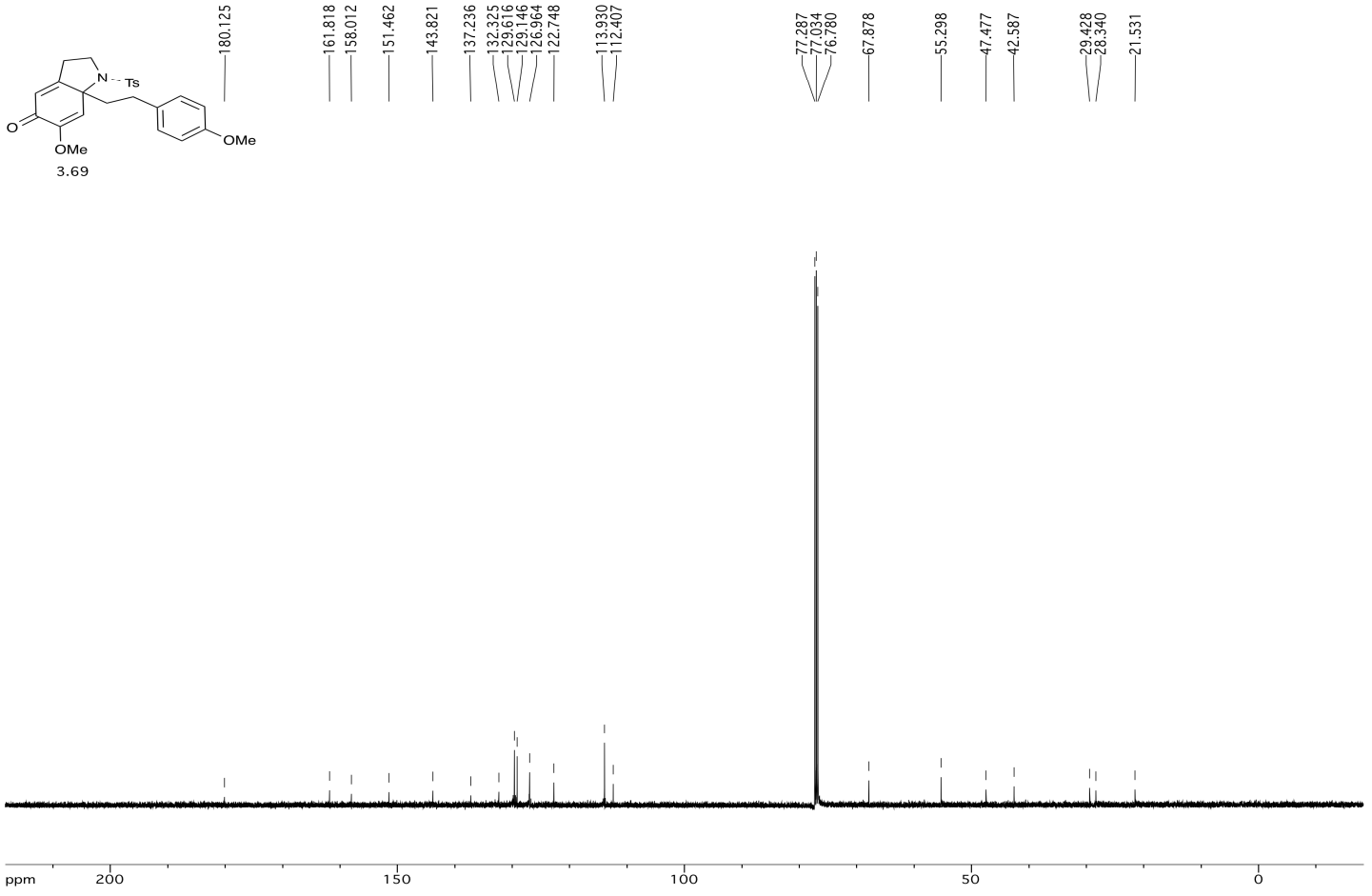
180.125
161.818
158.012
151.462
143.821
137.236
132.325
129.616
129.146
126.964
122.748
113.930
112.407
77.287
77.034
76.780
67.878
55.298
47.477
42.587
29.428
28.340
21.531
N
Ts
O
OMe
OMe
3.69
ppm
200
150
100
50
0

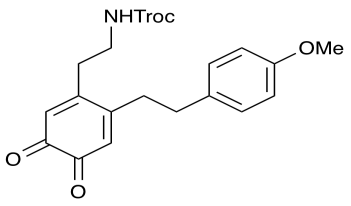
NHTroc
OMe
O
O

3.71

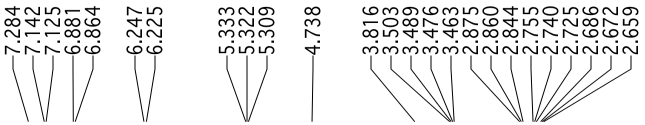
7.284
7.142
7.125
6.881
6.864
6.247
6.225
5.333
5.322
5.309
4.738
3.816
3.503
3.489
3.476
3.463
2.875
2.860
2.844
2.755
2.740
2.725
2.686
2.672
2.659

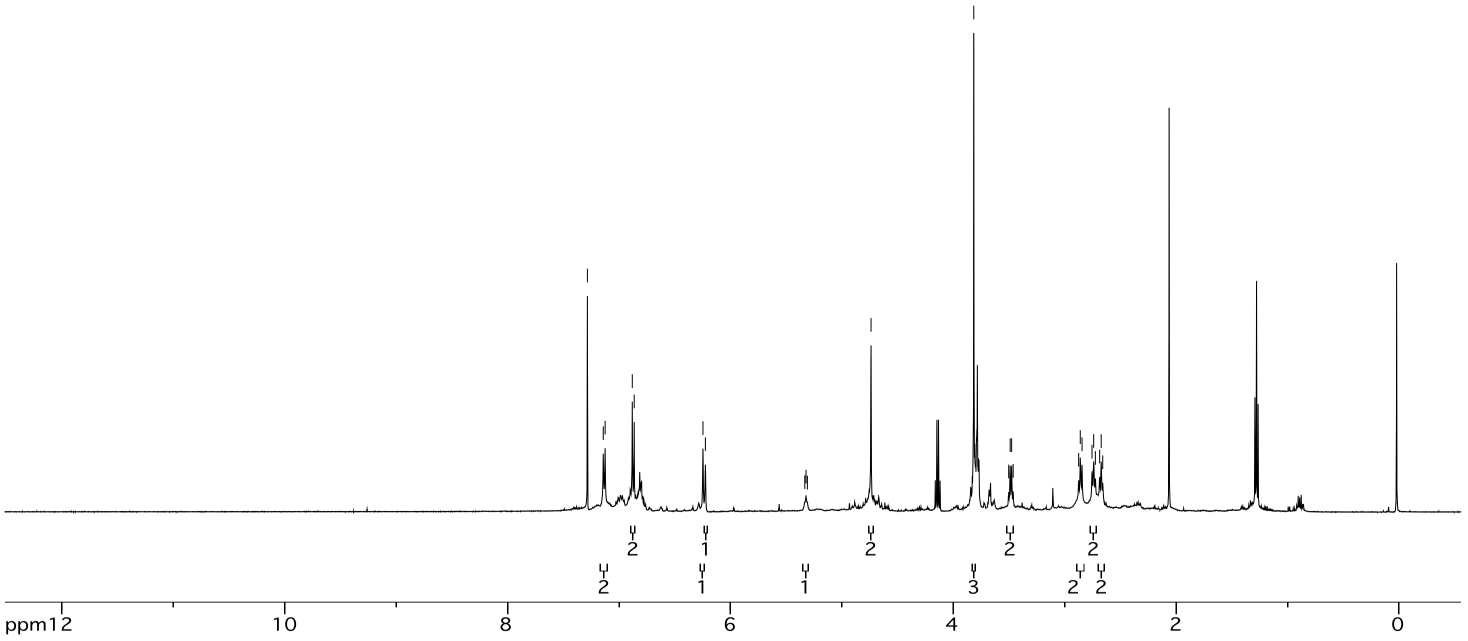
2
1
2
2
2
2
1
1
3
2
2
ppm12
10
8
6
4
2
0

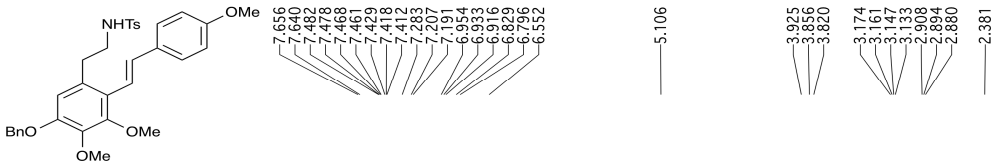
NHTs
OMe
BnO
OMe
OMe
7.656
7.640
7.482
7.478
7.468
7.461
7.429
7.418
7.412
7.283
7.207
7.191
6.954
6.933
6.916
6.829
6.796
6.552
5.106
3.925
3.856
3.820
3.174
3.161
3.147
3.133
2.908
2.894
2.880
2.381

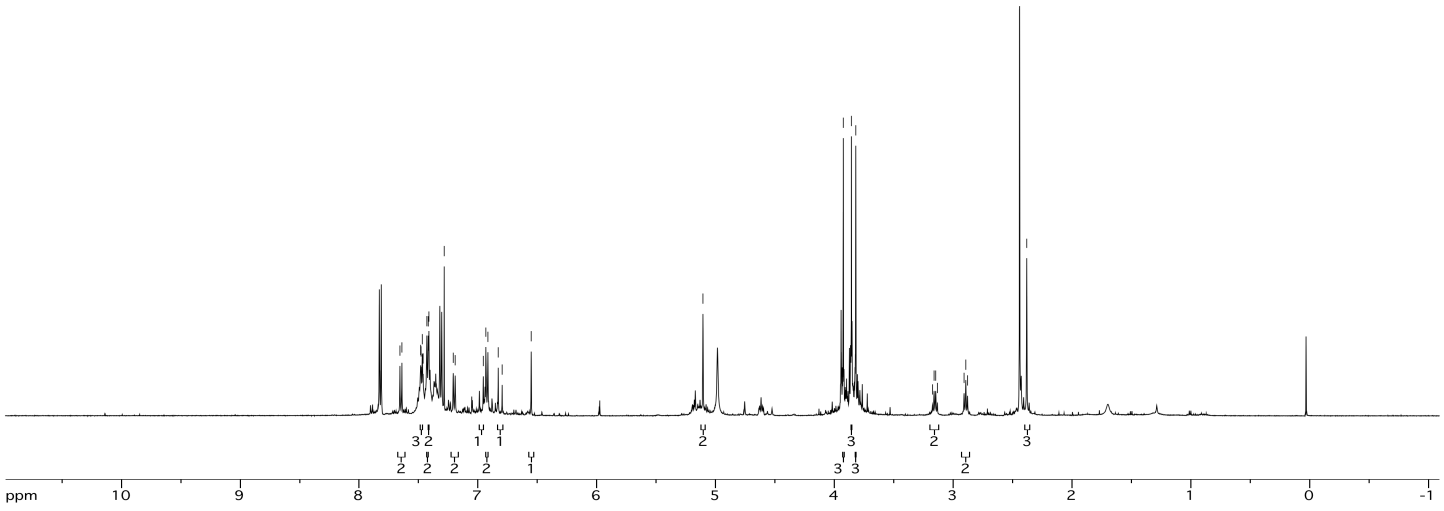
ppm
10
9
8
7
6
5
4
3
2
1
0
-1

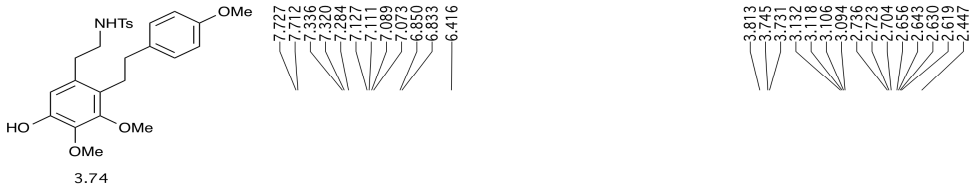
NHTs
OMe
HO
OMe
OMe
3.74
7.727
7.712
7.336
7.320
7.284
7.127
7.111
7.089
7.073
6.850
6.833
6.416
3.813
3.745
3.731
3.132
3.118
3.106
3.094
2.736
2.723
2.704
2.656
2.643
2.630
2.619
2.447

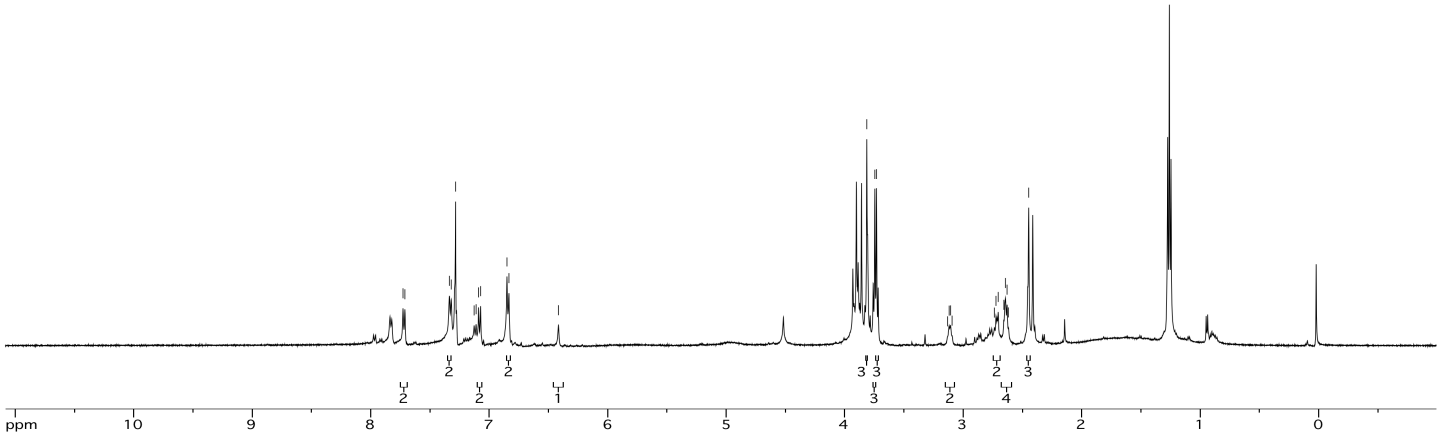
ppm
10
9
8
7
6
5
4
3
2
1
0

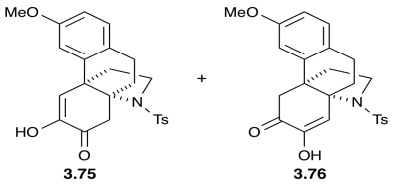
MeO
HO
O
N
Ts
3.75
+
MeO
O
OH
N
Ts
3.76

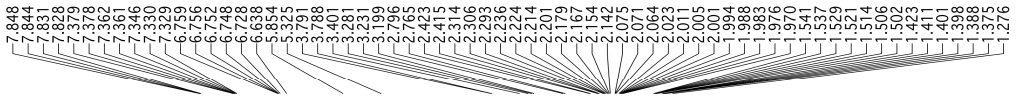
7.848
7.844
7.831
7.828
7.379
7.378
7.362
7.361
7.346
7.330
7.329
6.759
6.756
6.752
6.748
6.728
6.638
5.854
3.325
3.316
3.791
3.788
3.401
3.281
3.231
3.199
2.796
2.765
2.423
2.415
2.314
2.306
2.293
2.236
2.224
2.214
2.201
2.179
2.167
2.154
2.142
2.075
2.071
2.064
2.023
2.011
2.005
2.001
1.994
1.988
1.983
1.976
1.970
1.541
1.537
1.529
1.521
1.514
1.506
1.502
1.423
1.411
1.401
1.398
1.388
1.375
1.276

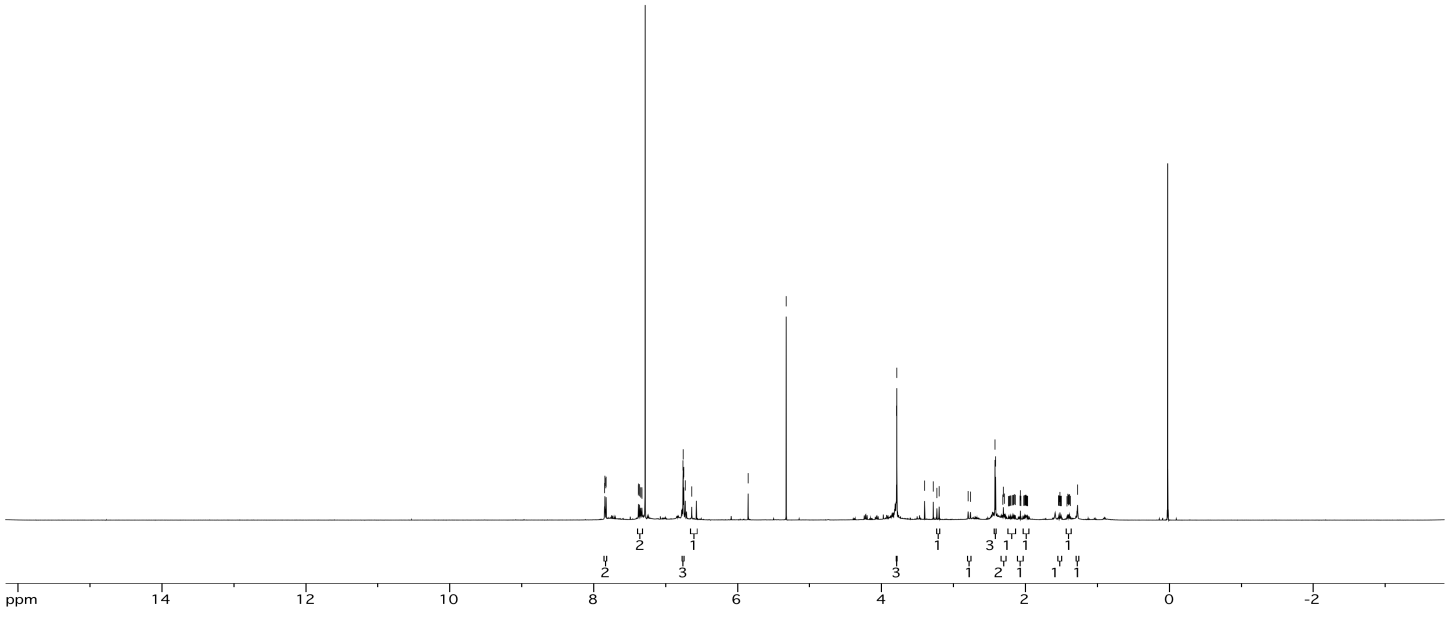
ppm
14
12
10
8
6
4
2
0
-2